

**Role played by the WD domain of  
ATG16L1 in defense against Salmonella  
infection in vivo**

**Weijiao Zhang**

**A Thesis submitted for the degree of Doctor of  
Philosophy (Ph.D)**

**Quadram Institute Bioscience &  
Norwich Medical School  
University of East Anglia  
2021**

This copy of the thesis has been supplied on condition that anyone who consults it is understood to recognise that its copyright rests with the author and that use of any information derived there-from must be in accordance with current UK Copyright Law. In addition, any quotation or extract must include full attribution.

## Abstract

Non-canonical autophagy, or LC3-associated phagocytosis (LAP), conjugates autophagy protein LC3 to endo-lysosome compartments to facilitate delivery of extracellular materials to lysosomes. The WD domain of autophagy protein ATG16L1 is required for conjugation of LC3 to endo-lysosomes during LAP, but is not required for LC3 conjugation during autophagy. Mice lacking the WD domain of ATG16L1 ( $\delta$ WD mice) are therefore defective in LAP, but can activate autophagy to maintain tissue homeostasis. This study has used  $\delta$ WD mice to determine the role played by the WD domain of ATG16L1 during *S. Typhimurium* infection "*in vivo*".

*S. Typhimurium* showed increased replication and virulence in  $\delta$ WD mice characterized by high mortality rate, severe weight loss, and enhanced dissemination of bacteria and lymphocytes to liver and spleen. Crosses with *LysM*<sup>cre</sup> and *villin*<sup>cre</sup> mice showed that expression of the WD domain of ATG16L1 in intestinal epithelial cells, rather than myeloid cells, protected against *S. Typhimurium*.

SopF is an *S. Typhimurium* SPI-1 T3SS effector thought to increase virulence by blocking the binding of the WD domain of ATG16L1 to the endo-lysosome v-ATPase to prevent recruitment of LC3 to *Salmonella* containing vacuoles. A SopF knockout *S. Typhimurium* strain (JH3009 <sup>$\delta$ SOPF</sup>), generated by lambda recombination, showed reduced virulence in control mice, but both wild type *S. Typhimurium* and JH3009 <sup>$\delta$ SOPF</sup> showed increased virulence in mice lacking the WD domain. This suggested that the WD domain restricted *S. Typhimurium* replication by additional pathways that are independent of the WD-v-ATPase axis blocked by Sop-F.

Fluorescent probes and biosensors showed that cells and tissues of  $\delta$ WD mice had raised intracellular cholesterol that accumulated at sites of replication. Replication

was reduced by cholesterol-lowering drugs. Taken together the results suggest that WD domain of ATG16L1 restricts *S. Typhimurium* replication in intestinal epithelial cells partly by reducing intracellular cellular cholesterol levels.

## **Access Condition and Agreement**

Each deposit in UEA Digital Repository is protected by copyright and other intellectual property rights, and duplication or sale of all or part of any of the Data Collections is not permitted, except that material may be duplicated by you for your research use or for educational purposes in electronic or print form. You must obtain permission from the copyright holder, usually the author, for any other use. Exceptions only apply where a deposit may be explicitly provided under a stated licence, such as a Creative Commons licence or Open Government licence.

Electronic or print copies may not be offered, whether for sale or otherwise to anyone, unless explicitly stated under a Creative Commons or Open Government license. Unauthorised reproduction, editing or reformatting for resale purposes is explicitly prohibited (except where approved by the copyright holder themselves) and UEA reserves the right to take immediate 'take down' action on behalf of the copyright and/or rights holder if this Access condition of the UEA Digital Repository is breached. Any material in this database has been supplied on the understanding that it is copyright material and that no quotation from the material may be published without proper acknowledgement.

# Contents

Abstract .....	1
List of abbreviations .....	10
List of tables.....	13
List of Figures .....	14
Acknowledgment .....	17
1. Introduction.....	19
1.1 Host defenses against pathogens.....	19
1.1.i. Physical barrier .....	19
1.1.ii. Innate immune systems.....	20
1.1.iii. Innate immune defences against bacterial pathogens.....	21
1.1.iv. Autophagy .....	22
1.1.v. LC3 lipidation .....	24
1.1.vi. Xenophagy .....	25
1.1.vii. Non-canonical autophagy and LC3 associated phagocytosis/endocytosis.....	26
1.1.viii. Role played by non-canonical autophagy and LC3 associated phagocytosis/endocytosis in immune regulation and disease.....	32
1.1.ix. Adaptive immune response .....	33
1.2 Generation of mice lacking non-canonical autophagy pathways such as LAP and LANDO.....	34
1.2.i. Domains of ATG16L1 important for autophagy and LAP.....	34
1.2.ii. Generation of mice defective in non-canonical autophagy/LAP. ....	37
1.3.i. Role played by ATG16L1 during gut homeostasis and inflammation.....	39
1.4 <i>Salmonella</i> and virulence factors .....	40
1.4.i. Basic introduction of <i>Salmonella</i> .....	40
1.4.ii. Non-typhoidal <i>Salmonella</i> (NTS).....	41
1.4.iii. Invasive Non-typhoidal <i>Salmonella</i> (iNTS).....	42
1.4.iv. Typhoidal <i>Salmonella</i> .....	43

1.4.v. Barriers to salmonella infection. ....	44
1.4.vi. Animal models. ....	45
1.4.vii. Mouse models. ....	46
1.4.viii. Genetically modified mice. ....	47
1.4.ix. The genome of Salmonella 、 ....	47
1.4.x. Salmonella pathogenic islands (SPIs). ....	48
1.4.xi. Other important virulence factors. ....	49
1.5 <i>Salmonella</i> -host interactions ....	55
1.5.i. How does <i>Salmonella</i> enter cells ....	55
1.5.ii. <i>Salmonella</i> intracellular lifestyle ....	57
1.6 The role of SopF in xenophagy ....	62
1.6.i. SopF ....	62
1.6.ii. v-ATPase ....	63
1.7 The role of cholesterol in Salmonella infection and replication ....	65
1.7.i. Cholesterol and <i>S. Typhimurium</i> infection ....	65
1.8 Hypothesis and Aim ....	67
Chapter 2. Materials and Methods ....	68
2.1 Mouse models ....	68
2.2 cell lines ....	68
2.3 Genotyping ....	69
2.4 Bone marrow stem cells extraction and differentiation ....	70
2.5 LPS Challenge in mice. ....	70
2.6 IL-1 $\beta$ enzyme-linked immunosorbent assay (ELISA) ....	71
2.7 JH3009 replication in HEKs and MEFs. ....	72
2.8 <i>S. Typhimurium</i> infection in mice and tissue harvesting ....	73
2.9 Bacterial dissemination to liver and spleen. ....	74
2.10 Luminex assay of pro-inflammatory cytokines in serums of infected mice	74
2.11 Tissue processing and embedding ....	75
2.12 Hematoxylin and Eosin (H&E) staining ....	76
2.13 Immunohistostaining of tissue sections ....	77

2.14 Tissue western blot.....	78
2.15 FITC-dextran treatment in mice.....	79
2.16 FACS analysis of immune cells populations in the liver .....	80
2.17 FACS analysis lamina propria lymphocytes from small intestine of mice ..	82
2.18 Lamda Red recombination to replace <i>SopF</i> with kanamycin cassette.....	83
2.19 P22 transduction of <i>SopF</i> mutation to <i>S. Typhimurium</i> strain JH3009 .....	85
2.20 Growth curve of JH3009 <sup>Δ<i>SopF</i></sup> .....	87
2.21 JH3009 <sup>Δ<i>SopF</i></sup> replication in MEFs.....	87
2.22 Immunofluorescent (IF) staining of LC-3 recruitment to <i>S. Typhimurium</i> ..	88
2.23 JH3009 <sup>Δ<i>SopF</i></sup> infection in control mice .....	89
2.24 JH3009 <sup>Δ<i>SopF</i></sup> infection in ΔWD mice .....	89
2.25 Filipin staining in MEFs .....	89
2.26 Membrane repair assay with digitonin.....	89
2.27 mCherry-D4H transfection in MEFs .....	90
2.28 Cholesterol visualization after cholesterol drug treatment. ....	91
2.29 <i>S. Typhimurium</i> replication in MEFs after T0901317 treatment.....	92
2.30 Filipin Staining of the small intestine .....	92
3. Generation and identification of mice that lack WD domain of Atg16L1 .....	94
3.1 Introduction.....	94
3.1.i. Background.....	94
3.1.ii. Domains of ATG16L1 important for autophagy and LAP.....	94
3.1.iii. Generation of mice defective in non-canonical autophagy/LAP.....	95
3.2 Results.....	98
3.2.i. Generation of ΔWD mice. ....	98
3.2.ii. Genotyping by PCR.....	100
3.2.iii. Examination of ATG16L1, autophagy and LAP in MEFs.....	101
3.2.iv. Examination of the truncated ATG16L1 by western blot in tissues..	101
3.2.v. The status of autophagy and LAP in fibroblasts and macrophages. ..	105
3.2.vi. ΔWD mice do not have the pro-inflammatory phenotype seen in mice lacking autophagy in myeloid cells.....	106

3.3 Discussion.....	108
3.3.i. Background.....	108
3.3.ii. Summary.....	110
Chapter 4. The loss of WD domain of ATG16L1 promotes <i>S. Typhimurium</i> replication ‘in vitro’ and increases <i>S. Typhimurium</i> sensitivity ‘in vivo’.....	112
4.1 Introduction.....	112
4.1.i. Background.....	112
4.2 Results.....	112
4.2. i. The loss of WD domain of ATG16L1 promotes <i>S. Typhimurium</i> replication in fibroblasts and epithelial cells. ....	112
4.2.ii. The Loss of the WD domain of ATG16L1 increases the sensitivity of mice to <i>S. Typhimurium</i> infection.....	114
4.2.iii. Increased lymphocyte infiltration was observed in the livers of $\delta$ WD mice.....	120
4.3 Discussion.....	123
4.3.i. Background.....	123
4.3.ii. Increased <i>Salmonella</i> replication in $\delta$ WD cells.....	124
4.3.iii. The Loss of the WD domain of ATG16L1 increases sensitivity of mice to <i>S. Typhimurium</i> infection. ....	125
4.3. iv. Summary.....	126
Chapter 5. WD domain of Atg16L1 control <i>S. Typhimurium</i> infection at intestinal epithelial surface in mice .....	127
5.1 Introduction.....	127
5.1.i. Background.....	127
5.1.ii. <i>LysM<sup>cre</sup></i> and <i>Villin<sup>cre</sup></i> .....	127
5.2 Results.....	128
5.2.i. Generation of mice lacking the WD domain of ATG16L1 in myeloid cells .....	128
5.2.ii Genotyping of $\delta$ WD <sup>phage</sup> mice. ....	131
5.2.iii. Analysis of tissue-specific expression of WD by western blot. ....	131
5.2.iv Generation of mice lacking the WD domain of ATG16L1 in intestinal	

epithelial cells. ....	132
5.2.v Genotyping of $\delta$ WD <sup>IEC</sup> mice. ....	132
5.2.vi Analysis of tissue-specific expression of WD by western blot.....	133
5.2.vii. $\delta$ WD <sup>IEC</sup> mice are more sensitive to <i>S. Typhimurium</i> compared with $\delta$ WD <sup>phage</sup> mice and control mice. ....	137
5.2. viii. Loss of Atg16L1's WD domain in the intestinal epithelium decreased intestinal permeability after <i>S. Typhimurium</i> infection .....	142
5.2.ix. FACs analysis of the lymphocyte population in the small intestine and liver of $\delta$ WD <sup>IEC</sup> and $\delta$ WD <sup>phage</sup> mice after <i>S. Typhimurium</i> infection. ....	144
5.3 Discussion.....	147
5.3.i. Background.....	147
5.3.ii. Role of different cells during <i>S. Typhimurium</i> infection.....	148
5.3.iii. LysMcre and Villincre .....	148
5.3.iv. Why does LAP in macrophages failed to play a significant role in controlling <i>S. Typhimurium</i> infection.....	150
5.3.v. <i>S. Typhimurium</i> infection and adaptive immunity.....	151
5.3.iv. Summary .....	151
Chapter 6. Generation and analysis of infection by a <i>SopF</i> deficient <i>S. Typhimurium</i> strain.....	153
6.1 Introduction.....	153
6.2. Results.....	154
6.2.i. <i>SopF</i> mutation in strain SL1344 via Lambda red recombination. ....	154
6.2.ii. <i>SopF</i> mutation transduced in strain JH3009.....	157
6.2.iii. Loss of <i>SopF</i> does not affect <i>S. Typhimurium</i> growth in LB.....	157
6.2.iv. The loss of <i>SopF</i> reduced the replication of <i>S. Typhimurium</i> in MEFs. ....	157
6.2.v. The loss of <i>SopF</i> promotes LC-3 recruitment to SCVs. ....	160
6.2.vi. Loss of <i>SopF</i> reduced <i>S. Typhimurium</i> virulence in mice.....	161
6.2.vii. <i>S. Typhimurium</i> lacking <i>SopF</i> show increased virulence in $\delta$ WD mice. ....	163

6.3 Discussion.....	166
6.3.i. Background.....	166
6.3.ii. Does the WD-vATPase axis block autophagy or non-canonical autophagy/LAP? .....	168
6.3.iii. Does the WD domain of ATG16L1 have functions in addition to recruiting LC3 via the WD-vATPase axis?.....	172
Chapter 7 The WD domain of ATG16L1 influences the distribution of cholesterol between the cytosol and the Salmonella containing vacuole.....	174
7.1 Introduction.....	174
7.1.i. Background.....	174
7.1.ii. Cholesterol.....	174
7.1.iii. Cholesterol and <i>S. Typhimurium</i> infection.....	175
7.2 Results.....	176
7.2.i. Loss of the WD domain of ATG16L1 raises cholesterol levels in the cytosol leading to a deficiency in membrane repair .....	176
7.2.ii. Salmonella co-localize with cytosolic cholesterol.....	180
7.2.iii. T0901317 and U18666A modulate cholesterol levels in cells. ....	183
7.2.iv. Reduced intracellular cholesterol levels inhibit Salmonella replication .....	184
7.2.v. Small intestine of mice lacking the WD domain of ATG16L1 have higher levels of intracellular cholesterol.....	185
7.3 Discussion.....	189
7.3.i. Background.....	189
7.3.ii. The lack of WD domain of ATG16L1 increases cellular cholesterol. ....	189
7.3.iii. Membrane repair, cholesterol and the WD domain of ATG16L1.....	190
7.3.iv. Plasma membrane or cytosolic cholesterol inhibits <i>S. Typhimurium</i> infection. ....	192
7.3.v. Other roles for cholesterol during <i>S. Typhimurium</i> infection. ....	193
7.3.vi. Summary.....	193

Chapter 8 Discussion and further perspective .....	195
8.1 Discussion. ....	195
8.2 Future perspective. ....	199
<b>Reference</b> .....	205

## List of abbreviations

peptidoglycan	PG
pattern recognition receptors	PRRs
NOD-like receptors	NLRs
Toll-like receptors	TLRs
C-type lectin receptors	CTLRs
RIG-like receptors	RLRs
pathogen-associated molecular patterns	PAMPs
reactive oxygen species	ROS
Autophagy-related protein	ATGs
phosphatidylinositol 3-kinase	PI3K
mammalian target of rapamycin	mTOR
microtubule-associated protein light chain 3	LC3
optineurin	OPTN
LC3 interacting region	LIR
vacuole ATPase	V-ATPase
LC3 associated phagocytosis	LAP
LC3 associated endocytosis	LANDO
dendritic cells	DCs
NADPH oxidase-2	NOX2
T cell receptor	TCR
major histocompatibility complex	MHC
amino acid	aa
lipopolysaccharide	LPS
nuclear factor $\kappa$ B	NF- $\kappa$ B

interferon-regulated factor	IRF
leucine-rich repeats	LRRs
systemic lupus erythematosus	SLE
<i>S. enterica</i> serotype Typhi	<i>S. Typhi</i>
<i>Salmonella enterica serovar</i> Typhimurium	<i>S. Typhimurium</i>
peripheral blood mononuclear cells	PBMCs
<i>Salmonella</i> pathogenic islands	SPIs
plasmid-encoded fimbriae	<i>pef</i>
<i>Salmonella</i> plasmid virulence	spv
self-transmissible virulence plasmid	pSLT
fetal calf serum	FCS
early endosome antigen 1	EEA1
Ras-related protein	Rab
lysosomal-associated membrane protein 1	LAMP1
Salmonella-induced filaments	SIFs
fluorescent activated cell sorting	FACS
Mass spectrum	MS
Wild type	WT
mouse embryonic fibroblasts	MEFs
Dulbecco's modified eagle medium	DMEM
penicillin-streptomycin	PS
Human embryonic kidney	HEK
specific pathogen-free	SPF
ethidium bromide	EtBr
ultraviolet	UV
bone marrow-derived macrophages	BMDMs
phosphate buffer saline	PBS
formalin fixed paraffin embedded	FFPE
enzyme-linked immunosorbent assay	ELISA
embryonic stem cell	ES

bovine growth hormone polyadenylation site	bGH-pA
colonies forming units	CFU
small intestine	SI

## List of tables

Table 1 Functions of SPI-1/2 effectors .....	
Table 2.1.....	Table 2.1.....
Table 2.2 FACS antibody .....	Table 2.2.....
Table 2.2.....	Table 2.2.....

# List of Figures

Figure 1.1 Autophagy as defense against infection.....	18
Figure 1.2 .....	21
Figure 1.3 .....	24
Figure 1.4 Xenophagy and LC-3 associated phagocytosis. ....	29
Figure 1.5 an overview of ATG16L1's isoforms, domains and protein interaction sites .....	35
Figure 1.7 Alternative splicing of mRNA of $\alpha$ , $\beta$ and $\gamma$ isoform of Atg16L1 .....	38
Figure 1.8 Different strategies used by Salmonella for invasion and proliferation in eukaryotic cells .....	56
Figure 1.9 Cell Type-Specific Salmonella Intracellular Life Cycle and SPI-2 T3SS effectors.....	60
Figure 3.1 Assay for determines autophagy level.....	96
Figure 3.2 Determine the presence of LAP by Zymosan phagocytosis.....	97
Figure 3.3 The final vector for mouse embryonic stem cell (ES) transfection....	99
Figure 3.4 Removal of neomycin cassette and flp gene .....	99
Figure 3.5 Genotyping of E230/ $\delta$ WD mice .....	100
Figure 3.6 A&B. Analysis of ATG16L1 and autophagy in cells from $\delta$ WD mice .....	102
Figure 3.6 C&D .....	104
Figure 3.7 Analysis of proinflammatory responses in $\delta$ WD mice.....	107
Figure 4.1 A&B Intracellular <i>S. Typhimurium</i> replication in HEK cells .....	114
Figure 4.1 C&D Intracellular <i>S. Typhimurium</i> replication in MEFs.....	114
Figure 4.2 A&B <i>S. Typhimurium</i> infection in $\delta$ WD and WT mice .....	115
Figure 4.2 C&D <i>S. Typhimurium</i> infection in $\delta$ WD and WT mice.....	116
Figure 4.2E <i>S. Typhimurium</i> infection in $\delta$ WD mice and WT controls .....	117

Figure 4.3 Liver histology from <i>S. Typhimurium</i> infected $\delta$ WD mice and WT controls.....	118
Figure 4.4 Spleen and small intestine histology from <i>S. Typhimurium</i> infected $\delta$ WD mice and WT controls .....	119
Figure 4.5 Gating Strategy for T cells.....	121
Figure 4.6 Gating strategy for Kupffer cells, BMD-monocytic macrophages and neutrophils.....	122
Figure 4.7 Analysis of lymphocytes infiltration in the liver of infected.....	123
Figure 5.1 Generation and identification of $\delta$ WD <sup>phag</sup> mice .....	130
Figure 5.2 Generation and identification of $\delta$ WD <sup>IEC</sup> mice .....	136
Figure 5.3 A Weight curve of $\delta$ WD, $\delta$ WDIEC, $\delta$ WDphage and control mice after JH3009 infection.....	138
Figure 5.4 Comparison of survival curves for $\delta$ WD, $\delta$ WDIEC, $\delta$ WDphage and control mice .....	140
Figure 5.5 Bacterial dissemination to liver and spleen on sixth day post infection .....	141
Figure 5.6 Gut permeability assay in $\delta$ WD, $\delta$ WDIEC, $\delta$ WDphage and control mice before and after JH3009 infection.....	143
Figure 5.7 A&B Lymphocyte population in liver and small intestine of $\delta$ WDphage mice and controls mice after JH3009 infection .....	145
Figure 5.7 C&D Lymphocyte population in liver and small intestine of $\delta$ WDIEC mice and controls mice after JH3009 infection .....	147
Figure 6.1 WD domain of ATG16L1 binds to vATPase .....	153
Figure 6.2 Lamda red recombination.....	155
Figure 6.3. Identification and characterization of SopF mutants.....	156
Figure 6.4 Replication of JH3009 $\delta$ SopF and JH3009 and LC3 recruitment in MEFs.....	160
Figure 6.5 A weight loss and bacterial dissemination for control mice infected with either JH3009 or JH3009 $\delta$ SopF.....	162

Figure 6.6 Infection of WT and $\delta$ WD mice with JH3009 $\delta$ SopF .....	164
Figure 6.7 A and B .....	168
Figure 6.7. C .....	169
Figure 6.8. Domains of ATG16L1 required for autophagy, bacterial autophagy or LAP .....	170
Figure 6.9. Assembly of T3SS complex makes a pore in the membrane of the SCV.....	172
Figure 7.1 Loss of the WD domain of ATG16L1 raises cholesterol levels in the cytosol leading to a deficiency in membrane repair .....	178
Figure 7.2 Salmonella co-localize with cytosolic cholesterol .....	181
Figure7.3 T0901317 and U18666A treatment in MEFs decrease/increase cellular cholesterol level and affect intracellular Salmonella replication .....	184
Figure 7.4 Filipin staining of small intestine .....	187
Figure 8.1 Main findings of this thesis .....	202
Figure 8.2 How does cholesterol accumulation affects Salmonella replication?	204

## **Acknowledgment**

I would like to extend my most sincere acknowledgments to my primary supervisor, Professor Tom Wileman for all his kind guidance and support throughout this Ph.D. I am extraordinarily lucky to come to UK and complete a Ph.D under his supervision. I thank all the science thoughts he taught me. Other than science, I learned a lot from him in oral and writing communication skills, as well as diagram drawing.

I really appreciate Dr. Yongping Bao for his care and support during my four-year study in Norwich. I would like also to thank Professor Ulrike Mayer for her kind help on transgenic mice breeding and maintenance, which would benefit me through my scientific career.

I want to thank Dr. Naiara Beraza and Anna, Mar, Sian in her group for their kind training and support on histology and FACs techniques which was involved throughout my Ph.D. I appreciated the kindness and patience they showed in training me and troubleshooting problems I met during my studies. It's impossible to finish this Ph.D without their help.

I would also like to thank Dr. Rob Kingsley and Luke, Gaetan, Haider from his group for their kind help in generating genetically modified Salmonella strains. This thesis wouldn't be complete without their help.

I really appreciated Dr. Penny Powell for all the guidance and support I received from her. She is very kind and helpful as both a supervisor in the lab and as the Dean of Postgraduate Research.

I would like to thank all my previous and current lab members for their help in this work. I thank Shashank for being a close buddy and a fantastic lab mates. It's very

nice to have a buddy working together on weekends. I admire his expertise, skills and experience in both lab work and management. I also appreciate his invitation to taste delicious Indian food. I appreciate Huanyu, who is a close friend, for his help in protein expression and purification during the project. I would also like to thank Dr. Timothy Pearson for all the tricks and methods he told me, which are very useful in troubleshooting and overcame all kinds of difficulties in the lab. I would like to thank Miss Lingzi Niu for all supports she provided with genotyping and management of transgenic mice. Last but not least I would like to thank Dr. Matthew Jefferson for being a monitor and friend in the lab and all his help during the study.

This thesis would never be finished without encouragement from my family. I would like to offer special thanks to Miss Nan Cheng for all the sacrifices she has made for my Ph.D and wellbeing.

I would like to thank all my friends who accompanied me during my Ph.D study in Norwich. I thank Chenghao Yue, Chengyang Liu, Junyu Liu, Zhengyu Zhang, Han Lin, Jiaoshan Li. I really appreciated them for making my stay comfortable, joyful and a learning experience.

Finally, I appreciate the China Scholarship Council for their financial support during my Ph.D study.

# **1. Introduction**

## **1.1 Host defenses against pathogens**

Humans face a broad range of microorganisms every day, many of which are pathogens. However, those infectious pathogens don't cause diseases on a regular basis due to a serious defense mechanism that has evolved over millions of years. Three levels of defense are identified, physical barriers, the innate immune system and the adaptive immune system (Delves 2011).

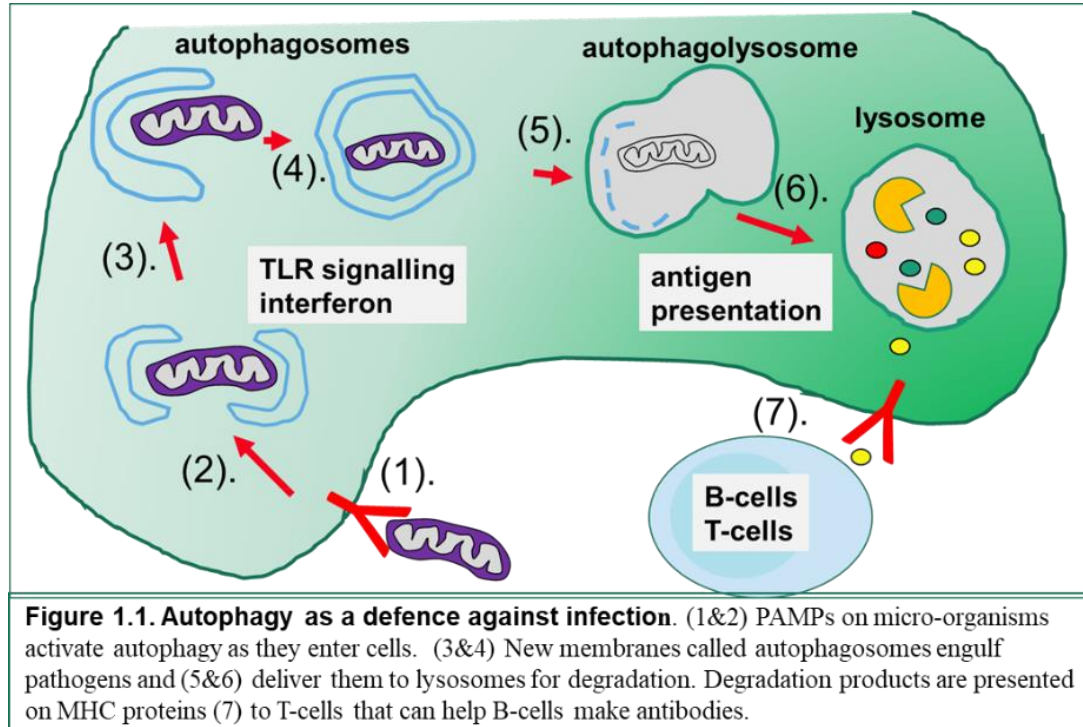
### **1.1.i. Physical barrier**

The best way to avoid diseases is to keep the pathogens out of the body. Physical barriers are represented by the skin and other epithelia which cover the surface of the gastrointestinal, respiratory, urogenital system and have been proven to be very effective. They provide not only physical but also biological and chemical barriers. The primary mechanical barrier is the tight junctions that link the epithelial cells. The internal mucosal epithelia, normally covered with mucosal secretions, can block the direct adhesion of pathogens to epithelial cells. In the intestinal mucosal, the mucus is secreted by specific goblet cells and provides a barrier covering epithelial cells (Lievin-Le Moal and Servin 2006). A chemical barrier is also in place to kill microbes or limit their growth. Those chemicals include a group of antibacterial enzymes, such as lactoperoxidase, lysozyme and phospholipase A2. Lysozyme disrupts the cell wall of both Gram-negative and Gram-positive bacteria by breaking peptidoglycan (PG) while phospholipase A2 kills bacteria by hydrolysing phospholipids in the cell membrane. Defensins, cathelicidins and histatins are anti-microbial peptides activated by proteolysis and secreted from epithelial surfaces. They are toxic to many microbes and disrupt the cell membrane. The biological barrier is microbiota, a microbial community composed of bacteria, archaea, protozoa, viruses and fungi. The microbiota in the intestine normally competes with the invading pathogens, such as

*Salmonella*, for space, nutrients and attachment sites. In addition, the microbiota can also secrete some metabolites and affect the replication. and virulence of pathogens (Vogt, Pena-Diaz et al. 2015).

### 1.1.ii. Innate immune systems

The innate immune response, the second level of defense, occurs when the pathogen starts to enter the body. Pathogens are normally recognized and killed by phagocytic cells, mainly macrophages and polymorphonuclear neutrophils. The phagocytic cells carry pattern recognition receptors (PRRs), including Toll-like receptors (TLRs), NOD-like receptors (NLRs), C-type lectin receptors (CTLRs) and RIG-like receptors (RLRs). PRRs can adhere to pathogen-associated molecular patterns (PAMPs) on the pathogen's surface. The binding of PRRs can increase the phagocytic ability of macrophages and neutrophils. Once inside the phagocytic cell, the microorganism can be killed by reactive oxygen species (ROS) with the assistance of low pH, lysozyme



and lactoferrin (Takeuchi and Akira 2010). Another important cell of the innate immune system is the natural killer cells, which can identify signals expressed by

infected cells and induce their apoptosis (Crouse, Xu et al. 2015).

### **1.1.iii. Innate immune defences against bacterial pathogens**

Many factors, such as lipopolysaccharide (LPS), PG, lipoproteins, flagellin, can activate TLRs, and these play an important role during *Salmonella* infection leading to activation of nuclear factor  $\kappa$ B (NF- $\kappa$ B) and transcription factors from the interferon-regulated factor (IRF) family. NLRs are soluble proteins within the cytosol and usually recognize PAMPs such as bacterial peptidoglycans with their C-terminal leucine-rich repeats (LRRs). NLRs are normally inhibited and activated when binding to PAMPs (Kim, Shin et al. 2016). NOD1 and NOD2 can activate autophagy machinery by recruiting ATG16L1 to the plasma membrane at the site of bacterial entry. Both canonical and non-canonical autophagy plays an important role in controlling intracellular pathogen infection and will be discussed below (Gomes and Dikic 2014). NOD1 and NOD2 also activate the NF- $\kappa$ B pathway whereas some other NLRs, such as NLRP2 and NLRP4, are negative regulators of the NF- $\kappa$ B pathway. Some other NLRs, such as NLRP1 and NLRP3 are inflammasome sensors (Sharma and Kanneganti 2016). Inflammasomes are a group of cytosolic protein complexes, consisting of an upstream sensor protein from the NLR family, an adaptor protein ASC and the effector caspase-1 (Henao-Mejia, Elinav et al. 2012, Sharma and Kanneganti 2016). Activation of inflammasome promotes caspase-1 to convert pro cytokines into active IL-1 $\beta$  and IL-18, and cleave Gasdermin D (Broz and Dixit 2016). N-terminal cleaved fragments induce programmed cell death apart from apoptosis, known as pyroptosis (Broz and Dixit 2016). These caspase-1 involved inflammasomes are defined as canonical inflammasomes, some other inflammasome pathways which don't involve caspase-1 are referred to as non-canonical inflammasomes. These pathways are activated by the sensing bacterial LPS in the cytosol and involve caspase-11 in mice and caspase-4 and caspase-5 in humans (Broz and Dixit 2016). The inflammasomes are first thought to be mainly activated in myeloid cells, professional cells from the immune system. However, some recent

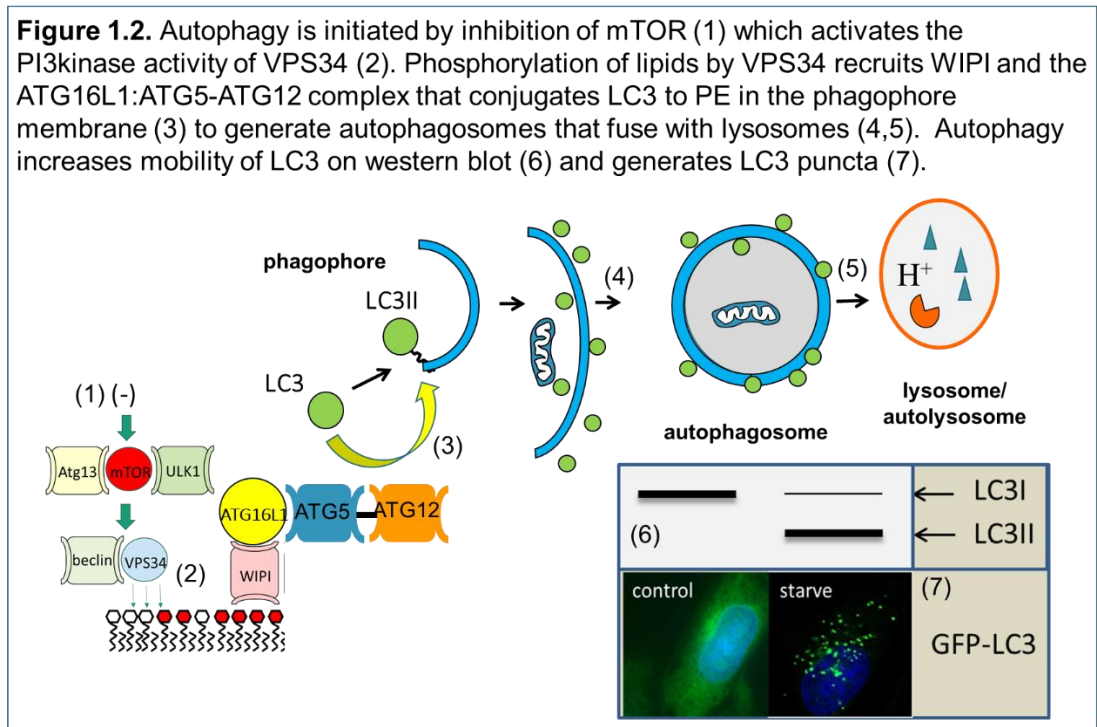
studies revealed that inflammasome-mediated defense plays a crucial role in the first line of defense against bacterial infection in various epithelium (Winsor, Krustev et al. 2019). Most epithelial inflammasome studies have been conducted in the intestinal mucosa, but some studies also reported that epithelial inflammasome also occurs in other epithelial surfaces, such as urinary bladder epithelium (Peeters, Wouters et al. 2015, Sellin, Maslowski et al. 2015, Sellin, Muller et al. 2018). Canonical inflammasome plays an important role in controlling enterobacterial, such as *Salmonella* and *Citrobacter rodentium* infection (Sellin, Maslowski et al. 2015). Canonical inflammasomes are triggered by intracellular bacteria, and a process referred to as epithelial cell extrusion, the expulsion of infected cells from the epithelium is carried out to reduce bacteria load in the epithelium. The process occurs without compromising epithelial integrity. Inflammasomes can induce epithelial death, promote epithelial cells to secrete a high level of IL-18 to recruit NK cells and neutrophils to the infection site. Inflammasomes are also reported to reduce tumor load in colon cancer, by triggering the removal of tumor-initiating cells (Sellin, Maslowski et al. 2015) and are involved in Crohn's disease (Opipari and Franchi 2015).

#### **1.1.iv. Autophagy**

Autophagy responds to pathogens that have entered cells. It is likely that autophagy evolved in early eukaryotes as a response to starvation allowing the cell to degrade organelles in lysosomes to provide a short-term source of energy. During the course of evolution, autophagy has been adapted to degrade damaged organelles and proteins to maintain cellular homeostasis and to defend the cell against invading microorganisms. In higher eukaryotes, autophagy communicates with the adaptive immune system by presenting microbial digestion products to B and T-cells (Fig 1.1).

The initial steps in autophagy are the formation and expansion of phagophore, an isolated membrane in the cytosol (Fig 1.2). The edges of the phagophore fuse together

to form a double-membrane structure which is called autophagosome. This is followed by the fusion of an autophagosome with lysosome to generate an autolysosome. The captured materials and the inner layer of the membrane are degraded (Klionsky, Abdalla et al. 2012). Autophagy-related proteins (ATGs) are a group of proteins that formed part of the autophagy machinery.



Autophagy proteins are generally split into four groups, the Atg1 kinase complex, the Vps34 class III phosphatidylinositol 3-kinase (PI3K) complex, two ubiquitin-like conjugation systems involving Atg8/LC3 and Atg12, and a membrane-trafficking complex involving Atg9 function. ULK1, an ATG1 homolog, forms a complex with ATG13 and Fip200 and serves as the key upstream kinase that induces autophagy (Kihara, Noda et al. 2001, Hara, Takamura et al. 2008, Jung, Jun et al. 2009). The complex is phosphorylated by the mammalian target of rapamycin (mTOR), which associates with ULK1-ATG13 complex and inhibits autophagy. During amino acid starvation or rapamycin treatment, mTOR dissociates from ULK1-ATG13 complex which results in the dephosphorylation of ULK1-ATG13 complex and induces autophagy. Activation of Vps34 complex, including BECN1, VPS15, ATG14L and VPS34, results in the generation of phosphatidylinositol 3-phosphate (PI3P). VPS34

functions by phosphorylating the inositol ring of the phosphatidylinositide to generate PI3P. Generation of PI3P at the sites of the autophagosome formation induces autophagy (Kihara, Noda et al. 2001, Chan 2009). PI3P plays a fundamental role in autophagy, such as autophagosome biogenesis, maturation and transport. PI3P production on the phagophore promotes the negative curvature and monitors the size of autophagosome. PI3P also facilitates the expansion and sealing of spherical structure and creates a membrane platform to concentrate and coordinate the effectors necessary for downstream signalling production and the progression of autophagy (Dall'Armi, Devereaux et al. 2013). The formation of autophagosome is controlled by two ATG related ubiquitin-like conjugation systems, ATG12 and ATG8, which play important roles in the expansion of phagophore. ATG12, the E1 enzyme, is activated by ATG7, then transferred to E2-like enzyme ATG10. From ATG10, ATG12 conjugate with an internal lysine residue of ATG5 to form ATG12-ATG5 complex. ATG12 - ATG5 conjugate with the coiled-coiled domain of ATG16L1, which results in the formation of ATG5-ATG12-ATG16L1 complex (Mizushima, Kuma et al. 2003). The common autophagy marker, ATG8 or microtubule-associated protein light chain 3 (LC3), conjugates ATG3 and ATG7, then was cleaved by ATG4 to form LC3-I. LC3I is conjugated to lipid phosphatidylethanolamine (PE) to form LC3-II. PI3P acts as a platform to bind WIPI2, which utilizes an alternative lipid-binding domain. WIPI2 is able to associate with ATG5-ATG12-ATG16L1 complex, which acts as E3 enzyme, to label the site LC3 lipidation (Proikas-Cezanne, Takacs et al. 2015). The identification of LC3-I to LC3-II on autophagosome punctae is considered as a key marker for autophagy (Klionsky, Abdalla et al. 2012) but some recent studies demonstrate LC3 lipidation on non-autophagy membranes suggest that this might not be always the case.

### **1.1.v. LC3 lipidation**

ATG8, a ubiquitin-like protein, was discovered first in yeast *S. cerevisiae* during the process of screening for macroautophagy-related proteins (Tsukada and Ohsumi

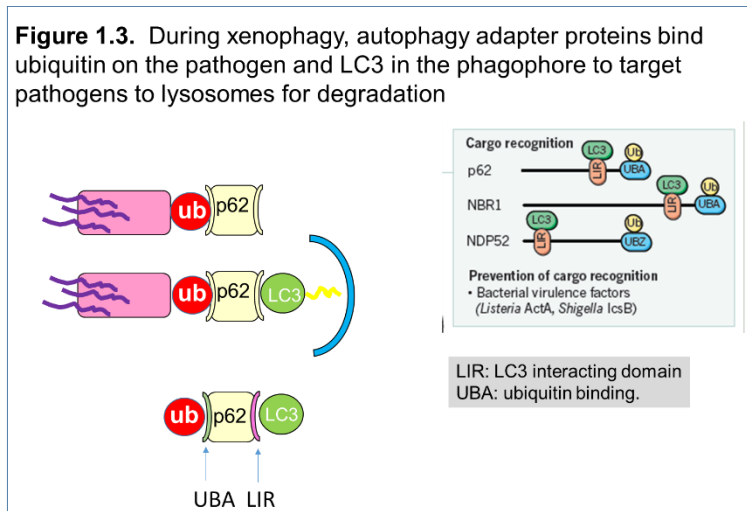
1993). Further sequencing analysis revealed that the LC3 protein family (LC3A,LC3B,LC3B2,LC3C) (Kuznetsov and Gelfand 1987) and GABARAP protein family (GARABAP, GARABAPL1, GARABAPL2) (Wang, Bedford et al. 1999) in human genome were homology yeast Atg8 and act as functional ATG8 gene (Legesse-Miller, Sagiv et al. 1998). Structure studies revealed that ATG8 protein process a core ubiquitin-like fold (Paz, Elazar et al. 2000). However, ubiquitin usually binds to the target proteins by conjugating its C terminal glycine residues with the latter's lysine residue through isopeptide binding. On the other hand, ATG8 usually conjugates to the amino headgroup of membrane lipid at the site of PE in vivo or both PE and phosphatidylserine in vitro (Ichimura, Kirisako et al. 2000, Sou, Tanida et al. 2006, Hanada, Noda et al. 2007). This process is often referred to as ATG8 or LC3 lipidation.

ATG8 (LC3) lipidation process is similar to ubiquitin conjugation. The c terminus of ATG8 (LC3) is cleaved by ATG4 to expose a glycine residue (Kirisako, Ichimura et al. 2000). With the consumption of ATP, ATG8 (LC3) binds to E1-like ATG7 through a cysteine residue. This binding process transferred ATG8 to ATG3, a E2 like enzyme. ATG3 mediates the attachment of ATG8 (LC3) exposed C-terminal glycine to the headgroup of PE with the presence of ATG12-ATG5-ATG16L1 complex, which greatly accelerates the process and is essential for ATG8 (LC3) lipidation in cell (Mizushima, Noda et al. 1999).

### **1.1.vi. Xenophagy**

Autophagy induced by foreign entities (bacteria, viruses, and other pathogens) is termed xenophagy. Xenophagy was first found when vacuoles containing bacterial such as group A *Streptococcus* and *Mycobacterium tuberculosis* were decorated within LC-3 (Gutierrez, Master et al. 2004, Nakagawa, Amano et al. 2004), and activation of autophagy decreased bacterial proliferation (Sharma, Verma et al. 2018). So how does xenophagy recognize intracellular bacteria? Some studies revealed that cytosolic bacteria are coated by ubiquitin chains (Figure 1.3) through the action of E3

ubiquitin ligase and then recognized by a group of adaptor molecules, including NDP52, p62, optineurin (OPTN), and TAX1BP (Watson, Bell et al. 2015, Herhaus and Dikic 2018, Samie, Lim et al. 2018). Those adaptor molecules serve as bridges between the coated pathogen and the nascent autophagosomes. All adaptors process



two common regions, an LC3 interacting region (LIR) to interact with LC3-II decorating autophagosomes and a ubiquitin-binding domain (Behrends and Fulda 2012, Xu, Yang et al. 2015). In addition,

those adaptors represent sequestosome-1-like receptors, a new type of PRRs, and play a role in innate immunity pathways (Deretic, Saitoh et al. 2013). Some intracellular bacteria reside in bacteria-containing vacuoles. The membrane of these vacuoles, either integrity or damaged, can bind to adaptors and recruit autophagic machinery to degrade the pathogens (Fujita, Morita et al. 2013), but the actual mechanism is little to be known. It was not until a recent study revealed that the vacuole ATPase (V-ATPase) plays a role in the recruitment of autophagic machinery to the vacuoles (Xu, Zhou et al. 2019).

### 1.1.vii. Non-canonical autophagy and LC3 associated phagocytosis/endocytosis.

During autophagy, LC3 is recruited to the phagophore to enhance the fusion of the autophagosome with lysosomes to ensure degradation of autophagy cargos (Figure 1.2 [5]). Interestingly, recent studies have revealed that the recruitment of LC3 to endosomes and phagosomes can increase the delivery of extracellular materials to lysosomes for degradation. During this process, lipidated LC3II is recruited to endo-

lysosome compartments such as phagosomes, endosomes, macropinosomes and lysosomes and this non-canonical pathway is referred to as LC3 associated phagocytosis (LAP) or LC3 associated endocytosis (LANDO)(Heckmann, Teubner et al. 2019). Both phagocytosis and endocytosis are processes whereby components of the plasma membrane, as well as particles (including pathogens), are internalized by cells through the invagination of the plasma membrane and the scission of membrane vesicles or vacuoles (Cossart and Helenius 2014). The main difference between them is the size of the particle. Phagocytosis is defined as the internalization of particles bigger than 0.5 $\mu$ m in size and endocytosis is generally reserved for internalization of small molecules and objects (Schille, Crauwels et al. 2018). In the bacterial pathogenesis field, phagocytosis is reserved for internalization of bacteria by professional phagocytes (Swanson, Johnson et al. 1999), such as macrophages, dendritic cells (DCs) and polymorphonuclear leucocytes whereas the uptake of bacteria into nonprofessional phagocytes is called internalization or bacterial-induced phagocytosis. Therefore, we will mainly discuss LAP in the context of professional and non-professional phagocytes (Henry, Hoppe et al. 2004, Zhang, Hoppe et al. 2010).

Both LAP and xenophagy are characterized by the lipidation of PE-conjugated LC3 (LC3-II) on pathogen-containing compartments and they share the same ubiquitin-like ATG conjugation system, which involves ATG3, ATG4, ATG5, ATG7, ATG10 ATG12 and ATG16L1. ATG12 is activated by ATG7 and transforms to ATG10, then binds to ATG5 to form a precursor for autophagosomes. LC3 is essential for the formation of autophagosomes. ProLC3 is converted to cytosolic LC3 (LC3-I), exposing a carboxyl-terminal Gly. LC3-I is also activated by ATG7 and transferred to a membrane bound form, LC3-II (Tanida, Ueno et al. 2004). So how is LAP/LANDO different from xenophagy? There is a molecular distinction between them, the major difference is shown in Figure 1.4 (Upadhyay and Philips 2019).

LAP is triggered by the activation of specific plasma membrane receptors, including PRRs, such as TLR-1/2/4/9, Dectin-1/2 and immunoglobulin Fc receptors, as well as phosphatidylserine detecting receptors (TIM-4) (Martinez, Almendinger et al. 2011, Henault, Martinez et al. 2012, Ma, Becker et al. 2012). LAP begins with the engulfment of cargo by receptor-mediated phagocytosis whereas autophagy begins with the formation of a double-membrane phagophore and under the control an initiation complex, which is composed of kinase ULK1, FIP200, ATG13 and ATG101. In contrast, LAP does not rely on the ULK1 kinase complex. In addition, mTOR, an autophagy inhibitor, does not play a role in LAP (Martinez, Almendinger et al. 2011). In contrast to the double-membraned autophagosome, LAP is characterized by a single membrane phagosome (Heckmann and Green 2019).

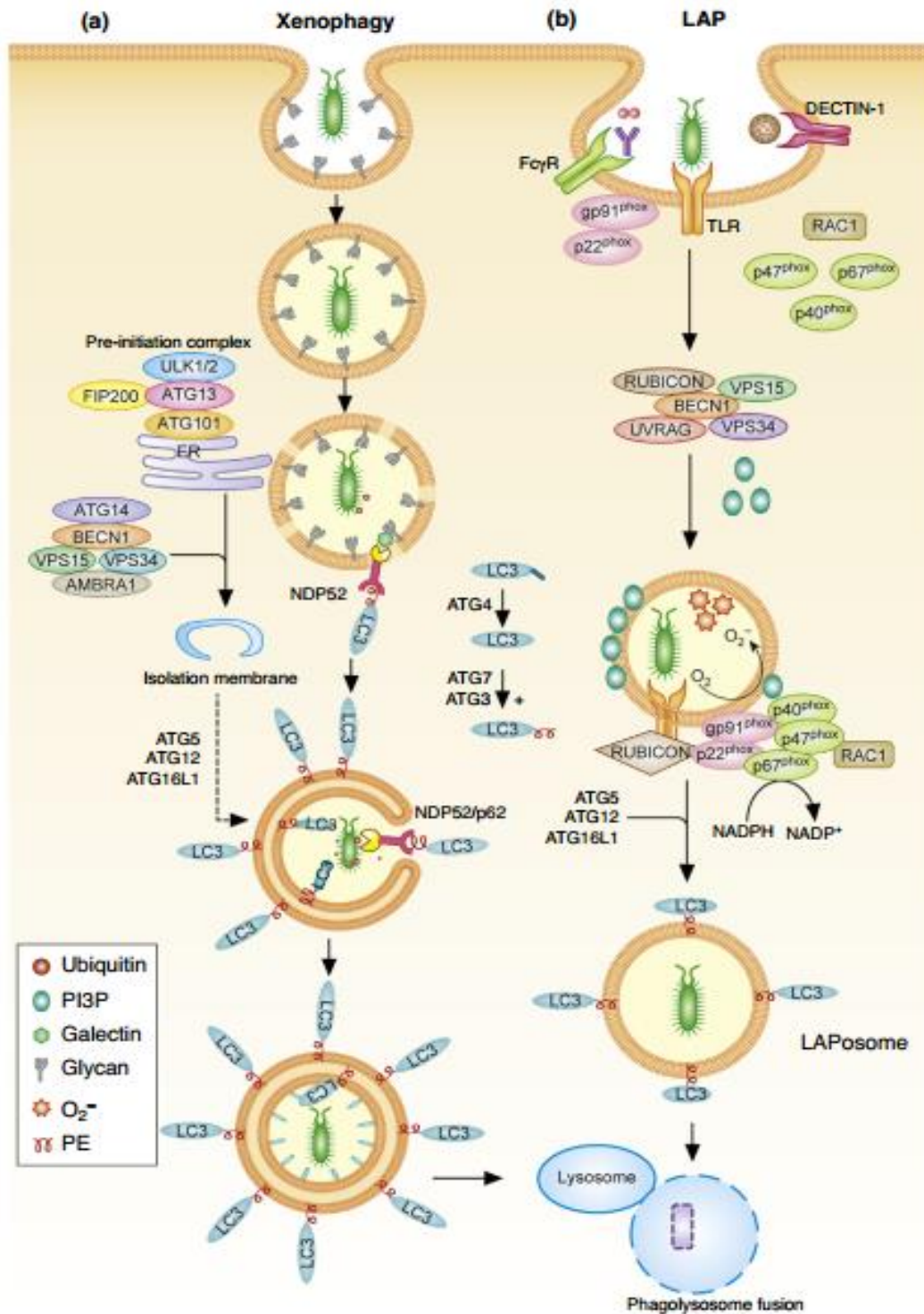


Figure 1.4 Xenophagy and LC-3 associated phagocytosis.

(a) Xenophagy is a form of canonical autophagy which selectively captures microbes in an autophagosome. Invading microbes disrupt the vacuolar membrane and gained access to the cytosol. Pathogenic antigens and damaged membranes are ubiquitinated by E3 ubiquitin ligase.

p62 and NDP52 bind ubiquitinated cargo, then autophagy machinery recruit LC-3 and link cargo to the autophagosomal membranes. Damaged vacuole membrane exposes luminal glycans, which are recognized by galectins and bind NDP52. ULK1 binds with ATG13, ATG101 and FIP200 to form ULK1 pre-initiation complex. VPS34 binds with ATG14L, BECLN1 and VPS15 to form PI3K complex, which is transformed to PI3P complex. PI3P complex provides binding sites for ATG5-ATG12-ATG16L1 which recruit LC3 to the autophagosome membrane. Thus, autophagy machinery targets cytosolic microbes or damaged vacuoles to LC-3 decorated double-membrane compartments. Then LC-3 promotes the fusion of the autophagosome with lysosome for degradation of sequestered microbes.

(b) LC-3 associated phagocytosis (LAP) LAP is usually triggered by receptors on the plasma membrane, such as TLRs, DECTIN-1, FcγRs, and TIM4. The receptor engagement recruits NADPH oxidase complex on phagosomes or endosomes, which is stabilized by RUBICON. RUBICON is also a key part of the PI3K complex which generates PI3P. PI3P binds to NADPH oxidase and generates ROS. ROS is required for the recruitment of LC-3 machinery to phagosomes. LC-3 is lipidated on a single membrane structure, referred to as LAPosomes and promotes its fusion with lysosomes for degradation. Figure is taken from (Upadhyay and Philips 2019).

The second stage in both autophagy and LAP is characterized by the PI3k complex which is responsible for producing PI3P. LAP and autophagy share a similar PI3K complex but vary in some of the ingredients. The PI3K complex involved in LAP includes RUBCN and UVRAG but not ATG14L. RUBICON, a RUN-domain-containing protein, is required for the generation of PI3P and acts as a molecular switch that promotes LAP while it shows an inhibitory effect in canonical autophagy (Matsunaga, Saitoh et al. 2009). The absence of RUBICON leads to a decrease in the stability of NADPH oxidase-2 (NOX2) complex on the membrane of the phagosome, which results in a decrease in ROS activity. ROS is not involved in xenophagy but is crucial for LAP because of its role in lipidation and maintenance of LC3. NOX2 is a multiprotein complex associated with phagosome membranes and can bind PI3P (Bedard and Krause 2007). NOX2 is responsible for the generation of ROS and can regulate the pH of the phagosome. A third stage is characterized by the conjugation systems involved in the processing and ligation of LC3 to either the phagophore (autophagy) or phagosome (LAP). Most of the processes do not show a difference in this step except for WIPI proteins, which cooperate with the ATG16L1 complex and determine the site of LC3 lipidation, which is dispensable in LAP (Romao, Gasser et al. 2013, Romao and Munz 2014). This left a gap between PI3K and LC3 lipidation machinery, leaving it an open question in LAP. In addition, as will be described in detail below, the WD-40 repeats in the C-terminal of ATG16L1 are essential for LAP but dispensable for autophagy (Fletcher, Ulferts et al. 2018). Another difference between xenophagy and LAP is the speed of LC3 lipidation. Some recent studies demonstrate that LC3 lipidation occurs rapidly upon the fully sealment of phagosome membrane and remains attached (Sanjuan, Dillon et al. 2007, Martinez, Malireddi et al. 2015), while the LC3 conjugates elongately on phagophore membrane during the process of canonical autophagy (Kabeya, Mizushima et al. 2004), which is reversible and ATG16L1 complex is released from the autophagosome soon after its formation (Mizushima, Kuma et al. 2003).

### **1.1.viii. Role played by non-canonical autophagy and LC3 associated phagocytosis/endocytosis in immune regulation and disease.**

The primary goal of phagocytosis is to degrade the extracellular cargo, such as pathogens. Therefore, the role of LAP in such degradation can help to control infection. Many studies using cell lines ‘*in Vitro*’ demonstrate that LAP can control the infection of fungus (*Candida albicans* and *Aspergillus fumigatus*), bacteria (*Legionella dumoffii*, *Listeria monocytogenes* and *Yersinia pseudotuberculosis*) and parasites (*Toxoplasma gondii*, *Plasmodium spec* and *Leishmania major*) (Schille, Crauwels et al. 2018). In most cases, the pathogens are engulfed by LAP and result in the clearance of the pathogen, and defects in LAP can result in immunological defects. For example, LAP knockout mice fail to efficiently clear *Aspergillus fumigatus* (Sprenkeler, Gresnigt et al. 2016). Phagocytosis can also have an immunoinhibitory effect, depending on the content of the cargo. For instance, LAP-induced degradation of outer membrane vesicles in DCs regulates Treg cells to express IL-10 that suppresses intestinal inflammation during inflammatory bowel disease (Chu, Khosravi et al. 2016).

LAP not only is connected to pathogen reorganization and clearance in the innate immune response but is also shown in that LAP activation promotes antigen presentation via presenting major histocompatibility complex (MHC) class II molecules to CD4<sup>+</sup> T cells. LAP accelerates phagosome fusing to lysosomes and stabilizes antigen levels, which results in prolonged MHC class II antigen presentation (Romao, Gasser et al. 2013). LAP activation also promotes MHC class II recruitment to phagosomes and sustains antigen presentation (Ligeon, Loi et al. 2018).

Macrophages play an important role in the elimination of apoptotic cells, a process known as efferocytosis, which is important in maintaining homeostasis. This process does not normally induce an immune response and is regarded as ‘immunological

silence' because of the inhibition of pro-inflammatory cytokines, such as IL-6, IL-18 (Xiao, Freire-de-Lima et al. 2008, Martin, Peters et al. 2014). LAP reduces immune responses to apoptotic bodies by delivering them to lysosomes for degradation (Martinez et al). Thus, apoptotic bodies accumulation in the tissues and phagocytic cells of LAP knockout mice generated by inactivation RUBICON and they develop an autoimmune disease similar to systemic lupus erythematosus (Martinez et al ) (Munoz, Lauber et al. 2010). Some recent studies also revealed that LAP protects against other forms of autoimmunity in mice and may oppose immune responses to cancers (Cunha, Yang et al. 2018). LAP may also play a role in cellular metabolism by providing the phagocytic cells with an energy substrate from nutrients, such as sugars, lipids, amino acids and nucleotides recycled from extracellular materials (Heckmann and Green 2019).

### **1.1.ix. Adaptive immune response**

Acquired or adaptive immune responses can recognize and develop responses against specific antigens. In contrast to innate, adaptive immunity is antigen-specific and can recognize millions of different antigen molecules. A connection between the innate and adaptive immune response is provided by DCs, which are relevant APCs. PAMPs stimulate DCs and promote their maturation. Matured DCs present antigens to T lymphocytes via MHC molecules and also activated naive T cells with B7 family ligands. T lymphocytes are activated after MHC molecules are presented by a T cell receptor (TCR) and classified either Th (CD4<sup>+</sup> T helper) cells or Tc (CD8<sup>+</sup> cytotoxic) cells, which is determined by the class of MHC presented (MHC-II for Th and MHC I for Tc). Then Th cells proliferate B lymphocytes to plasma cells and help them to generate antibodies against the antigen, while Tc cells recognize the antigen to kill it. After the infection, a small portion of B cells are transferred to memory B cells which persist independently of the antigen and can be activated during the second wave of infection by the same pathogen (Bonilla and Oettgen 2010).

## **1.2 Generation of mice lacking non-canonical autophagy pathways such as LAP and LANDO.**

Recruitment of LC3 to endolysosome compartments requires the ATG16L1:ATG5-ATG12 complex to conjugate LC3 to PE in the endo-lysosome membrane. Knock out of Atg16L1, Atg5, ATG3, ATG7 and Atg12 in mice results in neonatal lethality because they are unable to adapt to the starvation that follows a loss of placental nutrition (Kuma, Komatsu et al. 2017). Mice with tissue-specific loss of autophagy survive, but the tissues lacking autophagy show signs of inflammation and tissue damage because they accumulate ubiquitin-positive inclusions containing protein aggregates (Kuma, Komatsu et al. 2017). Mice lacking Atg5, Atg12 or Atg16L1 in specific tissues can be generated to study LAP but the simultaneous loss of autophagy will make it impossible to determine if and loss of function results from loss of autophagy, or LAP, or both. An alternative approach to studying LAP ‘*in vivo*’ has focused on the inactivation of RUBICON (Martinez, Malireddi et al. 2015, Martinez, Cunha et al. 2016). RUBICON is upstream of LC3 recruitment to endolysosome compartments (Figure 1.4) and RUBICON<sup>-/-</sup> myeloid cells are LAP-deficient and show defects in clearance of fungi, bacteria as well as dying and apoptotic cells. Unfortunately, as described above, the RUBICON<sup>-/-</sup> mice develop an autoimmune systemic lupus erythematosus (SLE) (Martinez, Cunha et al. 2016, Heckmann, Boada-Romero et al. 2017) and have elevated levels of inflammatory cytokines in serum making them unsuitable for studies of infection ‘*in vivo*’. The text below describes how an understanding of the roles played by different domains of ATG16L1 during autophagy and LAP provided a way to generate mice that retained autophagy but had a specific defect in non-canonical autophagy/LAP.

### **1.2.i. Domains of ATG16L1 important for autophagy and LAP.**

ATG16L1 is a 623 amino acid (aa) protein that acts as a part of the E3-ligase ATG12-ATG5-ATG16L1 complex (Fujita, Itoh et al. 2008). This complex conjugates PE to

LC3 and binds to membranes directly to determine the sites of the conjugation (Romanov, Walczak et al. 2012). Mammalian ATG16L1 is comprised of three domains (figure 1.5, taken from (Lystad, Carlsson et al. 2019)): the N-terminal ATG5 binding domain, central coiled-coiled domain joined by a linker region to a C-terminal WD domain. The ATG5 binding domain helps ATG16L1 interact with the ATG5-ATG12 conjugate. The CCD domain is important for oligomerization and acts as binding sites for various proteins involved in autophagy (Gammoh, Florey et al. 2013, Dooley, Razi et al. 2014) and the linker region has a site for FIP200 binding (Gammoh, Florey et al. 2013). A natural variant of ATG16L1, known as T300A, carries a mutation located in the linker region and provides cleavage sites for caspase 3 and caspase 7 (Hampe, Franke et al. 2007, Boada-Romero, Serramito-Gomez et al. 2016). This mutation caused a cleavage in aa 296-299 and separates the WD domain from the rest of the protein when caspase 3 is activated and has been proven to be a risk factor for Crohn's disease (Lassen, Kuballa et al. 2014, Murthy, Li et al. 2014).

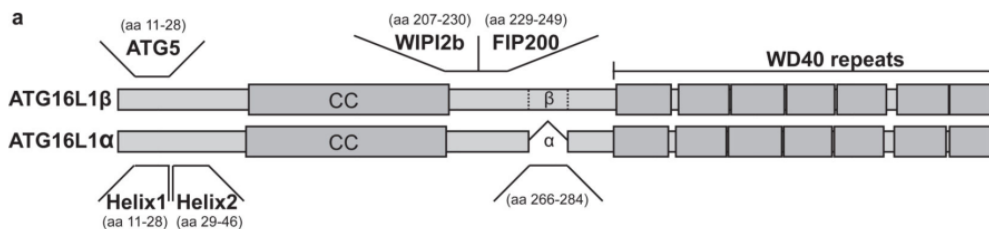


**Figure 1.5 an overview of ATG16L1's isoforms, domains and protein interaction sites.** The first 11-28 aa are amphipathic  $\alpha$ -helix which is responsible for ATG5 interaction. aa 28-44 are also  $\alpha$ -helix and are important for binding with both ATG5 and liposomes. The second membrane-binding domain is located in the region of aa 266-284. This region is not essential for LC3 lipidation induced by starvation and is missing in the  $\alpha$  isoform of ATG16L1. WIPI2b and FIP200 binds at 207-230aa and 229-249aa. A WD40 domain, consist of 7 WD repeats, is located in the C-terminal of ATG16L1. This domain is not required for canonical autophagy, but essential for LC3 lipidation on single membranes (LAP). Figure from (Lystad, Carlsson et al. 2019).

Experiments by Oliver Florey and colleagues studied recruitment of LC3 to endosomes and lysosomes subjected to osmotic stress by lysosomotropic agents as a model for non-canonical autophagy/LC3-associated phagocytosis (Fletcher, Ulferts et al. 2018). They showed that in contrast to autophagy, the PI3 kinase activity of VPS34 and recruitment of WIPI to membranes were not required for LAP. Reconstitution experiments using *ATG16L1*<sup>-/-</sup> HCT116 cells showed that *ATG16L1* lacking the WD domain were able to recruit LC3 to autophagosomes during autophagy, but were not able to recruit LC3 to endosomes swollen by lysosomotropic agents such as monensin. Site-directed mutation guided by a bioinformatic approach to identify amino acids likely to be involved in protein-protein interactions within the WD domain showed that N453, F467 and K490 are important for LAP (Fletcher, Ulferts et al. 2018).

Parallel studies by Lystad et al (2019) used liposome pull-down assays to identify membrane binding sites in *ATG16L1*. Two membrane-binding regions were identified, the first domain was located on 11-44 aa of the N-terminus. The first 11-28 aa are amphipathic  $\alpha$ -helix which is responsible for ATG5 interaction, aa 28-44 form an  $\alpha$ -helix and are also important for binding with both ATG5 and liposomes (Otomo, Metlagel et al. 2013, Kim, Hong et al. 2015). The second membrane-binding domain was located in the region of aa 266-319 (Lystad, Carlsson et al. 2019). This region was not essential for LC3 lipidation during autophagy induced by starvation. The role of both binding domains in LAP was examined by following LC3 lipidation of zymosan-induced phagosomes in *ATG16L1* KO RAW264.7 cells (Lystad, Carlsson et al. 2019). The N-terminal membrane binding sites (1-44 aa) were confirmed to be essential for both autophagy and LAP while the C-terminal membrane binding sites (266-319 aa) and the WD domain were essential for LAP but not autophagy.

## 1.2.ii. Generation of mice defective in non-canonical autophagy/LAP.

The studies above showed that the WD domain of ATG16L1 was required for LAP but not autophagy. This prompted our lab to generate mice lacking the WD domain of ATG16L1 to study the role played by non-canonical autophagy/LAP in vivo (figure 1.6). A stop codon was introduced at position E230 of Atg16L1 to preserve the ATG5

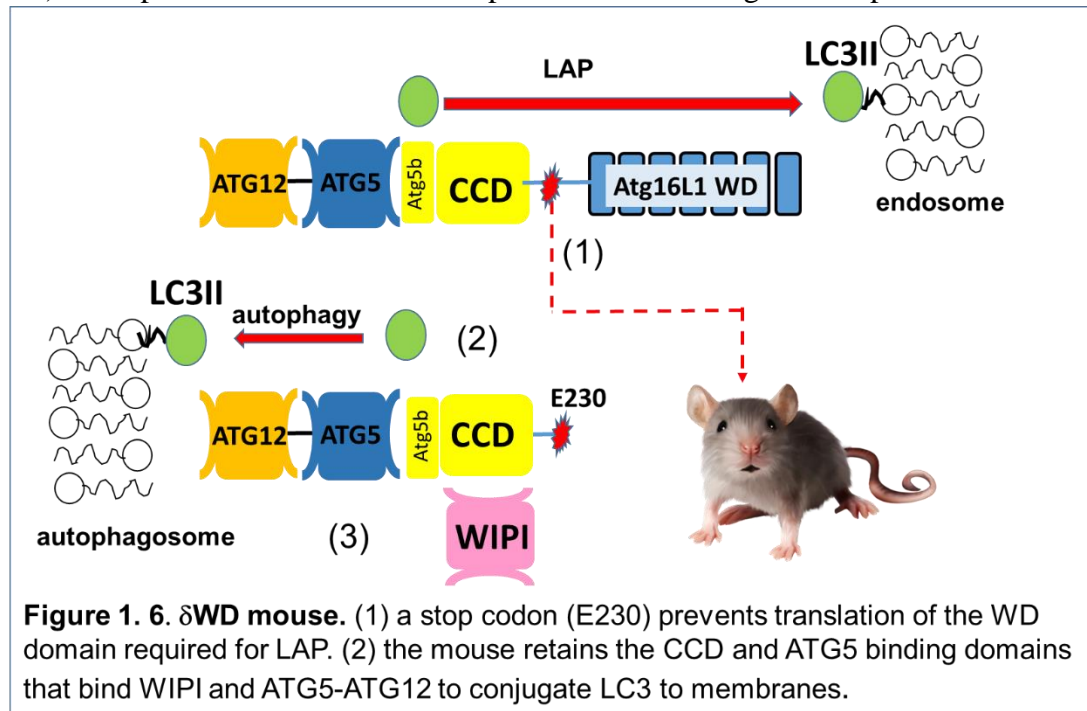


**Figure 1. 6.  $\delta$ WD mouse.** (1) a stop codon (E230) prevents translation of the WD domain required for LAP. (2) the mouse retains the CCD and ATG5 binding domains that bind WIPI and ATG5-ATG12 to conjugate LC3 to membranes.

binding domain and CCD WIPI2b binding site for autophagy and remove residues in the WD domain required for LAP. The mice were named  $\delta$ WD mice due to the knockout of the WD domain. They do however lack both the WD and the linker domains of ATG16L1.

Unlike  $ATG16L1^{-/-}$  and  $RUBICON^{-/-}$  mice, the  $\delta$ WD mice showed a similar growth rate and tissue homeostasis compared to the littermate controls, which makes them potential models for infection studies (Rai, Arasteh et al. 2019). Interestingly, during the characterization of the mice, gel filtration was performed on brain lysates. The results indicated that the binding of WIPI2b to Atg16L1 was different in the brain compared to the liver. This might be due to the  $\gamma$  isoform of Atg16L1, which is the major form of Atg16L1 in the mouse brain. Atg16L1 $\gamma$  expresses 2 more exons, exon 8 (57bp)

and 9 (48bp). Those 2 exons are missing or partly missing from the Atg16L1 $\alpha$  (exon 9 missing) and Atg16L1 $\beta$  (both missing), which are found as a major and minor form of Atg16L1 in the liver (Mizushima, Kuma et al. 2003). This might provide the possibility of different binding strategies in the brain compared with other tissues.

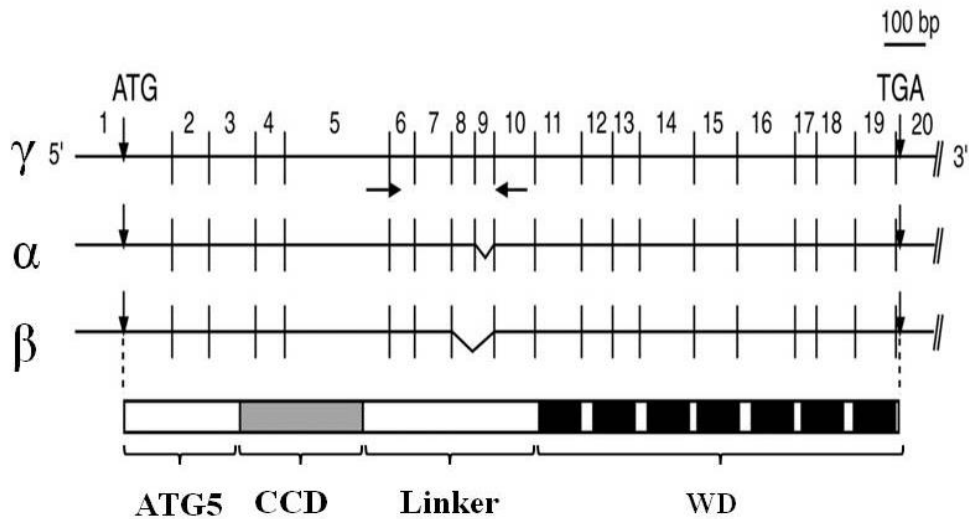


**Figure 1.7** Alternative splicing of mRNA of  $\alpha$ ,  $\beta$  and  $\gamma$  isoform of Atg16L1. The 20 exons of Atg16L1 are indicated by numbers above the line. The alternative spliced exons in  $\alpha$  and  $\beta$  are indicated as broken lines. exon 9 is missing in  $\alpha$  isoform of Atg16L1 while both exon 8 and 9 are missing in the  $\beta$  isoform. Corresponding domains are shown below the line as boxes of different patterns. Figure from (Mizushima, Kuma et al. 2003).

### **1.3.i. Role played by ATG16L1 during gut homeostasis and inflammation.**

The identification of the T300A mutation in ATG16L1 as a risk allele for Crohn's disease stimulated a great deal of interest in the function of ATG16L1 in the gut. The research has shown that ATG16L1 is involved in maintaining homeostasis of gut epithelium (Matsuzawa-Ishimoto, Shono et al. 2017, Lassen and Xavier 2018), especially in Paneth cells, which secrete antimicrobial peptides and proteins (Cadwell, Liu et al. 2008, Cadwell, Patel et al. 2009). Paneth cells are key mediators of host-microbe interactions, including homeostatic balance with colonizing microbiota and innate immune protection from enteric pathogens (Clevers and Bevins 2013). In addition, ATG16L1 in myeloid cells, particularly macrophages plays an important role in maintaining intestinal homeostasis via facilitating host-bacteria interactions including ROS production, MHC class II antigen presentation and lysosome trafficking (Zhang, Zheng et al. 2017). Studies have revealed that ATG16L1 in the gut epithelium plays an important role in preventing Salmonella infection (Conway, Kuballa et al. 2013). Most of the studies were focused on full-length ATG16L1, only a few of them were focused on the WD domain (Serramito-Gomez, Boada-Romero et al. 2019, Slowicka, Serramito-Gomez et al. 2019). Interestingly, the T300A variant of ATG16L1 cleavage site generates a cleavage site for Caspase 3 and Caspase 7. This variant is thought to cause a defect in autophagy and reduced anti-bacterial defense (Lassen, Kuballa et al. 2014, Salem, Nielsen et al. 2015).

## 1.4 *Salmonella* and virulence factors

### 1.4.i. Basic introduction of *Salmonella*

The *genus* of *Salmonella* is a group of Gram-negative bacteria named after Daniel Salmon, an American veterinary pathologist, whose research assistant, Theobald Smith, isolated the first strain of *Salmonella* (Nutrition 2008). *Salmonella*, intracellular, rod-shaped, non-spore-forming bacterial pathogens with a diameter of 0.7-1.5µm and a length of 2-5µm. which is motile and has a peritrichous flagellum (Jantsch, Chikkaballi et al. 2011). The genus belongs to the family of Enterobacteriaceae and contains two species, *Salmonella enterica*. and *Salmonella bongori*. *Salmonella bongori*. mainly infects cold-blooded animals, mostly reptiles and was first isolated from a lizard in 1966 (Le Minor, Chamoiseau et al. 1969). *Salmonella enterica*. can be further divided into seven subspecies, I, II, IIIa, IIIb, IV, VI, VII, and includes more than 2600 serotypes or serovars (Brenner, Villar et al. 2000, Tindall, Grimont et al. 2005, Agbaje, Begum et al. 2011, Ryan, O'Dwyer et al. 2017). The serovars were defined based on somatic lipopolysaccharide O and flagellar H antigen (Okoro, Kingsley et al. 2012). Among those subspecies, *Salmonella enterica* subtype I, is the most important and includes most of the pathogenic serovars which can infect a wide range of hosts, mostly mammals and birds, while subtypes II, IIIa, IIIb, IV, VI, VII are mostly reptile associated and can rarely transmit to human (Murray PR 2009, Baumler and Fang 2013). Within those serovars, some are highly host-adapted, such as *S. enterica* serotype Typhi (*S.Typhi*), which only infects human and non-human primates (Edsall, Gaines et al. 1960). In contrast, *Salmonella enterica* serovar Typhimurium (*S.Typhimurium*) can infect a wide range of hosts, including humans, livestock, domestic fowl, rodents, and birds (Rabsch, Andrews et al. 2002). *Salmonella enterica* can cause very different diseases and induce a different immune response in humans and other mammals (de Jong, Parry et al. 2012, Baumler and Fang 2013), and can be classified into typhoidal and non-typhoidal serovars (Feasey, Dougan et al. 2012, Maclennan 2014).

#### **1.4.ii. Non-typhoidal *Salmonella* (NTS)**

Non-typhoidal *Salmonella* (NTS) serotypes, such as *S.Typhimurium* and *Salmonella enterica serovar Enteritidis*, have a large host range and cause gastroenteritis, which is a diarrheal disease that usually limits the infection in intestine and mesenteric lymph nodes, in humans (Santos, Zhang et al. 2001). NTS salmonellosis occur worldwide in both developing and developed countries (Graham 2010, Majowicz, Musto et al. 2010, McCusker, Hokamp et al. 2014, Paine, Thornley et al. 2014, Lofstrom, Hintzmann et al. 2015, Van Cauteren, De Valk et al. 2015, Freidl, Schoss et al. 2018). There are about 94 million cases of NTS gastroenteritis each year and cause about 155,000 fatalities globally (Majowicz, Musto et al. 2010). Unlike global morbidity, the fatal cases are mostly restricted to developing countries, due to their poor health service and financial support (Majowicz, Musto et al. 2010). NTS infection is usually caused by engaging contaminated animal-derived food products, such as beef, pork, fish, milk and eggs (Threlfall, Ward et al. 1998, Nicolay, Thornton et al. 2011, Friesema, Schimmer et al. 2012, Friesema, de Jong et al. 2014, Fournier, Knox et al. 2015, Schroeder, Harries et al. 2016, Freidl, Schoss et al. 2018), but some previous studies also confirmed close contact with pets, including canines, felines, rodents, amphibians and reptiles can also be a reason of infection (Hohmann 2001, Mermin, Hutwagner et al. 2004, Braden 2006, Haeusler and Curtis 2013, Imanishi, Rotstein et al. 2014). Contaminated plants and vegetables can be another source of infection. Bean sprouts, tomatoes, fruits, peanuts, and spinach have all been associated with recent outbreaks (Centers for Disease and Prevention 2008, Berger, Shaw et al. 2009, Berger, Sodha et al. 2010, Barton Behravesh, Mody et al. 2011, Cavallaro, Date et al. 2011, Jackson, Griffin et al. 2013). There is also transmission from person to person (Mason 1909, Marr 1999, Hohmann 2001, Mermin, Hutwagner et al. 2004, Ortiz, Siegal et al. 2014). Patients infected with NTS normally show the common symptoms of watery diarrhea, nausea, vomiting, abdominal pain, and fever

after only 6-12 hours of infection (McGovern and Slavutin 1979, Glynn and Palmer 1992). Those symptoms will last no more than 10 days and the patients will recover without any sequelae because the infection is limited in the intestine (Glynn and Palmer 1992).

#### **1.4.iii. Invasive Non-typhoidal *Salmonella* (iNTS)**

Although NTS usually cause gastroenteritis in human, in some rare cases, *Salmonella* can break out of the intestine and invade the blood circulation and cause bacteremia and focal systemic disease, those bacteria are referred as invasive Non-typhoidal *Salmonella* (iNTS) (Mandal and Brennan 1988, Garcia Urena, Velasco Garcia et al. 1999). A few *Salmonella* serovars, such as Typhimurium, Dublin, Choleraesuis, have more ability or chance to cause this kind of disease than other serovars while the mechanism is still not fully understood (Wilkins and Roberts 1988, Rodriguez, de Diego et al. 1998, Haeusler and Curtis 2013). In Africa, iNTS is the major cause of bacteremia in both children and adults, especially HIV patients. The morbidity rate in African children is around 0.3% and can rise to 2-8% in adult HIV patients due to their deficiency in the immune system (Feasey, Dougan et al. 2012). During the infection, patients can suffer from hepatosplenomegaly, respiratory complications and most important, high fever. But unlike normal NTS infections, intestinal symptoms, such as diarrhea, usually don't occur (Feasey, Dougan et al. 2012). The mortality rate can go up to 20-25%, which makes it a major threat to public health (MacLennan 2014). Some recent studies attempt to uncover the reason for the high morbidity rate of iNTS infection in HIV patients. A few reports claimed that IL-12/IL-23 deficiency patients are highly susceptible to NTS infection and have a high chance of iNTS infection (MacLennan, Fieschi et al. 2004, van de Vosse and Ottenhoff 2006), but not Typhoidal *Salmonella* infection. This finding supported that an HIV-induced IL-12/IL23 deficiency may cause a high chance of iNTS infection, and IL-12/IL-23 pathway may play a key role in controlling NTS infection, but not in typhoidal *Salmonella* infection.

#### **1.4.iv. Typhoidal *Salmonella*.**

In contrast to NTS's broad host range, there are a few serovars of *S. enterica*, such as Typhi, Sendai, and Paratyphi A, B, or C, that are highly adapted to humans and non-human primates hosts (Meltzer and Schwartz 2010). Those highly adapted pathogens can cause enteric fever, an invasive, systemic, life-threatening disease, in humans (also named typhoid fever or paratyphoid fever when caused by *S. Typhi* or *S. Paratyphi*) (Buckle, Walker et al. 2012). Typhoidal *Salmonella* is responsible for more than 27 million cases and results in more than 200,000 death annually in the world, mostly in developing countries. This is due to the lack of clean water and adequate sanitation in those regions (Crump, Luby et al. 2004), which facilitate the spread of this pathogen by the fecal-oral route. In recent years, the serovar Paratyphi A has caused about 50% of total enteric fever cases worldwide, making it an emerging concern to public health (Ochiai, Wang et al. 2005, Meltzer and Schwartz 2010). The average incubation period of enteric fever is about 14 days, and the symptoms could last up to 21 days (Olsen, Bleasdale et al. 2003, Patel, Armstrong et al. 2010, Wangdi, Winter et al. 2012). Patients all show a high fever (39-40°C), other frequent symptoms are similar to those induced by iNTS, including abdominal pain, chill, headache, dry cough, nausea, anorexia, hepatosplenomegaly, rash, and diarrhea (Stuart and Pullen 1946).

A lot of studies in the past decade showed that both Typhoidal *Salmonella* and NTS patients can act as a chronic carrier even when they recovered and don't show any symptoms (Aserkoff and Bennett 1969, Hohmann 2001, Parry, Hien et al. 2002). This allows the bacteria to transmit between humans by the oral-fecal route. A few reports even described a recovered patient caused up to 200 human infections in early 1900 (Mortimer 1999, Van Detta 1999). Some suspected sites for *S. Typhi* to stay long-term in patients are the gallbladder and gallstones. Those sites can help the bacteria to hide from antibiotics and the host immune system and play an important role in the long-

term chronic carrier (Levine, Black et al. 1982).

#### **1.4.v. Barriers to salmonella infection.**

Both Typhoidal *Salmonella* and NTS infect humans via the epithelium of the small intestine (Liu, Ezaki et al. 1988). NTS infection in non-immunodeficient patients can induce a high inflammatory response and massive numbers of neutrophils that migrate across the small intestinal epithelium. Thus, the infections are usually limited to the ileum and colon (McCormick, Miller et al. 1995). NTS infection can also induce a very strong Th1 response. As a result, a high level of IFN- $\gamma$ , IL-18, IL-10, IL-12, IL-15 and TNF- $\alpha$  can be detected in the serum of the patients (Mizuno, Takada et al. 2003, Stoycheva and Murdjeva 2005). Several chemokines can also be expressed, resulting in the recruitment and activation of macrophages, dendritic cells and neutrophils which migrate to the small intestine, all acting as a unique marker for gastroenteritis (Kraus, Amatya et al. 1999). In contrast, typhoidal serovars only cause a very low inflammatory response in the mucosal surface of intestinal epithelium and break through it to gain access to the underlying lymphoid nodes and infect the residential mononuclear macrophages. *Salmonella* replicates in those phagocytes and quickly spreads into the liver, spleen, bone marrow, and gallbladder and causes systemic disease. Then a secondary infection to the small intestine might occur via bile transport of the enterohepatic cycle (Gordon 2008). The lack of mucosal intestinal inflammatory response and neutrophils migration in the lumen of the small intestine is thought to be the key factor causing the invasion of typhoidal serovars to the deeper gut tissues and promote its dissemination to systemic sites (House, Wain et al. 2001). The immune response to typhoidal serovars is quite complicated as they induce both humoral and cellular immune responses (Sztein 2007). Both CD4<sup>+</sup> and CD8<sup>+</sup> cells from enteric fever patients show strong and specific response to *S.Typhi* antigens. A few other studies revealed the gene expression of peripheral blood mononuclear cells (PBMCs) and level of cytokines in the serum of both vaccinated and infected individuals. Both the gene expression of IFN- $\gamma$  pathway cytokines, such

as IL-6, IL-8 and the level of serum IFN- $\gamma$  were all elevated during the acute phase of typhoid fever (Butler, Ho et al. 1993, Thompson, Dunstan et al. 2009, Sheikh, Khanam et al. 2011). Other research isolated PBMCs from volunteers who were orally vaccinated by an attenuated *S. Typhi* vaccine. The results showed that the PBMCs secreted Th1 cytokines, such as IFN- $\gamma$ , IL-10, TNF- $\alpha$  (Wahid, Salerno-Goncalves et al. 2007). Those results indicated that the immune response from *S. Typhi* is mostly Th-1 related. Compared to the bacteremia and leukopenia related septic shock caused by other Gram-negative bacteria, enteric fever is rarely associated with these symptoms, which indicate that typhoidal *salmonella* induces a different immune response to other Gram-negative counterparts (Pohan 2004, Tsolis, Young et al. 2008, Gal-Mor, Suez et al. 2012). This finding is confirmed by measuring the pyrogenic cytokine level, such as TNF- $\alpha$  and IL-1 $\beta$  in patients' serum. The secretion of TNF- $\alpha$  and IL-1 $\beta$  were suppressed during *S. Typhi* infection (Butler, Bell et al. 1978).

#### **1.4.vi. Animal models.**

Some animal species share the same physiological, behavioral, or other characteristics as humans during infection. Thus, animal models can be developed as important tools to study immunology, infectious disease and host-pathogen interactions (Ericsson, Crim et al. 2013). A few animal models were established to model the NTS-induced gastroenteritis in humans. The most successful model is a non-human primate model established in the 1970s (Kent, Formal et al. 1966, Rout, Formal et al. 1974). The use of non-human primates raises ethical concerns, is very expensive and is genetically complex. In recent years such studies have been limited to co-infection with simian immunodeficiency virus (SIV) to model the iNTS disease, which is common in HIV patients (Raffatellu, Santos et al. 2008). Furthermore, SIV-infected rhesus macaques can be used to test the safety and efficiency of the live *Salmonella* vaccine (Ault, Tennant et al. 2013). Another model for NTS infection is calves. *S. Typhimurium* is a natural pathogen for calves and causes a similar disease and symptoms compared to humans. Some valuable findings concerning host-Salmonella interaction have been

gained from calves (Costa, Paixao et al. 2012) but this model shares the same disadvantages as the non-human primate model (Santos, Zhang et al. 2001).

#### **1.4.vii. Mouse models.**

Mouse models are the most widely used animal model due to their low cost, easy handling, housing and easy access to genetic modification. But the mouse shows typhoid fever-like symptoms during NTS infection rather than mild gastroenteritis seen in humans. This can limit the use of mouse models. Some recent studies revealed that NTS serovars induce inflammation in the gut if they are able to outcompete gut residential microbiota (Stecher, Robbiani et al. 2007, Thiennimitr, Winter et al. 2011). Pretreatment of mice orally by antibiotics, such as streptomycin or kanamycin, before the oral gavage with *S. Typhimurium*, can help *Salmonella* to overcome gut microbiota (Sekirov, Tam et al. 2008). Thus, pretreatment with streptomycin becomes a widely used method to dissect both bacterial- and host-mediated mechanisms involved in NTS-induced intestinal inflammation (Hapfelmeier and Hardt 2005, Sekirov, Tam et al. 2008).

Because *S. Typhi*, *S. Paratyphi*, and *S. Sendai* have a limited host range, mostly adapted to humans, all efforts of establishing an animal model for enteric fever have been proven to be inadequate (Pasetti, Levine et al. 2003). The chimpanzee model is one of the closest to success, but it can only induce an enteric fever when infected with a very high dose ( $10^{11}$  cfu) (Edsall, Gaines et al. 1960). Therefore until recently, most of our understanding of enteric fever come from *S. Typhimurium* infection in mice. *S. Typhimurium* causes a very mild intestinal inflammation and shows typhoidal fever-like symptoms in mice. This model also allows the investigation of chronic *S. Typhi* carriage in humans as the bacteria will also be resident in the gallbladder (Menendez, Arena et al. 2009, Gonzalez-Escobedo, La Perle et al. 2013). Thus, NTS infection in mice provided some insight into typhoidal *Salmonella*

invasion, transmission and dissemination in the host. Although the response to NTS in mice is similar to the response to typhoidal serovars infection in humans (Santos, Zhang et al. 2001), the results derived from this model should be carefully analyzed before coming to a conclusion.

#### **1.4.viii. Genetically modified mice.**

With the rapid development of genetic modification in mice, a few new transgenic mouse models have been developed to study typhoidal *salmonella* infection. Mathur *et al.* discovered that the flagellin of *Salmonella* is recognized by the toll-like receptor (TLR) 11 in the mouse intestine (Mathur, Oh et al. 2012). They generated TLR 11 knockout mice since the TLR11 receptor is absent in humans. Those mice showed a very mild intestinal epithelium innate immune response due to the loss of an ability to recognize the bacteria after oral administration of both *S. Typhi* and *S. Typhimurium*. In the meantime, the bacteria cause a systemic infection, similar to enteric fever (Mathur, Oh et al. 2012, Shi, Cai et al. 2012). Another novel mouse model is the generation of immunodeficient mice via transgenics or radiation. Those mice lack the entire murine immune cells (B, T, antigen-presenting and NK cells) (Shultz, Ishikawa et al. 2007) but can be reconstituted with human CD34<sup>+</sup> hematopoietic stem cells. The cells will differentiate into human Th cells, Tc cells, NK cells, B cells, monocytes and antigen-presenting cells (APCs). In general, those chimeric mice have a humanized immune system and such mice can facilitate *S. Typhi* infection and its dissemination to the liver, spleen and gallbladder and make the observation of long-term persistence possible (Song, Willinger et al. 2010, Firoz Mian, Pek et al. 2011). These models suggest that the human immune system is essential for *S. Typhi* infection in mice, giving us a hint to establish new mice models to study typhoidal *Salmonella* infection.

#### **1.4.ix. The genome of Salmonella ,**

*S. Typhi* has a genome of about 4,8000,000 bp in length. The whole-genome encodes

more than 4,400 genes, of which about 200 genes (5%) are inactivated or disrupted (McClelland, Sanderson et al. 2004). These functionally disrupted genes are considered to be the result of a relatively short period of approximately 5,000 years of bacterial evolution (Roumagnac, Weill et al. 2006), (Parkhill, Dougan et al. 2001). Most of these silenced genes were confirmed in many *S. Typhi*, such as CT18 and Ty2 (Deng, Liou et al. 2003), and can also be found in *S. Paratyphi A* (McClelland, Sanderson et al. 2004, Holt, Thomson et al. 2009), but in contrast, most of them remain fully functional in *S. Typhimurium* (McClelland, Sanderson et al. 2001). These findings indicate that the evolution in *S. Typhi* and *S. Paratyphi A* is mainly reductive evolution involving loss of function during adaptation to human hosts (Dagan, Blehman et al. 2006). On the other hand, the whole genome length of *S. Typhimurium* is a little longer than those of *S. Typhi*, mostly ranging from 4,850,000 to 4,880,000 bp, (LT2, 4,857,432 bp; SL1344 4,878,012, bp; and ATCC 14028, 4,870,265 bp) (McClelland, Sanderson et al. 2001, Jarvik, Smillie et al. 2010, Kroger, Dillon et al. 2012). *S. Typhimurium* has far fewer pseudogenes compared to *S. Typhi*, about 1% of the whole genome is pseudogenes, 54 in SL1344, 38 in LT2 and 60 in ATCC 14028. These pseudogenes usually code proteins of unknown function or a nonspecific nature, and don't include virulence genes or factors (Branchu, Bawn et al. 2018).

#### **1.4.x. Salmonella pathogenic islands (SPIs).**

*Salmonella* pathogenic islands (SPIs) are specific regions that encode virulence-related factors involved in adhesion, invasion, toxin production, etc.) and can be found in the bacteria's chromosomes or plasmids (Foley, Lynne et al. 2008). Compared to other regions of the genome, SPIs are usually found next to a transfer RNA gene and flanked by repeated sequences. SPIs also have some different G+C percentages compared with other regions of the genome (Schmidt and Hensel 2004, Kaur and Jain 2012). In total, 23 SPIs were identified and characterized in *Salmonella*, within those SPIs, SPI 19-22 were only found in some very rare serovars, such as

Dublin and Gallinarium (Blondel, Jimenez et al. 2009). SPI 19-21 are 3 locations that encode the Type VI secretion system (T6SS). SPI-22 is also a T6SS encoding region identified in *S. bongori* (Wang, Zhu et al. 2019). SPI-23 were identified in sevarar Derby. The other SPI encoding genes play an important role in either invasion or intracellular survival. Effectors encoded by SPI-1,4,9,14 and 18 mostly play a role in the invasion of epithelial cells and macrophages, whereas the effectors from SPI-2,3,5,6,7,8,13,16 usually help *Salmonella* to survive and replicate in host cells and inhibit host immune response. Within those SPIs, the *S. Typhimurium* and *S. Typhi* genomes share 11 common SPIs, SPI1-6, 9,11,13 and 16. 6SPIs, SPI-7,8,10,15,17,18 are considered to be only found in *S. Typhi* genomes, not genomes of *S. Typhimurium*. Only SPI-14 is unique to *S. Typhimurium*. Among all the SPIs, the most important ones are SPI-1 and SPI-2, which both encode a type III secretion system (T3SS), which is T3SS1 and T3SS2. Over 40 effectors were identified in T3SS of *S. Typhimurium*, but nearly half of them were absent in *S. Typhi* (Johnson, Mylona et al. 2018). Some of the important effectors encoded by SPI-1 and 2 are listed in Table 1.

#### **1.4.xi. Other important virulence factors.**

Studies reported that *Salmonella* strains possess low copy serotype-specific plasmids (1-2 copies per cell). Within the plasmids, there is a salmonella plasmid virulence (*spv*) locus which encodes some virulence factors that are important for the replication of bacteria in reticuloendothelial tissues, such as the liver and spleen (Rotger and Casadesus 1999). For example, *S. Typhimurium* possesses a 90 kb self-transmissible virulence plasmid (pSLT) harboring an *spv* operon (Ahmer, Tran et al. 1999), which is involved in intramacrophage survival. pSLT also harbors a plasmid-encoded fimbriae (*pef*) operon (Gulig and Doyle 1993, Ahmer, Tran et al. 1999). Fimbriae are protein-like structures on bacteria that mediate interaction with host cells. Both *S. Typhimurium* and *S. Typhi* possess 13 putative fimbrial sequences, 8 of them were shared and 5 rest are sevarar-specific. Little is known about the actual function, condition of expression or roles in virulence for most of the fimbriae due to the very

low expression level by bacteria *in vitro* (Dufresne 2017). Another virulence factor is the flagella, which normally locates on the cell surface of many bacteria and contributes to pathogenicity and mortality. Flagella are usually encoded by *fliC* or *fljB*, which makes up H<sub>1</sub> and H<sub>2</sub> variants of H antigen and were used for serovar classification (Silverman and Simon 1980). Some *Salmonella* serovars display flagellin phase variation on their surface to minimize host immune response, which creates phenotypic heterogeneity of the flagellar antigens (van Asten and van Dijk 2005). However, the actual role and ability of flagella in pathogenesis, motility, adhesion and invasion mostly still remain unclear (van Asten and van Dijk 2005).

**Table 1 Functions of SPI-1/2 effectors**

Effectors	Functions	SPI	Presence in S.Typhi	Key References
SipA	Tight junction disruption; enhances actin filament assembly; SCV trafficking	SPI-1	Yes	(McGourty, Thurston et al. 2012)
SipB	Cholesterol binding of translocon compartment; induction of apoptosis in Macrophages and DCs	SPI-1	Yes	(Myeni, Wang et al. 2013, Knuff and Finlay 2017)
SipC	Translocon component; molecule translocation of mediates effector; promotes actin polymerization	SPI-1	Yes	(Myeni, Wang et al. 2013)
SipD	Translocon compartment	SPI-1	Yes	(Myeni, Wang et al. 2013, Glasgow, Wong et al. 2017)
SopA	Stimulates pro-inflammatory cytokine production	SPI-1	Yes	(Kamanova, Sun et al. 2016)
SopB	Prevents ROS induced apoptosis; enhance RhoG GATPase activity; tight junction disruption; phosphoinositide phosphatase; SCV trafficking	SPI-1	Yes	(Roppenser, Grinstein et al. 2012, Perrett and Zhou 2013, Ruan, Zhang et al. 2016, Garcia-Gil, Galan-Enriquez et al. 2018, Truong, Boddy et al. 2018)
SopD	Intracellular survival; SIF formation and SCV maturation	SPI-1	Yes	(Jennings, Thurston et al. 2017)
SopD2	Inhabits Rab7 activity; block the delivery of endocytic cargo to lysosomes	SPI-2	Yes	(D'Costa, Braun et al. 2015)
SopE	Promotes bacteria invasion and intracellular replication; Induce Caspase-1 activity; disrupt tight junctions; recruit Rab-5 to phagosomes and block <i>Salmonella</i> transport to lysosomes	SPI-1	Yes	(Madan, Krishnamurthy et al. 2008, Muller, Hoffmann et al. 2009, Humphreys, Davidson et al. 2012, Vonaesch,

SopE2	Guanine nucleotide exchange factor for Cdc42; promotes pro-inflammatory signaling and bacteria invasion	SPI-1	Yes	Sellin et al. 2014) (Boyle, Brown et al. 2006, Zhang, Riba et al. 2018)
SopF	Maintain the integrity of the nascent SCV membrane; block Atg16L1 binding to VAMP3 and inhibit xenophagy	SPI-1	Unclear	(Lau, Haeberle et al. 2019, Xu, Zhou et al. 2019)
SptP	Down regulating host membrane ruffling after bacteria entry; tyrosine phosphatase domain acts on ACK; vimentin;	SPI-1	Yes	(Johnson, Byrne et al. 2017)
AvrA	cysteine protease; inhibits NF- $\kappa$ B signaling and inflammation; stabilize tight junction	SPI-1/2	No	(Ye, Petrof et al. 2007, Liao, Petrof et al. 2008)
Slrp	Inhibits the release of IL-1 $\beta$	SPI-1/2	Yes	(Jennings, Thurston et al. 2017)
GogA	Inhibits NF- $\kappa$ B signaling	SPI-2	No	(Sun, Kamanova et al. 2016, Jennings, Esposito et al. 2018)
GogB	Inhibits NF- $\kappa$ B signaling	SPI-2	No	(Sun, Kamanova et al. 2016)
GtgA	Inhibits NF- $\kappa$ B signaling	SPI-2	No	(Sun, Kamanova et al. 2016)
GtgE	Promote replication in macrophages	SPI-1/2	No	(Jennings, Thurston et al. 2017)
PipA	Inhibits NF- $\kappa$ B signaling	SPI-2	Yes	(Jennings, Esposito et al. 2018)
PipB	Targeted to SIF	SPI-2	Yes	(Knodler, Vallance et al. 2003)
PipB2	Resistance to high temperature and PH; involved in kinesin-1 recruitment to SCV	SPI-1/2	Yes	(Knodler, Vallance et al. 2003, Henry, Couillault et al. 2006, Baison-

SpiC (SSaB)	Alter cell traffic and block SCV-lysosome fusion; translocation of SPI-2 effectors	SPI-2	Yes	Olmo, Cardenal-Munoz et al. 2012) (Freeman, Rappl et al. 2002, Yu, Ruiz-Albert et al. 2002)
SpvB	Inhabit autophagy to avoid degradation; induce apoptosis; scavenge iron from host cell and promote survival in macrophages	SPI-2	No	(Kurita, Gotoh et al. 2003, Chu, Gao et al. 2016, Li, Wang et al. 2016, Yang, Deng et al. 2019)
SpvC	Reduce inflammatory response in intestine; trigger the reverse transmigration of infected cells to blood stream	SPI-1/2	No	(Haneda, Ishii et al. 2012, Gopinath, Allen et al. 2019)
SpvD	Inhibits NF-κB signaling	SPI-1/2	No	(Rolhion, Furniss et al. 2016)
SrfJ	Responses to intracellular conditions	SPI-2	No	(Kim, Kim et al. 2009, Figueira and Holden 2012)
SsaJ	Prevent NADPH oxidase target SCV	SPI-2	No	(Hensel, Shea et al. 1997)
SsaV	Prevent NADPH oxidase target SCV; regulate translocon and effectors secretion	SPI-2	No	(Gallois, Klein et al. 2001, Yu, Grabe et al. 2018)
SseA	Chaperone for SseB, SseC and SseD	SPI-2	Yes	(Zurawski and Stein 2004)
SseB	Prevent NADPH oxidase target SCV	SPI-2	Yes	(Gallois, Klein et al. 2001)
SseF	Inhabits Rab1-mediated autophagy; promote bacterial survival and replication; contributes to Sif formation; tethers SCV to the Golgi network	SPI-2	Yes	(Kuhle and Hensel 2002, Abrahams, Muller et al. 2006, Deiwick, Salcedo et al. 2006, Yu, Liu et al. 2016, Feng, Jiang et

SseG	Inhabits Rab1-mediated autophagy; promote bacterial survival and replication; contributes to Sif formation; tethers SCV to the Golgi network	SPI-2	Yes	al. 2018) (Kuhle and Hensel 2002, Yu, Liu et al. 2016, Feng, Jiang et al. 2018)
SseJ	Modulation of phagosome membrane; cholesterol acyltransferase; SCV membrane dynamics	SPI-2	Yes	(Lossi, Rolhion et al. 2008, Kolodziejek and Miller 2015)
SseK1	Inhibits TNF $\alpha$ -stimulated NF- $\kappa$ B signaling; induce cell death in macrophages	SPI-2	No	(Gunster, Matthews et al. 2017, Newson, Scott et al. 2019)
SseK2	Inhibits TNF $\alpha$ -stimulated NF- $\kappa$ B signaling	SPI-2	No	(Zhang, He et al. 2019)
SseK3	Inhibits TNF $\alpha$ -stimulated NF- $\kappa$ B signaling	SPI-2	No	(Zhang, He et al. 2019)
SseL	Inhibits TNF $\alpha$ -stimulated NF- $\kappa$ B signaling; Inhibits autophagic clearance of cytosolic aggregates; induces late macrophage cell death; inhibits directional migration of macrophages and DCs	SPI-2	Yes	(Rytönen, Poh et al. 2007, Mesquita, Thomas et al. 2012, Geng, Wang et al. 2019)
SspH2	An E3 ubiquitin ligase; activates NOD1 signaling	SPI-2	No	(Jennings, Thurston et al. 2017, Shappo, Li et al. 2020)
SsrA	Prevent NADPH oxidase target SCV	SPI-2	No	(Gallois, Klein et al. 2001)
SteA	Suppress pro-inflammatory response; SIF formation, vacuolar membrane partitioning	SPI-1/2	Yes	(Domingues, Holden et al. 2014, Gulati, Shukla et al. 2019)
SteC	Induces assembly of F-actin mesh workaroud SCV	SPI-2	Yes	(Odendall, Rolhion et al. 2012)
SteD	Inhibits antigen presentation and T cell activation	SPI-2	Yes	(Johnson, Mylona et al. 2018)

## 1.5 *Salmonella*-host interactions

### 1.5.i. How does *Salmonella* enter cells

*Salmonella* is an intracellular bacterium found within a variety of eukaryotic cells, including both phagocytic and nonphagocytic cells. *Salmonella* invasion of the cells is the first and crucial step for bacterial proliferation, dissemination and transmission (Richter-Dahlfors, Buchan et al. 1997, Salcedo, Noursadeghi et al. 2001, Meyerholz, Stabel et al. 2002, Geddes, Cruz et al. 2007). It has long been believed that *Salmonella* enters the cells only by a trigger mechanism and is mediated by T3SS-1, which is encoded by SPI-1. The T3SS is a needle-like complex found in many Gram-negative bacteria and plays a major role in the invasion and intracellular proliferation (McGhie, Brawn et al. 2009). Some recent studies have revealed that *Salmonella* invades cells via some other mechanisms (Rosselin, Virlogeux-Payant et al. 2010, Wisner, Desin et al. 2010, Pardo-Roa, Salazar et al. 2019). For example, Murray et al. found SPI-1 deficient *S. Typhimurium* is sufficient to pass through intestinal epithelium and cause a systemic infection (Murray and Lee 2000). Furthermore, *S. Typhimurium* with a nonfunctional T3SS-1 is not impaired in causing systemic infection in mice and chickens (Galan and Curtiss 1989, Morgan, Campbell et al. 2004). A recent study demonstrated that *S. Enteritidis* and *S. Typhimurium* and some serovars from *S. Dublin* conserved an extra zipper mechanism and is mediated by Rck which is encoded by the *rck* gene on the large virulence plasmid (Rychlik, Gregorova et al. 2006, Rosselin, Virlogeux-Payant et al. 2010).

Trigger invasion requires the injection of various effectors, such as SipA, SipC, SopB, SopE, by needle-like T3SS-1 into the host cell, to induce membrane ruffles, a rearrangement of the host cells cytoskeleton. On the other hand, the Zipper entry mechanism is mediated by Rck and relies on the interaction of bacterial ligands with host cell receptors. These interactions caused local accumulation of action, and induce the only minor cytoskeletal rearrangement of actin and tighter membrane extension.

PagN is also an identified invasion factor in many *Salmonella* genuses, PagN binds to extracellular heparin sulfate proteoglycans to induce *Salmonella* invasion.

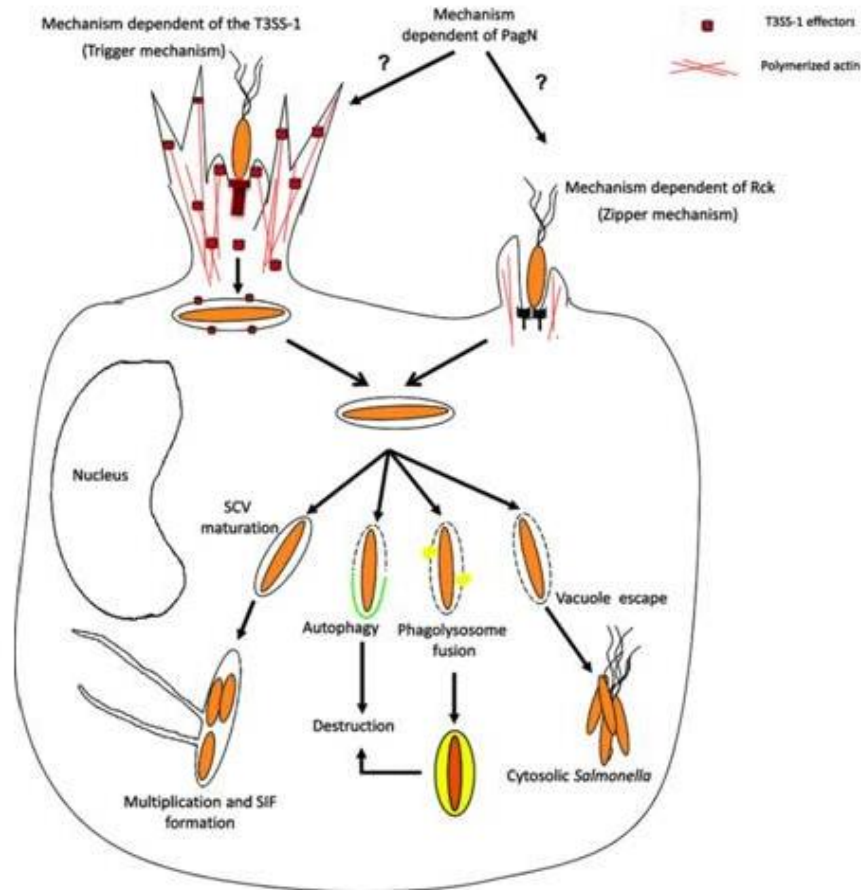


**Figure 1.8 Different strategies used by *Salmonella* for invasion and proliferation in eukaryotic cells.** *Salmonella* invades eukaryotic cells by the Trigger mechanism and Zipper mechanism. The trigger mechanism is mediated by T3SS-1 while the Zipper mechanism is mediated by Rck. Both of the mechanisms may be regulated by PagN.

Following bacterial entry into cells and the transition from a phagolysosome to an SCV nascent. Nascent SCVs can transform into mature SCVs, which lead to SIF formation and bacterial replication. SCV can also be targeted by LAP which induces SCV-lysosome fusion. Intracellular *Salmonella* may also be targeted by autophagy/xenophagy, both LAP and autophagy/xenophagy recognition of *Salmonella* generally lead to degradation. In epithelial cells, a small proportion of *Salmonella* can escape into cytosol and lead to hyper-replication of *Salmonella*.

Other unknown factors may also contribute to *Salmonella* invasion. The study of Rosselin et al. revealed *Salmonella* can enter some cell types without expressing Rck, PagN and T3SS-1 (Rosselin, Abed et al. 2011). *S. Typhimurium* also processes a unique ruffling independent invasion by the formation of myosin II rich stress fiber-like structure at the invasion site.

### **1.5.ii. *Salmonella* intracellular lifestyle**

Most intracellular bacteria internalize within membrane-bound compartments after their invasion. Some bacteria, such as *Listeria monocytogenes*, *Shigella flexneri* and *Francisella tularensis* escape from nascent vacuoles to enter the cytoplasm for rapid proliferation and replication (Ray, Marteyn et al. 2009). *Salmonella*, on the other hand, has been long considered as a vacuole pathogen because they only survive and replicates within SCVs. Nevertheless, growing evidence demonstrated that a proportion of intracellular *Salmonella* escape from SCVs and rapidly replicate in the cytoplasm of epithelial cells, but not macrophages. (Knodler, Vallance et al. 2010, Malik-Kale, Winfree et al. 2012). This escape is mainly due to the defect in vacuole maturation (Knodler, Nair et al. 2014).

After the invasion of host cells, SCVs develop a multiple-stage maturation step to facilitate its vacuole replication. Nascent SCVs are enriched in early endosomal markers, such as Rab5 and early endosome antigen 1 (EEA1). Then those markers are replaced by Rab7 and lysosomal-associated membrane protein 1 (LAMP1), which are late endosome and lysosome markers. Then SCVs were decorated with v-ATPase to allow the acidification of SCVs to pH4-5. Then SCVs are surrounded with actin and become matured SCVs. Matured SCVs migrate to perinuclear position and initiates the formation of *Salmonella*-induced filaments (SIFs), which promote the delivery of nutrients to SCVs and facilitate the vacuole bacterial replication (Knodler and Steele-Mortimer 2003, Salcedo and Holden 2003, Yu, Liu et al. 2016).

The intracellular growth of *Salmonella* is considered to be influenced by several factors, such as the site they replicate (vacuole or cytosolic), bacterial degradation by multiple innate immune responses and the type of host cell (Boumart, Velge et al. 2014). Cytosolic *Salmonella* replicates at a much higher rate compared with vacuole *Salmonella* and is referred to as hyper-replication (>100 bacteria per cell). A study revealed that hyper-replication only occurs in a minor percentage (<20%) of epithelial cells (Knodler, Nair et al. 2014). This hyper-replication in epithelial cells is always considered as transition steps that allow bacterial move out of cells and facilitates the interaction of *Salmonella* to neighboring cells in intestinal environments and *Salmonella* dissemination to organs to induce systemic infection (Cliffe, Humphreys et al. 2005, Knodler, Vallance et al. 2010). In contrast, Significantly lower *Salmonella* proliferation was observed in fibroblasts and macrophages compared with epithelial cells. *Salmonella* processes some effectors which prevent its overgrowth in fibroblasts, such as PhoP/PhoQ system (Cano, Martinez-Moya et al. 2001), while the cytosol of macrophages is been shown to be lethal for *Salmonella* (Beuzon, Salcedo et al. 2002).

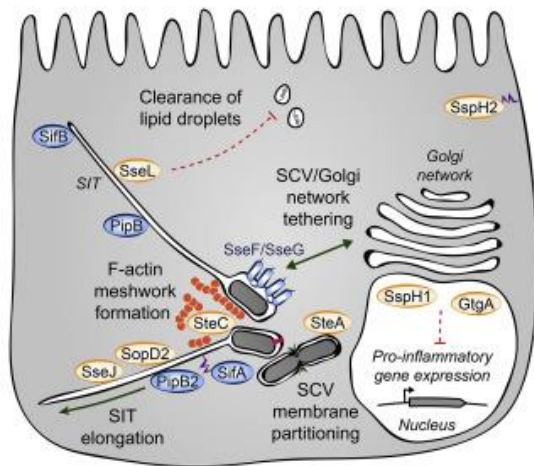
Two pathways are related to intracellular *Salmonella* degradation. One is rapid recruitment of LC3 to nascent SCVs to mediate SCV-lysosome fusion, or LC3 associated phagocytosis (Masud, Prajsnar et al. 2019, Masud, van der Burg et al. 2019). The second pathway is autophagy or xenophagy, a mechanism of capture both cytosolic and vacuolar *Salmonella* for degradation. Both of these pathways involve LC3 decoration of *Salmonella*.

A few recent studies have further revealed the mechanism of xenophagy/anti-bacterial autophagy. anti-bacterial autophagy-mediated pathogen engulfment depends on the recognition of dangerous signals from ubiquitin labelling of invading pathogens, mostly poly-ubiquitin coats. A study of Thurston et al. showed that galectin-8, a cytosolic lectin, is a monitor of endo-lysosomal integrity and limits *Salmonella*

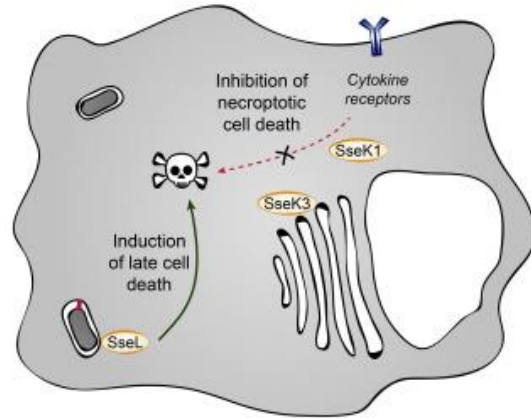
proliferation by binding to glycans on damaged SCVs, leading to ubiquitylation of SCV and recruitment of NDP52 to SCV to activate anti-bacterial autophagy. Cells lacking galectin-8 or NDP52, but not galectin-3 and galectin-9, failed to suppress proliferation of *S. Typhimurium*. The study also showed that hyper-proliferation of *S. Typhimurium* was observed in cells lacking galectin-8. The author also found that those hyper-proliferating *S. Typhimurium* are mostly negative for SCV marker LAMP1, indicating they are cytosolic *salmonella* (Thurston, Wandel et al. 2012).

Linear ubiquitin chain assembly complex (LUBAC) is a 600kDa ubiquitin ligase complex and is consists of HOIL-IL, HOIP and SHARPIN. LUBAC generates liner polyubiquitin chain to regulate NF- $\kappa$ B (Tokunaga and Iwai 2012). A few studies have focused on the role of LUBAC in bacterial and viral infections and found that LUBAC seems to play a role in TLR signaling pathways (Zak, Schmitz et al. 2011). A follow-up study was conducted by Noad et al. The authors determine the essential role of LUBAC in regulating cell-autonomous defense against cytosolic *S. Typhimurium*. LUBAC synthesizes M1-linked polyubiquitin and transfers the surface of cytosolic *S. Typhimurium*, not membrane of SCVs, into multivalent signaling platforms and recruitments two anti-bacterial pathways to degrade the cytosolic *S. Typhimurium*, anti-bacterial autophagy and NF- $\kappa$ B signaling. However, *Salmonella* has applied different strategies to avoid those host immune responses. For example, hyper-replication of *Salmonella* in epithelial cells is usually not targeted by autophagy/xenophagy (Knodler, Nair et al. 2014). *S. Typhimurium* processes SopF, a T3SS-1 virulence factor, to block the interactions between v-ATPase and the WD domain ATG16L1 to block LC3 recruitment to SCVs and inhabit xenophagy (Xu, Zhou et al. 2019). This will be discussed in the coming chapters.

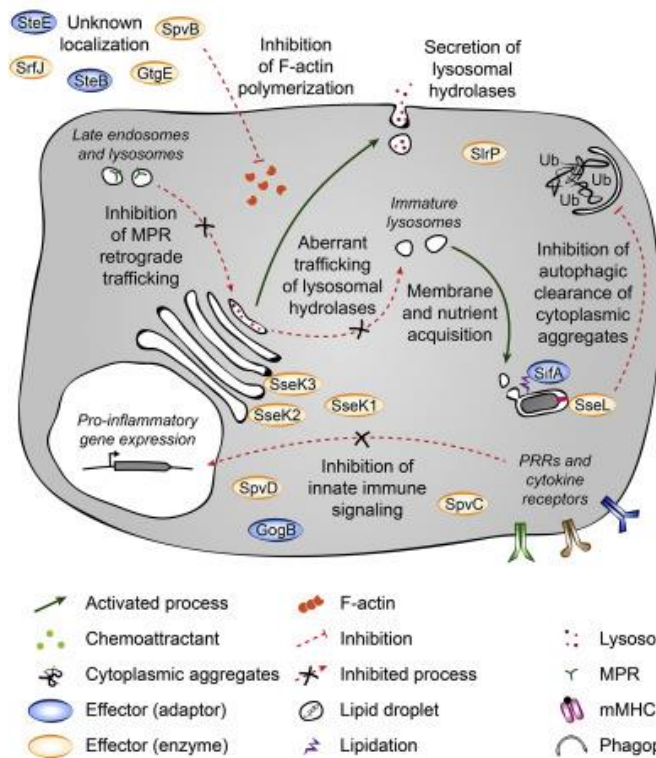
### A Epithelial cells



### B Macrophages



### C Epithelial cells and macrophages



### D Dendritic cells

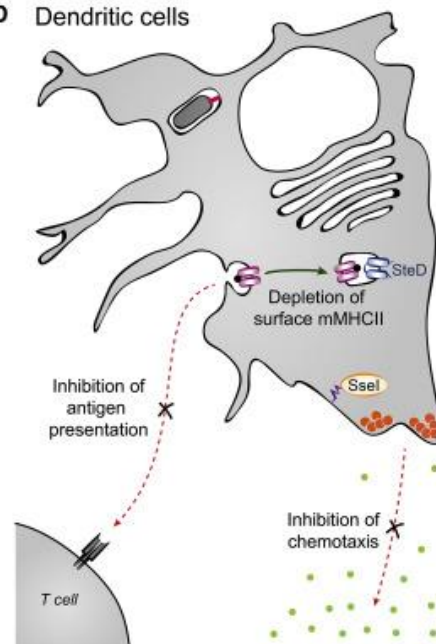


**Figure 1.9 Cell Type-Specific Salmonella Intracellular Life Cycle and SPI-2 T3SS effectors**

A. In *Salmonella*-infected epithelial cells, SseF and SseG, two transmembrane effectors, tether microcolony forming SCV the Golgi network. Vacuolar *Salmonella* replicates as the SCV membrane partition around them and encloses them into the individual vacuole. This process requires SifA and SteA. SCV forms a tubular extension called *Salmonella* induced tubules (SIT) with the function of SifA, PipB2, SseJ and SopD2. SteC is essential for the formation of an F-actin meshwork that surrounds the SCV microcolonies. SseL prevents cytoplasmic lipid droplets.

B. In *Salmonella*-infected macrophages, SseK1 and SseK3 inhibit necroptotic cell death, SseL induces cell death after phagocytosis of the bacteria.

C. In *Salmonella*-infected epithelial cells and macrophages, SifA plays important role in inhibiting mannose-6-phosphate receptors trafficking from late endosomes and lysosomes to Golgi network. This results in the secretion of lysosomal hydrolases and reduced lysosomal potency. In addition, SifA recruits late endosomes and lysosomes to SCV, whose contents act as a source of nutrients and membrane. SseL inhibits the clearance of cytoplasmic aggregates through autophagy pathway. SpvB inhibits F-actin polymerization. GogB, SseK1, SseK2, SseK3, GtgSA, SspH1, SpvC and SpvD inhibit innate immune signaling.

D. In *Salmonella*-infected DCs, transmembrane effector SteD depletes the surface MHC-II, which inhibits antigen presentation and result in reduced T cell proliferation. Furthermore, SseI prevents the directional migration of DCs.

## 1.6 The role of SopF in xenophagy

### 1.6.i. SopF

As one of the most studied bacterial models, more than 60 effector proteins were identified in *S. Typhimurium* over the past years various bioinformatics, biochemical and genetic methods. *STM1239* was first described as a protein of unknown function in *SL1344* genome. In 2014, the expression of *STM1239* was found to be regulated by HilA, an SPI-1 regulator (Brown, Rogers et al. 2014). In 2016, InvF, a transcriptional regulator of SPI-1 genes, was found to positively regulate *SopF* (Smith, Stringer et al. 2016). In 2017, Cheng et al. identified this protein as a novel SPI-1 T3SS effector protein by quantitative secretome profiling technology and renamed it *SopF* (Cheng, Wang et al. 2017). In this study, Cheng et al. also found that SopF promotes bacterial proliferation in macrophages and is required for full virulence of *S. Typhimurium* in C57BL/6 mice (Cheng, Wang et al. 2017).

A few further studies were focused on *SopF* in the following years. Lau et al. suggested that *SopF* is translocated by SPI-1 T3SS and its main role is maintaining integrity of the nascent SCV membrane. *SopF* mutants were shown to have increased access to the cytosol compared with WT *S. Typhimurium*. *SopF* mutants were also showed to have more associations with vacuole rupture markers (galectin-8) and key components of autophagy machinery, such as LC-3 and p62 (Lau, Haeberle et al. 2019). Another study further revealed this link between SopF and autophagy machinery (Xu, Zhou et al. 2019). In this study, the authors defined canonical autophagy as the non-selective autophagy which is triggered by nutrient deprivation and xenophagy as invading pathogen-induced autophagy. *S. Typhimurium* is a well-studied model of an intracellular bacterial pathogen widely used to study host-pathogen interactions of intracellular bacterial infection. But one problem is xenophagy was not robust during *S. Typhimurium* infection. In HEK cells, only around 20% of intracellular Salmonella were decorated with LC-3 and this percentage

further shrunk to about 5%-10% at 2 hours post-infection, indicating the possibility of unknown mechanisms behind this (Birmingham, Smith et al. 2006). Xu et al. conducted a transposon genetic screen and identified a new function of *SopF*. Deletion of *SopF* can increase antibacterial xenophagy activity while this phenotype can be abolished with overexpression of *SopF* in the cytoplasm. The authors also found that the expression of *SopF* in cells did not have any effect on canonical autophagy and LAP, but specifically block xenophagy and promote *S. Typhimurium* growth. Then they used a fluorescent activated cell sorting (FACS)-based genome-wide CRISPR Cas9 screen and identified a cluster of 5 genes encoding v-ATPase subunits along with most of the host ATG genes involved in xenophagy. The authors used Mass spectrometry (MS) and identified ATG5 and ATG16L1, and ATP6V1A, a major subunit of v-ATPase, as interacting partners specifically under conditions of bacterial infection. The authors then further demonstrated that v-ATPase interacts with the WD domain of ATG16L1 and recruits ATG16L1 to SCV membrane. This recruitment facilitates LC-3 lipidation on damaged SCV membrane and this interaction can be blocked by *SopF* catalyzing ADP-ribosylation of a component of the c-ring of the V-ATPase, ATP6V<sub>0</sub>C, without affecting v-ATPase's ability to pump protons or maintaining vacuole pH. Similar to the study of Lau et al. (Lau, Haeberle et al. 2019), data from mouse models showed that *SopF* is required for full virulence of *S. Typhimurium*. Loss of *SopF* caused more *S. Typhimurium* to be targeted by LC-3 in the small intestine of mice. Finally, the authors determine the protein structure of *SopF* and identified it as a member of the ADP-ribosyltransferase family. Then they further identified Gln124 of ATP6V<sub>0</sub>C, a v-ATPase component, as a target of ADP-ribosylation. Mutagenesis of Gln124 caused a complete silence of v-ATPase-dependent ATG16L1 recruitment to SCV and xenophagy, but again does not affect canonical autophagy. This study revealed a connection between *SopF* and xenophagy, and identified the main function of *SopF* in *S. Typhimurium* infection.

### **1.6.ii. v-ATPase**

v-ATPases are large, ATP-driven, multisubunit complexes that pump protons across membranes to acidify intracellular compartments (Vasanthakumar and Rubinstein 2020). This is crucial for endocytosis, membrane trafficking, protein degradation, and tumor metastasis (Vasanthakumar and Rubinstein 2020). V-ATPase is composed of two domains that operate like a rotor. ATP is hydrolyzed in the V<sub>1</sub> domain and the energy-derived movement of a rotary complex in the center, resulting in proton translocation through an integral V<sub>0</sub> domain. Multiple stalks connect both domains (Nishi and Forgac 2002). The isoform of subunit a, a subunit of V<sub>0</sub> which is about 100 kDa, is reported to control the targeting of V-ATPase to different cellular destinations (Forgac 2007). Xu *et al* identified ATG16L1 and ATG5 interacting with V-ATPase subunits from mass spectrometry after *Salmonella* infection of HeLa cells, indicating that V-ATPase recruits ATG16L1 to vacuole membrane. How does this happen? ATG16L1 has an ATG5 binding domain in its N-terminus and a middle coiled-coiled domain that mediates homodimerization. An additional C-terminal WD-40 repeat domain is presented in the ATG16L1 of mammals but not yeast. The most likely hypothesis is V-ATPase interacts with ATG16L1 to the vacuole membrane, then ATG16L1 recruits ATG5-ATG12 forming a complex and catalyze LC3 lipidation to the vacuole membrane. Thus, Xu *et al* generated several different forms of ATG16L1, including ATG16L1T<sup>281stop</sup>, which doesn't disrupt canonical autophagy but causes a defect in xenophagy. Pull-down experiments showed that this form of ATG16L1 failed to pull down V-ATPase in *Salmonella*-infected cells, which indicates the WD domain of ATG16L1 is critical for interacting with V-ATPase during xenophagy (Xu, Zhou et al. 2019). Interestingly, studies also revealed that V-ATPase is essential for LC3 lipidation on single membrane phagosomes and endosomes by recruiting ATG5 and LC3 to the membrane (Florey, Gammoh et al. 2015).

## **1.7 The role of cholesterol in Salmonella infection and replication**

### **1.7.i. Cholesterol and *S. Typhimurium* infection**

Cholesterol (C<sub>27</sub>H<sub>46</sub>O) was first isolated from human gallstones more than two centuries ago (Luo, Yang et al. 2020) and have been identified to be associated with many diseases. Cholesterol is largely hydrophobic and is biosynthesized in all mammalian cells. The majority of total cellular cholesterol resides on the plasma membrane and interacts with adjacent lipids to regulate the permeability and fluidity of the membrane (Liscum and Munn 1999). Besides, cholesterol can also interact with proteins on the plasma membrane, such as transmembrane proteins and sterol transport protein (Luo, Jiang et al. 2019, Wong, Gatta et al. 2019). Cholesterol often packs with sphingolipids and glycosylphosphatidylinositol-anchored proteins to form cholesterol-glycosphingolipid enriched membrane microdomains (rafts) in the plasma membrane. These microdomains play important roles in many cellular processes, such as signaling transduction, membrane trafficking, host-pathogen interactions (Sezgin, Levental et al. 2017), membrane fusion, and exocytosis (Churchward and Coorssen 2009, Linetti, Fratangeli et al. 2010). This microdomain is always targeted by bacterial and viral pathogens for entry or invasion of eukaryotic cells, some others take advantage of the cholesterol trafficking pathway to promote their replication. Viral examples include many common viruses, such as murine leukaemia virus, human T-cell leukaemia virus (Churchward and Coorssen 2009), human immunodeficiency virus type 1 (Liao, Cimasky et al. 2001, Popik, Alce et al. 2002, Viard, Parolini et al. 2002). Some bacteria also depend on cholesterol to invade cells, such as pathogenic FimH expressing *E.coli* strains (Baorto, Gao et al. 1997, Shin, Gao et al. 2000), *Mycobacterium bovis* (Ferrari, Langen et al. 1999, Gatfield and Pieters 2000), *Campylobacter jejuni* (Wooldridge, Williams et al. 1996) and *Chlamydia trachomatis* (Norkin, Wolfrom et al. 2001).

There were a few studies investigating the role of cholesterol during *S.Typhimurium* infection. Garner et al. determined the role of plasma membrane cholesterol in *S.Typhimurium* entry of non-phagocytic cells. Their study revealed that profound cholesterol redistribution was triggered by *S.Typhimurium* during bacterial entry into non-phagocytic cells. Their studies revealed that this redistribution relied on SPI-1 effectors. A defect in *S.Typhimurium* invasion was observed following the depletion of membrane cholesterol (Garner, Hayward et al. 2002). *Alvarea et al.* further investigated and identified plasma membrane cholesterol promotes *Salmonella* invasion by providing a target for SPI-1 T3SS docking to the plasma membrane (Alvarez, Glover et al. 2017). Plasma membrane cholesterol also plays some other roles during *Salmonella* infection. A few studies by Huang revealed that plasma membrane cholesterol plays critical role in *Salmonella*-induced anti-inflammatory response and *Salmonella*-induced autophagy in intestinal epithelial cells (Huang 2011, Huang 2014). Cholesterol was also found to play important role in vacuolar infection of *Salmonella*. Brumell et al. first found that SCV in HeLa cells is labeled with filipin at 6 hours post-infection (Brumell, Tang et al. 2001). Filipin is a polyene antibiotic that binds to 3 $\beta$ -hydroxysterols and emits a blue fluorescence (Wilhelm, Voilquin et al. 2019). But it was still not clear whether it was cholesterol or some other 3 $\beta$ -hydroxysterols which bind to filipin in SCVs. Catron et al. found that *S.Typhimurium* infection affects the host sterol biosynthetic pathway and identified the major sterol associated with SCV is cholesterol (Catron, Sylvester et al. 2002). They also found the association of cholesterol and SCV occurs at a very early stage of infection and increases after *Salmonella* replication. Up to 30% of cellular cholesterol accumulates around SCVs and this redistribution of host cholesterol is dependent on intracellular bacterial replication. They also identified a new marker of SCV, CD55, which suggests that SCV interacts with early endosomal, cholesterol-rich membranes during replication. Another study focused on the early stage of infection and revealed that cholesterol-rich SCVs were directly derived from the plasma membrane at the site of entry and maintained their high cholesterol level (Garner, Hayward et al. 2002). These

findings indicate that cholesterol plays a critical role during entry/invasion and intracellular replication of *Salmonella*.

## **1.8 Hypothesis and Aim**

The aim of this thesis is to determine the role of Atg16L1's WD domain in controlling *Salmonella* infection in cell lines, primary cells, as well as transgenic mice models.

According to the published literature, we made the following hypothesis:

1. WD domain of Atg16L1 controls *Salmonella* infection by recruiting LC-3 to SCV membrane and promote bacterial degradation through an innate immune pathway referred to as LC-3 associated phagocytosis.
2. Myeloid cells and intestinal epithelial cells play an important role during *Salmonella* infection. Mice with specific loss of Atg16L1's WD domain in either myeloid cell and intestinal epithelial cells were generated to study WD domain in which cell type is more important to *Salmonella* infection.
3. WD domain of Atg16L1 plays a crucial role in maintaining intracellular cholesterol homeostasis. Loss of Atg16L1's WD domain results in intracellular cholesterol accumulation, which promotes intracellular *Salmonella* replication.

## Chapter 2. Materials and Methods

### 2.1 Mouse models

Three transgenic mice models were used in this study.  $\delta$ WD mice were generated by Matyam Arasteh, a Ph.D student in our lab, and identified by the whole lab (Rai, Arasteh et al. 2019). Briefly, a stop codon was introduced at position E230 of Atg16L1 to preserve the ATG5 binding domain and CCD WIPI2b binding site for autophagy and remove residues in the WD domain required for LAP. The mice were named  $\delta$ WD mice due to the knockout of the WD domain, they do however lack both the WD and the linker domains of Atg16L1.  $\delta$ WD mice were then crossed twice with LysMcre mice or Villincre mice and then with Atg16<sup>fl/fl</sup> mice to generate  $\delta$ WD<sup>phage</sup> and  $\delta$ WD<sup>IEC</sup> mice. Atg16<sup>fl/fl</sup> mice have a flox site on both flanks of the Atg16L1 gene and were generated and kindly provided by Pro. Ulrike Mayer in the School of Biological Sciences, University of East Anglia. LysMcre mice and Villincre mice were purchased from The Jackson Laboratory. All mice were bred and maintained according to home office regulations in specific pathogen-free (SPF) ventilated cages. Mice were weaned at 3 weeks of age and ear notched for identification and genotyping.

### 2.2 cell lines

Wild type (WT) and  $\delta$ WD mouse embryonic fibroblasts (MEFs) were generated by serial passage of cells isolated from mice embryos harvested from pregnant females at 13.5 days into pregnancy. MEFs were cultured in Dulbecco's modified eagle medium (DMEM) (Gibco 21969035) supplied with 10% fetal calf serum (FCS) and 1% penicillin-streptomycin (PS) (Gibco,150700-63). Atg16L1KO MEFs were generated from Atg16L1<sup>fl/fl</sup> mice crossed with Rosa26-LacZ mice. The Atg16L1 gene was deleted with Adenovirus expressing Cre recombinase and isolated by FACS through activation of Lac Z expression after deletion of upstream stop sequences by the Cre

recombinase. Atg16KOL1 MEFs were cultured in DMEM (10% FCS+1% PS).  $\delta$ WD and WT Human embryonic kidney (HEK) cells provided by Prof. Oliver Florey in Babraham Institute and also cultured in DMEM supplied with 10% FCS and 1% PS.

## 2.3 Genotyping

Mice were ear notched after wean and small ear biopsies were collected for genotyping. Ear biopsies were lysed in 50  $\mu$ l of lysis buffer (0.1M Tris-HCl pH=8.5, 0.2 M NaCl, 0.005M EDTA, 0.2% SDS, 100 $\mu$ g/ml of proteinase K) at 55° C overnight. The lysates were diluted 20 times in water and used as a template for touchdown PCR. The details for PCR mix and reactions are listed in Table 2.1. Primer set 290 and 291 binds on both flanks of Atg16L1's exon 6 and amplifies a 291 bp product in WT mice or a 639 bp band in  $\delta$ WD mice due to the insertion of neomycin cassette. Primer sets 223 and 226 binds on both flanks of Atg16L1's exon2 and amplifies an 801 bp product in Atg16<sup>fl/fl</sup> mice or a 654 bp product in WT mice. The amplification is reduced to 253bp in cre expression tissues due to the removal of Atg16L1's exon 2 by cre. Primer set 15B and 19B binds on both flanks of cre enzyme and amplifies a 600 bp product if the cre gene is presented in the genome. At the end of PCR, the products were resolved on 1% agarose gel by performing electrophoresis at 200 volts for 1 hour. The gels were stained with ethidium bromide (EtBr) for 40 minutes and then imaged under ultraviolet (UV) light via ChemiDoc-It<sup>®</sup>2 810 Imager.

**Table 2.1**

**PCR mixture recipe:**

dNTP mix 1  $\mu$ l (25  $\mu$ M)  
 Buffer (10X with MgCl<sub>2</sub>) 5  $\mu$ l (1X)  
 Forward & reverse primer mix 1  $\mu$ l (20pM)  
 TODDNA polymerase 1  $\mu$ l (1:10 diluted)  
 Biopsy lysate (1:10 diluted) 3  $\mu$ l  
 Water = 39  $\mu$ l  
 Total = 50.0  $\mu$ l

**Sequence of primers used:**

290 (forward)  
 CAAATATGCCTTCAGAACTG  
 291 (reverse) : CAAATATGCCTTCAGAACTG  
 223 (forward)  
 CTGAACAGTTAAGTTCCTAG  
 226 (reverse)  
 CCAAGAGACACTGACATAGG  
 15B (forward)  
 GACGGAAATCCATCGCTCGAGCAG  
 19B (reverse)  
 GACATGTTTCAGGGATCGCAGGCG

**PCR program used: Touchdown PCR (Annealing temperature decreases from 65 °C to 56 °C at the rate of 1°C/cycle)**

95 °C – 10 minutes  
95 °C – 45 seconds  
65 °C – 1min (decreases 1 °C/ cycle) } 10 Cycles  
72 °C – 1 minute }  
95 °C – 45 seconds } 25 Cycles  
55 °C – 1 minute }  
72 °C – 1 minute }  
72 °C – 10 minutes }  
04 °C – forever (hold)

## **2.4 Bone marrow stem cells extraction and differentiation**

The cervical dislocation was used to sacrifice mice. Hind legs were harvested by scissors and muscles were removed by blades. Femur and tibia were cut open on both ends and then flushed with RPMI-1640 (Gibco, 21879-076, supplied with 1%PS) using a 10 ml syringe and 25 gauge needle. The flushed bone marrow cells were then passed through a cell strainer into a 50ml Falcom tube. Then the cells were centrifuged at 1000g for 5minutes. Supernatants were discarded after the centrifuge and cell pellets were resuspended in RPMI-1640 supplied with 50ng/ml of macrophages colony-stimulating factors (M-CSF, Peprotech 315-02), 10% FCS and 1% PS to differentiate them to bone marrow-derived macrophages (BMDMs). Then cells were placed in Petri dishes (no coating) and cultured in a 5% CO<sub>2</sub>, 37°C incubator for 6 days. The medium was replaced with fresh RPMI supplied with 50ng/ml of M-CSF on the third day after extraction.

## **2.5 LPS Challenge in mice**

Mice were injected with either PBS or 10mg/kg of LPS (Sigma L4130) via intraperitoneal (IP) route. Blood samples were collected at 90 minutes post-injection. The blood samples were placed in 4°C for one hour to allow them to clot. Then blood samples were centrifuged at 4°C, 3000 rpm for 10 minutes. Serum samples were transferred to clean Eppendorf, snapped frozen in liquid nitrogen and stored in -80 °C for further analysis of IL-1 $\beta$  concentration via IL-1 $\beta$  ELISA kit (Invitrogen, 88-7013-

22). ELISA was conducted according to the following step:

1. Plates were coated with capture antibody overnight at 4 °C.
2. The wells were washed with wash buffer (PBS with 0.05% Tween-20) 3 times in one-minute intervals.
3. Block the wells at room temperature (RT) for 1 hour with 200ul 1X ELISA Diluent. Wash the wells twice with 250ul wash buffer
4. Prepare a two-fold serial dilution of the IL-1 $\beta$  standard provided in the kit.
5. Add 100ul/well of the sample per well
6. Seal the plate and incubate at RT for 2 hours.
7. Aspirate the well and wash 3 times with wash buffer, 5 minutes each.
8. add 100ul/well of detection antibody and incubate for 1 hour at RT, seal the plate before incubation.
9. Aspirate the wells and wash 5 times with wash buffer, 5 minutes each.
10. Add 100ul of Streptavidin-HRP per well, seal the plate and incubate for 30 minutes at RT.
11. Wash for 7 times with wash buffer, 1-2 minutes each wash.
12. Add 100ul/well of TMB solution and incubate at RT for 15 minutes.
13. Add 100ul/well of stop solution.
14. Read the plate at the wavelength of 450nm.
15. Calculate the concentration according to the reading of standards.

The data were analyzed with turkey's test under one-way ANOVA.

## **2.6 IL-1 $\beta$ enzyme-linked immunosorbent assay (ELISA)**

After 6 days of differentiation, BMDMs were washed twice with warm PBS. Ice-cold PBS was added to the dish and the cells were incubated in the fridge for 20 minutes to allow them to detach. Detached cells were spun in 4°C at 1000g for 5 minutes and resuspended in fresh RPMI-1640 (10% FCS and 1% PS). BMDMs were counted by a cell counter (Biorad) and seeded at the concentration of 80,000 cells per well in 24 well plates. Then BMDMs were stimulated with 100ng/ml of LPS for 4 hours and

then treated with 150uM of BzATP (Sigma, 6396) for 30 minutes to activate P2X7 receptor. The supernatants were collected for further analysis of IL-1 $\beta$  concentration via ELISA kit (Invitrogen, 88-7013-22). ELISA was conducted according to the following step:

1. Plates were coated with capture antibody overnight at 4 °C.
2. The wells were washed with wash buffer (PBS with 0.05% Tween-20) 3 times in one-minute intervals.
3. Block the wells at room temperature (RT) for 1 hour with 200ul 1X ELISA Diluent. Wash the wells twice with 250ul wash buffer
4. Prepare a two-fold serial dilution of the IL-1 $\beta$  standard provided in the kit.
5. Add 100ul/well of the sample per well
6. Seal the plate and incubate at RT for 2 hours.
7. Aspirate the well and wash 3 times with wash buffer, 5 minutes each.
8. add 100ul/well of detection antibody and incubate for 1 hour at RT, seal the plate before incubation.
9. Aspirate the wells and wash 5 times with wash buffer, 5 minutes each.
10. Add 100ul of Streptavidin-HRP per well, seal the plate and incubate for 30 minutes at RT.
11. Wash for 7 times with wash buffer, 1-2 minutes each wash.
12. Add 100ul/well of TMB solution and incubate at RT for 15 minutes.
13. Add 100ul/well of stop solution.
14. Read the plate at the wavelength of 450nm.
15. Calculate the concentration according to the reading of standards.

The data were analyzed with turkey's test under one-way ANOVA.

## **2.7 JH3009 replication in HEKs and MEFs**

$\delta$ WD HEKs and WT HEKs were seeded in 6 well plates at the concentration of  $2 \times 10^5$  cells per well. On the next day, cells were infected with *S. Typhimurium* strain JH3009 at the MOI of 40-100 for 20 minutes. Cells were washed with PBS 3 times

and treated with DMEM supplied with 250 ug/ml of gentamycin for 2 hours to kill the extracellular bacteria. Then the medium is changed to DMEM supplied with 50ng/ml gentamycin for long-term culture. Cells were lysed with 0.1% deoxycholic acid at 2,4 and 8 hours post-infection and lysates were diluted in two-fold serial dilutions and plated on Streptomycin supplied agar plates overnight in a 37 °C incubator. The numbers of colonies in each dilution were counted to calculate intracellular bacteria. The intracellular growth was determined by the formula of CFU counts at 8hours post-infection divided by CFU counts at 2 hours post-infection. The data were analyzed by student's t-test.

$\delta$ WD MEFs, WT MEFs and ATG16L1KO MEFs were seeded in 6 well plates at the concentration of  $2 \times 10^5$  cells per well. On the next day, cells were infected with *S. Typhimurium* strain JH3009 at the MOI of 40-100 for 20 minutes. Cells were washed with PBS 3 times and treated with 250 ug/ml of gentamycin for 2 hours to kill the extracellular bacteria. Then the medium is changed to DMEM supplied with 50ng/ml gentamycin for long-term culture. Cells were lysed with 0.1% deoxycholic acid at 2,4 and 8 hours post-infection. The CFU counts at each time point and intracellular growth was determined as mentioned above. The data were analyzed by student's t test.

## **2.8 *S. Typhimurium* infection in mice and tissue harvesting**

*S. Typhimurium* strain JH3009 was kindly provided by Prof. Jay Hilton from the Institute of Food Research and is described previously (Hautefort, Proenca et al. 2003). Food and water were removed from mice at 4 hours prior to infection. Mice were orally gavaged with a bacterial dose of  $1-5 \times 10^8$ /mouse and monitored for weight loss, clinical symptoms over 6 days. All mice which received a 20% weight loss were sacrificed immediately. All surviving mice were sacrificed on the sixth-day post-infection. Livers and spleens were harvested and cut into two pieces, one of which was weighed and lysed in phosphate buffer saline (PBS), the second part is

fixed in 10% neutral buffered formalin (Sigma, HT501128). The small intestine was cut and rolled in a swiss roll formation and also fixed with 10% neutral buffered formalin.

## **2.9 Bacterial dissemination to liver and spleen.**

Livers and spleens were placed in 2 ml Eppendorf tubes with 2 sterilized magnified beads in each tube. Then tissues were lysed with a tissue homogenizer in 1 ml of PBS. The lysates were diluted in two-fold serial dilutions and plated on LB agar plates. The plates were incubated in a 37 °C incubator overnight and CFUs were counted on the next day. The data were calculated and represented as numbers of CFU per gram of tissue. The data were analyzed with student's t test.

## **2.10 Luminex assay of pro-inflammatory cytokines in serums of infected mice**

Serums were isolated as mentioned in section 2.5 and preserved in -80 °C. The pro-inflammatory cytokines (IL-1 $\beta$ , IL-6, IL-13 and TNF- $\alpha$ ) were measured by ProcartaPlex™ Simplex immunoassay kit (ThermoFisher Scientific, EPX01A-26015-901, EPX01A-26004-901, EPX01A-26005-901, EPX01A-26002-901, EPX01A-20607-901, EPX01A-20603-901) according to the following step:

1. Vortex each of the beads and add 50ul of each magnetic bead to the plate.
2. Securely insert the 96 well flat-bottom plates into a hand-held magnetic plate washer (EXP-55555-0000), and wait for 2 minutes to allow the beads to accumulate on the bottom of each well.
3. Aspirate the well completely by rapidly inverting the hand-held magnetic plate washer over the sink.
4. Add 150ul of wash buffer per well and wait for 30 seconds.
5. Aspirate the well completely by rapidly inverting the hand-held magnetic plate washer over the sink.

6. Centrifuge the standard at 2000g for 10s. Prepare the standard by adding 50 ul of Universal Assay Buffer. Gently vortex for 10 seconds at 2000g to collect the contents. Incubate the vial on ice for 10 minutes. Adjust the vials with Universal Assay Buffer to a total volume of 250 ul. Gently vortex for 10 seconds at 2000g to collect the contents.
  7. Prepare the 4 fold serial dilution of the standard with Universal Assay Buffer.
  8. Remove the plate from the hand-held magnetic plate washer, add 25 ul of Universal Assay Buffer and 25 ul of serum or standard. 50 ul of Universal Assay Buffer were added to the blank well.
  9. Seal the plate and then cover the plate with Black Microplate Lid. Shake at 500 rpm for 2 hours at RT.
  10. Perform the wash step in step 3 for 5 times.
  11. Add 25 ul of Detection Antibody mixture to each well/
  12. Seal the plate and then cover the plate with Black Microplate Lid. Shake at 500 rpm for 30 minutes at RT.
  13. Perform the wash step in step 3 for 5 times.
  14. Add 120 ul of Reading Buffer into each well.
  15. Seal the plate and then cover the plate with Black Microplate Lid. Shake at 500 rpm for 5 minutes at RT.
  16. Run the plate on a Luminex 200 instrument.
- The data were analyzed with student's t test.

## **2.11 Tissue processing and embedding**

The tissues harvested from mice were fixed in formalin and transferred to 70% ethanol the next day for short-term storage before further processing. Then tissues were dehydrated overnight in an automatic tissue processor (Lecia, ASP300S) with the process of 70% ethanol for 1 hour, 80% ethanol for 1.5 hours, 90% ethanol for 2 hours, ethanol absolute for 1, 1.5 and 2 hours, xylene for 0.5, 1 and 1.5 hours, paraffin wax for 1, 2 and 2 hours. The dehydrated tissues were submerged with melted paraffin

(Sigma, P2558) and embedded with an embedding station (Leica, EG1150). Tissues were placed in the correct orientation on a layer of partially solidified paraffin in metal moulds. Then melted paraffin was used to fill up the moulds. Then the entire moulds were placed on a precooled surface allowing them to cool down and solidify. Those formalin fixed paraffin embedded (FFPE) tissues were sectioned into 4 micron thick sections with a microtome (Microm, HM355S). Briefly, tissue blocks were precooled in the cold room and fixed on the holder of the microtome, and were trimmed to form a flat surface. Then several 4-micron sections were sliced from each block and flattened in warm water (42°C). These sections were stuck to glass slides (Thermofisher, J1800AMNS) and left to dry overnight.

## **2.12 Hematoxylin and Eosin (H&E) staining**

The dried sections were stained by H&E with the following process:

1. Histoclear (National diagnostics) I for 5 minutes
2. Histoclear II for 5 minutes
3. 100% ethanol for 2 minutes
4. 80% ethanol for 2 minutes
5. 70% ethanol for 2 minutes
6. Rinsing under running tap water for 5 minutes
7. Hematoxylin staining (Sigma, HHS128) for 2 minutes
8. Washing under running tap water for 5 minutes
9. 1% HCL in 70% ethanol for 15 seconds
10. Rinsing in water for about 10 seconds
11. 0.1% Sodium bicarbonate for 1 minute
12. Washing under running tap water for 5 minutes
13. Eosin solution (Sigma, HT110116) staining for 30 seconds
14. 70% Ethanol for 2 minutes
15. 80% Ethanol for 2 minutes

- 16.100% Ethanol for 2 minutes
- 17.Histoclear solution-II for 5 minutes
- 18.Histoclear solution-I for 5 minutes

Sections were mounted with DPX mounting media (Thermofisher, D/5319/05) and dried overnight at room temperature in a fume hood. All the sections were observed under a bright field microscope (Zesis).

## **2.13 Immunohistostaining of tissue sections**

Dried tissue sections obtained from section 2.11 were de-paraffinised and rehydrated by the following step.

- 1.Histoclear (National diagnostics) I for 5minutes
- 2.Histoclear II for 5 minutes
- 3.100% ethanol for 2 minutes
- 4.80% ethanol for 2 minutes
- 5.70% ethanol for 2 minutes
- 6.Rinsing under running tap water for 5 minutes

Antigen retrieval was performed by two 10-minutes microwaving (600W) in Citrate based antigen retrieval buffer. (0.053%w/v Tri Sodium Citrate dihydrate and 0.17%w/v Citric acid in distilled water). Sections were cooled at room temperature and then washed 3 times in PBS. Peroxidase activation was blocked by 10 minutes incubation with hydrogen peroxide in methanol (10%v/v) at room temperature. Then sections were again washed in PBS 3 times before incubation in blocking buffer (10% Goat serum and 0.3% TritonX-100 in PBS) for one hour to block non-specific binding. The sections were then stained with anti-mouse CD11b antibody at the dilution of 1:1000 (Abcam, ab133357) overnight at 4°C. The secondary antibody, HRP-anti-rabbit IgG (Dako, K4003) was diluted in antibody diluting buffer provided in the kit.

Sections were washed with PBS three times the next day and then incubated in secondary antibody at room temperature for one hour. The sections were again washed 3 times in PBS. The signal was developed by adding 2% v/v Chromogen in Substrate buffer to the sections. The first section was observed under a bright field microscope to determine the time for signal development and applied to all sections. The reaction was stopped by submerging in PBS, then the sections were counterstained with hematoxylin by the following step and mounted in DPX mounting solution. Sections were observed under a bright field microscope (Axioplan 2, Zeiss), pictures were taken with a coloured Axio Cam HRc camera with 10 times objective.

1. Hematoxylin staining (Sigma, HHS128) for 2 minutes
2. Washing under running tap water for 5 minutes
3. 1% HCL in 70% ethanol for 15 seconds
4. Rinsing in water for about 10 seconds
5. 0.1% Sodium bicarbonate for 1 minute
6. Washing under running tap water for 5 minutes
7. 70% Ethanol for 2 minutes
8. 80% Ethanol for 2 minutes
9. 100% Ethanol for 2 minutes
10. Histoclear solution-II for 5 minutes
11. Histoclear solution-I for 5 minutes

## **2.14 Tissue western blot**

3-month-old  $\delta$ WD<sup>IEC</sup> mice and control mice were sacrificed, gut epithelium was scrapped, collected and snap-frozen in liquid nitrogen. A proper amount of gut epithelium was resuspended in RIPA buffer (0.5% Sodium deoxycholate, 0.1% SDS, 50mM Tris, 150mM Sodium chloride, 1% TritonX-100, adjust the pH to 8.0) supplied with proteinase and phosphatase inhibitor (Sigma, P8340 and P5726) and lysed on ice

for 30minutes. Freezing and thawing cycles were used for further homogenization. Then the lysates were sonicated twice on ice and centrifuged at 16000Xg in the cold room to get rid of cell fragments. Supernatants were transferred into fresh Eppendorf tubes and the protein concentrations were determined by BCA assay kit (Thermofisher, 23225) according to the manufacturer's instructions. 15µg of protein was loaded in each well of precast SDS gel of 4-12% in BIS-TRIS buffer system (Thermofisher, NW04125BOX) and electrophoresed at 70 volts for 20minutes and then 100 volts for 90 minutes. Then proteins were transferred to PVDF membrane (Immunobilon, Millipore, IPFL00010) by wet transfer (280mA for 90minutes in 4°C) and blocked with blocking buffer (Thermofisher, 37576) for 1 hour at room temperature. The membrane was then probed in rabbit anti-ATG16L1 (MBL, M150-3) antibody and goat anti-β actin antibody (Abcam, ab8227) both diluted at the dilution of 1:1000 in blocking buffer overnight at 4°C. On the next day, the membrane was washed with TBST (Tris buffer saline Tween 20) (0.5% Tween 20) 3 times for 15 minutes each and probed with 680 anti-goat IgG and 800 anti-rabbit IgG at room temperature for 1 hour. Then the blot was again washed three times with TBST and imaged by Odyssey infrared system (LI-COR). The image was quantified by ImageJ software and the data was analyzed with student's t test.

## **2.15 FITC-dextran treatment in mice**

3-month-old  $\delta$ WD,  $\delta$ WD<sup>IEC</sup>, WT and control mice were orally gavaged with FITC-dextran (3000-5000 molecule weight, Sigma, 60842-46-8) to measure the intestinal permeability. FITC-Dextran was resuspended in PBS at the concentration of 80mg/mL in PBS. Mice were fasted for 4 hours and orally gavaged with 500mg/kg of body weight. Serum was collected at 2 hours post oral gavage and diluted 1:1 in PBS to measure the fluorescence spectrophotometrically in 96 well plates with the emission of 528 nm and excitation of 485 nm. FITC-Dextran concentration was determined by comparing the reading with a standard curve ranging from 0-20 ng/µl which is generated by diluting FITC-dextran in PBS. 4 mice from each group were

involved in the experiment and the data were analyzed by Turkey's test in One-way Anova.

*S. Typhimurium* challenged mice were orally gavaged with FITC-dextran at sixth day post infection. Then mice were sacrificed after 2 hours. FITC-dextran concentration in serums was determined with the procedures mentioned above. 6 mice from each group were involved in the experiment and the data were analyzed by student's t test in One-way Anova.

## **2.16 FACS analysis of immune cells populations in the liver**

Mice were sacrificed on sixth day post infection, livers were harvested and the triangular lobes were submerged in PBS-2%FCS (1.5ml Eppendorf tubes for each) and kept on ice. Then triangular lobes were transferred to collagenase buffer (1/40 of stock in PBS-2%FCS) in 24 well plates (one triangular lobe per well) and cut into pieces with curved scissors. The plates are incubated for 30 minutes at 37 °C. Livers were broken into small pieces after the incubation by passing them up and down with a syringe. The small pieces of liver were smashed against a 70µm cell strainer. Then cells were washed through the strainer with 15ml of PBS-2%FCS into a 15ml falcon tube. The samples were centrifuged in a precooled centrifuge at 13000rpm for 10 minutes. The supernatants were discarded and cell pellets were resuspended in 5 ml of 35% Percoll (GE Healthcare, 17-5445-01) in PBS/FBS at room temperature and centrifuged at 1700rpm for 40 minutes at room temperature. A brown ring can be observed on top of the supernatant, discard the supernatant and the brown ring without disturbing the cell pellet. Resuspend the pellet in 2-3 ml of Red blood cell lysis buffer (eBioscience, 00-4333-57) for 3 minutes. Transfer the cells to FACS tubes and top up with PBS-2%FCS. Centrifuge at 1300 rpm for 10 minutes in cold.

Prepare two sets of antibodies, one for T cells, other for macrophages and neutrophils.  
T cells: CD45-APC-cy7 (BD Pharmigen), CD8-PE (eBioscience), CD3-APC

(eBioscience), CD4-Percp5.5 (BD Pharmigen). macrophages and neutrophils: CD45-APC-Cy7 (BD Pharmigen), CD11b-PE (BD Pharmigen), F4/80-FITC (Miltenyi), Ly6G-APC (Miltenyi), Ly6C-Vio Blue (Miltenyi). These antibodies were diluted in 1/200 dilutions in PBS/2%FCS.

**Table 2.2 FACS antibody**

Antibody	Company	Catalog Number	Dilution
CD45-APC-cy7	BD Pharmigen	561037	1:200
CD8-PE	eBioscience	12-0081-82	1:200
CD3-APC	eBioscience	17-0032-82	1:200
CD4-Percp5.5	BD Pharmigen	560650	1:200
CD11b-PE	BD Pharmigen	557321	1:200
F4/80-FITC	Miltenyi	130-117-509	1:200
Ly6G-APC	Miltenyi	130-123-854	1:200
Ly6C-VioBlue	Miltenyi	130-102-929	1:200

Discard the supernatant and stained the cells in 95µl of antibody solution for 30 minutes in the fridge. Wash the cells with PBS/2%FCS and resuspend cells in 200µl of PBS/2%FCS and analyzed the cells with a BD cell sorter. The results were analyzed by Flowjo software. The results showed the average percentage of indicated cell types in CD45 positive cells of 10 mice from indicated mice strain. The data were analyzed by student's t test.

## **2.17 FACS analysis lamina propria lymphocytes from small intestine of mice.**

Small intestines were harvested from *S. Typhimurium* infected mice on sixth day post infection. The small intestine was cut open on the lid of Petri dishes to remove the content, then those pieces were shaken in PBS/2%FCS and moved to 10 ml of buffer (PBS+2%FBS, DTT 0.1mM, EDTA 2mM). Then the small intestines were incubated at 37 °C for twenty minutes with 200 rpm of shaking. Then vortex the tubes for 15 seconds until cloudy. Catch the lamina propria into a new falcon tube with 15 ml of digestion media (15ml RPMI, 2µM Calcium Chloride, 0.25mg/ml of Collagenase) and cut lamina propria into small pieces with scissors and incubate at 37 °C for 10 minutes with 200 rpm of shaking. After the incubation, the liquid was passed through a cell strainer and the remaining small pieces of tissues were smashed with a syringe.

Cell strainers were washed with RPMI until the volume reached 30ml. Centrifuge the tubes for 10 minutes at 2000 rpm in 4 °C. Discard the supernatant and resuspend in 10ml of RPMI. Prepare the Percoll gradients in 50 ml Falcon tubes by adding 15 ml of 30% Percoll (4.5ml of 100% osmotic Percoll, 10.5 ml of RPMI) and then underlay 5 ml of 100% Percoll (4.45ml Percoll, 0.5ml 10XDPBS and 0.05ml 1M HEPES) with a Pasteur pipette. Layer the cells on to 30% Percoll gradient. Centrifuge at room temperature for 30 minutes (acceleration to 3 and break to 0). A white ring of immune cells was formed between the layer of 100% and 30% Percoll. Collect this layer carefully with a Pasteur pipette and try to avoid any Percoll. Transfer the collected cells to a 50 ml Falcon tube and top up with 30ml RPMI and resuspend the cells by vortexing. Cells were centrifuged for 7 minutes with 2000 rpm at 4 °C and transferred to FACS tubes. Then the antibody staining and FACS analysis were performed as described in section 2.16.

## **2.18 Lamda Red recombination to replace *SopF* with kanamycin cassette**

Primers were designed to amplify the kanamycin cassette from pKD4 vector. Gene *SopF* was identified at the 1282936-1284060 location in the complete genome of *S. Typhimurium* strain SL1344 (Genbank Accession number: NC\_016810.1). The 50 bp sequence upstream and downstream of *SopF* gene were used to design primers for amplification of DNA fragments for homologous recombination. The third set of primers were designed to identify the replacement of *SopF* with kanamycin cassette. All the primers used were in Table 2.2

**Table 2.2**

Name	Primer Sequence (5'-3')
Kanamycin_F orward	GTGTAGGCTGGAGCTGCTTCG
Kanamycin_Re verse	CATATGAATATCCTCCTTAGT
SopF_Amplify _Forward	TACGTCAGCGAAAGTGAATGCTATATTAGTCATAAAAATTCA GGAGACAT GTGTAGGCTGGAGCTGCTTCG
SopF_Amplify _Reverse	CATATGAATATCCTCCTTAGTTGCGCTCATGATCATTTAAAGC TCTTTTAAAGAGACTGATAATAAGCTTG
SopF_Identify _Forward	GTAGGCTGGAGCTGCTTCG
SopF_Identify _Reverse	AGAGACTGATAATAAGCTTG

1. TBH (Terrific broth+hygromycin) was prepared from powder (invivogen) in a fume hood according to provider instructions.
2. *S. Typhimurium* strain SL1344 which carries pSIM18 plasmid was cultured overnight in 5 ml of TBH at 30 °C with 200 rpm shaking. On the next day, 5 ml of overnight culture was inoculated to 150 ml of sterile TBH and incubated at 30 °C with 200 rpm of shaking. Grow the culture to the mid-exponential period (OD<sub>600</sub> ~0.3).
3. In the meantime, amplify the kanamycin cassette with primer set SopF\_Amplify\_Forward and SopF\_Amplify\_Reverse. PCR products were purified by a PCR clean up kit (Qiagen, 28106). DNA concentration was measured by Nanodrop. The purified products were stored in 4 °C for further use.
4. Collect the bacteria culture and heat shock it in 42 °C water bath for 15 minutes. Then cool down the culture on ice immediately for 10 minutes.
5. Transfer the culture to sterile centrifuge tubes and spin bacteria down at 4000 rpm for 10 minutes at room temperature. Discard the supernatant and resuspend the pellet with 75 ml of ice cold sterile water.
6. Spin down the bacteria at 4000 rpm for 10 minutes at room temperature. Resuspend

all bacteria in 1.5 ml sterile ice cold water. Then bacterial cells were washed 5 times with 1.5 ml of sterile ice cold water, through resuspension and spinning down at 9000G for 2 minutes at room temperature.

7. Resuspend the bacterial cells in 150µl of sterile ice cold water. Prepare the bacterial cell/DNA mix in pre cold sterile Eppendorf tubes by adding 2,4,8µl of purified PCR products to 40µl of bacterial cells. Water is added to the bacterial culture as a negative control. Bacterial cell/DNA mixes were transferred to electroporation cuvettes and set to E2 on MicroPulser™ Electroporator for electroporation.

8. Immediately after the electroporation, 400µl of SOC media (800µl SOB+100µl 1M Glucose) was added to each cuvette. Then the cells were transferred to sterile Eppendorf tubes for recovery at 37 °C for 2.5 hours.

9. Plate out the cells on LB agar plates supplied with kanamycin. The plates were incubated overnight at 37 °C.

10. Colonies were picked and grown in LB supplied with 50ng/ml of kanamycin. Bacteria were lysed by boiling for PCR with primer set SopF\_Identify\_Forward and SopF\_Identify\_Reverse. At the end of PCR, the products were resolved on 1% agarose gel by performing electrophoresis at 200 volts for 1 hour. The gels were stained with ethidium bromide (EtBr) for 40 minutes and then imaged under ultraviolet (UV) light via ChemiDoc-It®2 810 Imager. The correct colonies were named SL1344<sup>δSopF</sup>, grown in LB and frozen in glycerol for long term storage.

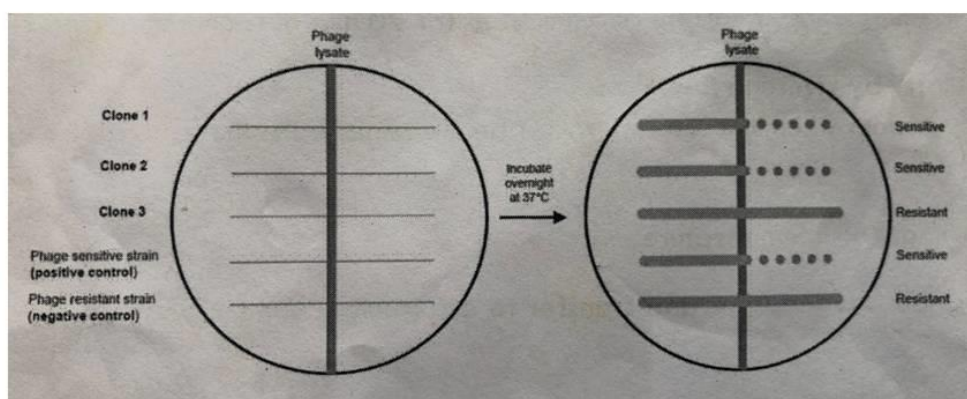
## **2.19 P22 transduction of SopF mutation to *S. Typhimurium* strain JH3009**

1. Grow 5 ml of SL1344<sup>δSopF</sup> in LB supplied with 50 ng/ml of kanamycin overnight at 37 °C with 200 rpm shaking.

2. The next day, heat the top agar. Put liquid agar (0.5%) in water bath at 50 °C. Mix 100µl of overnight culture with 10µl of 10 fold serial diluted P22 lysates (kindly provided by Dr. Rob Kingsley from Quadram Institute). Incubate the mixtures in a 37 °C water bath for 20 minutes.

3. Add 3 ml of top agar in each mixture and mix. Then pour the mixture over warmed LB agar plates and spread by moving plates in continuous circular motions. Then the agar plates were incubated at 37 °C for 4-6 hours. Determine the optimal dilution by selecting the plate with a gradual plaque formation with a confluence peak at around 4 hours.
4. Scrape the top agar containing the lysates with a sterile spreader and collect them in 50 ml tubes with 3 ml of LB. 100µl of chloroform was added to each tube and mixed thoroughly by vortexing followed by a 20 minutes incubation period at room temperature.
5. Centrifuge the mixture at 4000 rpm for 5 minutes. Collect the supernatant which contains the P22 phage lysates and transfer it to a 1.2 ml cryopreservation vial (Corning). 50µl of chloroform was added to sterile the phage lysates. The lysates were stored in 4 °C for further use.
6. Grow up a 5 ml overnight culture of JH3009 in LB supplied with 75 ng/ml of Streptomycin overnight at 37 °C with 200 rpm shaking. On the next day, 100µl of overnight culture were mixed with 10 fold serial dilutions of P22 lysates or 10µl of LB as negative controls. The mixture was incubated in 37 °C incubator for 15 minutes. Then add 1 ml of LB supplied with 10mM EGTA(Ethylene glycol-bis(2-aminoethylether)-*N,N,N',N'*-tetraacetic acid) and further incubate in 37 °C for another hour.
7. Spin down the bacterial cells at 14000 rpm for 5 minutes at room temperature. Discard all but 100µl of supernatant and resuspend the bacteria by pipetting. Spread the suspension on LB agar plates supplied with 50ng/ml of kanamycin and 10mM EGTA and incubated in a 37 °C incubator overnight.
8. The colonies were picked the next day and examined using PCR with the primer set of SopF\_Identify\_Foward and SopF\_Identify\_Reverse. Then the correct clones were grown in LB supplied with 50ng/ml of kanamycin. Then cultures were diluted in LB and spread on Evans Blue-Uranine (EBU) plates supplied with 50ng.ml of kanamycin to detect the phage contaminated colonies. The phage contaminated colony is

expected to show a dark green color on EBU plates. The plates were incubated in a 37 °C incubator overnight. The next day, pick light green/white colonies from the plates and test their sensitivity to P22 phage as described in Figure 2.1. Briefly, make a strip of P22 lysates on an EBU plate and stack the colonies you want to test through the P22 strip. Then incubate the plate overnight at 37 °C. Choose the phage sensitive clone the next day. Those phage sensitive clones were named JH3009<sup>δSopF</sup>.



## 2.20 Growth curve of JH3009<sup>δSopF</sup>

5 ml of either JH3009 or JH3009<sup>δSopF</sup> were culture overnight at 37 °C. The next day, both JH3009 and JH3009<sup>δSopF</sup> were inoculated into fresh LB at the ratio of 1:33. The culture was collected at 30,60, 90, 120,150,180,240 and 360 minutes post infection. The OD<sub>600</sub> value was determined by a spectrum reader. The data were analyzed with Bonferroni post test in two way ANOVA .

## 2.21 JH3009<sup>δSopF</sup> replication in MEFs

δWD MEFs and WT MEFs were seeded in 6 well plates at the concentration of 2X10<sup>5</sup> cells/per well. On the next day, cells were infected with *S. Typhimurium* strain JH3009<sup>δSopF</sup> at the MOI of 40-100 for 20 minutes. Cells were washed with PBS 3 times and treated with 250 ug/ml of gentamycin for 2 hours to kill the extracellular bacteria. Then the medium is changed to DMEM supplied with 50ng/ml gentamycin for long term culture. Cells were lysed with 0.1% deoxycholic acid at 2,4 and 8 hours

post infection. The CFU counts at each time point and intracellular growth was determined as mentioned in section 2.7.

## **2.22 Immunofluorescent (IF) staining of LC-3 recruitment to *S. Typhimurium***

WT and  $\delta$ WD MEFs were seeded on coverslips at the concentration of 10000 cells per well in 24 well plates and allow them to attach overnight. On the next day, both WT and  $\delta$ WD MEFs were infected with either JH3009 or JH3009 <sup>$\delta$ SopF</sup> for 20 minutes at an MOI of 40. Then cells were washed 3 times with PBS and extracellular *S. Typhimurium* was removed by culturing in DMEM supplied with 250ng/ml of gentamycin. Cells were fixed with methanol at 30minutes, 60 minutes and 120 minutes post infection. Then cells were then blocked with 5% goat serum, 0.1% TritonX in PBS for 30 minutes and stained with rabbit polyclonal anti-Salmonella antibody (1:2000, Abcam, ab35156) and mouse anti-LC3 monoclonal antibody (1:200, G2, saint cruz) overnight at 4 °C. The cells were washed three times with PBS on the next day and stained with Alexa-488 Goat anti-rabbit IgG (Thermofisher, A-11008) and Alexa-594 donkey anti-mouse IgG (Thermofisher, A21203), both at the dilution of 1:2000. Then the cells were again washed 3 times with PBS. After washing, cells were counterstained with 4', 6 diamidino-2-phenylindole (DAPI) (Thermo Fisher Scientific, 10116287) and mounted with Fluoromount-G (Cambridge Bioscience). Cells were imaged on a Zeiss Imager M2 Apotome microscope with a 63x, 1.4 NA oil-immersion objective. The LC-3 positive *Salmonella* ratio was determined by numbers of LC-3 positive *Salmonella* divided by the numbers of total Salmonella in 20 images. The number of cells in each image (field of view) was determined via DPAI staining. LC-3 positive *Salmonella* was determined by co-localization of LC-3 and *Salmonella* and the total number of Salmonella in each image was determined by Alexa-488 staining. The data was presented as the ratio of LC-3 positive *Salmonella* at indicated timepoints and were analyzed with Bonferroni post test in two way ANOVA.

## **2.23 JH3009<sup>δSopF</sup> infection in control mice**

8-12 weeks old control mice from  $\delta\text{WD}^{\text{phage}}$  and  $\delta\text{WD}^{\text{IEC}}$  group (mice which don't carry the cre gene, one allele floxed Atg16L1 and other allele Atg16L1 $\delta\text{WD}$ , these mice can be considered as heterozygous  $\delta\text{WD}$  mice, which showed no difference compared with WT mice in previous studies) were orally gavaged with *S. Typhimurium* strain JH3009<sup>δSopF</sup>. Food and water were removed 4 hours prior to the challenge. Weight curve, survival curve, *S. Typhimurium* dissemination to liver and spleen were determined by the methods mentioned in sections 2.8 and 2.9.

## **2.24 JH3009<sup>δSopF</sup> infection in $\delta\text{WD}$ mice**

8-12 weeks old  $\delta\text{WD}$  mice and littermate control mice were oral gavaged with *S. Typhimurium* strain JH3009<sup>δSopF</sup>. Food and water were removed 4 hours prior to the challenge. Weight curve, survival curve, *S. Typhimurium* dissemination to liver and spleen were determined by the methods mentioned in sections 2.8 and 2.9.

## **2.25 Filipin staining in MEFs**

WT and  $\delta\text{WD}$  MEFs were seeded on coverslips at the concentration of 10000 cells per well in 24 well plates. After 48 hours, the cells were fixed with 2.5% Paraformaldehyde (PFA) in PBS and then stained with 0.1 $\mu\text{g}/\text{ml}$  of Filipin (Sigma, F4767) for 16 hours. Cells were washed and mounted with Fluoromount-G (Cambridge Bioscience). Cells were imaged on a Zeiss Imager M2 Apotome microscope with a 63x, 1.4 NA oil-immersion objective.

## **2.26 Membrane repair assay with digitonin.**

WT,  $\delta\text{WD}$  and ATG16L1KO MEFs were seeded in 24 well plates at the concentration of  $1 \times 10^5$  cells per well and allowed to attach overnight. After 48 hours, the cells were treated with 1.25, 2.5, 5, 10, 20, 40 $\mu\text{g}/\text{ml}$  of digitonin diluted in Tyrode's buffer

(10 mM HEPES, 10 mM glucose, 5 mM potassium chloride, 140 mM sodium chloride, 1 mM EGTA, 1 mM magnesium chloride, 2 mM calcium chloride, pH 7.4) for 20 min at 37 °C. Then cells were washed with PBS<sup>+/+</sup> (including Calcium) and the media is replaced with Tyrode's buffer with calcium for 10 minutes to allow the membrane to repair. Then cells were stained with 0.4mg/ml of Propidium Iodide (PI) dissolved in Tyrode's buffer with calcium. Cells were fixed with 2.5% PFA in PBS and counterstained with DAPI. The cells were imaged on a Zeiss microscope with a 10X objective. Three wells were seeded for each concentration/cell type. One image per well was taken to determine the percentage of membrane damaged cells in each digitonin concentration/cell type. The percentage of cells with membrane damage was determined by the numbers of PI-stained nuclei divided by the numbers of DAPI stained nuclei. The data were presented as percentage of membrane damaged cells in all cells and analyzed via Bonferroni post test in two way ANOVA.

## **2.27 mCherry-D4H transfection in MEFs**

WT and  $\delta$ WD MEFs were seeded on coverslips at the concentration of 10000 cells per well in 24 well plates and allow the cells to attach overnight. The next day, cells were transfected with mCherry-D4H with Lipofectamine LTX according to the manufacturer's instructions. Briefly, DNA (800ng/well) and Lipofectamine LTX (1 $\mu$ l/well) were diluted in Opti-MEM (Gibco) and then mixed by a vortex. The mixture was incubated at room temperature and then added to the cells. Cells were fixed with 2.5% PFA in PBS at 48 hours post transfection. Cells were washed and mounted with Fluoromount-G (Cambridge Bioscience) overnight. The next day, cells were imaged on a Zeiss Imager M2 Apotome microscope with a 63x, 1.4 NA oil-immersion objective. The CTCF(corrected total cell fluorescence) was analyzed by ImageJ software and calculated with this formula: the corrected total cell fluorescence (CTCF).  $CTCF = \text{Integrated Density} - (\text{Area of selected cell} \times \text{Mean fluorescence of background readings})$ . Image of 30 random single WT or cells were taken to determine the CTCF value by ImageJ. Data were presented as mean  $\pm$  SD and

analyzed by student's t test.

WT and  $\delta$ WD MEFs were transfected with mCherry-D4H as mentioned above. Transfected MEFs were infected with JH3009 (GFP expressing *Salmonella*) at the MOI of 40. Then cells were washed 3 times with PBS and extracellular *S. Typhimurium* was removed by culturing in DMEM supplied with 250ng/ml of gentamycin. Cells were fixed with 2.5% PFA at 4hours post infection. After washing, cells were counterstained with 4', 6 diamidino-2-phenylindole (DAPI) (Thermo Fisher Scientific, 10116287) and mounted with Fluoromount-G (Cambridge Bioscience). Cells were imaged on a Zeiss Imager M2 Apotome microscope with a 63x, 1.4 NA oil-immersion objective. mCherry-D4H is a fluorescent probe that binds to cholesterol on the cytosolic leaflet of the plasma membrane and intracellular organelles. The co-localization of cholesterol and *Salmonella* was determined by the mCherry surrounding of GFP-labelled *Salmonella* strain JH3009.

## **2.28 Cholesterol visualization after cholesterol drug treatment.**

WT and  $\delta$ WD MEFs were plated at  $1 \times 10^5$  cells per well in 24-well tissue culture plates with glass coverslips. On the next day, MEFs were transfected with mCherry-D4H as described in section 2.28. At 48 hours post transfection, cells were treated with 30  $\mu$ M T0901317 (Sigma Aldrich, T2030) or 3  $\mu$ g ml<sup>-1</sup> U18666A (Sigma Aldrich, 3309-71-2) for 4 h and 24 h respectively. Then cells were fixed with 2.5% PFA in PBS and mounted with Fluoromount-G (Cambridge Bioscience) overnight. The next day, cells were imaged on a Zeiss Imager M2 Apotome microscope with a 63x, 1.4 NA oil-immersion objective.

## **2.29 *S. Typhimurium* replication in MEFs after T0901317 treatment**

WT and  $\delta$ WD MEFs were seeded in 24 well plates at the concentration of  $1 \times 10^5$  cells per well. On the next day, cells were infected with *S. Typhimurium* strain JH3009 at the MOI of 40 for 20 minutes. Cells were washed with PBS 3 times and treated with 250 ug/ml of gentamycin for 2 hours to kill the extracellular bacteria. Then the medium is changed to DMEM supplied with 50ng/ml gentamycin for long term culture. Cells were lysed with 0.1% deoxycholic acid at 2,4, 6 and 8 hours post infection. The CFU counts at each time point and intracellular growth was determined as mentioned in section 2.7.

## **2.30 Filipin Staining of the small intestine**

Small intestine from  $\delta$ WD, WT,  $\delta$ WD<sup>IEC</sup> mice and control mice were harvested, flushed with ice cold PBS and fixed in 10% neutral buffered formalin (Sigma, HT501128). Then tissues were dehydrated overnight in an automatic tissue processor (Lecia, ASP300S) with the process of 70% ethanol for 1 hour, 80% ethanol for 1.5 hours, 90% ethanol for 2 hours, ethanol absolute for 1, 1.5 and 2 hours, xylene for 0.5, 1 and 1.5 hours, paraffin wax for 1, 2 and 2 hours. The dehydrated tissues were submerged with melted paraffin (Sigma, P2558) and embedded with an embedding station (Leica, EG1150). 4 micron thick sections were obtained as described in section 2.12. Prior to staining, tissue sections were rehydrated in the following procedure:

1. Histoclear (National diagnostics) I for 5 minutes
2. Histoclear II for 5 minutes
3. 100% ethanol for 3 minutes
4. 100% ethanol for 3 minutes
5. 95% ethanol for 3 minutes
6. 95% ethanol for 3 minutes

7. 75% ethanol for 3 minutes

8. Rinsing under running tap water for 5 minutes

Then the small intestine was incubated in  $100 \mu\text{g ml}^{-1}$  filipin III (Sigma) diluted in PBS<sup>+</sup> for 2 h at room temperature and counterstained with 0.4mg/ml of PI. The sections were imaged with Zeiss Imager M2 Apotome microscope with a 20x objective.

## **3. Generation and identification of mice that lack WD domain of Atg16L1**

### **3.1 Introduction**

#### **3.1.i. Background**

Recruitment of LC3 to endolysosome compartments requires the ATG16L1:ATG5-ATG12 complex to conjugate LC3 to PE in the endo-lysosome membrane. Knock out of Atg16L1, Atg5, or Atg12 in mice results in neonatal lethality because they are unable to adapt to the starvation that follows the loss of placental nutrition. Mice with tissue-specific loss of autophagy survive, but the tissues lacking autophagy show signs of inflammation and tissue damage because they accumulate ubiquitin-positive inclusions containing protein aggregates (Kuma, Komatsu et al. 2017). Mice lacking Atg5, Atg12 or Atg16L1 in specific tissues can be generated to study LAP but the simultaneous loss of autophagy will make it impossible to determine if loss of function results from loss of autophagy, or LAP, or both. An alternative approach to studying LAP *in vivo* has focused on the inactivation of RUBICON (Martinez, Malireddi et al. 2015, Martinez, Cunha et al. 2016). RUBICON is upstream of LC3 recruitment to endolysosome compartments and *rubcn*<sup>-/-</sup> myeloid cells are LAP-deficient and show defects in clearance of fungi, bacteria, and dying and apoptotic cells. Unfortunately, the RUBICON<sup>-/-</sup> mice develop an autoimmune systemic lupus erythematosus (SLE) (Martinez, Cunha et al. 2016, Heckmann, Boada-Romero et al. 2017) and have elevated levels of inflammatory cytokines in serum making them unsuitable for studies of infection *in vivo*.

#### **3.1.ii. Domains of ATG16L1 important for autophagy and LAP.**

Experiments by Oliver Florey and colleagues (Fletcher, Ulferts et al. 2018) studied

recruitment of LC3 to endosomes and lysosomes subjected to osmotic stress by lysosomotropic agents as a model for non-canonical autophagy/LAP (LAP). They showed that in contrast to autophagy, the PI3 kinase activity of VPS34 and recruitment of WIPI to membranes were not required for LAP. Reconstitution experiments using ATG16L1<sup>-/-</sup> cells showed that ATG16L1 lacking the WD domain was able to recruit LC3 to autophagosomes during autophagy, but was not able to recruit LC3 to endosomes swollen by lysosomotropic agents such as monensin. Site-directed mutation guided by a bioinformatic approach to identify amino acids likely to be involved in protein-protein interactions within the WD domain showed that N453, F467 and K490 are important for LAP.

Parallel studies by Lystad et al (2019) used liposome pull-down assays to identify membrane binding sites in ATG16L1. Two membrane-binding regions were identified, the first domain was located on aa 11-44 of the N-terminus. The first aa 11-28 are amphipathic  $\alpha$ -helix which is responsible for ATG5 interaction, aa 28-44 form an  $\alpha$ -helix and are also important for binding with both ATG5 and liposomes (Otomo, Metlagel et al. 2013, Kim, Hong et al. 2015). The second membrane binding domain was located in the region of aa 266-319 (Lystad, Carlsson et al. 2019). This region was not essential for LC3 lipidation during autophagy induced by starvation. The role of both binding domains in LAP was examined by following LC3 lipidation of zymosan-induced phagosomes in ATG16L1 KO RAW264.7 cells (Lystad, Carlsson et al. 2019). The N-terminal membrane binding sites (aa 1-44) were confirmed to be essential for both autophagy and LAP while the C-terminal membrane binding sites (aa 266-319) and the WD domain were essential for LAP but not autophagy.

### **3.1.iii. Generation of mice defective in non-canonical autophagy/LAP.**

The studies above showed that the WD domain of ATG16L1 was required for LAP but not autophagy. This prompted the lab to generate mice lacking the WD domain of ATG16L1 to study the role played by non-canonical autophagy/LAP in vivo. A stop

codon was introduced at position E230 of Atg16L1 to preserve the ATG5 binding domain and CCD WIPI2b binding site for autophagy and remove residues in the WD domain required for LAP. The mice were named  $\delta$ WD mice due to the knockout of the WD domain, they do however lack both the WD and the linker domains of ATG16L1.

In the experiments below cells taken from the mice were analysed using standard assays for autophagy and LAP (Figure 3.1 and 3.2). Figure 3.1 shows the autophagy pathway where substrates are bound to adaptor protein p62 which brings them into autophagosomes by binding LC3 in the autophagosome membrane. Autophagy results in degradation of both p62 and LC3 which can be measured by western blot. Steady state levels of p62 and LC3 are higher in autophagy KO cells (bottom left). Autophagy leads to conversion of LC3I to LC3II, which can be seen by increased mobility of LC3 on western blot, or formation of LC3 puncta by microscopy (bottom right). LAP can be analyzed by a method referred to as LAP assay. BMDMs were generated from mice and treat with Zymosan particles or polystyrene beads which are good substrates for phagocytosis. The presence of LAP can be determined via the recruitment of LC3 to phagosomes formed after uptake of Zymosan particles or polystyrene beads (figure 3.2).

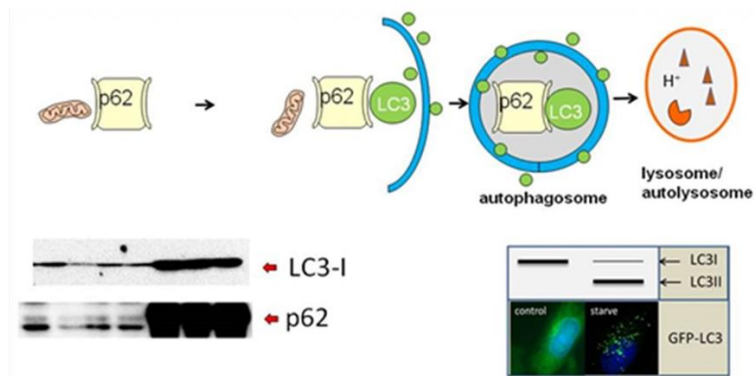


**Figure 3.1 Assay for determines autophagy level.** Cargos are recognized by p62/SQSRM 1 protein. Both p62/SQSRM 1 and LC3 are part of autophagosome and degrade in lysosomes (top

panel). During the process of autophagy, LC-1 is transformed into LC3-II. A block in autophagy causes p62/SQSRM1 accumulation (bottom left panel). Autophagosomes can be also identified by LC-3 positive puncta after starvation (bottom right panel).

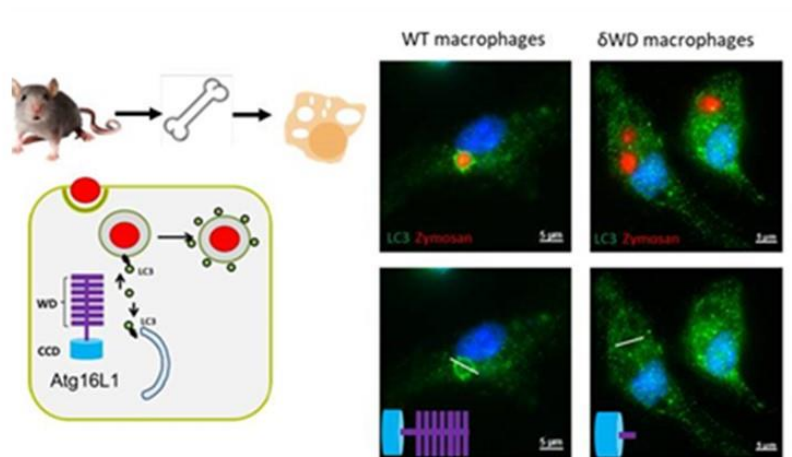


**Figure 3.2 Determine the presence of LAP by Zymosan phagocytosis.** Bone marrow cells were isolated from mice and differentiated into bone marrow derived macrophages (BMDMs). Then BMDMs were feed with Zymosan and fixed for LC-3 staining. The presence of LAP is determined by LC-3 positive puncta which surround zymosan.

## 3.2 Results

### 3.2.i. Generation of $\delta$ WD mice.

Atg16L1 protein in mammalian cells carries C-terminus WD40 repeats, which are reported recently to play a role in non-canonical autophagy or LAP *in vitro* (Fletcher, Ulferts et al. 2018). To examine the role played by the WD repeat *in vivo*, mouse models lacking WD40 domain were generated by Maryam Arasteh, a Ph.D student in our lab. Translation of the WD40 domain was prevented by introducing two stop codons after glutamate 230 in exon 6. This site was chosen so it would preserve the WIPI2b binding site which is required for autophagy. The final vector for mouse embryonic stem cell (ES) transfection contains bovine growth hormone polyadenylation site (bGH-pA), frt sequences and a neomycin resistance gene for the positive clone selection (Figure 3.3). The ES cells with correct homologous recombination were identified by PCR and Southern blot and injected into mouse blastocyst and transplanted into surrogate female mice. The presence of the correct mutation in delivered chimeras was identified by PCR. Chimeras with the mutation were crossed with flp mice to remove the neomycin resistance gene via flp-frt mediated excision. The offspring were crossed with C57BL/6 mice to remove the flp gene and the pure heterozygous mice were crossed together to obtain homozygous mice. These mice were named Atg16L1<sup>E230</sup> or  $\delta$ WD mice because they lack the WD domain (Figure 3.4). Further study of  $\delta$ WD revealed that they are fertile and maintain body weight and tissue homeostasis (Rai, Arasteh et al. 2019).

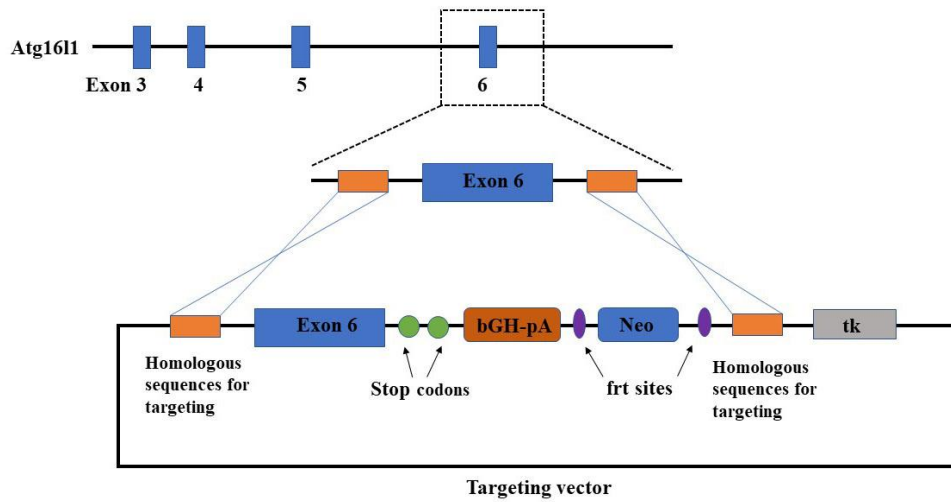


**Figure 3.3** The final vector for mouse embryonic stem cell (ES) transfection. The vector contains bovine growth hormone polyadenylation site (bGH-pA), frt sequences and a neomycin resistance gene for the positive clone selection.



**Figure 3.4** Removal of neomycin cassette and flp gene. Chimeras with the mutation (*Atg16L1<sup>δWD</sup> neo*) were crossed with flp mice (*Atg16L1 Flp*) to remove the neomycin resist gene via flp-frt mediated excision. The offspring (*Atg16L1<sup>δWD</sup>: Atg16L1 Flp*) were crossed with C57BL/6 mice

(Atg16L1: Atg16L1) to remove the flp gene and the pure heterozygous mice (Atg16L1<sup>dWD</sup> neo: Atg16L1).

### 3.2.ii. Genotyping by PCR

$\delta$ WD mice were genotyped by PCR using a set of primers (290-291) designed to bind upstream and downstream of exon 6. The 290-291 primer set amplified a 291 bp fragment in the case of WT control mice. In the case of  $\delta$ WD mice, because of the insertion of stop codons in the vector sequence, the amplified fragments are 639bp, much longer than WT littermate control. The heterozygous mice with one copy of the mutant gene and one copy of the WT gene amplified two fragments, one 639 bp band representing the mutant copy of the gene and one 291 band which represents the WT copy of the gene (Figure 3.5).

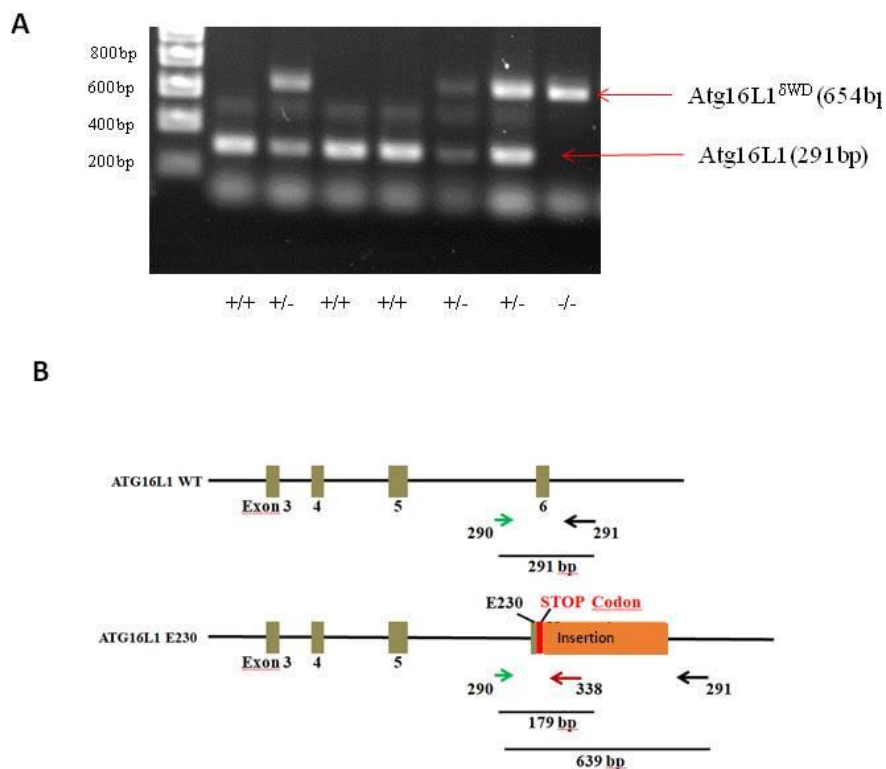


**Figure 3.5 Genotyping of E230/ $\delta$ WD mice.** A. The 290-291 primer set amplified a 291 bp

fragment in the case of WT control mice. In the case of  $\delta$ WD mice, because of the insertion of stop codons in vector sequence, the amplified fragments are 639bp, much longer than WT littermate control. **B.** The binding sites of primers for identification.

### **3.2.iii. Examination of ATG16L1, autophagy and LAP in MEFs.**

Heterozygous mice were crossed in a timed mating and the pregnant females were sacrificed after 13.5 days. The E13.5 embryos were used to make mouse embryonic fibroblasts (MEFs) and lysates were analyzed by western blot (figure 3.6A).

Control MEFs (lanes 1&2, 5&6) expressed  $\alpha$  and  $\beta$  ATG16L1 isoforms and convert LC3I to LC3II after starvation in HBSS. Cells lacking ATG16L1 (FL KO lanes 3 &4) lacked ATG16L1 signal, accumulated p62 and do not convert LC3I to LC3II after starvation with HBSS. MEFs from  $\delta$ WD mice (E230 lanes 7&8) lack full length ATG16L1 but, similar to control MEFs, convert LC3I to LC3II during autophagy and do not accumulate p62.

These results indicate that the full-length ATG16L1 is missing in  $\delta$ WD MEFs.  $\delta$ WD MEFs also showed a normal level of autophagy while ATG16L1 full-knockout MEFs didn't show any sign of autophagy after starvation. Autophagy level is determined via the transformation of LC-3I to LC-3II and degradation of p62/SQSRM1. Figures were taken from a published manuscript from our lab, and the  $\delta$ WD was labeled as E230 in the figures (Rai, Arasteh et al. 2019). I acknowledge Dr. Shashank Rai for providing this piece of valuable data.

### **3.2.iv. Examination of the truncated ATG16L1 by western blot in tissues**

Protein extracts were isolated from liver, brain and muscle of  $\delta$ WD and WT mice. Then protein concentrations were measured by BCA assay and loaded on a precast gel.

Liver, brain and muscle from WT mice showed a full-length ATG16L. Figure 3.6 B lane 1 represents liver of  $\delta$ WD mice with two bands representing  $\alpha$  (63kDa) and  $\beta$  (71 kDa) isoforms, lane 2 represent muscle and lane 3 represents the brain which expressed the  $\beta$  isoform. The  $\delta$ WD tissue showed a truncated version of ATG16L1 around 30 kDa (Figure 3.4 B lanes 4,5 and 6). These results indicate that the WD domain is knocked out in the tissue of  $\delta$ WD mice. Figures were taken from a published manuscript from our lab, and the  $\delta$ WD was labeled as E230 in the figures (Rai, Arasteh et al. 2019).

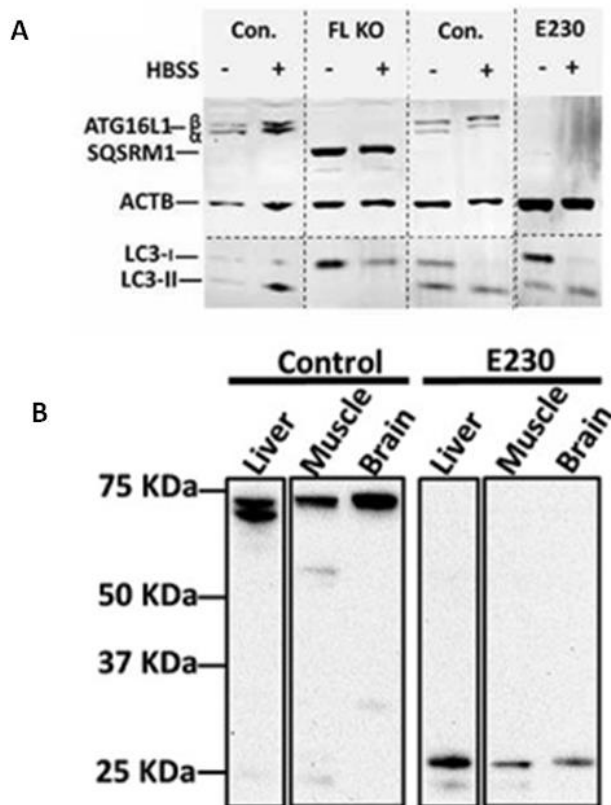


**Figure 3.6 A&B.** Analysis of ATG16L1 and autophagy in cells from  $\delta$ WD mice.

**A.** Analysis of MEFs. MEFs generated from control mice (Con: lanes 1,2 and 5&6), autophagy defective mice\* (FL KO: lanes 3&4) or  $\delta$ WD mice (E230: lanes 7&8) were lysed before and after incubation in HBSS for 2 hours as indicated to activate autophagy. Cell lysates were analyzed by

western blot for the indicated proteins. Antibody against ATG16L1 identified  $\alpha$  (63kDa) and  $\beta$  (71 kDa) isoforms of ATG16L1 which were missing from FL KO and  $\delta$ WD MEFs. HBSS induced conversion of LC3I to LC3II in control and  $\delta$ WD MEFs, but not FL KO. FL KO MEFs showed high levels of p62 absent from the other cells. \* FL KO cells were derived from a mouse carrying an additional truncation to the CCD of ATG16L1 to E226 that prevents WIPI binding and autophagy (Rai, Arasteh et al. 2019).

**B.** Tissue western blot to examine the truncated ATG16L1 in  $\delta$ WD mice. Liver, brain and muscle from WT mice showed a full-length ATG16L1. Lane 1 represents the liver of WT mice with two bands representing  $\alpha$  (63kDa) and  $\beta$  (71 kDa) isoforms of ATG16L1, lane 2 represent muscle, and lane 3 represents the brain which lacked the  $\alpha$  isoform. The  $\delta$ WD muscle and brain tissue showed loss of full length ATG16L1 but expressed a truncated version of ATG16L1 around 30 kDa (lanes 4,5 and 6).

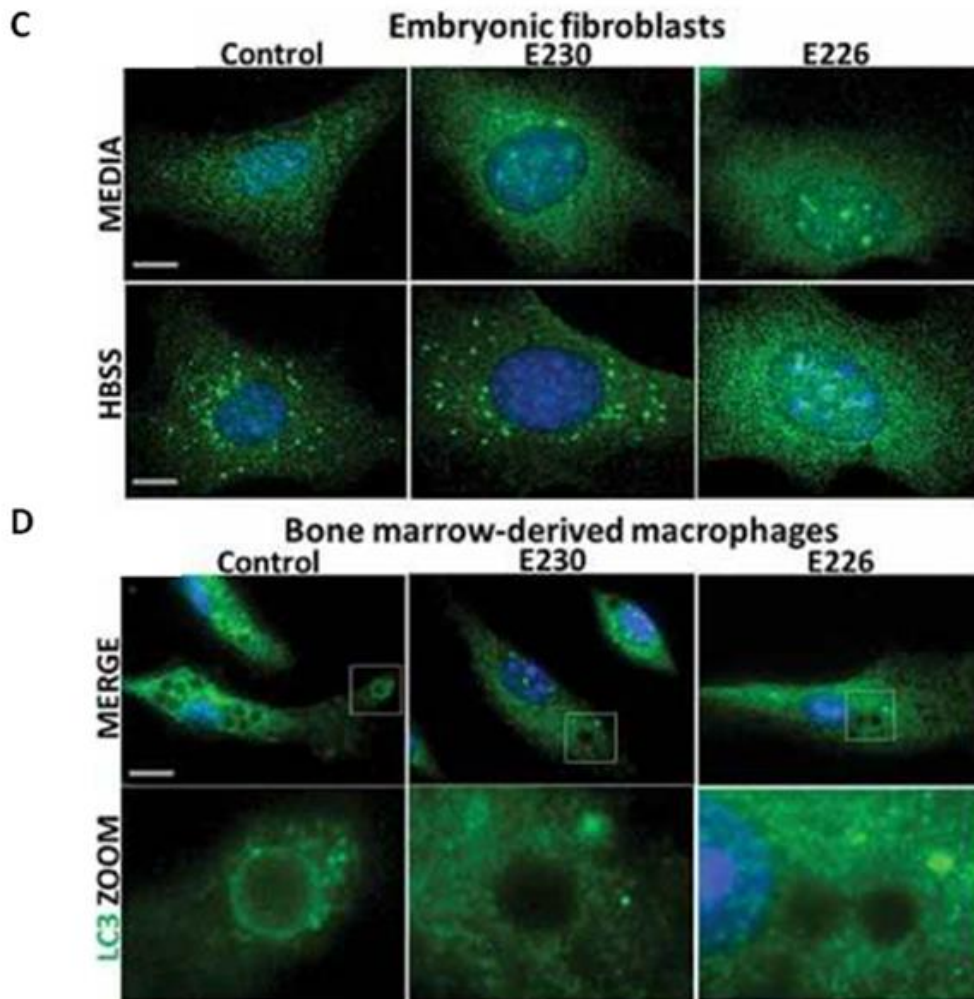


**Figure 3.6 C&D. C. Generation of LC3 puncta following activation of autophagy by HBSS.**

Skin fibroblasts from  $\delta$ WD (E230) and control mice showed LC3-positive puncta (green) after starvation in HBSS. In contrast, no LC-3 positive puncta were observed in FL KO cells (E226).

**D Recruitment of LC3 to phagosomes.** BMDMs from control mice and  $\delta$ WD mice were incubated with Pam3CSK4 coated polystyrene beads to assay for phagocytosis. Cells were incubated with Pam3csk4-coupled polystyrene beads for 1.5 hours in complete media to induce LAP and immunostained for endogenous LC3 (green). Boxed regions highlighting internalised beads are enlarged and shown in the lower panel. Magnification 63X, scale bars 10 $\mu$ m. Although all the BMDMs showed phagocytosis of the beads, only the control BMDMs showed LC3 translocation to phagosomes containing beads. In contrast, phagosomes

containing beads in  $\delta$ WD BMDMs were negative for LC3 which indicates the loss of LAP in  $\delta$ WD mice

### **3.2.v. The status of autophagy and LAP in fibroblasts and macrophages.**

The activation of autophagy was examined via a standard starvation assay involving incubation of cells in HBSS for 2 hours to starve cells followed by immunoblot of LC3-II and p62/SQSTM1 (Figure 3.6A).  $\delta$ WD cells (E230: lanes 7&8) and WT cells (Con: lanes 1&2, 5&6) showed the generation of the faster migrating LC3-II after starvation indicating the conjugation of LC3 to PE during the formation of autophagosomes. Furthermore, levels of autophagy substrate p62/SQSTM1 in  $\delta$ WD MEFs were the same as seen for control. In contrast, the western blots show that Atg16L1 full knockout (FL KO: lanes 3&4) cells were unable to convert LC3I to LC3II and a level of p62/SQSTM1 was increased compared to control. When examined by microscopy (Figure 3.6C) skin fibroblasts from  $\delta$ WD and control mice after starvation in HBSS showed LC3-positive puncta. In contrast, no LC-3 positive puncta were observed in FL KO cells. Figures were taken from a published manuscript from our lab and the  $\delta$ WD was labeled as E230 in the figures (Rai, Arasteh et al. 2019).

Bone marrow stem cells were isolated and cultured in RPMI-1640 with 50ng/ml of M-CSF to generate bone marrow-derived macrophages (BMDMs). BMDMs from control mice and  $\delta$ WD mice were incubated with Pam3CSK4 coated polystyrene beads to assay for phagocytosis (Figure 3.6D). Although all the BMDMs showed phagocytosis of the beads, only the control BMDMs showed LC3 translocation to phagosomes containing beads. In contrast, phagosomes containing beads in  $\delta$ WD BMDMs were negative for LC3 which indicated the loss of LAP in  $\delta$ WD mice (Figure 3.6 D lower panel). Taken together these results suggest that loss of the WD domain of ATG16L1 prevents LAP but doesn't disrupt autophagy. Figures were taken

from a published manuscript from our lab (Rai, Arasteh et al. 2019).

### **3.2.vi. $\delta$ WD mice do not have the pro-inflammatory phenotype seen in mice lacking autophagy in myeloid cells.**

Myeloid cells, including macrophages, neutrophils, DCs and eosinophils, are widely distributed throughout the body and play an important role in innate and adaptive immunity (Bao and Cao 2011, Murray and Wynn 2011). The lysozyme-M-cre system (LysMcre) has been used widely to inactivate genes in myeloid cells. Mice lacking Atg14, Fip200, Atg5, Atg7, or Atg16L1 in myeloid cells show a proinflammatory immune system that generates high proinflammatory cytokine production after stimulation by pathogens and PAMPS, such as lipopolysaccharide (LPS) (Liu, Zhao et al. 2015). The observation that complete loss of ATG16L1 from myeloid cells resulted in increased secretion of proinflammatory cytokines made it possible that a similar phenotype would be seen for  $\delta$ WD mice lacking the  $\delta$ WD domain of ATG16L1. This was tested by comparing the pro-inflammatory responses of BMDM from WD mice with BMDM from control mice, and with mice where LysMcre had been used to induce complete loss of ATG16L1 from myeloid cells. The mice lacking ATG16L1 in myeloid cells were named  $\delta$ ATG16<sup>phage</sup>.

BMDMs from WT control,  $\delta$ WD and  $\delta$ ATG16<sup>phage</sup> mice were treated with 1 $\mu$ g/ml of LPS for 4 hours followed by treatment with BzATP, a P2X7 receptor agonist, for 30 minutes to activate NLRP3. Supernatants were collected and IL-1 $\beta$  concentrations were measured by ELISA. Untreated BMDMs (Mock) and BMDMs only treated with BzATP (BzATP control) showed only a very low basic production of IL-1 $\beta$ , which is below the detection limit of 4pg/ml. IL-1 $\beta$  production in  $\delta$ ATG16<sup>phage</sup> BMDMs rose to 300pg/ml and was significantly higher than the IL-1 $\beta$  production from  $\delta$ WD and control BMDMs, while there is no significant difference between the IL-1 $\beta$  production of  $\delta$ WD and control BMDMs (Figure 3.7 A).

To investigate if the same phenotype would be observed *in vivo*, WT control,  $\delta$ WD and  $\delta$ ATG16<sup>phage</sup> mice were given intraperitoneal injections of either PBS or LPS at the concentration of 10mg/kg. Blood samples were collected at 90 minutes post injection and serum were isolated to measure IL-1 $\beta$  concentration by ELISA. Again, serum from  $\delta$ ATG16<sup>phage</sup> showed a significantly higher concentration of IL-1 $\beta$  (around 150ng/ml) compared to the other groups, both of which were lower than 50 ng/ml. All these data indicate that  $\delta$ WD mice do not have the proinflammatory phenotype seen in autophagy negative mice (Figure 3.7 B).

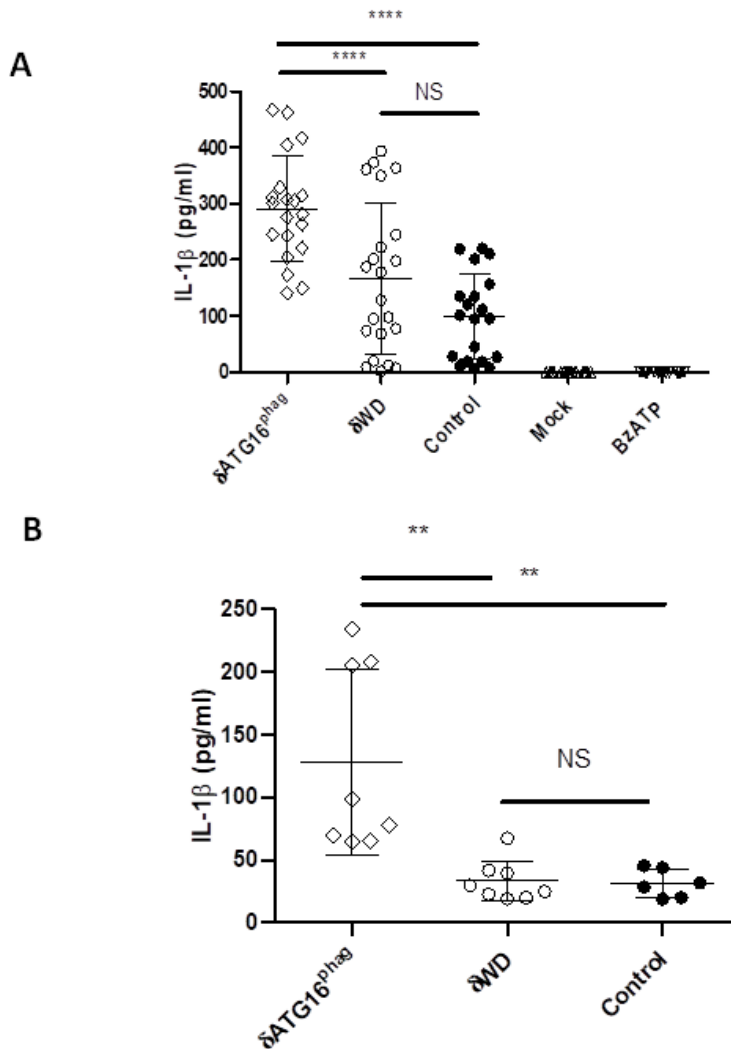


**Figure 3.7 Analysis of proinflammatory responses in  $\delta$ WD mice. A.** IL-1 $\beta$  production in BzATP and LPS treated BMDMs.  $\delta$ WD BMDM, WT BMDM and  $\delta$ ATG16<sup>phage</sup> BMDM were treated with LPS for 4 hours and then BzATP for 30 minutes.  $\delta$ WD BMDM produced a similar

amount of IL-1 $\beta$  while the  $\delta$ ATG16<sup>phage</sup> BMDMs produced a significantly higher amount of IL-1 $\beta$  compared with control mice. The data represents IL-1 $\beta$  concentration in supernatant from 20 independent wells of BMDM. **B** IL-1 $\beta$  production in serum after LPS challenge. Serum from  $\delta$ WD mice showed no difference in IL-1 $\beta$  production compared with WT serum. Serum from  $\delta$ ATG16<sup>phage</sup> showed a significantly higher amount of IL-1 $\beta$  after LPS challenge. The data represents IL-1 $\beta$  concentration in the serum of 8 mice of each strain. The data were analyzed with turkey's test under one-way ANOVA. ( $*p<0.05$   $**p<0.01$ ,  $****p<0.0001$ )

### **3.3 Discussion**

#### **3.3.i. Background**

Atg16L1 possesses a WD40 domain in higher eukaryotes, such as mammals, plants and insects, compared with Atg16L1 in yeast which expresses a much smaller protein made up of the coiled coil domain (CCD) and N-terminal ATG5 binding domain (Fujioka, Noda et al. 2010). The WD domain makes up more than 50% of the protein and is not required for canonical autophagy. Recent work has shown that the WD domain is required for LC3 lipidation at the surface of endocytic compartments, such as macropinosomes and phagosomes, to facilitate its fusion with lysosomes to degrade the contents (Fletcher, Ulferts et al. 2018, Rai, Arasteh et al. 2019). The WD domain also provides a platform for protein interactions to regulate endocytic pathways, which are responsible for the rapid removal of endocytosed materials or pathogens (Malhotra, Warne et al. 2015). Some recent studies also showed that the WD domain interacts with important proteins of pathogen identification, such as NLRs, TRIMs and TMEMs (Travassos, Carneiro et al. 2010, Boada-Romero, Letek et al. 2013, Kimura, Jain et al. 2015). These important functions suggested that the WD domain may have evolved to respond to changes in endocytic compartments such as those that occur during the entry of pathogens or damaged material. One of these responses triggers the recruitment of LC3 to endocytic pathways and this has been called LAP and/or non-canonical autophagy.

This chapter describes mice that are unable to express the WD domain of ATG16L1 because a stop codon has been inserted after the CCD. The mutation preserves the CCD and linker residues up to glutamate at position 230 (E230) of ATG16L1 that are required for WIPI2 binding and autophagy (Dooley, Razi et al. 2014). Expression of the truncated ATG16L1 at the predicted size of 27kDa in MEFs and tissues was confirmed by western blot. Functional assays following the translocation of LC3 to membranes and conversion of LC3I to LC3II showed that the mice maintained autophagy but had a selective loss of non-canonical autophagy/LAP. This suggested that they would be a useful model system to study the role played by non-canonical autophagy/LAP *in vivo*.

Previous reports had shown that loss of the CCD or complete loss of ATG16L1 in myeloid cells disrupts canonical autophagy and caused a rise in pro-inflammatory cytokine production (Saitoh, Fujita et al. 2008, Lu, Yokoyama et al. 2016). Meaningful studies of infection *in vivo* would require that the  $\delta$ WD mice did not show a similar pro-inflammatory phenotype. The pro-inflammatory immune response caused by loss of autophagy from myeloid cells has been shown to slow invasion of pathogens such as influenza virus (IAV). Lu et al, reported that deletion of genes essential for conventional autophagy (e.g. Atg5, Atg7, Atg14, Atg16L1, FIP200) in mice leads to raised pro-inflammatory cytokine expression in the lung, which significantly increased resistance to IAV infection in those mice (Lu, Yokoyama et al. 2016). Thus, we tested the possibility that loss of the WD domain may increase pro-inflammatory cytokine production by following IL-1 $\beta$  production from BMDM incubated with LPS and purine receptor agonist, BzATP, and by challenging mice with LPS and measuring IL-1 $\beta$  production in serum. As reported previously (Lu, Yokoyama et al. 2016), the complete knockout of ATG16L1 in myeloid cells increased IL-1 $\beta$  production from BMDMs and increased levels of IL-1 $\beta$  in serum. In contrast, IL-1 $\beta$  responses to LPS in  $\delta$ WD mice and  $\delta$ WD BMDMs did not differ significantly compared with controls. This was consistent with a previous study from

the lab where  $\delta$ WD mice also did not show any difference in IL-1 $\beta$ , IL-12p70, IL-13 and TNF- $\alpha$  levels in serum compared to WT control mice (Rai, Arasteh et al. 2019). We also measured the frequency of B cells, T cells, macrophages and neutrophils in splenocytes as a measure of immunological homeostasis. These cell populations were the same as control mice showing that the loss of the WD domain did not result in major changes to the immune system. All those data indicate that  $\delta$ WD mice are a good model to study the role of LAP in pathogenic infection.

Rubicon stabilizes the PHOX: NOX2 complex and allows ROS to facilitate the binding of ATG16L1 to the membrane of endo-lysosomes. During the course of this study, a few studies knocked out LAP in myeloid cells by LysMcre driven mediated loss of Rubicon or NOX2. These mice which relied on the knockout of Rubicon, showed a deficiency to remove bacterial and fungal pathogens, as well as apoptotic cells. Deletion of Rubicon also increased production of IL-1 $\beta$ , IL-6 and TNF- $\alpha$  and caused autoimmune disease that resembles systemic lupus erythematosus, and result in a slower growth rate compared with WT mice (Martinez, Malireddi et al. 2015, Martinez, Cunha et al. 2016, Heckmann, Boada-Romero et al. 2017, Heckmann, Teubner et al. 2020). It is hard to predict if these alterations in the immune system would affect infection studies. In contrast, Previous works in our lab showed that  $\delta$ WD mice can maintain tissue homeostasis and preserve normal growth rate over time compared with WT mice (Rai, Arasteh et al. 2019). This makes  $\delta$ WD mice a better model to study the role of LAP in pathogenic infection compared with Rubicon or NOX2 knockout mice.

### **3.3.ii. Summary**

Expression of the WD domain of ATG16L1 can be prevented by inducing 2 stop codons at the end of the CCD of ATG16L1. This prevents translation of the WD domain but preserves the WIPI2B binding sites required for autophagy. These  $\delta$ WD mice showed a loss in LAP but not canonical autophagy. Despite the loss of WD

domain,  $\delta$ WD mice do not have the proinflammatory phenotype seen following the loss of autophagy from myeloid cells. The mice are fertile, have a normal growth rate and maintain tissue homeostasis and are therefore suitable for infection studies.

# **Chapter 4. The loss of WD domain of ATG16L1 promotes *S. Typhimurium* replication ‘in vitro’ and increases *S. Typhimurium* sensitivity ‘in vivo’**

## **4.1 Introduction**

### **4.1.i. Background**

*S. Typhimurium* is an intracellular bacteria that causes a systemic typhoid fever in mice. Several ‘in vitro’ studies using cells in culture suggest that LAP may play an important role in bacterial infections, such as *Legionella dumoffii*, *Burkholderia pseudomallei*, *Listeria monocytogenes* (Schille, Crauwels et al. 2018). The previous chapter showed that cells cultured from mice lacking the WD domain of ATG16L1 were defective in LAP and that the  $\delta$ WD mice did not show the pro-inflammatory phenotype associated with ATG16L1 KO. The  $\delta$ WD mouse, therefore, provides a unique opportunity to study the role played by the WD domain of ATG16L1, and by implication, LAP during infection ‘in vivo’. In this chapter  $\delta$ WD mice, and cells derived from them were used to determine if the loss of WD domain caused increased sensitivity to *S. Typhimurium* infection.

## **4.2 Results**

### **4.2. i. The loss of WD domain of ATG16L1 promotes *S.***

#### ***Typhimurium* replication in fibroblasts and epithelial cells.**

MEFs and HEK cells were seeded in 6 well plates to allow attach overnight. On the next day, cells were infected with *S. Typhimurium* strain JH3009 for 20 minutes. Cells were washed with PBS 3 times treated with 250 ug/ml of gentamycin for 2 hours to

kill the extracellular bacteria. Then cells were lysed with 0.1% deoxycholic acid and serial dilutions of lysates were plated on streptomycin agar plates and CFUs were counted to calculate intracellular bacteria.  $\delta$ WD HEKs had significantly higher intracellular *Salmonella* than WT HEKs at 8 hours post-infection while the reading at 2 hours and 4 hours post infection showed no difference (Figure 4.1 A). The intracellular growth was determined by CFU at 8 hours post infection divided by CFU at 2 hours post infection. (Figure 4.1B). This data is mostly used to determine the replication rate of intracellular bacteria. The rate of growth of *Salmonella* was greater in  $\delta$ WD cells. To further investigate the role of autophagy and LAP in *S. Typhimurium*, a similar experiment was conducted with WT,  $\delta$ WD and Atg16L1 full knockout MEFs. The CFU counts from Atg16KO MEFs showed the highest counts and were significantly higher than WT MEFs at both 4hours and 8 hours post infection ( $p<0.01$  at 4 hours and  $p<0.0001$  at 8 hours). The CFU from  $\delta$ WD MEFs were intermediate between WT and full Atg16KO MEFs, counts from  $\delta$ WD MEFs were significantly higher than WT MEFs at 8 hours post infection ( $p<0.01$ ) (Figure 4.1 C). ATG16L1 full knockout MEFs have a significantly higher intracellular growth compared with both  $\delta$ WD and WT MEFs ( $p<0.05$  compared with  $\delta$ WD MEFs and  $p<0.0001$  compared with WT MEFs), while intracellular growth in  $\delta$ WD MEFs was significantly higher compared with WTMEFs ( $p<0.001$ ) (Figure 4.1D) These data indicate that *S. Typhimurium* has a higher replication rate in  $\delta$ WD MEFs compared with WT MEFs. A potential role of LAP/WD domain in controlling *S. Typhimurium* infection was also identified.

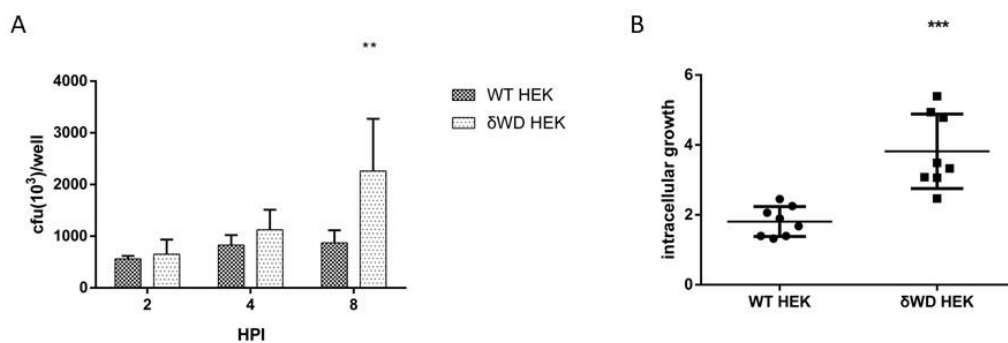


**Figure 4.1 A&B Intracellular *S. Typhimurium* replication in HEK cells.** A  $\delta$ WD and WT HEK cells were seeded in 24 well plates and infected with *S. Typhimurium*. Intracellular *S. Typhimurium* replication was assessed from CFUs. A significantly higher number of *S. Typhimurium* were found in  $\delta$ WD HEK compared with WT HEK at 8 hours post infection. The data represent CFU reading from 6 independent wells and were analyzed with Bonferroni post test in two way ANOVA (\*\* $p < 0.01$ ). B The intracellular growth in  $\delta$ WD and WT HEK was determined by dividing CFU at 8 hours post infection with those at 2 hours post infection. The intracellular growth in  $\delta$ WD HEKs was significantly higher than in WT HEKs. The data were analyzed with student's t test (\*\* $p < 0.01$ ).

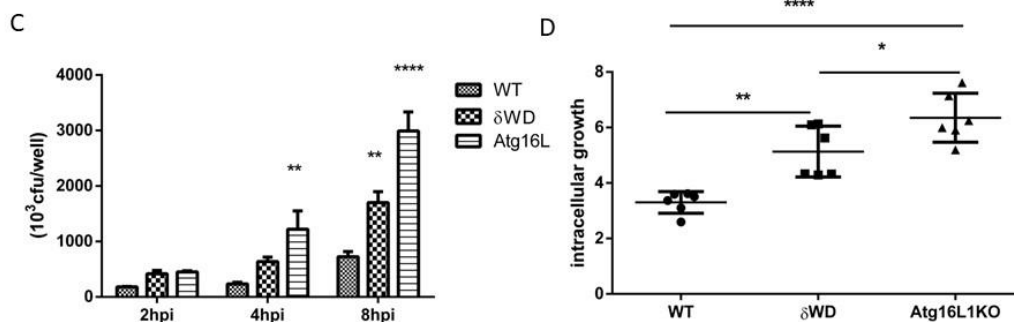


**Figure 4.1 C&D Intracellular *S. Typhimurium* replication in MEFs.** C Intracellular Replication in  $\delta$ WD, WT and Atg16L1 full knockout MEFs. MEFs were infected with *S. Typhimurium* and intracellular replication were assessed from CFUs. The data represent CFU reading from 6 independent wells and were analyzed with Bonferroni post test in two way ANOVA (\*\* $p < 0.01$ , \*\*\*\* $p < 0.0001$ ). D Intracellular growth was determined in  $\delta$ WD, WT and Atg16L1 full knockout MEFs. The data were analyzed with Turkey test under one way ANOVA (\*\* $p < 0.01$ , \*\*\*\* $p < 0.0001$ ).

#### 4.2.ii. The Loss of the WD domain of ATG16L1 increases the sensitivity of mice to *S. Typhimurium* infection.

To further investigate the role of the WD domain in *S. Typhimurium* infection.,  $\delta$ WD mice and WT littermate controls were infected with  $1.5 \times 10^8$  CFU of *S. Typhimurium* strain JH3009 by oral gavage and observed and weighed every day. Any mice which

suffered 20% weight loss or greater were sacrificed. The weight curve is shown in Figure 4.2 A showed more rapid weight loss in  $\delta$ WD mice (about 15% on average) compared with littermate controls (about 6% on average) at 6 days post-infection. Similarly, 7 of 20 (35%) of  $\delta$ WD mice died or suffered 20% weight loss before the challenge endpoint at 6 days. In contrast, only 1 of the 20 (5%) control mice died before the endpoint (Figure 4.2 B). Then mice

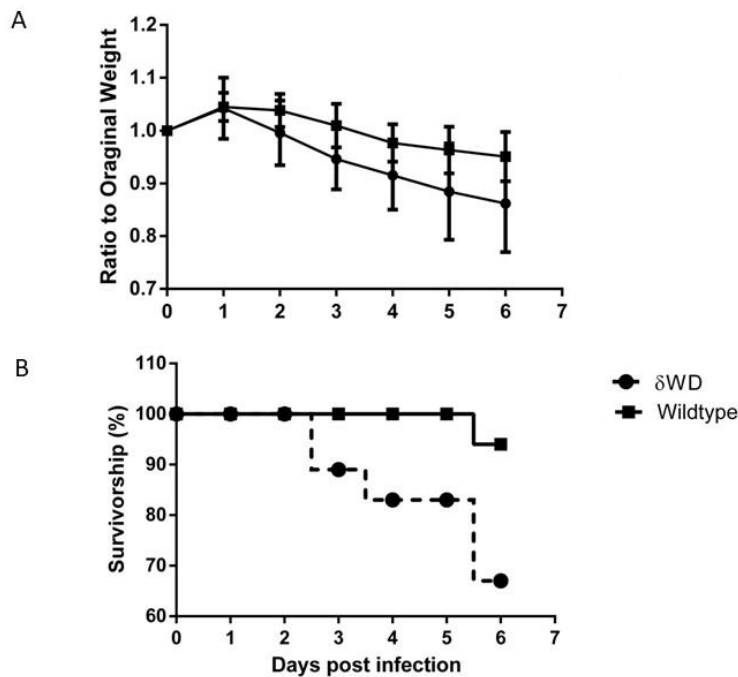


**Figure 4.2 A&B *S. Typhimurium* infection in  $\delta$ WD and WT mice.** 20 mice from each group were infected with  $1.5 \times 10^8$  CFU of *S. Typhimurium* strain JH3009. A. Weight curve after indicated days. B. Survival curve over indicated days, 7 of 20 (35%) of  $\delta$ WD mice died or suffered 20% weight loss before the challenge endpoint at 6 days. In contrast, only 1 of the 20 (5%) control mice died before the endpoint.

were sacrificed on sixth day post infection. The liver and spleen were harvested and observed for gross signs of tissue damage and lysed to measure bacterial dissemination by colony counting (Figure 4.2C&D). Obvious infectious foci were observed in livers and spleens from  $\delta$ WD mice (Figure 4.2C). Bacterial infiltration

was assessed by homogenizing liver or spleen and plating serial dilutions on agar plates for estimation of CFU (Figure 4.2D). A two-fold increase in bacterial dissemination in liver and spleen were observed in  $\delta$ WD mice compared with WT mice.

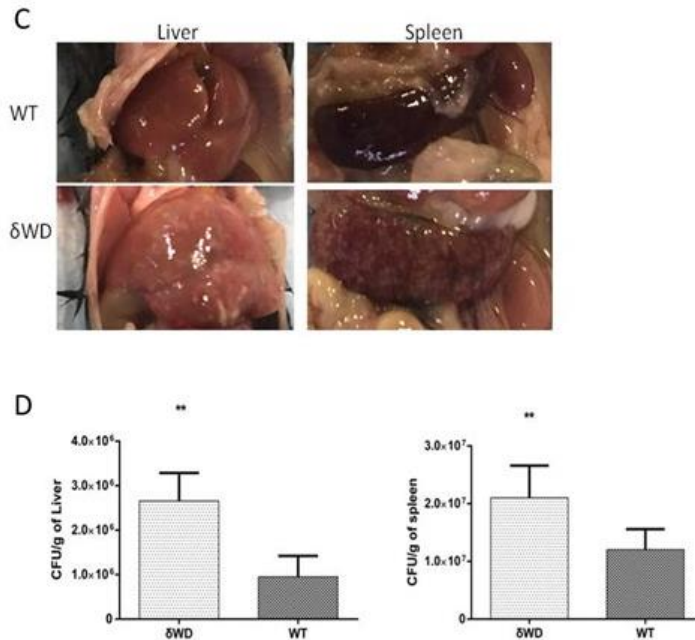


**Figure 4.2 C&D S. Typhimurium infection in  $\delta$ WD and WT mice.** C. Representative pictures of tissues from infected mice.  $\delta$ WD has a severely damaged liver and spleen compared with WT mice. *S. Typhimurium* dissemination to liver and spleen was assessed from CFU counts from tissue homogenates of 20 mice. A two-fold increase in bacterial dissemination to liver and spleen were observed in  $\delta$ WD mice compared with WT mice. The data were analyzed with student's t test (\*\* $p < 0.01$ ).

Serum were isolated and used to determine the pro-inflammatory cytokine level, such as IL-1 $\beta$ , IL-6, IL-13 and TNF- $\alpha$ , by Luminex assay (Figure 4.2E). Serum from  $\delta$ WD mice have a significantly lower level of IL-1 $\beta$ , IL-6, IL-13 compared with the serum from WT mice (Figure 4.2 E,  $p < 0.05$  for IL-1 $\beta$ ,  $p < 0.05$  for IL-6,  $p < 0.001$  for IL-13), while the level of TNF- $\alpha$  didn't show any difference.

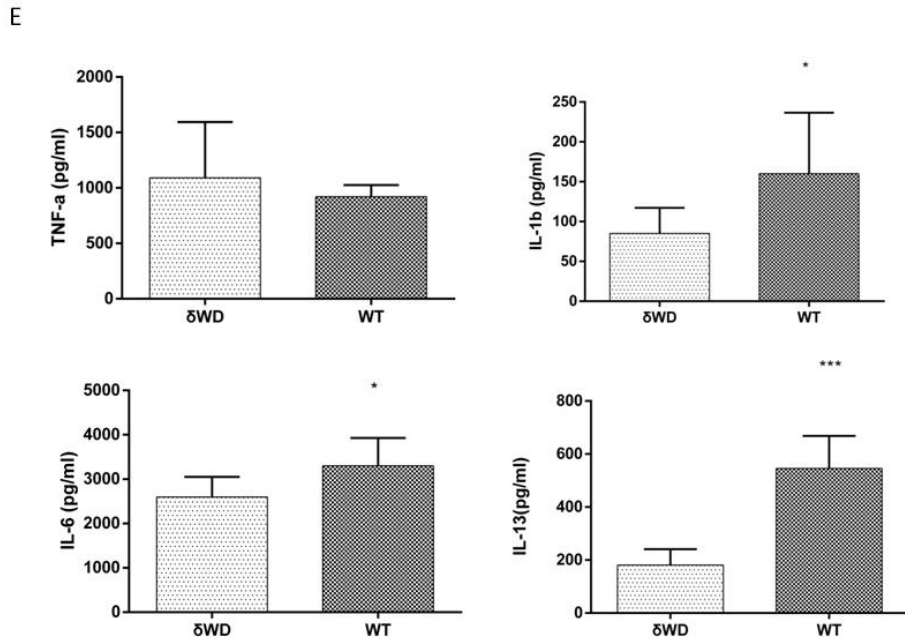


**Figure 4.2E S. Typhimurium infection in  $\delta$ WD mice and WT controls.** E. Serum were isolated and used to determine the pro-inflammatory cytokine level, such as IL-1 $\beta$ , IL-6, IL-13 and TNF- $\alpha$ , by Luminex assay. Serum from  $\delta$ WD mice have a significantly lower level of IL-1 $\beta$ , IL-6, IL-13 compared with the serum from WT mice, while the level of TNF- $\alpha$  didn't show any difference. The data were analyzed with student's t test (\* $p < 0.05$ , \*\* $p < 0.01$ , \*\*\* $p < 0.001$ ).

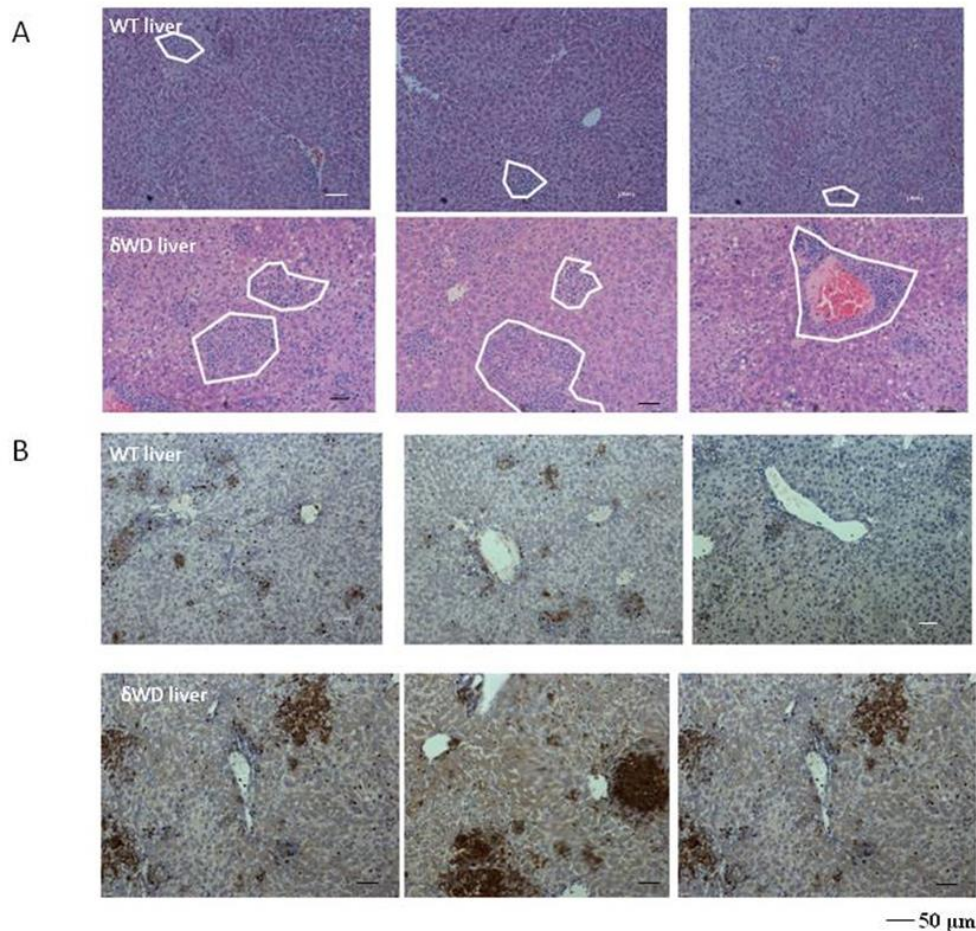


**Figure 4.3 Liver histology from *S. Typhimurium* infected  $\delta$ WD mice and WT controls. **A.** H&E staining of liver from infected  $\delta$ WD mice and WT controls. Liver from infected  $\delta$ WD mice showed large areas of granuloma (outlined in white). **B.** IHC (CD11b) staining of the infected liver to stain macrophages. The granuloma of  $\delta$ WD liver showed large clusters of CD11b positive macrophages.**

The above results showed increase dissemination of bacteria in  $\delta$ WD mice lacking the WD domain of ATG16L1. Increased bacterial dissemination to tissue induce macrophages infiltration, which is confirmed via histology and FACS analysis.

Figure 4.3 shows H&E staining of liver from infected  $\delta$ WD mice and control mice. Each picture represents a separate mouse. Large areas of granuloma (Figure 4A) were observed in  $\delta$ WD liver, while only small areas of granuloma were observed in WT liver. Granulomas are big clusters of macrophages that attempt to isolate the area of infection when the immune system can't eliminate the pathogen and are generally

considered as areas of persistent infection. The areas of granuloma were also examined by immunohistochemistry (IHC) of CD11b staining, which confirmed the cluster of macrophages in granuloma (Figure 4.3 B.) H&E staining of the spleen is shown in Figure 4.4 A. Damaged areas were found in  $\delta$ WD spleen and were circled in white but not found in WT spleen. H&E stainings of the small intestine after infection were shown in Figure 4.4 D, not much difference was observed between WT mice and  $\delta$ WD mice.

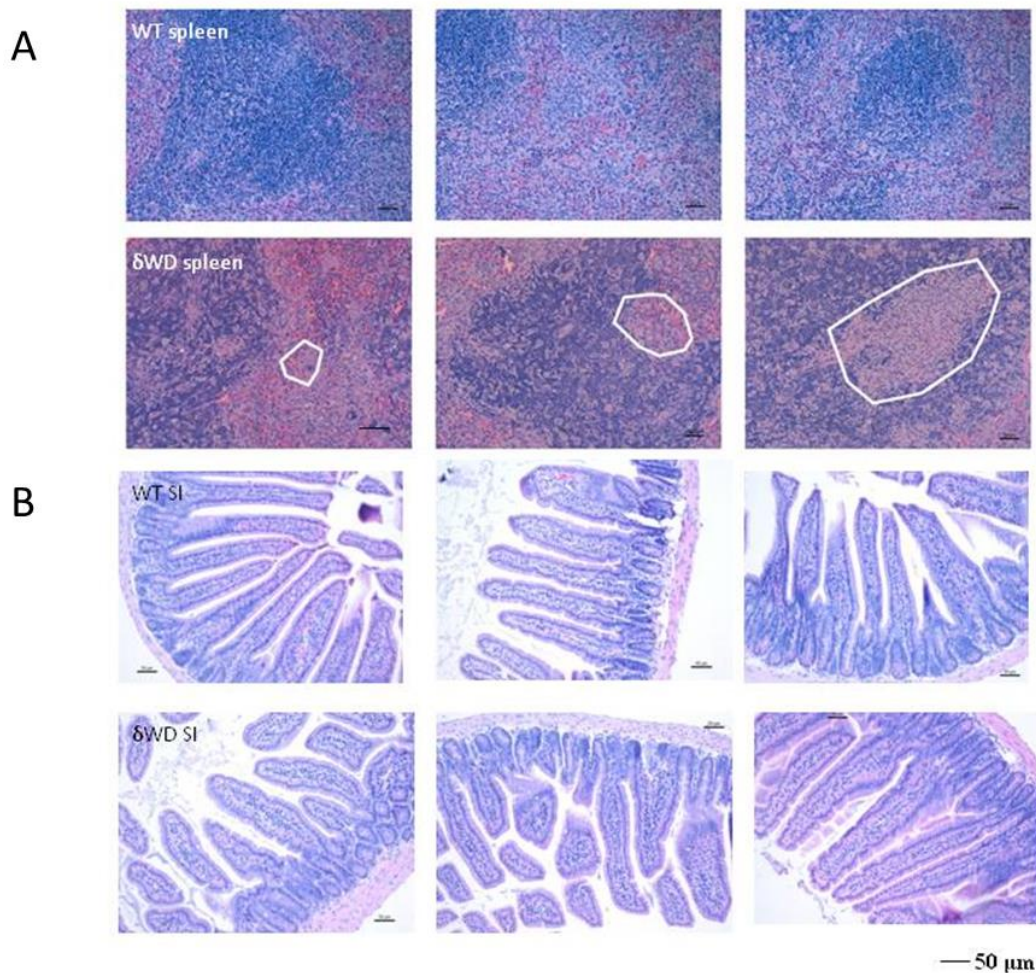


**Figure 4.4 Spleen and small intestine histology from *S. Typhimurium* infected  $\delta$ WD mice and WT controls. A.** H&E staining of infected spleen, area of damage were observed in  $\delta$ WD spleen, but not WT spleen. **B** H&E staining of small intestine from infected mice. Not much difference was observed between WT and  $\delta$ WD mice.

### **4.2.iii. Increased lymphocyte infiltration was observed in the livers of $\delta$ WD mice**

Liver lobes were cut into small pieces in collagenase buffer and lymphocytes from liver were isolated. Lymphocytes from the livers of  $\delta$ WD mice and WT mice were measured by staining with 2 sets of antibodies, one for T cells, other for macrophages and neutrophils. Figures 4.5 and 6 show the gating strategy for  $CD3^+CD4^+$  and  $CD3^+CD8^+$  and myeloid cells. Bacterial dissemination and liver damage are linked with lymphocytes infiltration into liver. Lymphocytes were first gated with CD3 positive T cells and then gate for CD4 (Th) and CD8 (Tc). Significant more Th cells and Tc cells were detected in the liver of  $\delta$ WD mice compared with WT mice. Myeloid cells were separated by CD11b and F4/80. Bone marrow-derived (BDM) monocytic macrophages are infiltrated macrophages and identified by high expression of CD11b and F4/80. Kupffer cells are liver residential macrophages and express a lower level of F4/80 compared with BDM monocytic macrophage. Neutrophils are identified by their expression of CD11b and Ly6G. Significant more infiltrated macrophages ( $CD11b^+F4/80^{hi}$ ) and neutrophils ( $CD11b^+Ly6G^+$ ) were detected in livers of  $\delta$ WD mice compared with WT mice, while less Kupffer cells were found in the livers of  $\delta$ WD mice compared with WT mice.

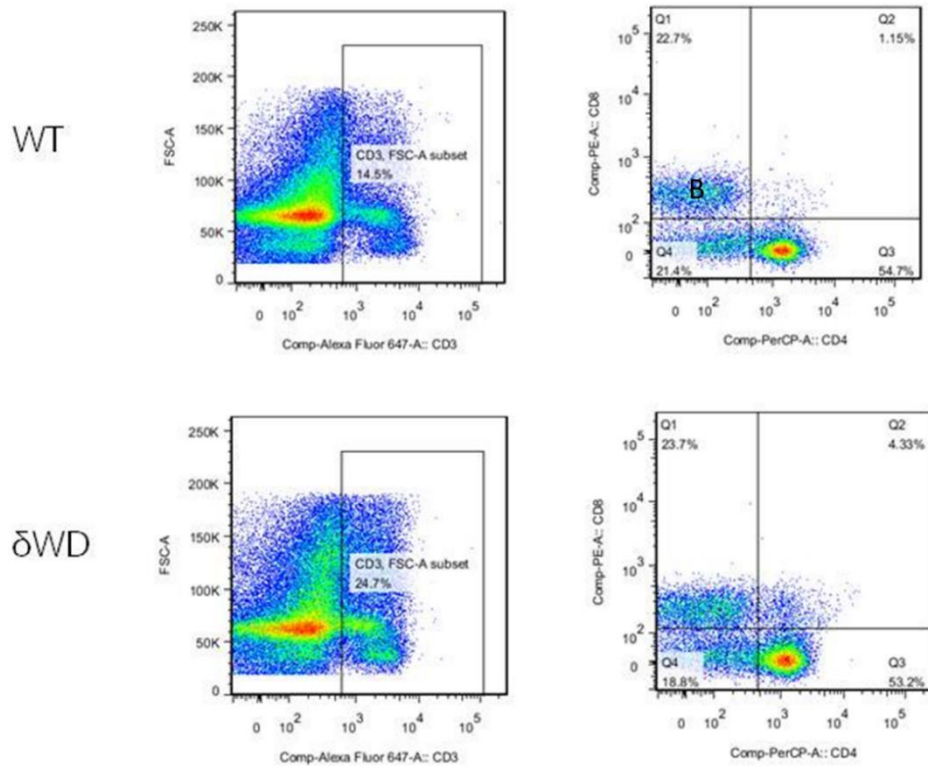


**Figure 4.5 Gating Strategy for T cells.** CD4 positive T cells and CD8 positive T cells. Cells were first gated for CD3 positive cells in CD45 positive and then gate for CD4 and CD8.

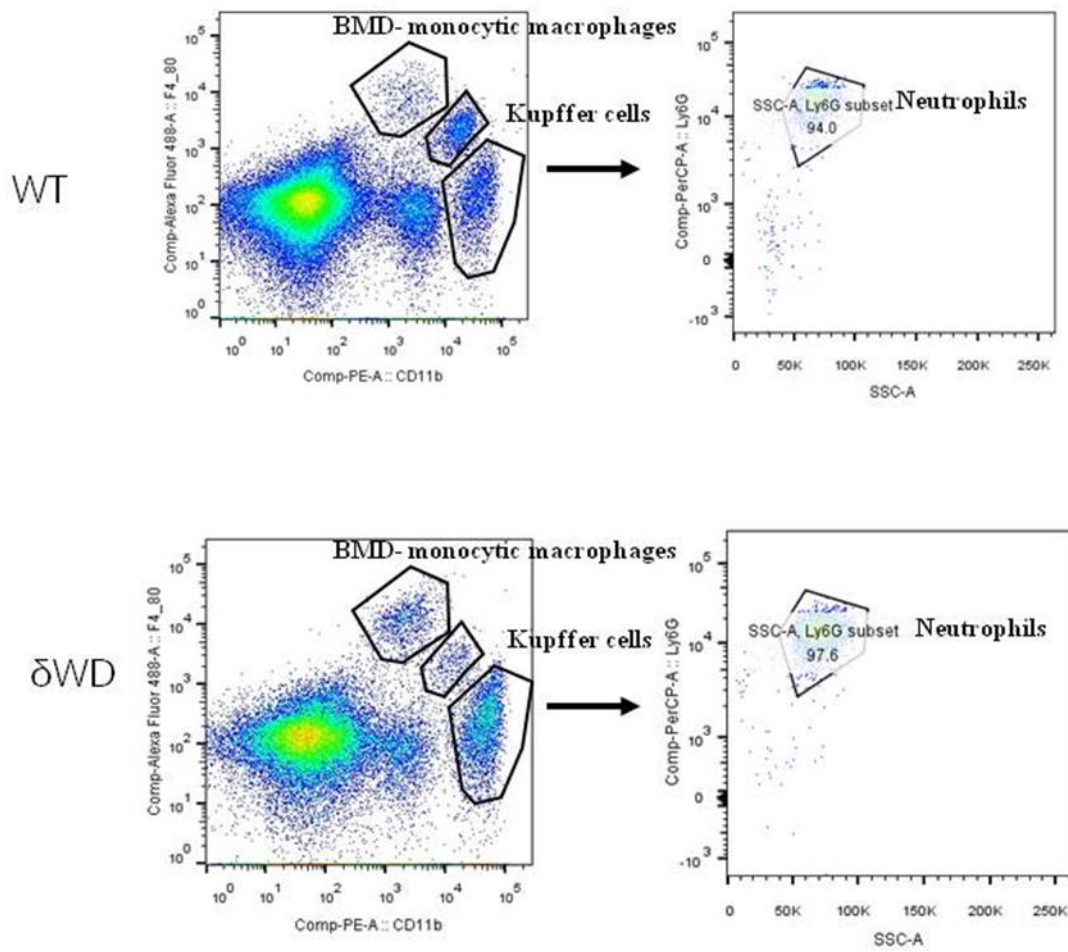


**Figure 4.6 Gating strategy for Kupffer cells, BMD-monocytic macrophages and neutrophils.**

Cells were separated by CD11b and F4/80 expression. The population of Kupffer cells, BMD-monocytic macrophages and neutrophils were shown in the graph.

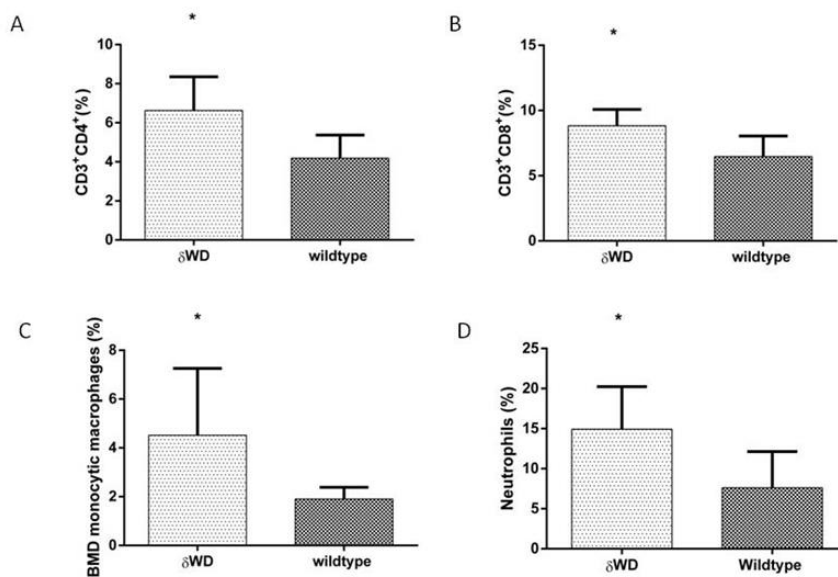


**Figure 4.7 Analysis of lymphocytes infiltration in the liver of infected  $\delta$ WD mice and WT mice** by FACS. Lymphocytes were stained with 2 sets of antibodies. T cells: CD45-APC-cy 7, CD8-PE, CD3-APC, CD4-Percp5.5. Macrophages and neutrophils: CD45-APC-Cy7, CD11b-PE, F4/80-FITC, Ly6G-PerCp5.5, Ly6C Pacific Blue. All data were presented as the percentage of total CD45<sup>+</sup> cells and analyzed by student's t-test. A and B more CD4+T and CD8+T-cells were found in the liver of  $\delta$ WD mice ( $p < 0.05$ ). Higher numbers of bone marrow-derived (BMD) monocytic macrophages (C) and (D) infiltrated livers of  $\delta$ WD mice ( $p < 0.05$ ).

## 4.3 Discussion

### 4.3.i. Background

Earlier work on the role played by ATG16L1 in maintaining homeostasis in the gut epithelium and during innate immune defense at the epithelial surfaces focused on the role played by autophagy in protection against viral and bacterial pathogens (Matsuzawa-Ishimoto, Shono et al. 2017, Lassen and Xavier 2018, Wang, Sharma et al. 2021). Cadwell et al. generated mice hypomorphic for Atg16L1. These mice expressed low levels of ATG16L1 in all tissues and they showed that ATG16L1, and by implication autophagy, plays important roles in the granule exocytosis in Paneth

cells. Paneth cells secreted antimicrobial peptides into the lumen of the gut and are key mediators of host-microbe interactions, including homeostatic balance with colonizing microbiota and innate immune protection from enteric pathogens. (Cadwell, Liu et al. 2008, Cadwell, Patel et al. 2009). The discovery that a T300A mutation in Atg16L1 is a risk allele for Crohn's disease stimulated several studies investigating the effect of the mutation on T300A during infection. Most of these studies have used cells in culture. Both full-length ATG16L1 and its T300A variant were shown to protect mice from *Salmonella* infection (Conway, Kuballa et al. 2013, Lassen, Kuballa et al. 2014, Salem, Nielsen et al. 2015), but these studies did not address the role played by the WD domain of ATG16L1 during microbial infection. Thus, we decided to study the role of the WD domain and LAP during *Salmonella* infection with our unique  $\delta$ WD mice models and cells derived from them.

#### **4.3.ii. Increased *Salmonella* replication in $\delta$ WD cells**

*Salmonella* CFU in  $\delta$ WD HEKs and MEFs were significantly higher than the number of bacteria in WT counterparts at 8 hours post infection (Figure 4.1 A and B). The intracellular growth, measured as fold increase between 2 and 8 hours post infection, indicates similar results,  $\delta$ WD cells showed a significantly higher growth compared with WT cells (Figure 4.1 C and D). LAP is thought to reduce intracellular replication by degrading intracellular *Salmonella* by delivering them to lysosomes. Interestingly, cells lacking all of the ATG16L1 protein were more susceptible than  $\delta$ WD cells to infection. This showed that autophagy (or the ATG5 binding domain and CCD of ATG16L1) played an additional role in controlling *Salmonella* replication.

These results are similar to those of Messer et al. who infected T300A and WT HCT116 with *S. Typhimurium* and found that T300A cells were more susceptible to *S. Typhimurium* infection, and also have defects in controlling intracellular *S. Typhimurium* replication (Messer, Murphy et al. 2013). This suggests that the T300A mutation may affect the function of ATG16L1 in controlling *S. Typhimurium*

infection through either disrupting the WD domain or cleave the Atg16L1 protein.

#### **4.3.iii. The Loss of the WD domain of ATG16L1 increases sensitivity of mice to *S. Typhimurium* infection.**

After confirming LAP/WD domain plays a role in controlling *S. Typhimurium* replication *in vitro* in cells, we infected  $\delta$ WD mice and WT littermate controls with *S. Typhimurium* strain JH3009. The  $\delta$ WD mice showed higher mortality and more severe weight loss (Figure 4.2 A and B). Gross observation and H&E staining showed that livers from  $\delta$ WD showed signs of serious damage with large numbers of granulomas compared to WT mice. Liver damage was associated with infiltration of lymphocytes, more Th cells (CD3<sup>+</sup>CD4<sup>+</sup>), Tc cells (CD3<sup>+</sup>CD8<sup>+</sup>), macrophages (CD11b<sup>+</sup>F4/80<sup>hi</sup>) and neutrophils (CD11b<sup>+</sup>Ly6G<sup>+</sup>). Similar results were observed for the spleen where  $\delta$ WD showed severe splenic disruption of white pulp and necrosis compared to WT mice. Analysis of *S. Typhimurium* dissemination to liver and spleen showed a significantly higher bacterial burden in  $\delta$ WD mice.

Lassen et al. studied the IL-1 $\beta$  production in serums 6 days after *S. Typhimurium* infection in WT and T300A mice. T300A mice produced more IL-1 $\beta$  compared with WT mice. The author also isolated cells from the spleen and lymph nodes from T300A and WT mice and a similar result with more IL-1 $\beta$  production in T300A cells was observed (Lassen, Kuballa et al. 2014). The role played by ATG16L1 in controlling IL-1 $\beta$  production is controversial but some studies suggest that autophagy degrades cytosolic pro- IL-1 $\beta$  and therefore reduces the availability of pro-IL-1 $\beta$  for processing and secretion during inflammation (Wu and Lu 2019). If this is the case IL-1 $\beta$  responses from  $\delta$ WD mice should be similar to controls because, unlike autophagy  $-/-$  mice, the  $\delta$ WD mice can activate autophagy. The increased levels reported for T300A might be because the T300A mutation leads to degradation of ATG16L1 protein leading to a loss of autophagy (Lassen, Kuballa et al. 2014), while the  $\delta$ WD mutation does not disturb autophagy at all. In contrast, pro-inflammatory

cytokine production were significantly decreased in the serum of  $\delta$ WD mice compared with WT littermate controls. A significantly low level of IL-13 was observed in the serum of  $\delta$ WD mice compared with WT littermate controls. IL-13 is secreted by many innate immune cells such as eosinophils, basophils, mast cells, dendritic cells, natural killer cells, and is shown to have an anti-inflammatory effect. Furthermore, IL-13 has been proven to be involved in many gastrointestinal diseases, such as Crohn's disease. IL-13 maintains homeostasis in the gut and may play a protective role in limiting intestinal epithelium injuries (Mannon and Reinisch 2012). Thus, the low expression of IL-13 in  $\delta$ WD mice might be one of the reasons for increased sensitivity to *S. Typhimurium* infection.

#### **4.3. iv. Summary**

Loss of the WD domain of Atg16L1 promoted *S. Typhimurium* replication in HEKs and MEFs.  $\delta$ WD mice also showed more sensitivity to *S. Typhimurium* infections compared with WT mice.  $\delta$ WD mice suffered a higher mortality rate and more severe weight loss.  $\delta$ WD mice also have more bacterial dissemination and areas of persistent infection and damage (granulomas) in their liver and spleen compared with WT mice. More T cells, macrophages and neutrophils infiltration were observed in  $\delta$ WD mice compared with control mice.

# **Chapter 5. WD domain of Atg16L1 control *S. Typhimurium* infection at intestinal epithelial surface in mice**

## **5.1 Introduction**

### **5.1.i. Background**

Previous experiments revealed that mice lacking the WD domain of ATG16L1 showed increased severity of *S. Typhimurium* infection. The next experiments were designed to determine the role played by the WD domain in specific tissues during the infection. Intestinal epithelial cells (IECs) are the first line of defense providing a barrier to infection that plays an important role against gastroenteritis, such as *S. Typhimurium* infection. Myeloid cells also play a role in *S. Typhimurium* infection, such as secreting proinflammatory cytokines at the site of infection, engulfing and degrading bacteria that invade through intestinal epithelium and presenting antigens to activate adaptive immune responses. At present, it is not known if the WD domain protects against infection in IECs or myeloid cells, or both. Thus, we generated mice that specifically lost the WD domain in IECs or myeloid cells to further study the role of Atg16L1's WD domain during *S. Typhimurium* infection.

### **5.1.ii. *LysM<sup>cre</sup>* and *Villin<sup>cre</sup>***

*LysM-cre* mice express cre in myeloid cells targeting the M lysozyme locus. Published studies on the mice show deletion efficiency of 83-98% in mature macrophages and near 100% in granulocytes. Partial deletion (16%) could be detected in CD11c positive dendritic cells (Clausen, Burkhardt et al. 1999). *Villin-cre* mice are generated using the expression of cre under the control of a 9 kb regulatory region of the murine villin gene. *Villin-cre* recombined at day E9 in visceral endoderm and is

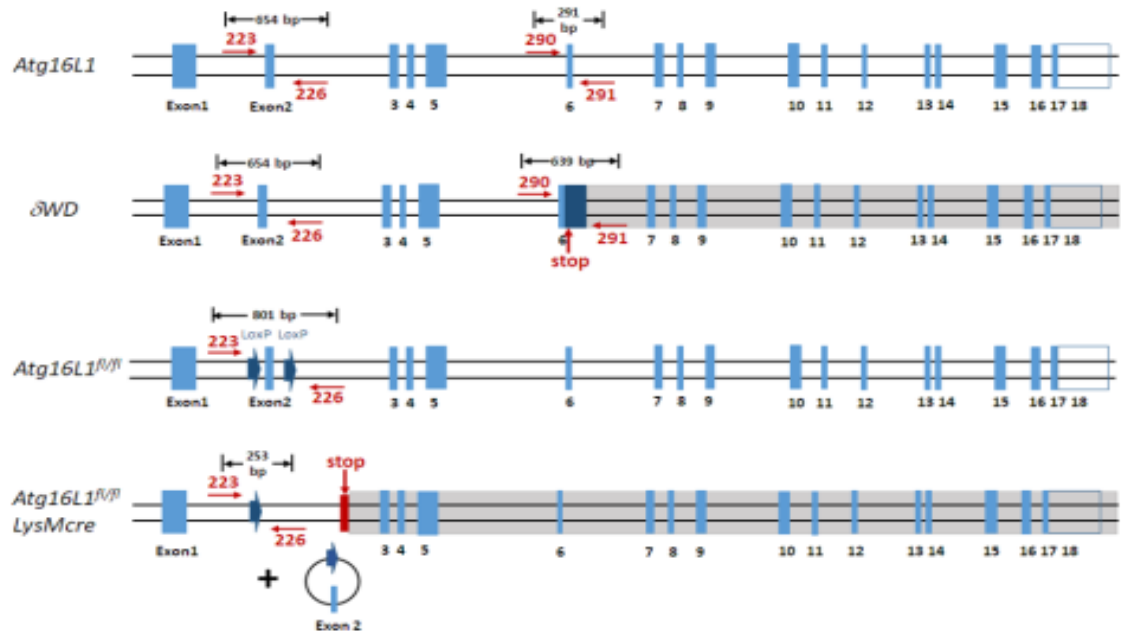
expressed in the entire intestinal epithelium at day E12.5, but not in other tissues. Furthermore, cre expression is maintained throughout the entire adulthood (el Marjou, Janssen et al. 2004).

## **5.2 Results**

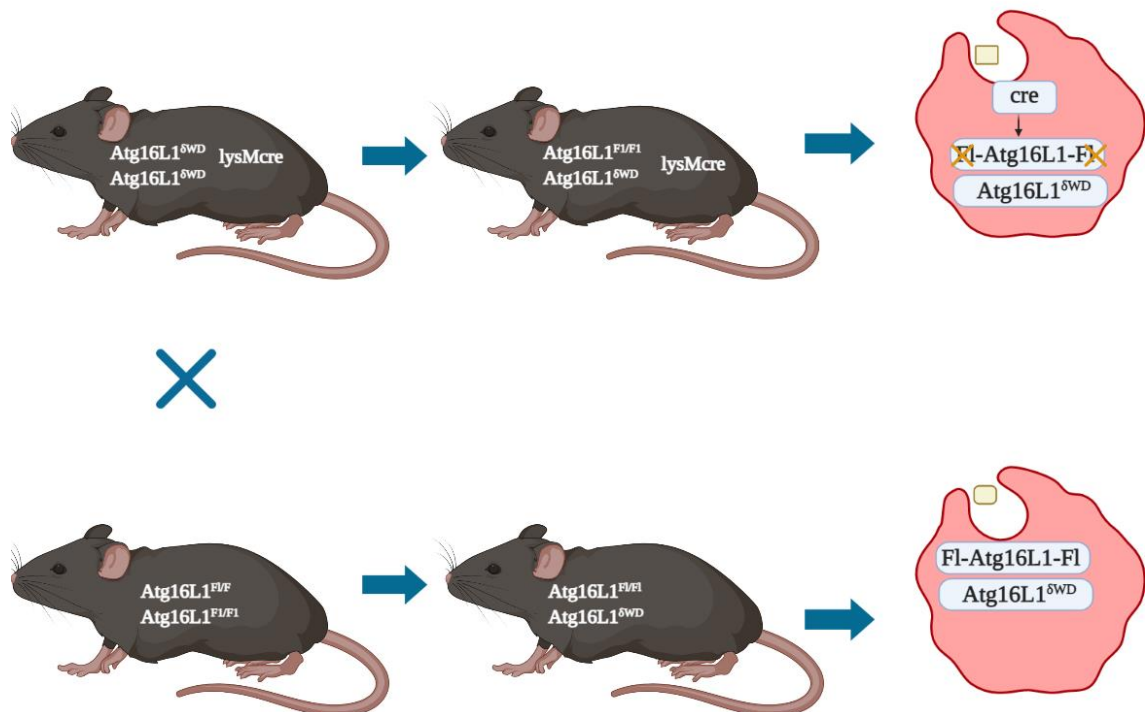
### **5.2.i. Generation of mice lacking the WD domain of ATG16L1 in myeloid cells**

LysMcre mice were crossed with  $\delta$ WD mice to generate mice expressing LysMcre with one allele of normal Atg16L1 and one allele of atg16L1 $\delta$ WD. Then these mice were crossed again with  $\delta$ WD mice to generate mice expressing LysMcre with both alleles atg16L1 $\delta$ WD (Figure not shown). The offspring were crossed with mice that have both alleles of Atg16L1 flanked by two floxp sites (Atg16L1<sup>F1/F1</sup>). All the offspring from this cross will have one allele of Atg16L1 in  $\delta$ WD form and one allele of floxed Atg16L1, which will be removed by cre enzyme (Figure 5.1 A). Thus, the offspring which do not express LysMcre are equivalent to heterozygous  $\delta$ WD mice (Atg16L1:atg16L1 $\delta$ WD), which have been shown to perform the same as WT littermate controls in some of the earlier studies from our lab (Rai, Arasteh et al. 2019, Wang, Sharma et al. 2021). The offspring which express LysMcre are heterozygous (Atg16L1:atg16L1 $\delta$ WD) in all tissues except myeloid cells expressing the cre enzyme where the floxed Atg16L1 is removed leaving one copy of  $\delta$ WD form of Atg16L1 (Figure 5.1 B). These mice were named  $\delta$ WD<sup>phage</sup> mice.

A.



B.



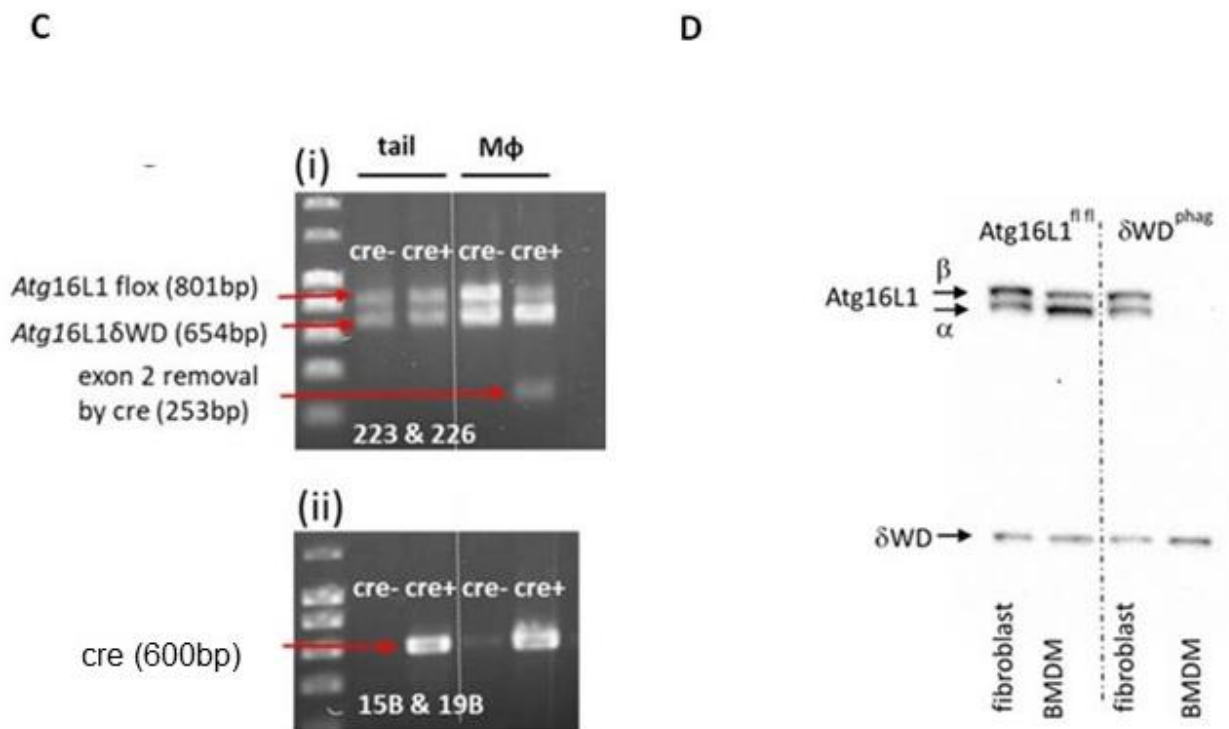


**Figure 5.1** Generation and identification of  $\delta\text{WD}^{\text{phag}}$  mice

**A** Mice were genotyped by 2 sets of primers, 223-226 and 15B-19B. Primer 223-226 binds upstream and downstream of the floxp sites in exon 2 and is designed to examine the removal of floxp sites by cre enzyme. This primer set amplifies a fragment of 654 bp when the copy of *Atg16L1* is not flanked by floxp site, or an 801 bp fragment when *Atg16L1* is flanked by floxp. The amplified fragments reduce in size to 253 bp when the sequence between floxp sites is removed by the cre enzyme. Primer set 15B-19B is designed to bind to upstream and downstream of the cre enzyme and amplifies a 600bp fragment if cre gene is present

**B.** Homozygous  $\delta\text{WD}$  mice carrying *LysMcre* were crossed with *atg16L1*<sup>fl/fl</sup> mice. 50% of progeny are *atg16L1*<sup>fl/ $\delta\text{WD}$</sup>  and carry *LysMcre*. Cre recombinase expressed in myeloid cells of these mice inactivates *Atg16L1* by removing exon 2 from *Atg16L1* ( $\delta\text{WD}^{\text{phag}}$ ). The myeloid cells only express  $\delta\text{WD}$ . Cre recombinase is not expressed in non-myeloid tissues and *Atg16L1* is preserved to induce LAP. 50% of progeny provide littermate controls because they lack *LysMcre* and preserve *Atg16L1* in all tissues.

**C** PCR identification  $\delta\text{WD}^{\text{phag}}$  mice. A 253 bp amplification was detected in BMDMs of cre positive mice, but not in tails and BMDMs from cre negative mice, indicating the knockout of

floxed Atg16L1.

**D** Atg16L1 expression in BMDMs and skin fibroblasts of Atg16L1<sup>fl/fl</sup> mice or  $\delta$ WD<sup>phage</sup> mice. two bands around 66 kDa were observed in skin fibroblasts of both mice strain and BMDMs of Atg16L1<sup>fl/fl</sup>, representing both  $\alpha$  and  $\beta$  isoforms of Atg16L1, but those two bands were not seen in BMDMs of  $\delta$ WD<sup>phage</sup> mice, indicating the specific knockout of floxed Atg16L1 in myeloid cells of  $\delta$ WD<sup>phage</sup> mice.

### **5.2.ii Genotyping of $\delta$ WD<sup>phage</sup> mice.**

Mice were genotyped by 2 sets of primers, 223-226 and 15B-19B. Primer 223-226 binds upstream and downstream of the floxp sites (Figure 5.1A, which is located in exon 2 of Atg16L1, and is designed to examine the removal of floxp sites by cre enzyme. 223-226 amplifies a fragment of 654 bp when the copy of Atg16L1 is not flanked by floxp sites, for example,  $\delta$ WD mice and WT mice. When Atg16L1 is flanked by floxp the primer set 223-226 amplifies a fragment of 801 bp. The amplified fragments reduce in size to 253 bp when the sequence between floxp sites is removed by the cre enzyme (Figure 5.1 B). Primer set 15B-19B is designed to bind to upstream and downstream of the cre enzyme and amplifies a 600bp fragment if cre gene is present (Figure 5.1 B).

Tails tissue from mice and BMDMs cultured from the mice were lysed and analyzed by PCR (Figure 5.1C). DNA extracted from mouse tail tissue or bone marrow-derived macrophages (M $\Phi$ ) were analyzed by PCR. (i) Samples from  $\delta$ WD<sup>phag</sup> mice (indicated by cre+) and littermate controls (cre-). The 253bp PCR product seen in macrophages DNA of cre+  $\delta$ WD<sup>phag</sup> strains indicates specific removal of exon 2 from Atg16L1 in myeloid cells. (ii) PCR primers verify the presence of cre recombinase (cre+). The 600 bp band indicated the presence of cre recombinase, while no band was amplified when there was no cre enzyme.

### **5.2.iii. Analysis of tissue-specific expression of WD by western blot.**

Skin fibroblasts from control mice lacking LysMcre (*Atg16L1<sup>fl/fl</sup>*) and  $\delta$ WD<sup>phag</sup> both showed two bands around 70kDa, which represents  $\alpha$  and  $\beta$  isoforms of ATG16L1, and a third band around 25kDa, which represent the truncated ATG16L1 $\delta$ WD.  $\delta$ WD<sup>phag</sup> mice express LysMcre in myeloid cells, which was indicated by the removal of full-length ATG16L1 from BMDMs but not skin fibroblasts. The protein lysates from BMDMs of control mice lacking LysMcre (*Atg16L1<sup>fl/fl</sup>*) also showed three bands, one for truncated ATG16L1 $\delta$ WD around 25 kDa, two for  $\alpha$  and  $\beta$  isoforms of full-length ATG16L1. In contrast, protein lysates from BMDMs of  $\delta$ WD<sup>phag</sup> showed only one band truncated ATG16L1 $\delta$ WD around 25 kDa, indicating that the full-length ATG16L1 was knocked out in myeloid cells of  $\delta$ WD<sup>phag</sup> mice (Figure 5.1 D).

#### **5.2.iv Generation of mice lacking the WD domain of ATG16L1 in intestinal epithelial cells.**

The mice with WD knockout in IECs were created with the same strategy as the  $\delta$ WD<sup>phage</sup> only mice expressing cre under the control of the villin promoter were used to remove *Atg16L1* from intestinal epithelial cells. The mice were named  $\delta$ WD<sup>IEC</sup> mice (Figure 5.2 A).

#### **5.2.v Genotyping of $\delta$ WD<sup>IEC</sup> mice.**

The primers used to detect *Atg16L1* alleles are the same as those used for the analysis of  $\delta$ WD<sup>phage</sup>. The small intestine was harvested from  $\delta$ WD<sup>IEC</sup> mice and control mice. The small intestines were separated from the duodenum, jejunum and ileum. All parts were cut open and washed with PBS to get rid of debris. The intestinal epithelium was scraped and DNA was extracted. Then the mice were genotyped with 223-226 and 15B-19B primers. The results are shown in Figure 5.2 B and are similar to the genotyping result of  $\delta$ WD<sup>phag</sup> mice. 223-226 amplified two fragments which are 801bp and 654 bp in all tail lysates, representing one allele *atg16L1* $\delta$ WD, other allele floxed *Atg16L1*. The DNA extracts from the small intestine of control mice (indicated

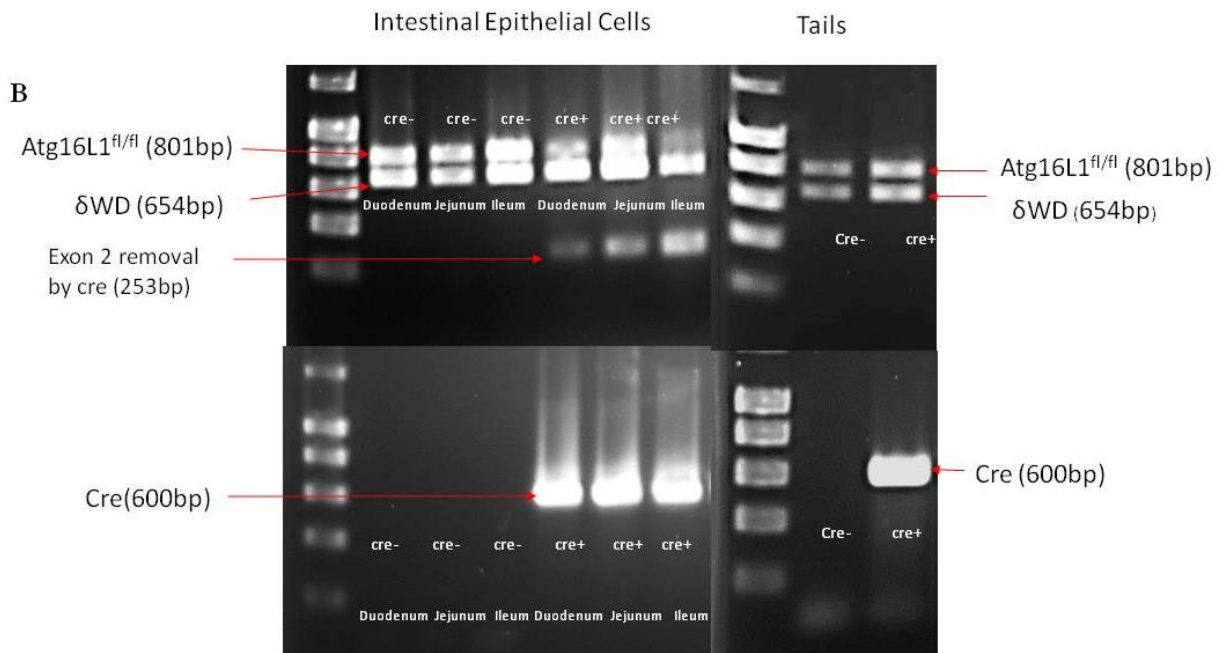
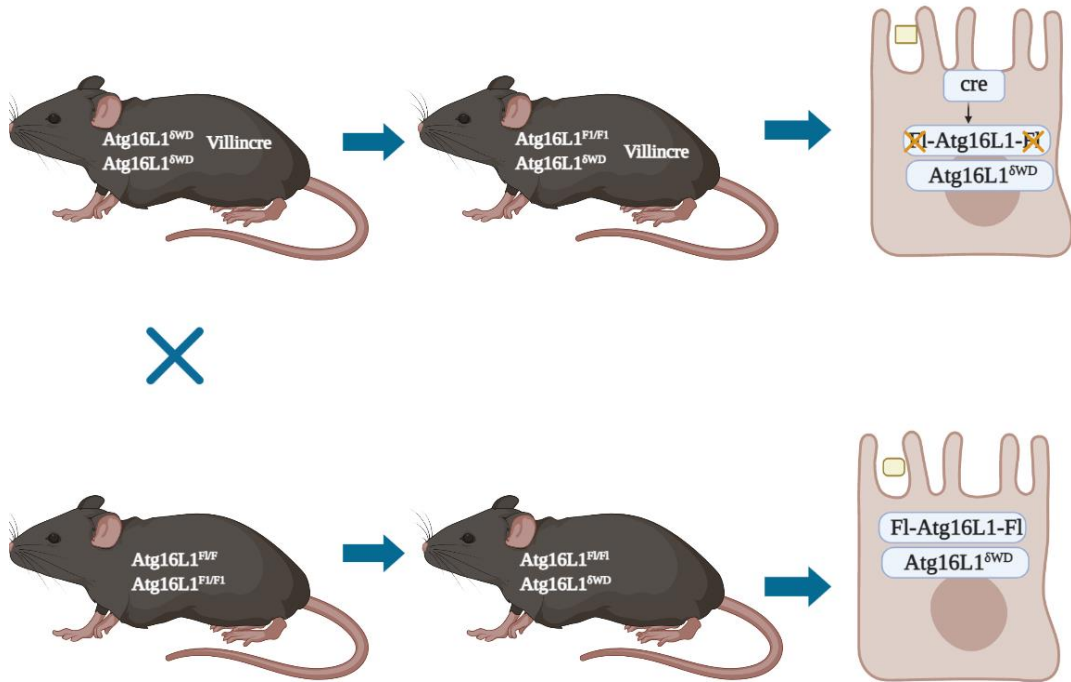
by cre-) mice also amplified two fragments which are 801bp and 654 bp, while an extra 253 bp fragment was amplified in all three parts of the small intestine (duodenum, jejunum, and ileum) of  $\delta\text{WD}^{\text{IEC}}$  mice (indicated by cre+). The 801 bp band was also very faint compared with the 801 bands of control mice, indicating that the floxed Atg16L1 was knocked out in most of the harvested cells. The existence of this faint band was probably due to some other cells apart from the epithelium were harvested.

### **5.2.vi Analysis of tissue-specific expression of WD by western blot**

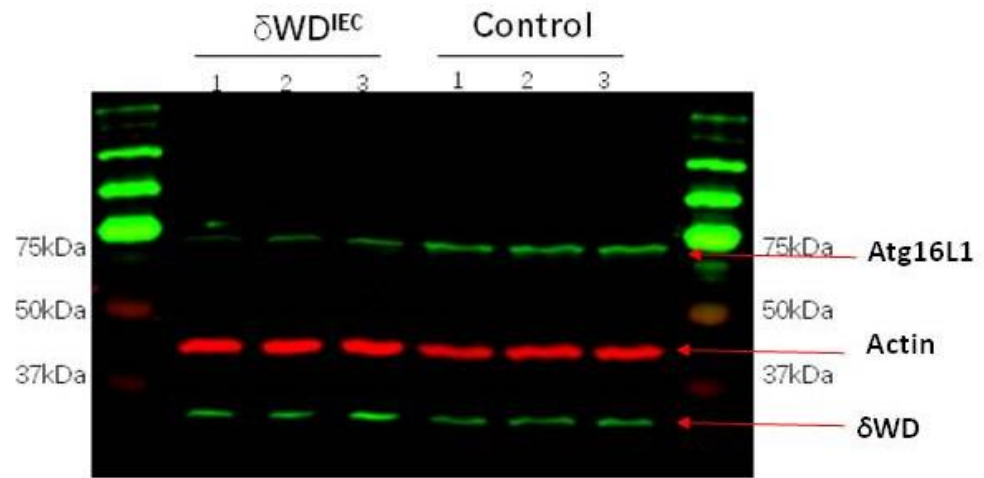
Protein lysates from cells scraped from intestinal epithelium of 3  $\delta\text{WD}^{\text{IEC}}$  mice and 3 littermate controls were exacted and immunoblotted for Atg16L1. The full-length Atg16L1 which is around 70 kDa was observed in gut epithelial cells of 3 control mice. In contrast, only very faint bands were seen in  $\delta\text{WD}^{\text{IEC}}$  mice at the same size (probably due to some other parts of the small intestine were accidentally scraped) (Figure 5.2 C). The full length (FL) Atg16L1 were quantified against actin using ImageJ software. The ratio of FL Atg16L1 to actin of each mouse was shown in Figure 5.2 D. A significantly higher ratio of FL Atg16L1 to actin was observed in Control mice compared to  $\delta\text{WD}^{\text{IEC}}$  mice, indicates that a significantly lower level of FL Atg16L1 was expressed in the intestinal epithelium of  $\delta\text{WD}^{\text{IEC}}$  mice. The data was analyzed with student's t test ( $p < 0.01$ ). A much brighter band representing truncated ATG16L1 was found in 3  $\delta\text{WD}^{\text{IEC}}$  mice compared with control mice. All those results indicate that only a truncated Atg16L1 around 25 kDa was found in target tissues of  $\delta\text{WD}^{\text{phage}}$  and  $\delta\text{WD}^{\text{IEC}}$  mice, confirming the knockout of full-length Atg16L1 in target tissues.



A



C



D

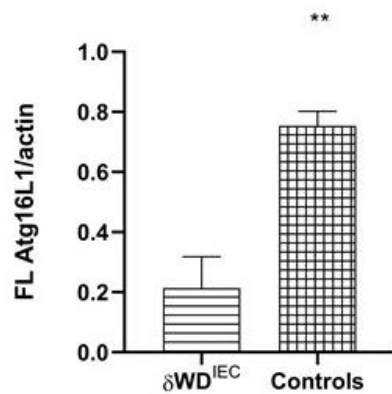


**Figure 5.2 Generation and identification of  $\delta$ WD<sup>IEC</sup> mice**

**A.** Homozygous  $\delta$ WD mice carrying Villin<sup>Cre</sup> were crossed with *atg16<sup>fl/fl</sup>* mice. Cre is expressed in gut epithelial cells of 50% of progeny and removes the full-length *atg16L1*, which maintains LAP. Those mice are  $\delta$ WD<sup>IEC</sup> mice. Other 50% of progeny does not express cre is determined as control mice, which have a full-length ATG16L1 to maintain LAP.

**B.** The 253bp PCR product seen in amplification from DNA extracts of the small intestine of cre+  $\delta$ WD<sup>IEC</sup> mice, indicating the removal of exon 2 from Atg16L1 in gut epithelial cells. In contrast, the amplification from DNA extracts of tail tissue showed 2 bands (654bp and 801 bp) which indicate that one allele of Atg16L1 and another allele floxed Atg16L1. The DNA extracts from the

small intestine and tail tissue of control mice (indicated by cre-) mice also amplified two fragments which are 801bp and 654 bp.

C. Protein lysates from cells scraped from intestinal epithelium of 3  $\delta\text{WD}^{\text{IEC}}$  mice and 3 littermate controls were extracted and immunoblotted for Atg16L1. The full-length Atg16L1 which is around 70 kDa was observed in gut epithelial cells of 3 control mice. In contrast, only very faint bands were seen in  $\delta\text{WD}^{\text{IEC}}$  mice at the same size (probably due to some other part of the small intestine was accidentally scraped).

D. The bands of full length (FL) Atg16L1 and actin were quantified by ImageJ. The ratio of FL Atg16L1 to actin was shown. A significantly higher ratio of FL Atg16L1 to actin was observed in Control mice compared to  $\delta\text{WD}^{\text{IEC}}$  mice, indicates that a significantly lower level of FL Atg16L1 was expressed in the intestinal epithelium of  $\delta\text{WD}^{\text{IEC}}$  mice. The data were analyzed with student's t test ( $p < 0.01$ ).

### **5.2.vii. $\delta\text{WD}^{\text{IEC}}$ mice are more sensitive to *S. Typhimurium* compared with $\delta\text{WD}^{\text{phage}}$ mice and control mice.**

The mice were weighed at indicated days post infection and the ratio of weight at indicated days post infection to the weight of before oral gavage is shown in Figure 5.3A and B.  $\delta\text{WD}^{\text{IEC}}$  mice lost about 12% of their weight on average and this weight loss was significantly greater compared with WT,  $\delta\text{WD}^{\text{phage}}$  mice and littermate controls, all of which lost about 5% of their weight on average at the sacrificing time point.  $\delta\text{WD}$  mice lost the most percentage of weight (15% on average) in all five groups (Figure 5.3 A). The weight loss was analyzed by two-way ANOVA (Bonferroni post test). Both  $\delta\text{WD}$  mice and  $\delta\text{WD}^{\text{IEC}}$  mice showed significantly greater weight loss compared with the other three groups ( $p < 0.05$  at third day post infection and  $p < 0.01$  at fourth, fifth and sixth day post infection).

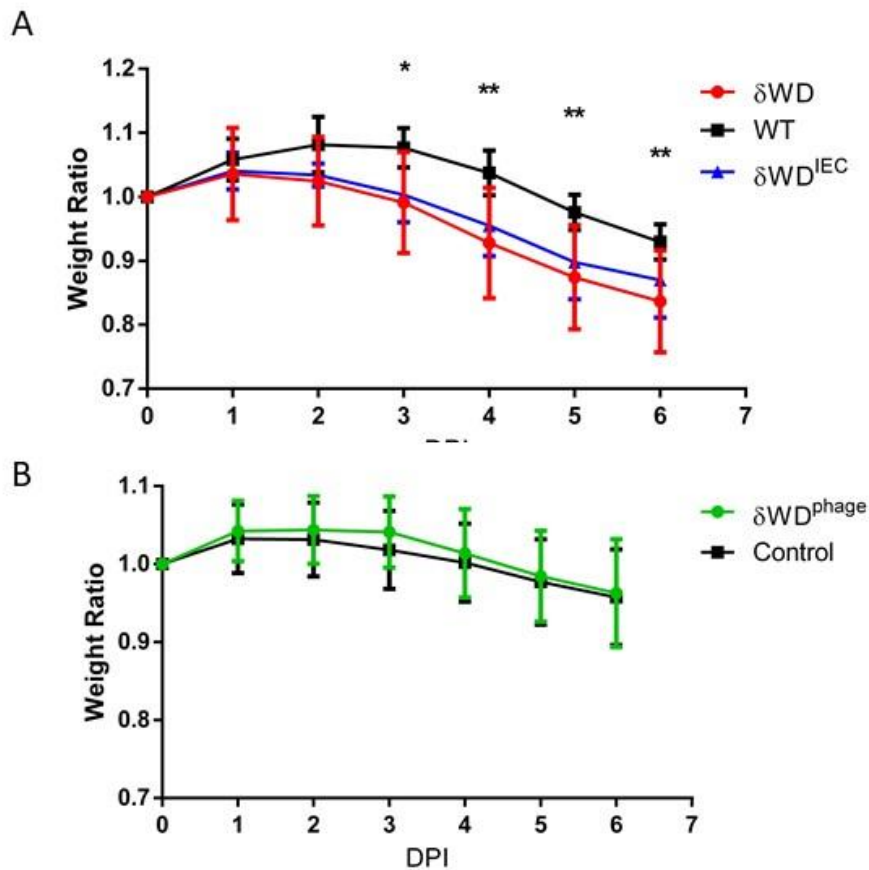


**Figure 5.3** A Weight curve of  $\delta$ WD,  $\delta$ WD<sup>IEC</sup>,  $\delta$ WD<sup>phage</sup> and control mice after JH3009 infection. Mice were infected with  $1.5 \times 10^8$  CFU of *S. Typhimurium* strain JH3009 by oral gavage and weighed on the days indicated. **A.**  $\delta$ WD,  $\delta$ WD<sup>IEC</sup> showed a more severe weight loss compared with wild type mice. **B.** In contrast,  $\delta$ WD<sup>phage</sup> didn't show any difference in weight loss compared with control mice. The weight loss was measured in 20 mice from each group at the beginning of the challenge, while the sacrificed mice were removed after the day of sacrifice. The weight loss was analyzed with Bonferroni post test in two way ANOVA. (\* $p < 0.05$  \*\* $p < 0.01$ )

Figure 5.4 shows the survival curve of all 5 groups,  $\delta$ WD<sup>IEC</sup> and  $\delta$ WD mice suffered a mortality rate of around 30% (35% in  $\delta$ WD mice and 30% in  $\delta$ WD<sup>IEC</sup> mice), while mice from all three other groups survived the 6 day challenge. The specific tissues where LAP was knocked out were shown on the left of Figure 5.4. The bacterial

dissemination to the liver and spleen was measured in a serial dilution of tissue lysates. CFU in the liver of  $\delta\text{WD}^{\text{IEC}}$  mice was significantly higher than CFU in the liver of  $\delta\text{WD}^{\text{phage}}$  mice and wild type mice ( $p < 0.05$  compared with WT and  $p < 0.01$  compared with  $\delta\text{WD}^{\text{phage}}$ ) but showed no significant difference from the CFU found in the liver of  $\delta\text{WD}$  mice. Similarly, the liver of  $\delta\text{WD}$  mice had significantly higher amounts of bacteria compared with livers of  $\delta\text{WD}^{\text{phage}}$  mice and WT mice ( $p < 0.05$  compared with WT and  $p < 0.01$  compared with  $\delta\text{WD}^{\text{phage}}$ ). Bacterial counts from  $\delta\text{WD}^{\text{phage}}$ , littermate controls, and WT mice showed no significant difference between each other (Figure 5.5 A). The CFU counts in the spleen showed a similar result.  $\delta\text{WD}$  and  $\delta\text{WD}^{\text{IEC}}$  mice had significantly more bacteria in their spleen compared with  $\delta\text{WD}^{\text{phage}}$  and WT mice. The CFU values from the livers and spleens of littermate control mice had a very large SD and it was difficult to show a significant difference compared with the other 4 groups (Figure 5.5 B).

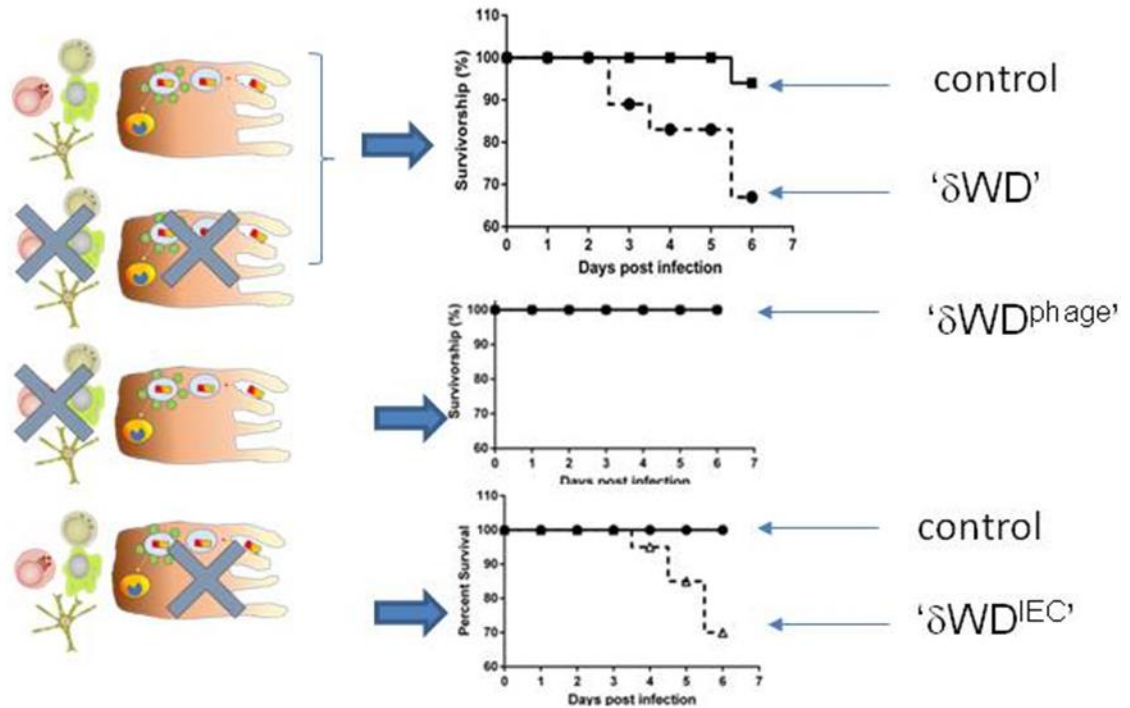


**Figure 5.4** Comparison of survival curves for  $\delta$ WD,  $\delta$ WD<sup>IEC</sup>,  $\delta$ WD<sup>phage</sup> and control mice.

20 mice from each group were orally gavaged with  $1-5 \times 10^8$  CFU of *S. Typhimurium* strain JH3009 and weighed daily for weight loss. All mice which experienced 20% weight loss were sacrificed. The left panel shows the location of LAP loss in different mice strains. The upper panel showed the survival curve of WT and  $\delta$ WD mice. 7 of the 20  $\delta$ WD mice were sacrificed before the endpoint, while only 1 WT mice were sacrificed due to severe weight loss. The middle panel showed the survival curve of  $\delta$ WD<sup>phage</sup> mice and its littermate controls. All 20 of  $\delta$ WD<sup>phage</sup> mice and 20 littermate controls survived the challenge. The lower panel showed the survival curve of  $\delta$ WD<sup>IEC</sup> mice and littermate controls. 6 of the 20  $\delta$ WD<sup>IEC</sup> were sacrificed due to weight loss while all littermate controls survived until the endpoint.

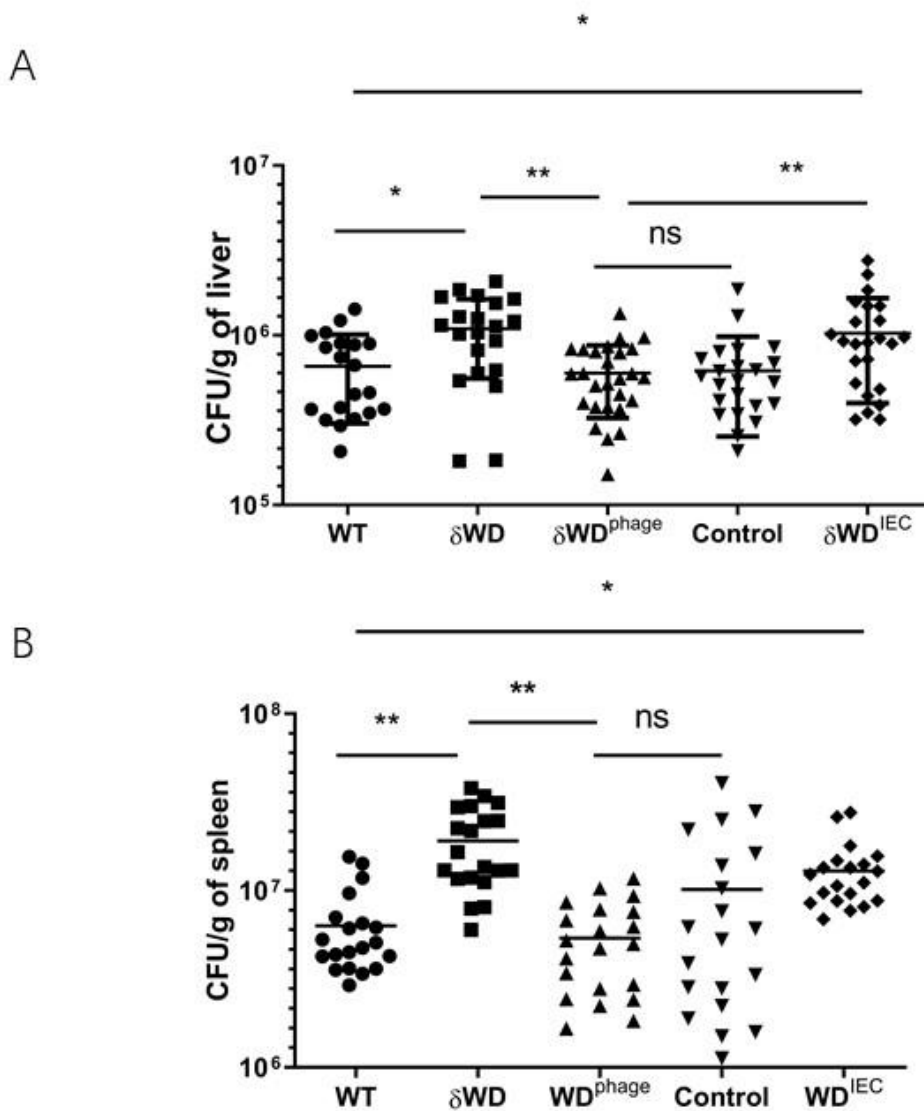


**Figure 5.5 Bacterial dissemination to liver and spleen on sixth day post infection.**

**A** The two strains of mice which have WD knocked out in their intestinal epithelium showed a higher number of bacterial disseminations to their liver compared with other three groups (n=20). Whereas  $\delta$ WD<sup>phage</sup> showed no difference from control mice despite their loss of WD in myeloid cells. The data were analyzed with Turkey's test in one-way ANOVA. (\* $p$ <0.05 \*\* $p$ <0.01)

**B**  $\delta$ WD and  $\delta$ WD<sup>IEC</sup> mice have a significantly higher number of *Salmonella* disseminating to the spleen compared with WT and  $\delta$ WD<sup>phage</sup> mice.  $\delta$ WD<sup>phage</sup> mice showed no difference from WT mice. The data were analyzed with Turkey's test in one-way ANOVA. (\* $p$ <0.05 \*\* $p$ <0.01).

## **5.2. viii. Loss of Atg16L1's WD domain in the intestinal epithelium decreased intestinal permeability after *S. Typhimurium* infection**

The intestinal epithelium lining the intestinal tract and act as a barrier that protects against pathogens, decreased intestinal epithelium was found to be associated with many diseases. Thus, it's crucial to investigate the role of WD domain in maintaining intestinal permeability before and after *S. Typhimurium* infection. 4-kDa dextran conjugated with FITC (FITC-dextran) passively crosses the intestinal epithelium once orally administered. The concentration of FITC-dextran in plasma represents a marker for the integrity of gut epithelium and can be easily measured by fluorimeter (Woting and Blaut 2018).

Mice were orally gavaged with FITC-dextran at the concentration of 500mg/kg body weight. Plasma was collected at 2 hours post oral gavage and measured for FITC concentration at the emission of 528 nm and excitation of 485nm. The readings were analyzed by one-way ANOVA (Turkey's test). The results for 4 mice from each group are shown in Figure 5.6 A. There was no difference in the concentration of FITC-dextran in the plasma of all four strains of mice involved in the experiment. This result indicates that the loss of WD in intestinal epithelium does not affect intestinal permeability without *S. Typhimurium* infection.

Plasma was collected from mice on sixth day post infection and measured for FITC-dextran concentration. A significantly higher level of FITC-dextran concentration was found in the plasma of  $\delta$ WD and  $\delta$ WD<sup>IEC</sup> mice when compared with WT or controls (Figure 5.6 B and C). In contrast, no difference was found between the plasma of  $\delta$ WD<sup>phage</sup> mice and control mice (Figure 5.6 D). Thus, WD domain of Atg16L1 helps to maintain the permeability of intestinal epithelium during *S. Typhimurium* infection.

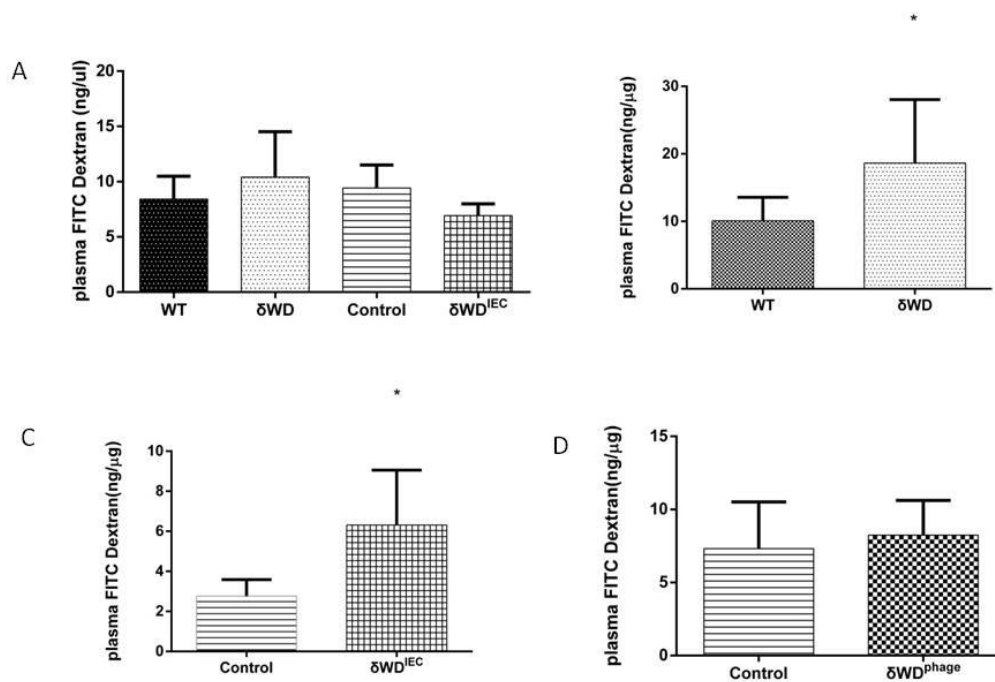


**Figure 5.6 Gut permeability assay in  $\delta$ WD,  $\delta$ WD<sup>IEC</sup>,  $\delta$ WD<sup>phage</sup> and control mice before and after JH3009 infection** **A** FITC-dextran concentration in plasma of 4  $\delta$ WD,  $\delta$ WD<sup>IEC</sup>,  $\delta$ WD<sup>phage</sup> and control mice before JH3009 infection. No differences were observed between all four groups, indicating loss of WD does not affect gut permeability before infection. The data were analyzed with Turkey's test in one-way ANOVA. **B** FITC-dextran concentration in plasma of 8  $\delta$ WD and 8 WT mice. A significantly higher concentration was observed in  $\delta$ WD mice ( $p < 0.05$ ). **C** FITC-dextran concentration in the plasma of 6  $\delta$ WD<sup>IEC</sup> mice and 6 control mice after JH3009 infection.  $\delta$ WD<sup>IEC</sup> showed a significantly higher ( $p < 0.05$ ) concentration of FITC-dextran in their plasma compared with control mice. **D** FITC-dextran concentration in plasma of 10  $\delta$ WD<sup>phage</sup> mice and 10 control mice after JH3009 infection. No difference was observed between them. The data in B, C and D were analyzed with student's t test ( $*p < 0.05$ ).

### **5.2.ix. FACs analysis of the lymphocyte population in the small intestine and liver of $\delta\text{WD}^{\text{IEC}}$ and $\delta\text{WD}^{\text{phage}}$ mice after *S.***

#### **Typhimurium infection.**

Lymphocytes were isolated from liver lobes and lamina propria of 8 mice in each group as mentioned in sections 2.17 and 2.18. Single-cell suspensions were prepared in PBS/2%FCS. Lymphocytes from the liver and small intestine were stained with 2 sets of antibodies, one for T cells, another for macrophages and neutrophils. Kupffer cells ( $\text{CD45}^+\text{CD11b}^{\text{low}}\text{F4/80}^{\text{hi}}$ ) are liver residential macrophages whereas BMD monocytic macrophages ( $\text{CD45}^+\text{CD11b}^+\text{F4/80}^{\text{hi}}$ ) are infiltrating macrophages migrated to the liver. Macrophages in lamina propria were identified by  $\text{CD45}^+\text{CD11b}^+\text{F4/80}^+$ . All neutrophils were identified with staining of  $\text{CD45}^+\text{CD11b}^{\text{high}}\text{F4/80}^{\text{low}}\text{Ly6G}^+$ . The results were shown in Figure 5.7. The specific tissues where LAP was knocked out were shown on the left of Figure 5.7. Figure 5.7 A and B showed the lymphocyte population from lamina propria and liver of  $\delta\text{WD}^{\text{phage}}$  mice and controls. Figure 5.7 C and D showed the lymphocyte population from lamina propria and liver of  $\delta\text{WD}^{\text{IEC}}$  mice and littermate controls. No significant differences were found in any of the cell populations.

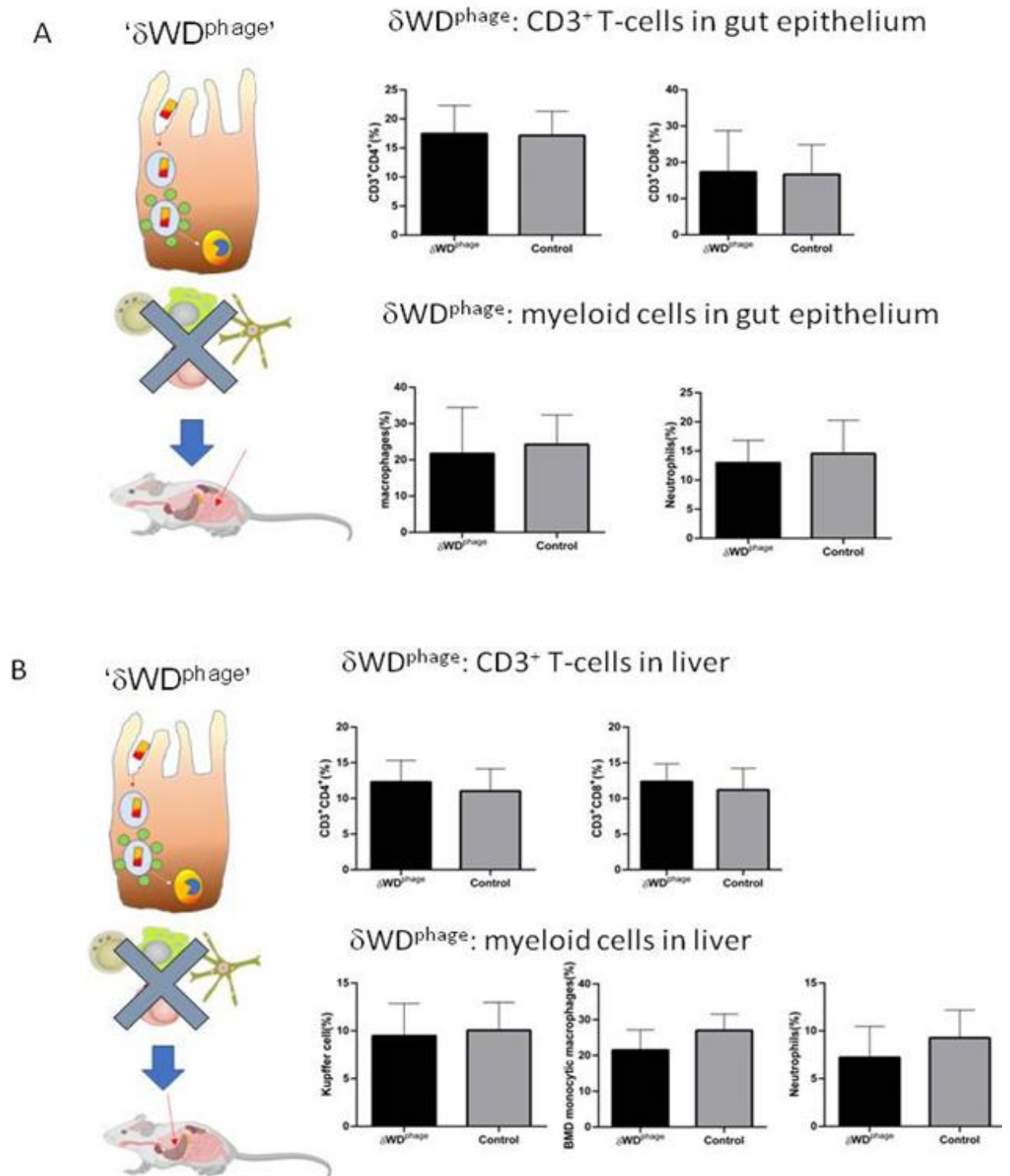
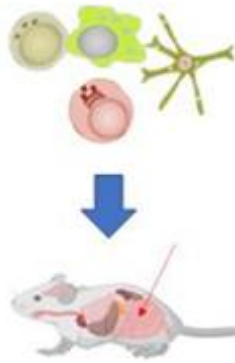
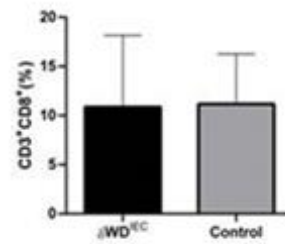
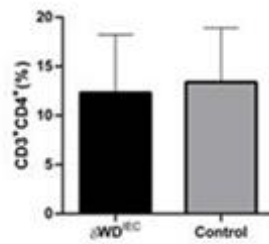
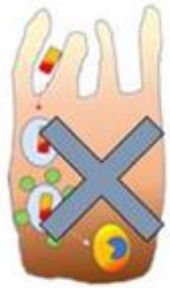


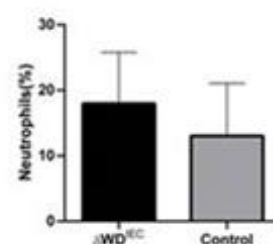
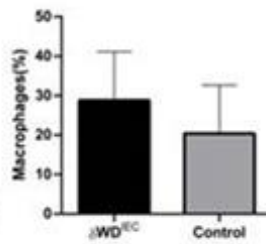
**Figure 5.7 A&B** Lymphocyte population in liver and small intestine of  $\delta$ WD<sup>phage</sup> mice and controls mice after JH3009 infection. 8  $\delta$ WD<sup>phage</sup> mice and 8 control mice were infected with JH3009. On day 6, lymphocytes were analyzed in homogenized tissue by FACS. The panel A shows percentage of Th cells (CD45<sup>+</sup>CD3<sup>+</sup>CD4<sup>+</sup>), Tc cells (CD45<sup>+</sup>CD3<sup>+</sup>CD8<sup>+</sup>) macrophages (CD45<sup>+</sup>CD11b<sup>+</sup>F4/80<sup>+</sup>) and neutrophils (CD45<sup>+</sup>CD11b<sup>high</sup>F4/80<sup>low</sup>Ly6G<sup>+</sup>) in CD45 positive cells

isolated from the small intestine. Panel B shows percentage of Th cells ( $CD45^+CD3^+CD4^+$ ), Tc cells ( $CD45^+CD3^+CD8^+$ ), Kupffer cells ( $CD45^+CD11b^{low}F4/80^{hi}$ ), BMD monocytic macrophages ( $CD45^+CD11b^+F4/80^{hi}$ ) and neutrophils ( $CD45^+CD11b^{high}F4/80^{low}Ly6G^+$ ) in CD45 positive cells isolated from livers of infected mice. All data were analyzed with student's t-test and no significant differences were observed in all cell populations.

C  $\delta$ WD<sup>IEC</sup>  $\delta$ WD<sup>IEC</sup>: CD3<sup>+</sup> T-cells in gut epithelium

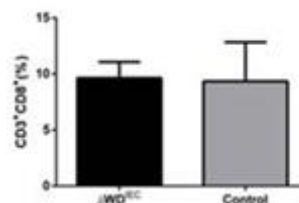
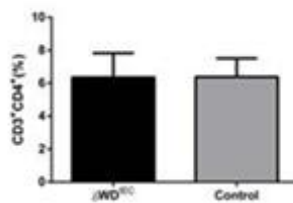


$\delta$ WD<sup>IEC</sup>: myeloid cells in gut epithelium



D  $\delta$ WD<sup>IEC</sup>

$\delta$ WD<sup>IEC</sup>: CD3<sup>+</sup> T-cells in liver



$\delta$ WD<sup>IEC</sup>: myeloid cells in liver

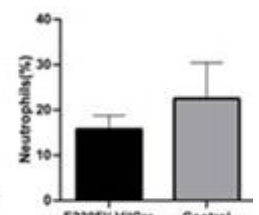
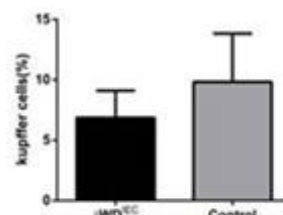
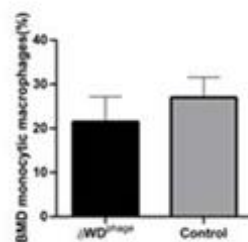


**Figure 5.7 C&D Lymphocyte population in liver and small intestine of  $\delta$ WDIEC mice and controls mice after JH3009 infection.** 8  $\delta$ WD<sup>IEC</sup> mice and 8 control mice were infected with JH3009. On day 6, lymphocytes were analyzed in homogenized tissue by FACS. The panel A shows percentage of Th cells (CD45<sup>+</sup>CD3<sup>+</sup>CD4<sup>+</sup>), Tc cells (CD45<sup>+</sup>CD3<sup>+</sup>CD8<sup>+</sup>) macrophages (CD45<sup>+</sup>CD11b<sup>+</sup>F4/80<sup>+</sup>) and neutrophils (CD45<sup>+</sup>CD11b<sup>high</sup>F4/80<sup>low</sup>Ly6G<sup>+</sup>) in CD45 positive cells isolated from the small intestine. Panel B shows percentage of Th cells (CD45<sup>+</sup>CD3<sup>+</sup>CD4<sup>+</sup>), Tc cells (CD45<sup>+</sup>CD3<sup>+</sup>CD8<sup>+</sup>), Kupffer cells (CD45<sup>+</sup>CD11b<sup>low</sup>F4/80<sup>hi</sup>), BMD monocytic macrophages (CD45<sup>+</sup>CD11b<sup>+</sup>F4/80<sup>hi</sup>) and neutrophils (CD45<sup>+</sup>CD11b<sup>high</sup>F4/80<sup>low</sup>Ly6G<sup>+</sup>) in CD45 positive cells isolated from livers of infected mice. All data were analyzed with student's t-test and no significant differences were observed in all cell populations.

## 5.3 Discussion

### 5.3.i. Background

LAP was first identified in macrophages in 2007 by *Sanjuan et al.* (Sanjuan, Dillon et al. 2007), and was further studied in recent years. Some recent studies identified many non-phagocytic cells, such as epithelial cells also processes a LAP-like pathway that protects from pathogens, Heckman et al identified a similar process in microglia and named it LC-3 associated endocytosis (Heckmann, Teubner et al. 2019). Many *in vitro* studies revealed LAP controls many intracellular bacterial pathogens by delivering them to lysosomes for degradation (Schille, Crauwels et al. 2018), such as *Legionella dumoffi* (studied in macrophages and HEKs), *Burkholderia pseudomallei* (studied in macrophages), *Shigella flexneri* (studied in colonic epithelial cells and MEFs), *Listeria monocytogenes* (studied in macrophages and H4 neuroglioma cells), *Yersinia pseudotuberculosis* (studied in macrophages and HEK cells) and *Mycobacterium tuberculosis* (studied in macrophages) (Schille, Crauwels et al. 2018). LAP in myeloid cells also plays an important role in the adaptive immune system by presenting antigens to T cells (Ligeon, Romao et al. 2017).

### **5.3.ii. Role of different cells during *S. Typhimurium* infection**

*S. Typhimurium* is a major cause of gastrointestinal infections. Those infections mainly remain localized in the small intestine and are generally resolved rapidly. However, *S. Typhimurium* infections can become systemic when the gut epithelial barrier is breached. Then bacteria invade macrophages or DCs and survive within them. Macrophages and DCs carry *S. Typhimurium* into the blood and other tissues, causing a systemic infection (Fabrega and Vila 2013). There are also studies confirming that *Salmonella* mostly replicates within macrophages and neutrophils in liver and spleen. Host cells, such as neutrophils and mononuclear cells, are recruited over time to *Salmonella* infection sites. Incoming cells could provide a steady source of new cells for the expanding bacterial population to colonize (Watson and Holden 2010). Thus, two major cell types played an important role in *S. Typhimurium* infection, gut epithelial cells and macrophages/neutrophils. Conditional mutagenesis in mice has been made possible through the combination of gene targeting techniques and site-directed mutagenesis, using the bacteriophage P1-derived Cre/loxP recombination system. To further study the role of LAP in *S. Typhimurium* infection, we used the loxp-cre system and generated mice with specific loss of LAP in either gut epithelial cells or myeloid cells.

### **5.3.iii. LysMcre and Villincre**

The possibility of this approach depends on the availability of transgenic mice in which the recombinase Cre is expressed in specific cell lineages or tissues. LysM-cre mice were generated with the expression of cre in myeloid cells targeting the M lysozymes locus. In a previous study, a deletion efficiency of 83-98% was observed in mature macrophages and near 100% in granulocytes. Partial deletion (16%) could be detected in CD11c positive dendritic cells (Clausen, Burkhardt et al. 1999). On the other hand, Villin-cre is generated with the expression of cre under the control of a 9 kb regulatory region of the murine villin gene. Villin-cre was recombined at day E9 in

visceral endoderm and expressed in the entire intestinal epithelium at day E12.5, but not in other tissues. Furthermore, cre expression was maintained throughout the entire adulthood (el Marjou, Janssen et al. 2004). LysMcre mice and Villincre mice were crossed with  $\delta$ WD mice and then *atg16<sup>fl/fl</sup>* mice to generate specific LAP knockout mice in myeloid cells and intestinal epithelial cells. Then these mice were identified by genotyping and western blots. The generation of these mice will allow us to study the role of LAP at different stages of infection.

Many studies have reported that ATG16L1 and its T300A variant have many functions in maintaining gut epithelial homeostasis and promoting anti-*Salmonella* effects. (Cadwell, Liu et al. 2008, Conway, Kuballa et al. 2013, Messer, Murphy et al. 2013, Bel, Pendse et al. 2017). In vitro studies suggest that LAP in myeloid cells, such as neutrophils and macrophages, targets intracellular *S.Typhimurium* and other bacterial pathogens in phagosomes for degradation (Fabrega and Vila 2013, Masud, Prajsnar et al. 2019, Masud, van der Burg et al. 2019). Macrophages also play a critical role in systemic infection of *S.Typhimurium* via acting as transporters for bacteria dissemination to other tissues (Fabrega and Vila 2013). ATG16L1 in myeloid cells also plays an important role in maintaining intestinal homeostasis and facilitates host interactions (Zhang, Zheng et al. 2017). But little is known about the role played by the WD domain of ATG16L1 (LAP) in either gut epithelial cells or myeloid cells in controlling *S.Typhimurium* infection in *vivo*. Thus, we made the hypothesis that LAP/WD domain functions in gut epithelium and myeloid cells might play important roles in controlling systemic *S. Typhimurium* infection in *vivo*. To study this, we generated  $\delta$ WD<sup>phage</sup> mice (LAP knockout in myeloid cells) and  $\delta$ WD<sup>IEC</sup> (LAP knockout in intestinal epithelial cells).

We conducted a FITC-dextran assay to check the intestinal permeability prior to the challenge and found that all mice strains showed a similar level of FITC-Dextran in the plasma which indicates that there was no significant difference between mice

strains before infection.  $\delta\text{WD}^{\text{IEC}}$  showed a higher mortality rate and more severe weight loss compared with control mice while  $\delta\text{WD}^{\text{phage}}$  showed a similar weight loss and mortality rate with controls (Figure 5.3 A and B) despite the loss of LAP/WD domain in myeloid cells. The  $\delta\text{WD}^{\text{IEC}}$  and  $\delta\text{WD}$  mice showed a higher amount of bacteria dissemination to the liver and spleen compared with  $\delta\text{WD}^{\text{phage}}$ , control and WT mice, while  $\delta\text{WD}^{\text{phage}}$  did not show significant difference with controls and WT mice (Figure 5.3 C). Results from post infection gut permeability assay showed a similar result,  $\delta\text{WD}^{\text{IEC}}$  and  $\delta\text{WD}$  mice have more disruptions in gut permeability compared with WT and control mice, while  $\delta\text{WD}^{\text{phage}}$  mice showed no difference with control mice (Figure 5.4 B-D). These results indicate that LAP/WD domain in gut epithelial cells plays an important role in controlling *S. Typhimurium* infection in vivo, while loss of LAP/WD in myeloid cells did not significantly impact the susceptibility to *S. Typhimurium* infection in mice.

#### **5.3.iv. Why does LAP in macrophages failed to play a significant role in controlling *S. Typhimurium* infection**

A study conducted by Conway et al. used a specific knockout of ATG16L1 in gut epithelium mice model and found that lack of full-length ATG16L1 caused an abnormality in Paneth cells and increased mice susceptibility to *S. Typhimurium* infection. In contrast, despite the increase in pro-inflammatory cytokines production caused by loss of full-length ATG16L1 in mononuclear cells, the abolition of ATG16L1 in mononuclear cells did not increase the virulence of *S. Typhimurium* in mice (Conway, Kuballa et al. 2013). In the present study, we also found that loss of LAP/WD domain in gut epithelial cells, not myeloid cells, played crucial role in controlling *S. Typhimurium* infection in mice. Myeloid cells, such as macrophages, act as transporters for *S. Typhimurium* dissemination from gut epithelium to other tissues and sites for *S. Typhimurium* replication in liver and spleen (Watson and Holden 2010). Macrophages also play a crucial role in the adaptive immune response by presenting antigens to T cells. It is very interesting that an innate pathway that limits intracellular

bacterial survival and promotes antigen presentation in macrophages failed to play significant roles in controlling *S.Typhimurium* infection in vivo. Digging deep into the literature, *S.Typhimurium* has developed many effectors and mechanisms to promote their survival and replication in macrophages (Linehan and Holden 2003, Thompson, Liu et al. 2011, Richardson 2015, Rao, Xu et al. 2020, Yeom, Shao et al. 2020, Jiang, Wang et al. 2021), therefore it is not surprising that *S.Typhimurium* can impair or escape from the LAP pathway in macrophages.

### **5.3.v. *S.Typhimurium* infection and adaptive immunity**

Wei et al. studied the immune responses to IP injection of three different strains of *S.Typhimurium* in C57/BL6 mice (Wei, Huang et al. 2019). In this study, the authors discovered that only an attenuated *S.Typhimurium* strain, CVCC541, induced anti-*S.Typhimurium* adaptive immune response at 11 days post infection, while SL1344, a highly virulent strain, and CMCC-50115, another attenuated strain failed to induce a significant adaptive immune response. In the present study, we infected six times backcrossed transgenic mice, which can be considered as full C57/BL6 background, with an SL1344 background *S.Typhimurium* strains, and the challenge took place for six days. Thus, it was not surprising that adaptive immune response did not take any part in the challenge. It would be interesting to determine the role of LAP in presenting antigens during *S.Typhimurium* infection with an attenuated strain, such as CVCC541 and determine the role of LAP in the activation of *S.Typhimurium* specific adaptive immune response at a later time point (such as antibody titers in serum and anti-Salmonella specific T cell response).

### **5.3.iv. Summary**

Mice with specific loss of WD domain in myeloid cells and intestinal epithelial cells were generated and identified with genotyping and western blot.  $\delta$ WD and  $\delta$ WD<sup>IEC</sup> showed a more severe weight loss and higher mortality rate during *S. Typhimurium*

infection compared with  $\delta\text{WD}^{\text{phage}}$  mice and controls.  $\delta\text{WD}$  and  $\delta\text{WD}^{\text{IEC}}$  mice also have a more disrupted intestinal epithelium and higher bacterial dissemination to tissues compared to  $\delta\text{WD}^{\text{phage}}$  mice and controls.

# Chapter 6. Generation and analysis of infection by a *SopF* deficient *S. Typhimurium* strain.

## 6.1 Introduction.

In some recent studies, a gene *SL1344\_1177* has been identified in the *S. Typhimurium* genome and named *SopF* (Cheng, Wang et al. 2017, Xu, Zhou et al. 2019). *SopF* is translocated by T3SS1 into the cells and helps to maintain the integrity of nascent salmonella-containing vacuole (SCV) membranes. Furthermore, *SopF* is thought to inhibit the degradation of *S. Typhimurium* by autophagy (xenophagy) by preventing the recruitment of LC3 to SCV membrane. Recent work suggests that during infection damage to the vacuole membrane is sensed by the vacuolar ATPase (V-ATPase) and this signals the binding of ATG16L1 to the V-ATPase and conjugation of LC3 to PE in the vacuole membrane. *SopF* is thought to act as a virulence factor by blocking the interaction between v-ATPase and WD domain of Atg16L1(Xu, Zhou et al. 2019) (Fig. 6.1).

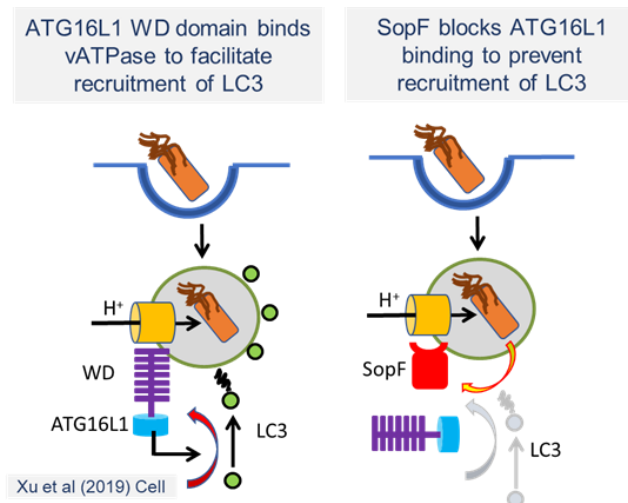


**Figure 6.1** WD domain of ATG16L1 binds to vATPase, which is located on the membrane of SCVs to facilitate LC3 recruitment to SCV and activate xenophagy. *SopF* block this interaction and prevents LC3 recruitment to the SCV membrane.

Xu et al have studied the v-ATPase/ATG16L1 pathway in great detail. A genome-wide CRISPR Cas9 screen showed that v-ATPase subunits were involved in xenophagy (Xu, Zhou et al. 2019). Mass spectroscopy showed that the major subunit of v-ATPase bound ATG16L1 during bacterial infection and that the interaction required the WD domain of ATG16L1. SopF was shown to be an ADP-ribosyltransferase and ADP-ribosylation of Gln124a in ATP6V<sub>0</sub>C blocked binding to ATG16L1 and xenophagy. Given the link between Sop-F, virulence and the WD domain of ATG16L1 we generated a *SopF* deficient *SL1344* strain by lambda red recombination and transduced the mutation into *JH3009* via P22 transduction.

## 6.2. Results.

### 6.2.i. *SopF* mutation in strain SL1344 via Lambda red recombination.

*SopF* deficient SL1344 strain was generated by lambda red recombination as described in materials and methods. Briefly, gene *SopF* was identified at the 1282936-1284060 location in the complete genome of *S. Typhimurium* strain SL1344. A set of primers about 70bp long were designed, 20bp of primer were designed to amplify the kanamycin cassette and the rest 50bp were used to flank it with 50bp sequence flanking the *SopF* gene in *S. Typhimurium* strain SL1344 genome. Then the amplified fragment was transformed into SL1344 carrying pSIM18 plasmid by electroporation

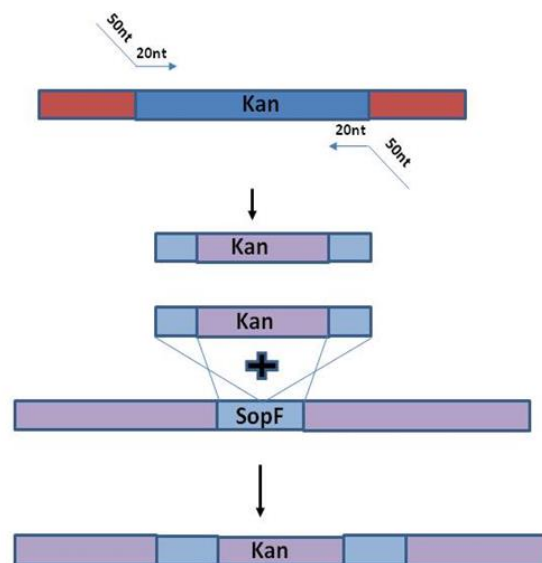
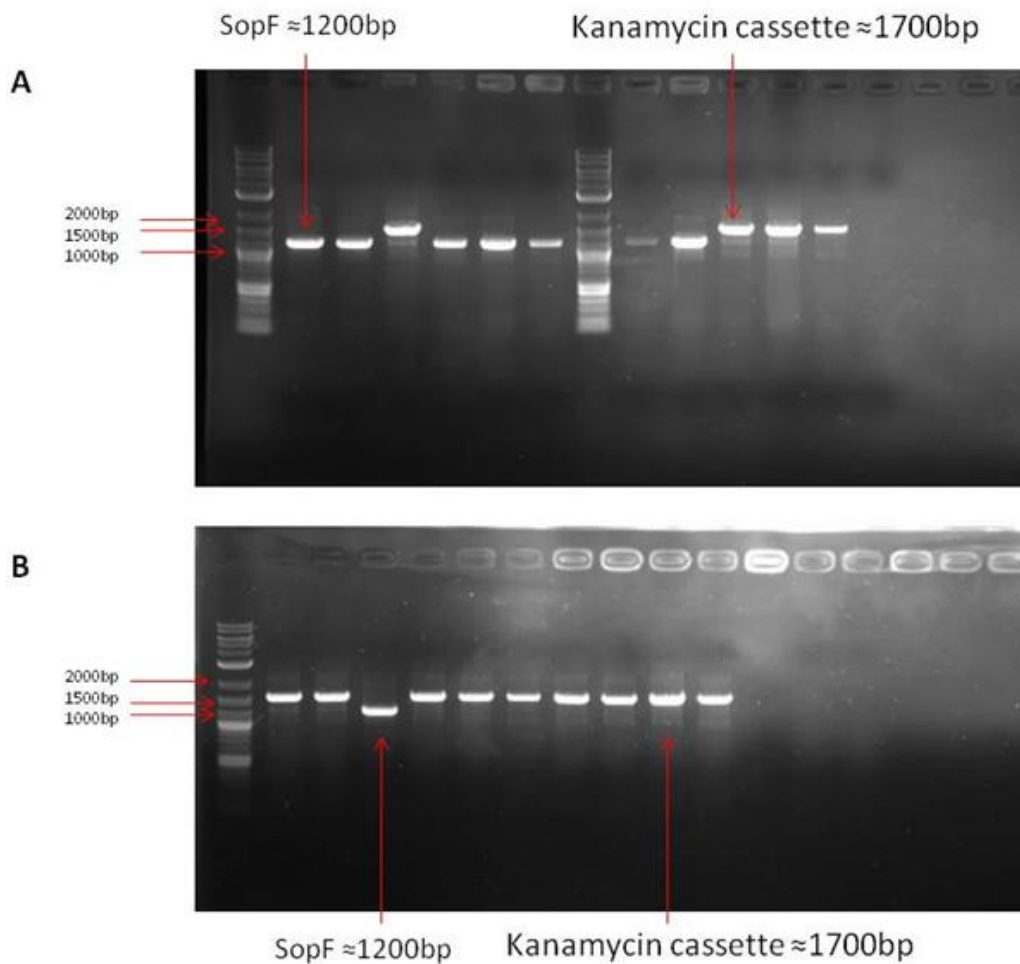


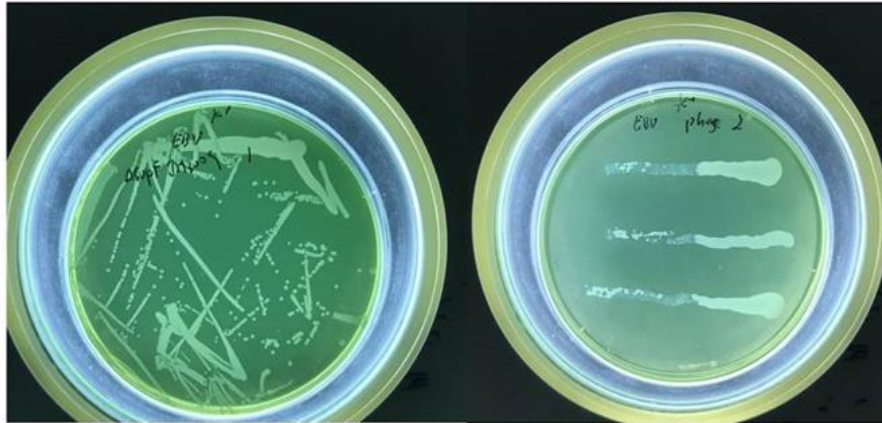
(Figure 6.2).

**Figure 6.2 Lamda red recombination.** Kanamycin cassette flanked with 50 bp of sequence upstream and downstream of *SopF* gene were amplified with PCR. The fragment is transformed into SL1344 carrying pSIM18 plasmid by electroporation for homogenous recombination.

Bacterial cultures after electroporation were spread on kanamycin agar plates for selection and colonies were picked the next day. 11 colonies were picked after the recombination and PCR was used to identify the replacement of *SopF* gene with a kanamycin resistance cassette. As shown in Figure 6.3 A, in 4 of 11 lanes, the amplifications were around 1700bps instead of 1200 bps, suggesting that *SopF* gene (around 1200bp) was replaced with a kanamycin cassette (around 1700 bp). The strain was named SL1344<sup>ΔSopF</sup>.



C



D

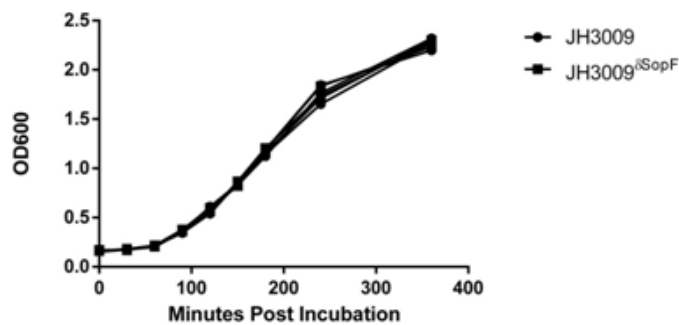


**Figure 6.3. Identification and characterization of SopF mutants.** **A.** In four of the eleven colonies, 1200bp SopF gene was replaced with 1700bp kanamycin resistance cassette. **B.** Colonies obtained from P22 transduction were identified with PCR. In nine of the ten colonies, 1200bp SopF gene was replaced with 1700bp kanamycin resistance cassette. **C.** Left picture, JH3009<sup>ΔSopF</sup> were plated on EBU plates to examine any remains of P22 bacteriophage. Right picture: sensitivity analysis of JH3009<sup>ΔSopF</sup> to P22 bacteriophage. Briefly, make a strip of P22 lysates on an EBU plate and stack the colonies you want to test through the P22 strip. All three colonies showed a reduction in growth after passing the P22 strip, indicating all three colonies are suitable for further gene modification via P22 transduction. **D.** OD<sub>600</sub> growth curve of JH3009 and JH3009<sup>ΔSopF</sup>, no difference is observed between the two strains, indicating that knockout of SopF showed no deficiency in growth.

### **6.2ii. *SopF* mutation transduced in strain JH3009.**

P22 transduction was performed as described in the Materials and Methods section and was examined by PCR. Briefly, P22 bacteriophage was incubated with SL1344<sup>δSopF</sup> overnight for genetic uptake. Then those P22 were incubated with JH3009 for gene transduction. As shown in Figure 6.3 B, one lane showed amplification of 1200 bp (*SopF*) while the rest 9 lanes showed amplification of 1700bp (kanamycin cassette). This result indicates that *SopF* was knocked out in 9 of 10 colonies. Two of the 9 positive colonies were stored in glycerol and these knockout strains were named JH3009<sup>δSopF</sup>. Then we plated the JH3009<sup>δSopF</sup> on EBU plates, the result is shown in Figure 6.3 C. There was no bacteriophage contamination in JH3009<sup>δSopF</sup> because all the colonies were white and clear, with no sign of lysis from bacteriophage (Figure 6.3 C left panel). This result indicates there was no P22 contamination in JH3009<sup>δSopF</sup> in the colonies we collected and the JH3009<sup>δSopF</sup> we generated were good to use in experiments. A routine check of sensitivity to P22 was examined by stripping test. All two strains showed sensitivity to P22 and were still fit for further transduction with P22 bacteriophage (Figure 6.3 C right panel). This test should be conducted in all transgenic bacterial stains after P22 transduction and only those which are still sensitive to P22 should be selected. This is to secure the possibility of further transduction via P22 bacteriophage.

### **6.2iii. Loss of *SopF* does not affect *S. Typhimurium* growth in LB.**

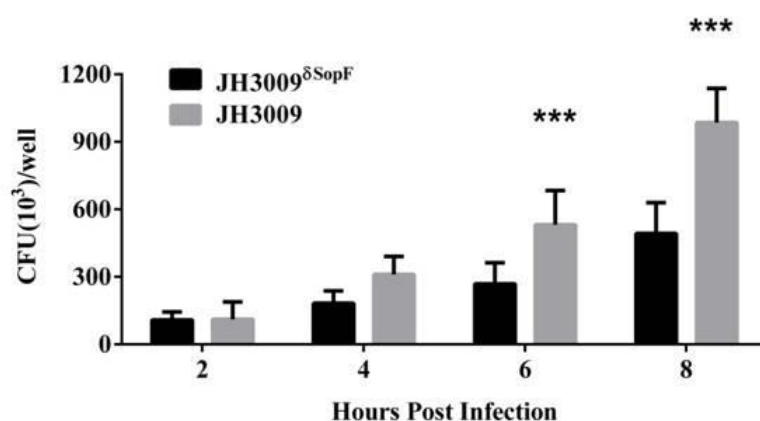
To determine the effect of *SopF* on *S. Typhimurium* growth, OD<sub>600</sub> of JH3009<sup>δSopF</sup> and JH3009 were measured at indicated time points after inoculation. The results were shown in Figure 6.3 D and there was no difference in OD<sub>600</sub> reading between the two strains, indicating that *SopF* doesn't play a role in *S. Typhimurium* replication in LB.

### **6.2iv. The loss of *SopF* reduced the replication of *S. Typhimurium* in MEFs.**

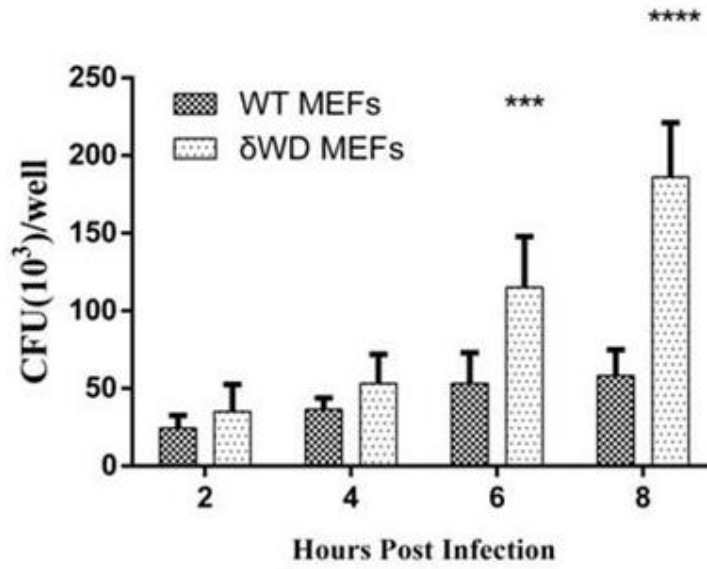
WT MEFs cells were seeded in 6 well plates at the concentration of  $2 \times 10^5$  cell/well and incubated overnight to allow them to attach. Cells were infected with JH3009 $^{\delta\text{SopF}}$  or JH3009 at the MOI of 40 for 2, 4, 6 and 8 hours respectively. Cells were lysed and spread on agar plates. The CFU readings are shown in Figure 6.4 A. The CFU counts in JH3009 infected cells were significantly higher than JH3009 $^{\delta\text{SopF}}$  infected cells at 6 and 8 hours post infection ( $p < 0.001$ ). These results showed that SopF increases replication of JH3009 in MEFs 'in vitro'.

To test the impact of WD loss on the intracellular replication of SopF deficient *S. Typhimurium* strain, WT and  $\delta\text{WD}$  MEFs were seeded in 24 well plates overnight and infected with JH3009 $^{\delta\text{SopF}}$  at the MOI of 40 for 2, 4, 6 and 8 hours respectively. Cells were lysed and spread on agar plates supplied with kanamycin for selection. The CFU readings were shown in Figure 6.4 B. The CFU counts in  $\delta\text{WD}$  MEFs are significantly higher than those in WT MEFs at 6 and 8 hours post infection ( $p < 0.05$  at 6 hours and  $p < 0.001$  at 8 hours).

A



B



C

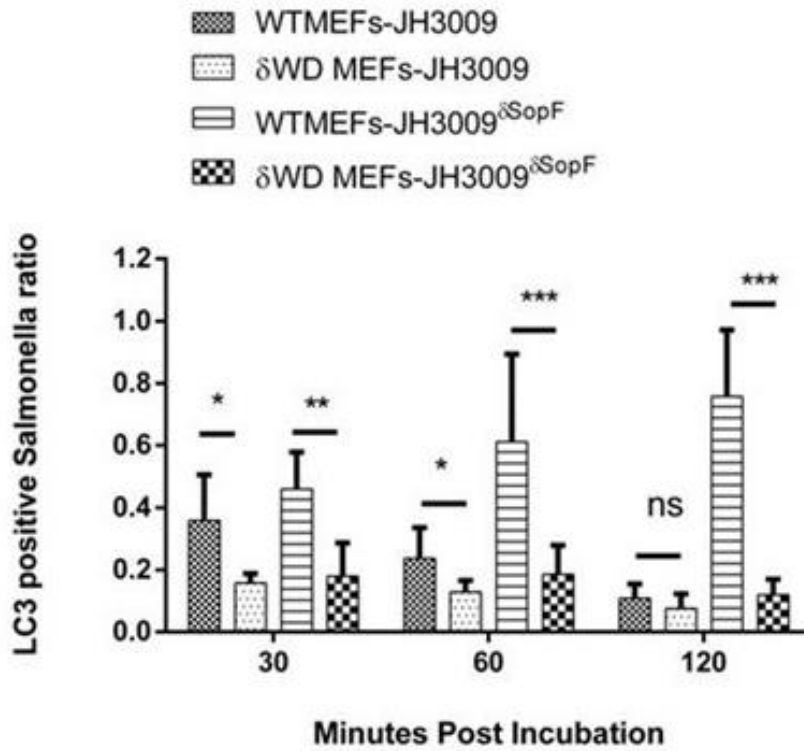


**Figure 6.4 Replication of JH3009 $\delta$ SopF and JH3009 and LC3 recruitment in MEFs. A.** WT MEFs cells were infected with JH3009 $\delta$ SopF or JH3009 at the MOI of 40 for indicated times. Cells were lysed and spread on agar plates to determine CFU. The CFU counts in JH3009 infected cells were significantly higher than JH3009 $\delta$ SopF infected cells at 6 and 8 hours post infection. The data represent CFU readings from 6 independent wells and were analyzed with Bonferroni post test in two way ANOVA (\*\* $p < 0.001$ ) **B** WT and WD MEFs cells were infected with JH3009 $\delta$ SopF at the MOI of 40 for indicated times. Cells were lysed and spread on agar plates to determine CFU. The data represent CFU readings from 6 independent wells and were analyzed by Bonferroni post test in two way ANOVA ( $p < 0.05$  at 6 hours and  $p < 0.001$  at 8 hours). **C** WT and  $\delta$ WD MEFs were infected with JH3009 $\delta$ SopF or JH3009 and fixed at indicated time points and stained with anti-*Salmonella* and anti-LC3 antibodies to count LC3-positive vacuoles. The LC-3 positive *Salmonella* ratio was determined by numbers of LC-3 positive *Salmonella* divided by the numbers of total *Salmonella* in 20 images. The number of cells in each image (field of view) was determined via DPAI staining. Data is analyzed with Bonferroni post test in two way ANOVA. (\* $p < 0.05$  and \*\* $p < 0.01$ ).

### **6.2.v. The loss of *SopF* promotes LC-3 recruitment to SCVs.**

MEFs were infected with JH3009 $\delta$ SopF or JH3009 at the MOI of 40 for 2, 4, 6 and 8 hours. Cells were fixed with methanol and stained with anti-LC3 and anti-*Salmonella* antibodies. The results are shown in Figure 6.4 C. The infection of WT MEFs with WT JH3009 resulted in a decrease in LC3 recruitment to vacuoles with time. This fell from approx. 35% at 30mpi, 25% at 60mpi and 10% at 120mpi. In contrast in WT MEFs infected with JH3009 $\delta$ SopF, there was a time-dependent increase in the ratio of LC3 decorated *S. Typhimurium* (~40% at 30mpi, ~50% at 60mpi, ~80% at 120mpi). This shows that SopF inhibited the recruitment of LC3 to SCV. When the experiment was repeated for  $\delta$ WD MEFs, which are unable to recruit LC3 to membranes, LC3 positive vacuoles remained below 20% at all time points. These results indicated that recruitment of LC3 to the vacuole requires the WD domain of ATG16L1 and the loss of SopF promotes LC3 recruitment to SCVs most easily seen at 60-120 minutes post-

infection.

It was difficult to see a reduction in LC3 decorated *S. Typhimurium* in MEFs infected with JH3009 compared to JH3009<sup>ΔSopF</sup> at 30 minutes post infection, indicating that SopF does not affect LC-3 recruitment to Salmonella/SCVs at the early stage of infection (non-canonical autophagy/LAP). This may reflect the time taken for the onset of secretion of SopF from the bacteria via the T3SS1 and/or the time taken for levels of SopF in the cytosol to reach concentrations able to inhibit interactions between ATG16L1 and the V-ATPase.

#### **6.2.vi. Loss of SopF reduced *S. Typhimurium* virulence in mice.**

WT control mice were oral gavaged with either JH3009<sup>ΔSopF</sup> or JH3009 and weighed daily for 6 days (Figure 6.5). All the mice survived the challenge (data not shown). The mice infected with JH3009<sup>ΔSopF</sup> group gained weight at the start of the experiment and then lost weight over the next 5 days. The control JH3009 group also lost weight with a statistically significant increase over JH3009<sup>ΔSopF</sup> group – at 6 days. Then mice were sacrificed at the sixth day post infection, liver and spleen were harvested and lysed. Bacterial dissemination to liver and spleen were measured by serial dilutions of tissue lysates onto kanamycin plates. Dissemination of bacteria to the liver and spleen is shown in Figure 6.5, panels B and C. JH3009 group showed greater dissemination to liver and spleen compared with the JH3009<sup>ΔSopF</sup> group. This shows that the virulence of *S. Typhimurium* is decreased in the absence of SopF and is consistent with a model where SopF prevents binding of the WD domain of ATG16L1 to the V-ATPase to reduce translocation of LC3 to the vacuole and subsequent delivery to lysosomes for degradation.

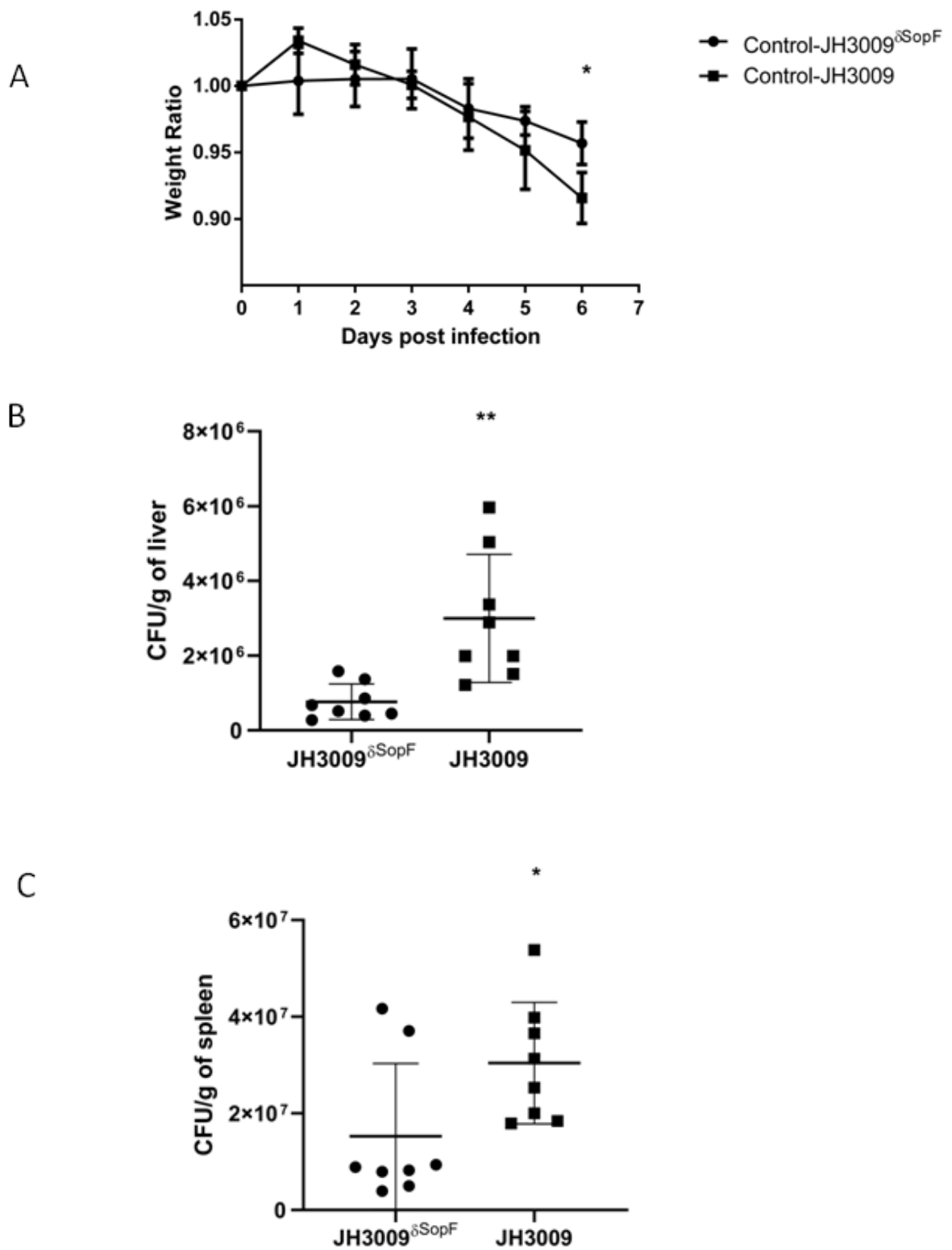


**Figure 6.5** A weight loss and bacterial dissemination for control mice infected with either JH3009 or JH3009<sup>ΔSopF</sup>. **A.** Weights loss within 6 days post infection. 8 WT control mice were infected with either JH3009<sup>ΔSopF</sup> or JH3009. Mice infected with JH3009<sup>ΔSopF</sup> showed only a very

mild weight loss while JH3009 infected mice showed about 10% weight loss. Data were analyzed with Bonferroni post test in two way ANOVA. ( $*p<0.05$ ) **B.** CFU counts in the liver of challenged mice. **C.** CFU counts in the spleen and liver of challenged mice. Significantly less bacterial dissemination was observed in liver and spleen of JH3009 <sup>$\delta$ SopF</sup> infected mice at 6 days post infection. Data were analyzed with student's *t*-test ( $**p<0.01$  and  $*p<0.05$ ).

### **6.2.vii. *S. Typhimurium* lacking SopF show increased virulence in $\delta$ WD mice.**

The results above suggested that Sop-F increased virulence by preventing the binding of the WD domain of ATG16L1 to the V-ATPase blocking the removal of *S. Typhimurium* by autophagy. If this were the case the virulence of JH3009 and JH3009 <sup>$\delta$ SopF</sup> *S. Typhimurium* should be the same in  $\delta$ WD mice because the target for SopF is missing. 10  $\delta$ WD mice were oral gavaged with JH3009 <sup>$\delta$ SopF</sup> and weighed once per day for 6 days. As seen following infection with WT JH3009,  $\delta$ WD mice lost significantly more weight during the period (Figure 6.6 A). One of ten  $\delta$ WD mice were found dead during the experiment while 3 others were sacrificed during the experiment due to severe weight loss. All the WT mice survived the challenge (Figure 6.6 B). All surviving mice were sacrificed on the sixth day post infection. Livers and spleens were lysed and serial dilutions were plated on ager plates. The results are shown in Figure 6.6 C and D. There are a significantly higher number of *S. Typhimurium* in the liver and spleen of  $\delta$ WD mice compared with WT mice ( $p<0.01$  in liver and  $p<0.001$  in spleen).

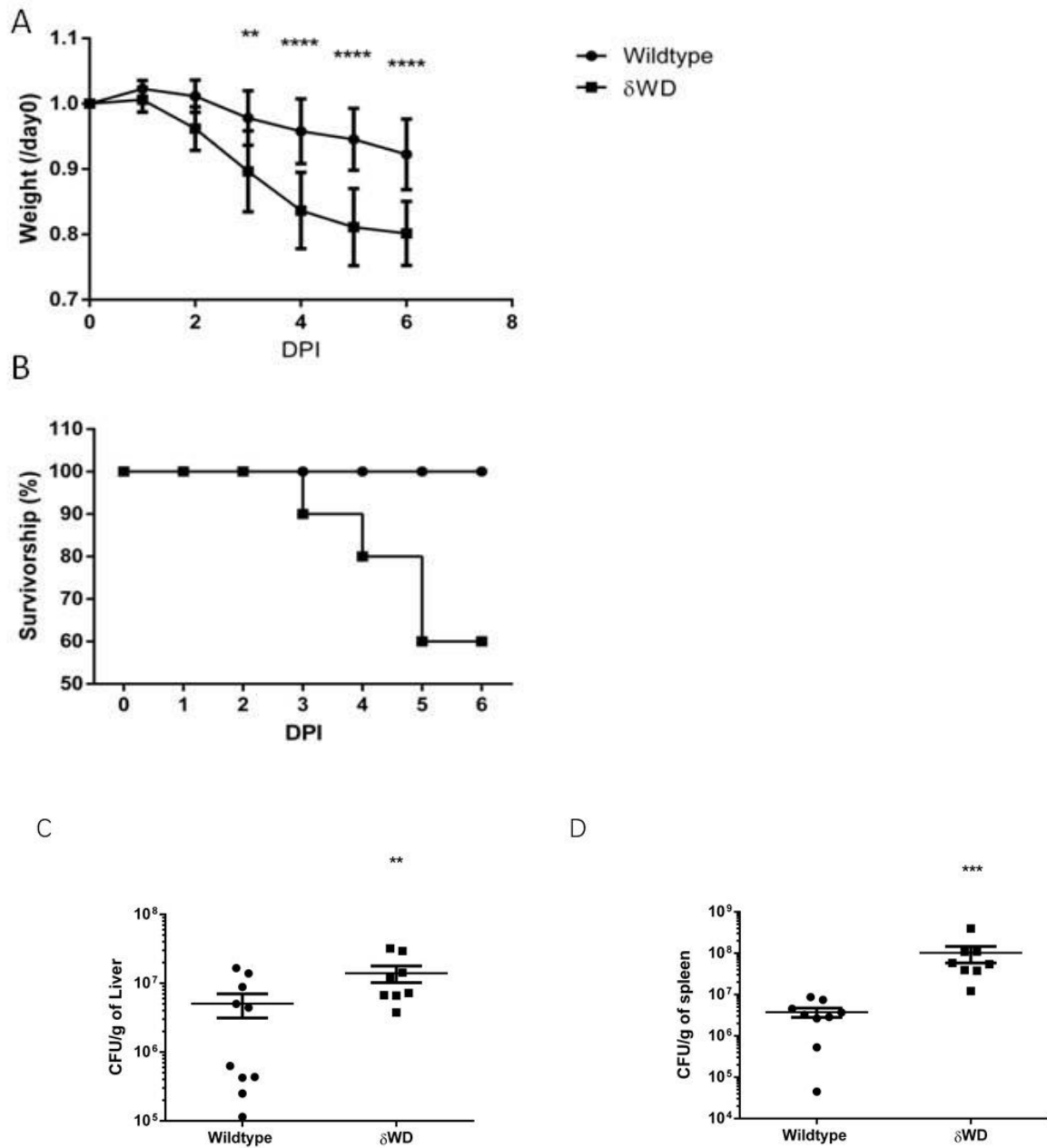


**Figure 6.6 Infection of WT and  $\Delta$ WD mice with JH3009 $\Delta$ SopF.** **A.** Weight curve of 10  $\Delta$ WD mice and 10 WT controls until 6 days post infection.  $\Delta$ WD mice showed significantly higher weight loss compared with WT mice. Data were analyzed with Bonferroni post test in two way ANOVA. (\*\* $p < 0.01$  and \*\*\* $p < 0.001$ ) **B.** Survival curve of 10 WT and 10  $\Delta$ WD mice after JH3009 $\Delta$ SopF infection.  $\Delta$ WD mice suffered 40% mortality rate while all the WT mice survived the challenge. **C&D.** Bacteria counts in liver of JH3009 $\Delta$ SopF infected mice and bacteria dissemination to the spleen of JH3009 $\Delta$ SopF infected mice.  $\Delta$ WD mice showed significantly higher bacterial

dissemination to liver and spleen compared with WT mice. Data were analyzed with student's t-test (\*\* $p < 0.01$  and \*\*\* $p < 0.001$ ).

## 6.3 Discussion.

### 6.3.i. Background.

STM1239 was first identified by *Cheng et al.* in 2017 and named *SopF* (*Cheng, Wang et al.* 2017). *SopF* is an SPI-1 T3SS effector and is thought to play an important role in bacterial virulence (*Cheng, Wang et al.* 2017). Recent studies focusing on *SopF* found that *SopF* plays an important role in the intracellular survival of *S. Typhimurium* by promoting nascent SCV stability and blocking xenophagy (*Lau, Haeberle et al.* 2019, *Xu, Zhou et al.* 2019). Importantly, in the study of *Xu et al.*, they propose that the v-ATPase on SCV membrane binds with WD domain of ATG16L1 to recruit LC3 to activate xenophagy. This raised the possibility that the increased sensitivity of  $\delta$ WD mice to *S. Typhimurium* might arise because the mice lack the WD domain of ATG16L1 and cannot use the v-ATPase pathway to recruit LC3 to the SCV. *Xu et al.* show that *SopF* silencing in *S. Typhimurium* resulted in an increasing level of ‘xenophagy’, increasing recruitment of LC3 to about 80% of intracellular *SopF* deficient *S. Typhimurium* at 2 hours post infection, while this ratio was 10% in WT *Salmonella*. This phenotype could be abolished by overexpressing *SopF* in cells infected with the *SopF* mutant. *SopF* mutant *S. Typhimurium* also showed reduced virulence in mice, resulting in more LC3 decorated *S. Typhimurium* in the small intestine and less bacterial dissemination to liver and spleen, and the virulence can be restored by reexpression of *SopF*.

Most of the results presented in this thesis are in agreement with *Xu et al.* *SopF* was replaced by a kanamycin cassette in JH3009 by lambda red recombination and P22 transduction and was named JH3009 <sup>$\delta$ SopF</sup>. Successful removal of *SopF* was confirmed by PCR and the mutation did not alter the growth kinetics of *S. Typhimurium* on nutrient agar. WT and  $\delta$ WD MEFs were infected with either JH3009 or JH3009 <sup>$\delta$ SopF</sup>, and fixed at increasing times to determine the percentage of LC3 decorated *Salmonella*. At early time points (30-60 minutes) the percentage of LC3- decorated *S.*

Typhimurium observed in WT MEFs infected with JH3009 or JH3009<sup>δSopF</sup> were similar at about 40%. Much of this recruitment of LC3 required the WD domain because only 15% of *S. Typhimurium* recruited LC3 in  $\delta$ WD MEFs. This data suggests that WD-dependent LC3 recruitment is not blocked by SopF at early times of infection. At 120 minutes post infection the number of LC3 decorated *S. Typhimurium* increased to 80% for JH3009<sup>δSopF</sup> in WT MEFs. Again, this required the WD domain because LC3 recruitment was much lower at 10% for  $\delta$ WD MEFs. The low levels of LC3 labelling seen in  $\delta$ WD mice indicate WD-independent recruitment of LC3, as would occur during autophagy.

In our study, the virulence of JH3009<sup>δSopF</sup> in mice was also examined in transgenic mice models. It was predicted that *S. Typhimurium* lacking SopF would be less virulent because they cannot inhibit the WD-vATPase pathway used to recruit LC3 to the vacuole. Control mice from the  $\delta$ WD<sup>phage</sup> study were infected with JH3009 or JH3009<sup>δSopF</sup>. These mice are heterozygous and have one allele of *atg16L1δWD* and another allele a normal full-length *Atg16L* which has been shown to maintain LAP at levels seen in WT mice (Rai, Arasteh et al. 2019). Although all the mice survived the challenge, mice infected with JH3009<sup>δSopF</sup> gained weight over the first two days compared with the mice infected with WT JH3009, and showed low bacterial dissemination to liver and spleen. These data confirmed that the loss of SopF and the WD-vATPase axis reduced the virulence of *S. Typhimurium* in WT mice.

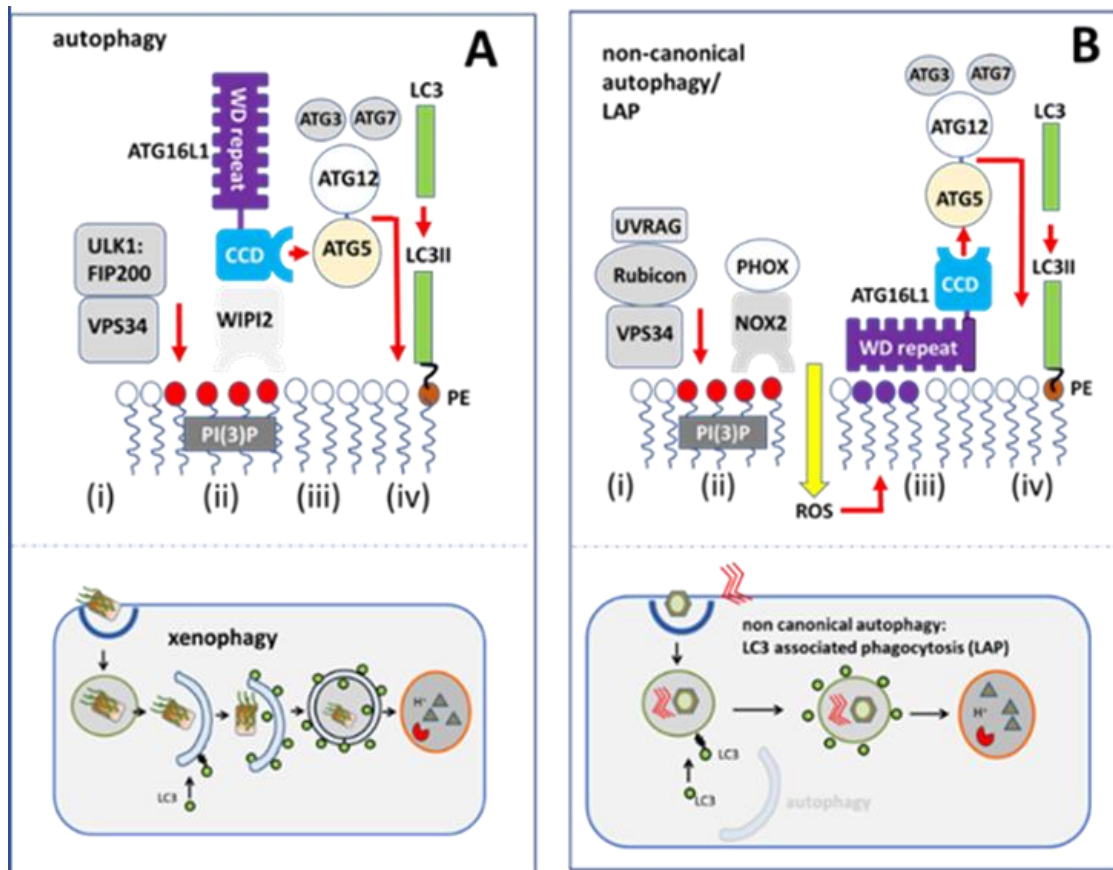


**Figure 6.7 A and B.** **A.** During xenophagy membranes phosphorylated by VP34 (i&ii) recruit WIPI which binds the CCD domain of ATG16L1 to recruit the ATG5-ATG12 complex (iii) required to conjugate LC3 to PE (iv). **B.** During LAP, endolysosome membranes phosphorylated by VP34: Rubicon (i) recruit the NOX2 complex (ii). ROS production (iii) provides a signal for binding of the ATG16L1 WD domain, allowing the CCD to recruit ATG5-ATG12 complex (iv) for LC3 conjugation to PE.

### 6.3.ii. Does the WD-vATPase axis block autophagy or non-canonical autophagy/LAP?

At first, it was difficult to compare the work in this thesis with that published by Xu et al in 2019 because of the definitions used by Xu et al for xenophagy, bacterial autophagy and LAP. The interpretations of these pathways used in this chapter are shown in Figure 6.7. Several studies have shown that during infection between 10 and 20% of the *S. Typhimurium* escape the SCV and enter the cytosol where they become substrates for conventional/canonical autophagy (Figure 6.7 A). This has been called

xenophagy and in common with autophagy is independent of the WD domain of ATG16L1, but does require ULK1/FIP200. Phosphorylation of lipids by the VPS34 PI3 kinase provides a platform for the recruitment of WIPI2 which can bind ATG5 to recruit the ATG5-ATG12:ATG16L1 complex required to conjugate LC3 to PE (Mizushima and Komatsu 2011).

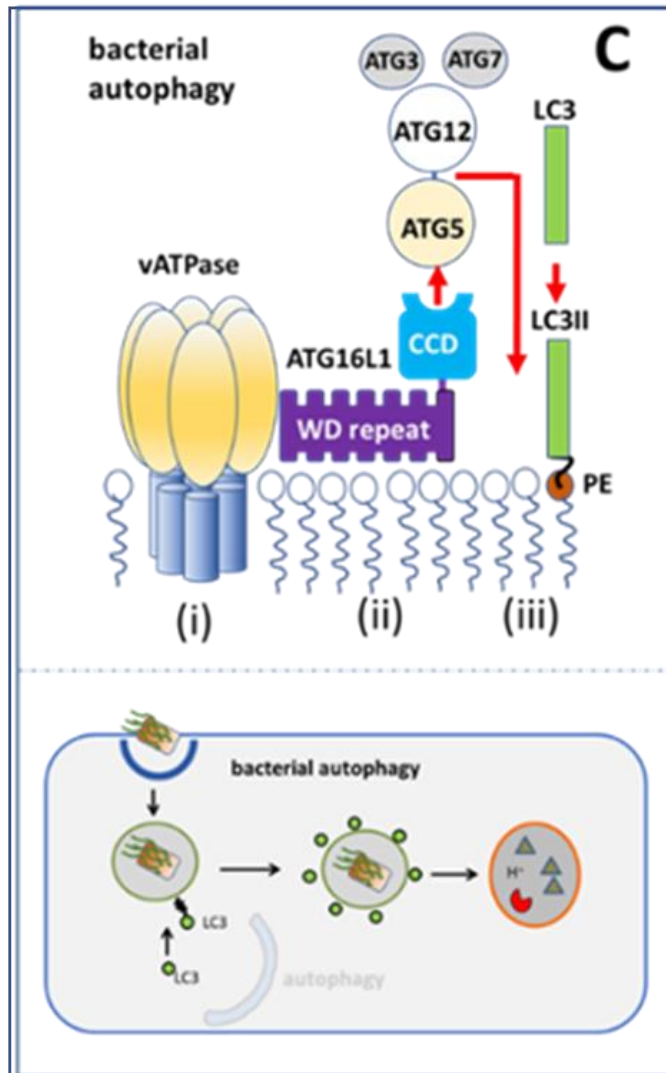


**Figure 6.7. C.** During bacterial autophagy, the WD domain of ATG16L1 binds the vATPase (i) allowing the CCD of ATG16L1 to recruit the ATG5-ATG12 complex (ii) for LC3 conjugation to PE (iii).

The  $\delta$ WD mouse model used in this study has a defect in the recruitment of LC3 to single membraned endolysosome compartments. This has been called non-canonical

autophagy/LAP and more recently LC3 associated endocytosis (LANDO) (Figure 6.7 B). The mice do not have defects in autophagy which involves recruitment of LC3 to double membraned autophagosomes. LAP (panel B) involves conjugation of LC3 to single membrane endo-lysosome compartments by pathways dependent on ROS signaling, UVRAG and RUBICON. Importantly, LAP requires the WD domain of ATG16L1 to bind lipids in endo-lysosome compartments and the CCD to recruit ATG5-ATG12 for LC3 conjugation to PE. Xu et al describe the WD-vATPase dependent recruitment of LC3 to vacuoles containing *S. Typhimurium* as xenophagy and/or bacterial autophagy (Figure 6.7 panel C). It seems unlikely that this is classical xenophagy because the WD-vATPase axis recruits LC3 to vacuoles containing vacuole markers Rab5, Rab7 and LAMP2 suggesting endo-lysosome compartments rather than autophagosomes. Furthermore, LC3 recruitment did not require FIP200 which is required for autophagy and SopF is unable to inhibit autophagy activated by Torin-1, even though it inhibits the WD-vATPase (Xu, Zhou et al. 2019).

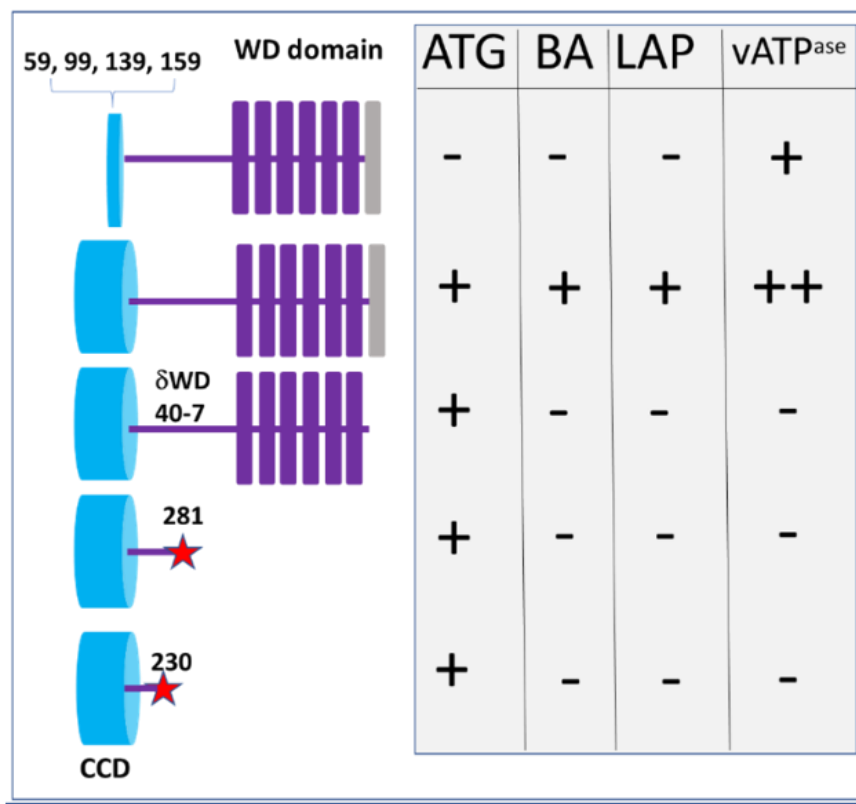
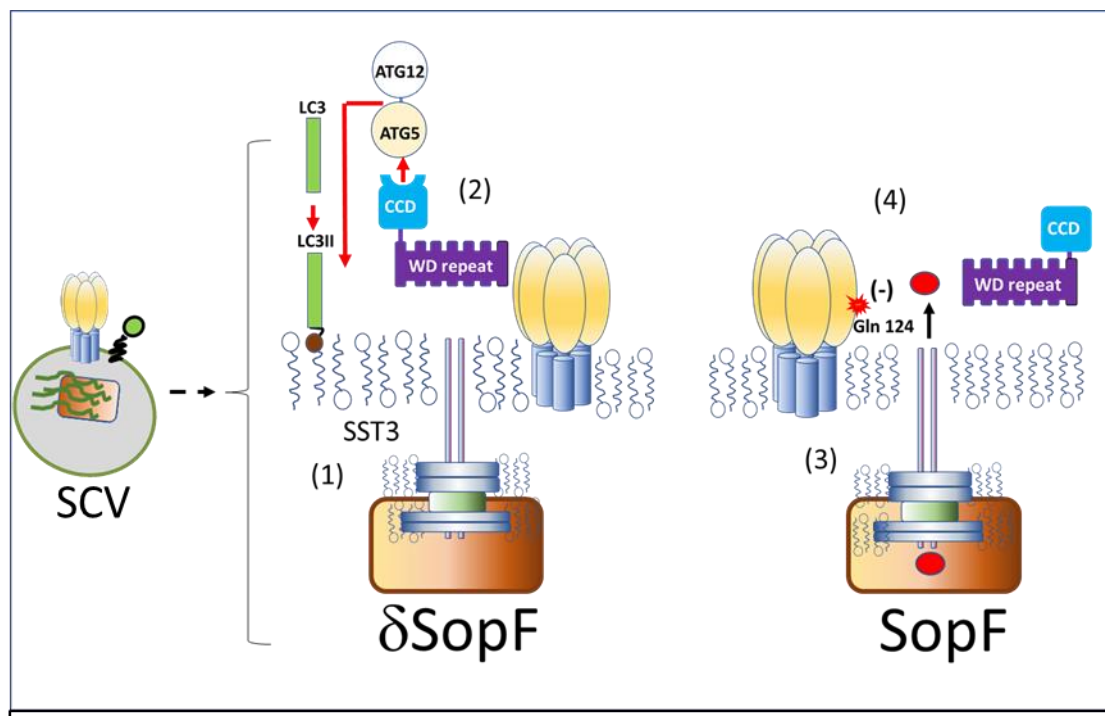


Figure 6.8. Domains of ATG16L1 required for autophagy, bacterial autophagy or LAP.

Xu et al. also carried out deletion analysis to locate domains of ATG16L1 required for recruitment of LC3 and binding to the vATPase. Figure 6.8 shows that the domains required for bacterial autophagy (BA) are different from autophagy (ATG) but the same as those required for LAP, suggesting that bacterial autophagy is very similar to LAP. BA required the ATG5 binding domain (59-139) within the CCD domain, to recruit ATG5-ATG12, and the last of the 7WD repeats. Interestingly, sites (N453, F467 and K490) identified as important for LAP (Fletcher, Ulferts et al. 2018) are in 4<sup>th</sup> WD repeat rather than 7, and LC3 recruitment to SCV in HeLa cells did not require UVRAG or RUBICON. This suggests that BA may be independent of ROS signaling and RUBICON and is not therefore classical LAP. It is possible that direct binding of the WD domain of ATG16L1 bypasses a need to bind the membranes of the endolysosome compartment and therefore uses the 7thWD domain to bind v-ATPase rather than the 4<sup>th</sup> WD domain required for membrane binding.

Figure 6.9 provides a model describing the WD v-ATPase axis and its role in bacterial autophagy. The diagram on the left shows the SCV containing *S. Typhimurium* labelled with LC3. *S. Typhimurium* within endosome-derived SCVs switch on the type III secretion (1) system leading to the assembly of the SST3 complex which extends a needle-like projection into the limiting membrane of the SCV. Xu et al (2019) have shown that the SCV is unable to retain fluorescent dyes or lysotracker. This suggests that the needle projection of the SST3 may increase membrane permeability (2) and trigger binding of ATG16L1 to the ATP6VOC subunit of the vATPase via the 7th WD domain/ $\beta$ -propeller. The CCD domain of ATG16L1 recruits ATG5-ATG12 required for conjugation of LC3 to PE in the SCV membrane providing a signal for fusion with lysosomes. LC3 recruitment is most obvious when *S. Typhimurium* lack SopF ( $\delta$ SopF). When *S. Typhimurium* expresses SopF (3) the virulence factor is secreted via the SST3 complex into the cytosol where it uses ADP-ribosylation to modify Gln 124 in the ATP6VOC subunit required for binding to the WD domain of ATG16L1. The ATP6VOC cannot respond to increased membrane

permeability by binding ATG16L1 and recruitment of LC3 and targeting to lysosomes are inhibited.



**Figure 6.9.** Assembly of T3SS complex makes a pore in the membrane of the SCV (1). This pore provides a docking site for ATG16L1, whose WD domain binds to vATPase on SCV membrane and conjugates LC3 to PE (2). SopF secreted by T3SS (3) block the binding of the WD to v-ATPase to prevent conjugation of LC3 (4).

### 6.3iii. Does the WD domain of ATG16L1 have functions in addition to recruiting LC3 via the WD-vATPase axis?

'*In vitro*' experiments by Xu et al showed that WT SL1344 *S. Typhimurium* generates more CFU than the SopF mutant when grown in HeLa cells and, in agreement with this thesis, they show that WT *S. Typhimurium* shows increased dissemination to liver and spleen '*in vivo*'. This shows that the v-ATPase-WD pathway suppresses replication, and this is inhibited by SopF both '*in vitro*' and '*in vivo*'. The availability of mice lacking the WD domain of ATG16L allowed us to determine whether the v-ATPase-WD axis was the only interaction reducing virulence, or if the WD domain had additional roles. Interestingly, results in chapter 4 (Fig 4.1) showed that there was

greater replication of WT *S. Typhimurium* in HEK cells reconstituted with ATG16L1 lacking the WD domain, and in  $\delta$ WD MEFs compared to control. Similarly, ‘*in vivo*’ challenge experiments in chapter 4 (Fig 4.2) showed that WT *S. Typhimurium* is more virulent in  $\delta$ WD mice where the WD target for SopF is missing. One possibility is that expression of SopF is too low to inhibit all the functions of the WD domain. However, in this chapter recruitment of LC3 to vacuoles by WT *S. Typhimurium* was the same for WT and  $\delta$ WD MEFs up to the timepoint of two hours post infect. The levels of SopF expressed in infected MEFs were sufficient to block the WD-dependent recruitment of LC3 to vacuoles between 60 and 120 minutes (Figure 6.4B). If the WD domain of ATG16L1 restricts *S. Typhimurium* replication only by the WD-v-ATPase axis that is blocked by SopF, the intracellular replication rate of *S. Typhimurium* should be very similar in WT and  $\delta$ WD MEFs. But this is not the case seen in our study. This raises the possibility that WD restricts *S. Typhimurium* replication by additional pathways that are independent of the WD-v-ATPase axis that is blocked by SopF.

# **Chapter 7 The WD domain of ATG16L1 influences the distribution of cholesterol between the cytosol and the Salmonella containing vacuole**

## **7.1 Introduction**

### **7.1.i. Background**

Recent reports have suggested that ATG16L1 may play a role in modulation of intracellular cholesterol trafficking. Both CCD and WD of ATG16L1 were involved in this process. Loss of either CCD or WD causes cholesterol accumulation in cells. (Tan, Mellouk et al. 2018). Studies also indicate that cytosolic cholesterol accumulates around SCVs and is linked to rapid Salmonella replication in cells (Catron, Sylvester et al. 2002, Garner, Hayward et al. 2002, Lossi, Rolhion et al. 2008, Nawabi, Catron et al. 2008). These findings suggested that ATG16L1's WD domain restricts *S. Typhimurium* replication by maintaining intracellular cholesterol homeostasis, which is independent of WD-v-ATPase axis. Thus, this chapter focuses on whether the loss of the WD domain of ATG16L1 promotes Salmonella replication by affecting cellular cholesterol levels.

### **7.1.ii. Cholesterol**

Cholesterol is very hydrophobic and the majority of total cellular cholesterol resides on the plasma membrane and interacts with adjacent lipids to regulate the permeability and fluidity of the membrane (Liscum and Munn 1999). Cholesterol often packs with sphingolipids and glycosylphosphatidylinositol-anchored proteins to form cholesterol-glycosphingolipid enriched membrane microdomains called lipid rafts in the plasma membrane. These microdomains play important roles in many cellular processes during host pathogen interactions (Sezgin, Levental et al. 2017),

membrane fusion, and exocytosis (Churchward and Coorssen 2009, Linetti, Fratangeli et al. 2010). This microdomain is often targeted by bacterial and viral pathogens for entry or invasion of eukaryotic cells, some others take advantage of the cholesterol trafficking pathway to promote their replication.

### **7.1.iii. Cholesterol and *S. Typhimurium* infection**

Cholesterol (C<sub>27</sub>H<sub>46</sub>O) was first isolated from human gallstone more than two centuries ago (Luo, Yang et al. 2020) and has been identified to be associated with many diseases. There were a few studies that revealed the role of cholesterol during *S. Typhimurium* infection. Garner et.al determined the role of plasma membrane cholesterol in *S. Typhimurium* entry of non-phagocytic cells. Their study revealed that profound cholesterol redistribution was triggered by *S. Typhimurium* during bacterial entry into non-phagocytic cells. Their studies revealed that this redistribution relied on SPI-1 effectors. A defect in *S. Typhimurium* invasion was observed following the depletion of membrane cholesterol (Garner, Hayward et al. 2002). Alvarea et.al further investigated and identified plasma membrane cholesterol promote *Salmonella* invasion by providing a target for SPI-1 T3SS docking to the plasma membrane (Alvarez, Glover et al. 2017). Plasma membrane cholesterol also plays some other roles during *Salmonella* infection. A few studies of Huang revealed that plasma membrane cholesterol plays critical roles in *Salmonella*-induced anti-inflammatory response and *Salmonella*-induced autophagy in intestinal epithelial cells (Huang 2011, Huang 2014). Cholesterol was also found to play important roles in vacuolar infection of *Salmonella*. Brumell et.al first found that SCVs in HeLa cells are labeled with filipin at 6 hours post infection (Brumell, Tang et al. 2001). Filipin is a polyene antibiotic that binds to 3 $\beta$ -hydroxysterols and emits a blue fluorescence (Wilhelm, Voilquin et al. 2019). But it was still not clear whether it was cholesterol or some other 3 $\beta$ -hydroxysterols which bind to filipin in SCVs. Catron et.al found that *S. Typhimurium* infection affects the host sterol biosynthetic pathway and identified the major sterol associated with SCVs is cholesterol (Catron, Sylvester et al. 2002).

They also found the association of cholesterol and SCVs occurs at a very early stage of infection and increases after *Salmonella* replication. Up to 30% of cellular cholesterol accumulates around SCVs, which is dependent on intracellular bacterial replication. They also identified a new marker of SCVs, CD55. CD55, or decay-accelerating factor, is a member of the glycosylphosphatidylinositol (GPI)-anchor proteins family. GPI anchor proteins conserve a C-terminal post-translational lipid modification and are important for maintaining cholesterol rich compartments and cellular uptake of folate (Chatterjee, Smith et al. 2001). These findings suggests that SCV interacts with early endosomal, cholesterol-rich membranes during replication. Another study focused on the early stage of infection and revealed that cholesterol-rich SCV were directly derived from the plasma membrane at the site of entry and maintained this high cholesterol level (Garner, Hayward et al. 2002). These findings indicate that cholesterol plays a critical role during entry/invasion and intracellular replication of *Salmonella*.

## **7.2 Results**

### **7.2.i. Loss of the WD domain of ATG16L1 raises cholesterol levels in the cytosol leading to a deficiency in membrane repair**

Filipin is a fluorescent probe that binds cholesterol and filipin staining is a standard way to measure cholesterol levels (Wilhelm, Voilquin et al. 2019). Intracellular cholesterol can also be measured using a DH4 probe that binds cholesterol. When mCherry-D4H is expressed in the cytosol it binds cholesterol on the cytosolic leaflet of the plasma membrane and intracellular organelles. WT MEFs and  $\delta$ WD MEFs were either stained with filipin or transfected with mCherry-D4H to visualize the intracellular cholesterol accumulation. Representative pictures were shown in Figure 7.1 A. The DH4 probe (left) gave strong labelling of intracellular vesicles and the number of DH4 positive vesicles was greatly increased in  $\delta$ WD MEFs. The signal from filipin was also located to intracellular vesicles but these were more difficult to

image because of the blue fluorescence signal. The corrected total cell fluorescence (CTCF) of D4H was measured by ImageJ software (Figure 7.1 B).  $\delta$ WD MEFs have a significantly higher fluorescence level compared with WT MEFs.

Cholesterol is known to regulate stiffness of the plasma membrane (Anishkin and Kung 2013) and exocytosis of lysosomes (Xu, Toops et al. 2012). ATG5, an important ATG16L1 binding partner, was previously shown to mediate cholesterol efflux from macrophage foam cells by a mechanism that remains poorly understood (Ouimet, Franklin et al. 2011). Tan et al. identified the role of ATG16L1 in promoting plasma membrane repair, in which both CCD and WD were involved (Tan, Mellouk et al. 2018). A digitonin titration assay was performed to determine if the loss of the WD domain from ATG16L1 in the  $\delta$ WD MEFs resulted in defects in plasma membrane repair. The cells were treated with serial dilution of digitonin (from 1.25-40  $\mu$ g/ml) for 20 minutes to generate small holes in the plasma membrane and then incubated in  $\text{Ca}^{2+}$  buffers for 10 minutes to allow them to repair. Membrane permeability was assessed by adding propidium iodide (PI) to label the nuclei of cells unable to repair membranes. Cells were then fixed in PFA, and counterstained with DAPI. The membrane repair efficiency was determined by the calculating percentage of PI-stained cells to DAPI stained cells. More PI stained cells indicated less efficiency in membrane repair. Figure 7.1 C showed that increasing concentrations of digitonin decreased the ability of cells to repair membranes. The WT MEFs were more resistant to digitonin than both the  $\delta$ WD and Atg16L KO MEFs. The WT MEFs showed defects in membrane repair in a digitonin range of 8-32 $\mu$ g/ml, this decreased by approximately half to 4-16  $\mu$ g/ml for  $\delta$ WD MEFs. The Atg16L1 KO MEFs showed the greatest sensitivity with 100% defect in repair at 4  $\mu$ g/ml. The results showed that the  $\delta$ WD MEFs have defects in membrane repair, and an apparent increased sensitivity of Atg16L1KO MEFs compared to  $\delta$ WD MEFs makes it possible that non-canonical functions of WD domain work together with autophagy to repair membranes.

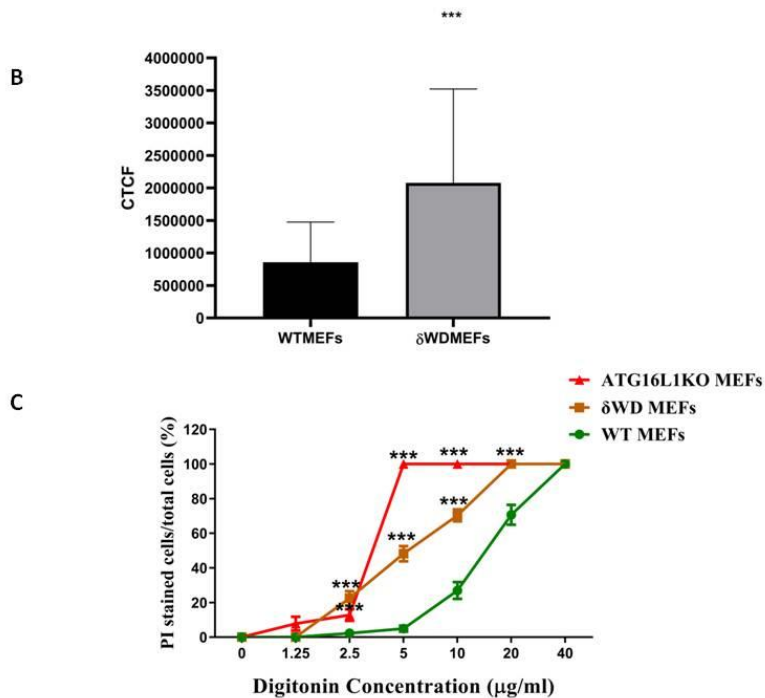
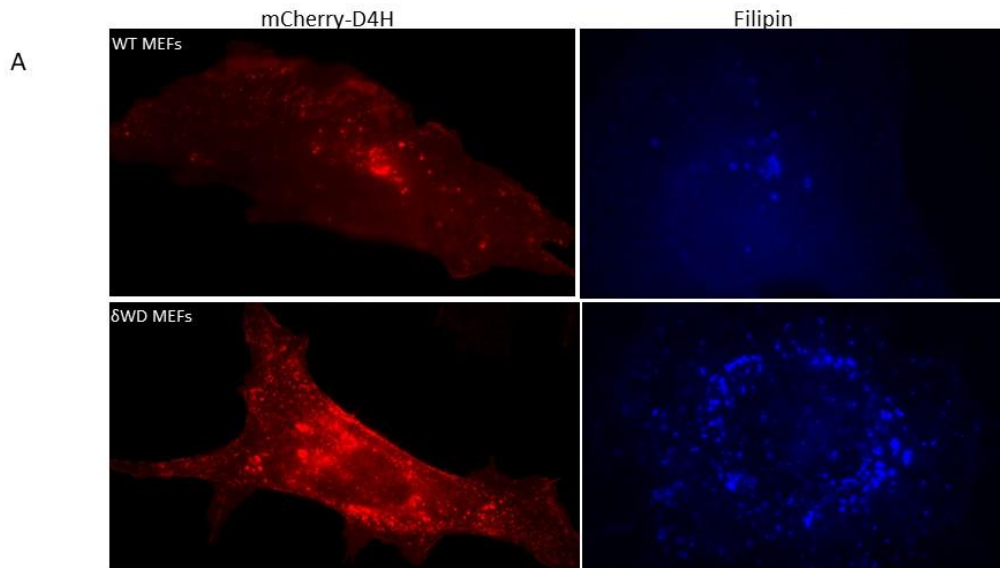


**Figure 7.1 Loss of the WD domain of ATG16L1 raises cholesterol levels in the cytosol leading to a deficiency in membrane repair** **A** left panel represents mCherry-D4H transfection of WT and deltaWD MEFs, the right panel shows Filipin staining of WT and deltaWD MEFs. Both staining showed that there are more cholesterol compartments in deltaWD MEFs compared with WT MEFs. **B** mCherry-D4H binds cholesterol on the cytosolic leaflet of the plasma membrane and intracellular organelles. Thus, mCherry density in cells can be used to measure cholesterol level in mCherry-DH4 transfected cells. The data represent the mean  $\pm$  SD of corrected cell total fluorescence

(CTCF) value of 30 WT or  $\delta$ WD MEFs measured by ImageJ after mCherry-D4H transfection. This result indicates that there is a significantly higher level of cholesterol in  $\delta$ WD MEFs compared with WT MEFs. The data were analyzed with student's t-test ( $p < 0.001$ ). C shows the percentage of PI-positive cells after increasing the concentration of digitonin treatment. Percentage of PI positive cells raise to 100% after only 5 $\mu$ g/ml of digitonin treatment in ATG16L1KO MEFs, while this concentration is 20 $\mu$ g/ml in  $\delta$ WD MEFs and 40 $\mu$ g/ml in WT MEFs. Percentage of PI positive cells from 3 wells per digitonin concentration were calculated. This data indicates that the MEFs used in this study showed the same deficiency in membrane repair as reported. The data is analyzed by Bonferroni post test in two way ANOVA and both ATG16L1KO MEFs and  $\delta$ WD MEFs were compared with WT MEFs for difference (\*\* $p < 0.01$  and \*\*\* $p < 0.001$ ).

### **7.2.ii. Salmonella co-localize with cytosolic cholesterol**

To determine if *Salmonella* co-localize with intracellular cholesterol,  $\delta$ WD MEFs and WT MEFs were transfected with mCherry-D4H for 48 hours and then infected with GFP-expressing JH3009 for 4 hours. Then cells were fixed with PFA and imaged with an Apotome microscope. The GFP-JH3009 showed strong co-localization with mCherry-D4H labeled cholesterol (Figure 7.2), which indicated that cholesterol accumulated around the site of intracellular *Salmonella* and matched with the previous studies (Catron, Sylvester et al. 2002, Garner, Hayward et al. 2002, Lossi, Rolhion et al. 2008, Nawabi, Catron et al. 2008). Despite  $\delta$ WD cells showing much more cellular cholesterol, there is no difference in cholesterol association with *Salmonella* between  $\delta$ WD and WT MEFs (Figure 7.2).

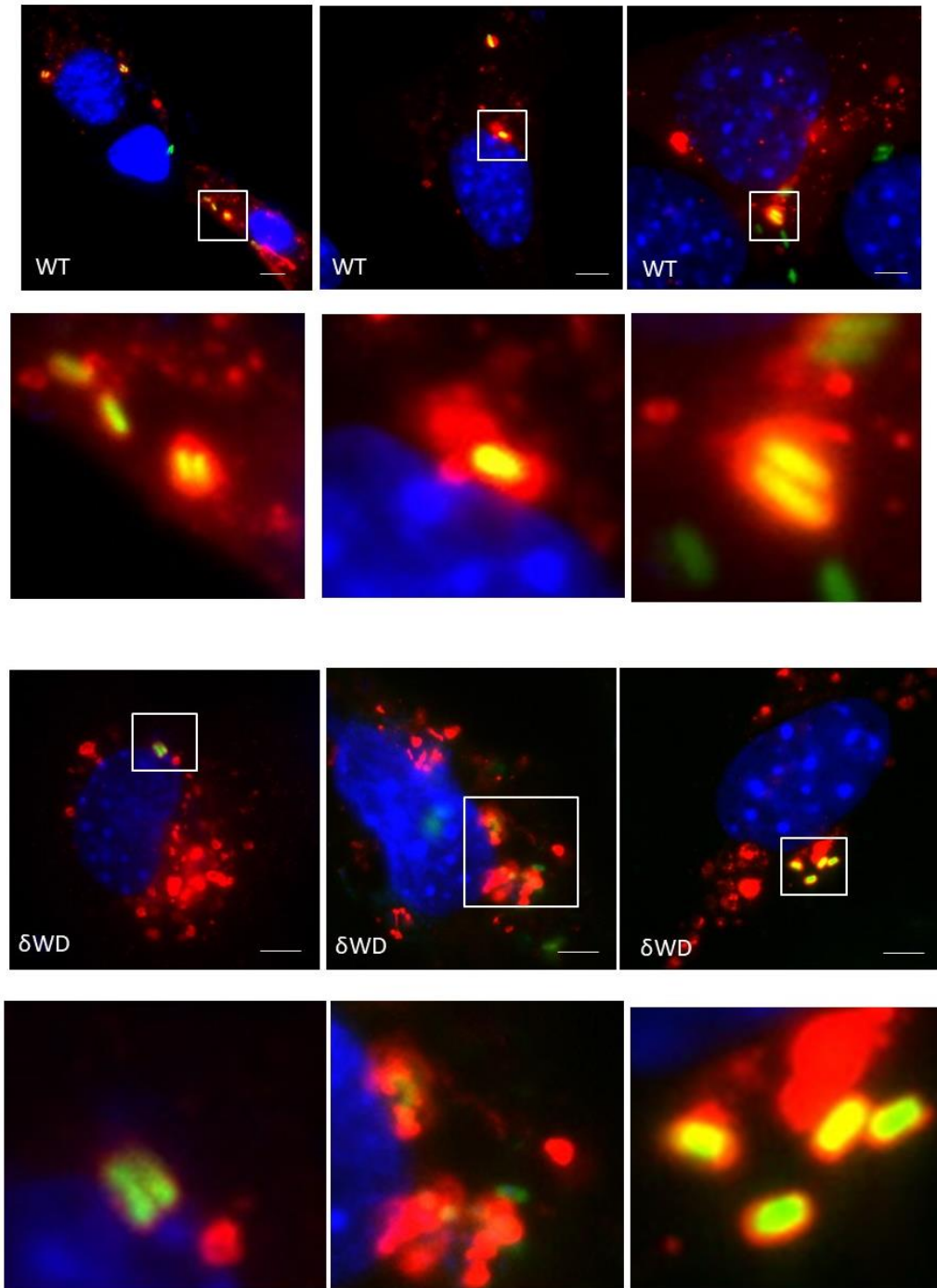


**Figure 7.2 Salmonella co-localize with cytosolic cholesterol**  $\delta$ WD MEFs and WT MEFs were transfected with mCherry-D4H for 48 hours and then infected with JH3009 for 4 hours. Then cells were fixed with PFA and imaged with an Apotome microscope. The GFP-JH3009 showed strong co-localization with mCherry-D4H labeled cholesterol. Despite  $\delta$ WD cells showing much more cellular cholesterol, there is no difference in cholesterol association with Salmonella between

$\delta$ WD and WT MEFs. Boxed regions highlighting co-localization of GFP-JH3009 and mCherry-D4H are enlarged and shown in the lower panel. Magnification 63X, scale bars: 10  $\mu$ m.

### 7.2.iii. T0901317 and U18666A modulate cholesterol levels in cells.

Drugs that modulate cholesterol levels in cells were used to further investigate the relationship between intracellular cholesterol and salmonella replication. T0901317 and U18666A were used to reduce/increase cholesterol levels in both  $\delta$ WD MEFs and WT MEFs.  $\delta$ WD MEFs treated with T0901317 showed a decrease in cholesterol levels, which is confirmed by mCherry-D4H transfection (Figure 7.3 A middle panel). WT MEFs treated with U18666A showed an increase in cholesterol level, which was also confirmed by mCherry-D4H staining (Figure 7.3 A right panel).

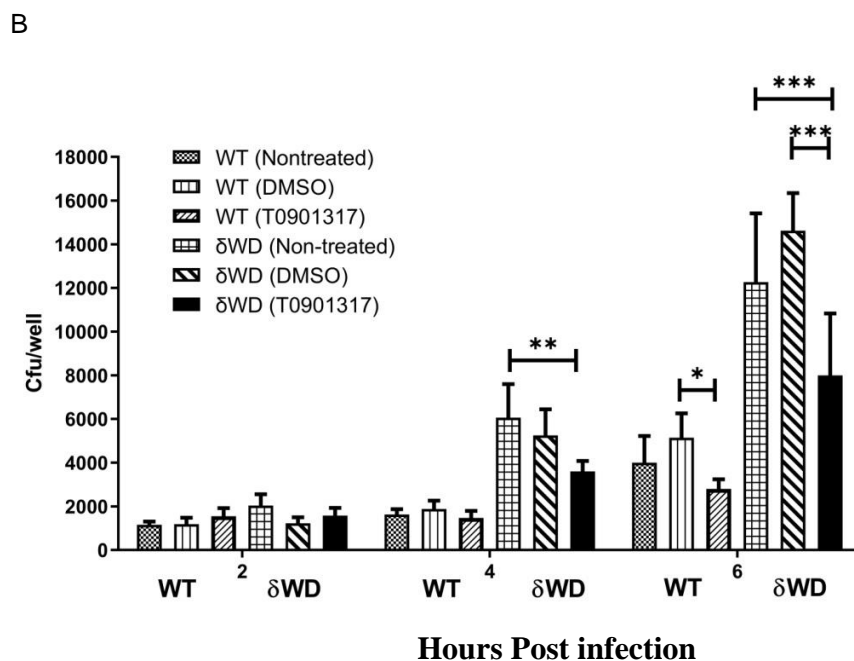
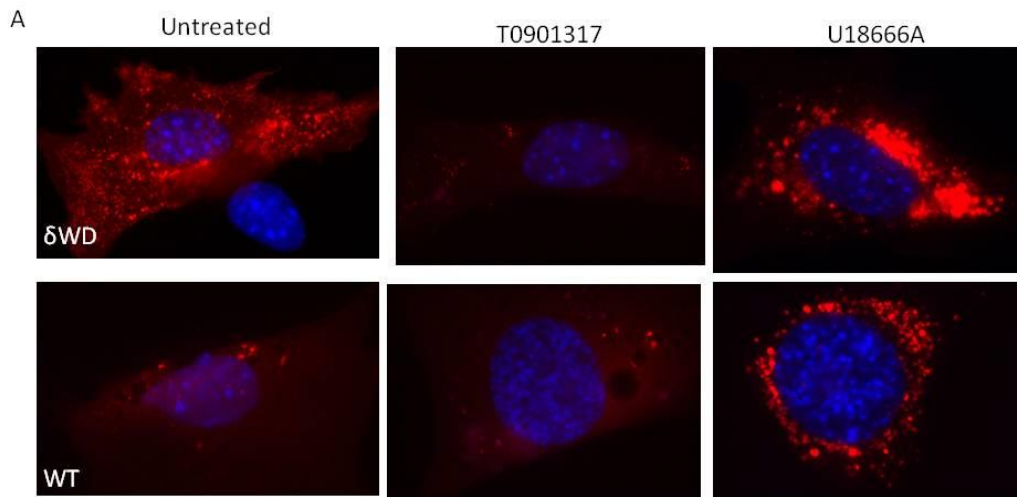


### **Figure 7.3 T0901317 and U18666A treatment in MEFs decrease/increase cellular cholesterol level and affect intracellular Salmonella replication**

**A** WT and  $\delta$ WD MEFs were treated with T0901317 and U18666A. WT and  $\delta$ WD MEFs were transfected with mcherry-D4H and then treated with T0301317 for 4 hours, cholesterol level was reduced after T0901317 treatment in both WT and  $\delta$ WD MEFs (middle panel). In the right panel, WT and  $\delta$ WD MEFs were treated with U18666A after mCherry-D4H transfection. Both WT and  $\delta$ WD MEFs showed an increase in cholesterol levels.

**B** WT and  $\delta$ WD MEFs were seeded in 24 well plates at a concentration of  $2 \times 10^4$  cell per well ( $n=6$ ). On the next day, cells were treated with T0901317 for 4 hours and then infected with JH3009. At the indicated time points, cells were lysed and plated on agar plates. Salmonella counts significantly reduced at 4 hours post infection in  $\delta$ WD MEFs and 6 hours post infection in both WT and  $\delta$ WD MEFs. The data is analyzed by Bonferroni post test in two way ANOVA ( $*p < 0.05$ ,  $**p < 0.01$  and  $***p < 0.001$ ).

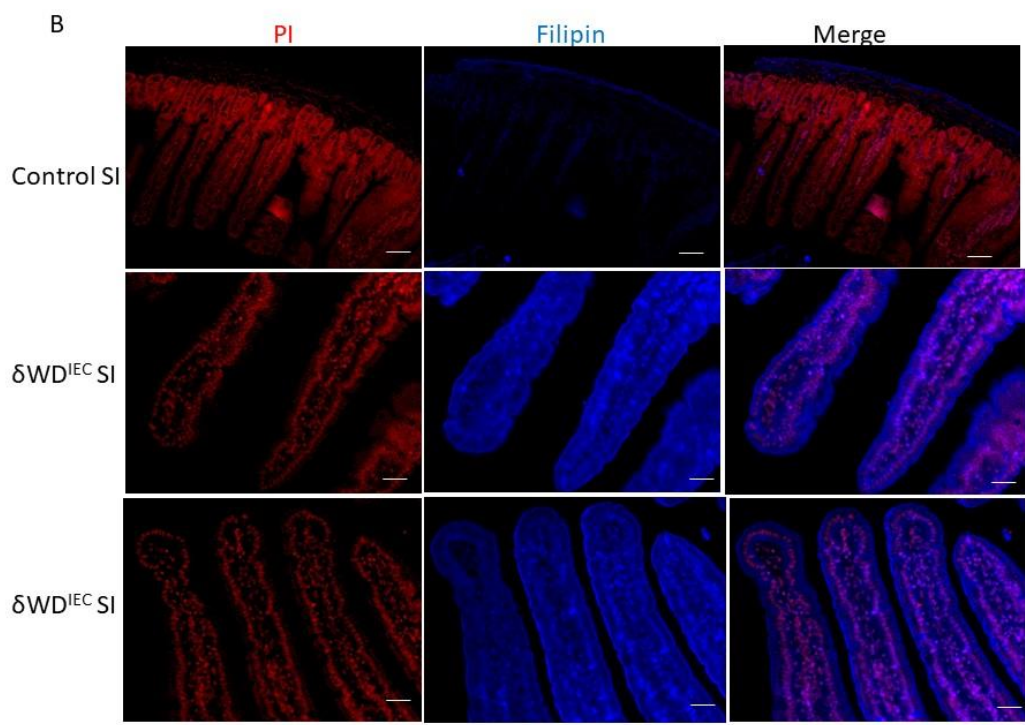
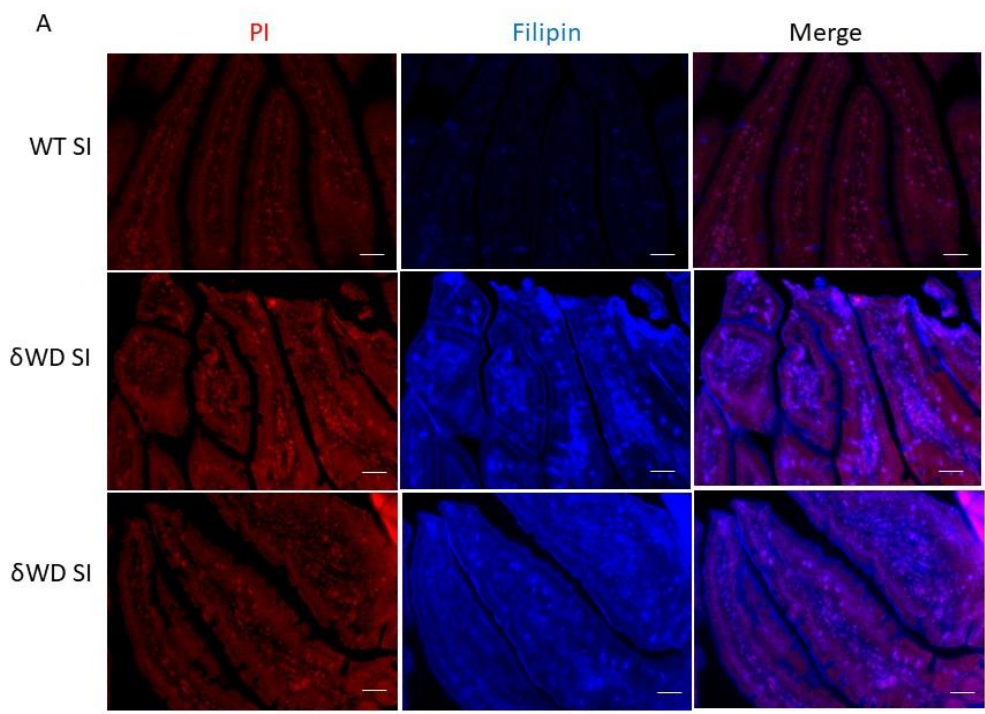
### **7.2.iv. Reduced intracellular cholesterol levels inhibit Salmonella replication**

To examine the link between intracellular cholesterol level and Salmonella replication,  $\delta$ WD and WT MEFs were treated with T0901317 for 4 hours prior to JH3009 infection. Cells were lysed at 2, 4, and 6 hours after infection and lysates were spread on agar plates and CFU were counted on the second day. The results were shown in Figure 7.2 B. The bar graphs compare untreated and DMSO controls with cells incubated with T0901317 at each time point with the WT MEFs shown on the left at each time point. The CFU count was higher for  $\delta$ WD cells at each time point and the counts were unaffected by DMSO. Replication appeared to occur earlier in the  $\delta$ WD MEFs with high numbers evident at 4 hours and increasing at 6 hours. In each case, the CFU counts were significantly reduced after T0901317 treatment. Replication was evident at 6 hours in WT MEFs and CFU were again reduced by T0901317, indicating that a reduction in cytosolic cholesterol levels limits intracellular Salmonella replication.

## **7.2.v. Small intestine of mice lacking the WD domain of ATG16L1**

### **have higher levels of intracellular cholesterol.**

After confirming that the loss of WD domain results in cholesterol accumulation in MEFs, we further investigated the cholesterol level in the small intestine of  $\delta$ WD mice. Small intestines were harvested from  $\delta$ WD mice and WT mice and fixed in formalin overnight and then transferred to 70% ethanol. Then tissues were embedded in paraffin and cut with a microtome. The sections were dewaxed and stained with filipin for 2 hours at room temperature to image cholesterol. After filipin staining, the sections were counterstained with PI to identify nuclei and imaged with an Apotome microscope. The left panel showed the PI staining (red) of the SI, PI is a dye which often used to stain cells and nucleic acid. The quantum yield of PI is enhanced 20-30 fold after binding to DNA. Thus, the nucleus is defined as the bright red dots in the left panel. Filipin binds to cholesterol and showed as blue in the middle panel. The merged image is in the right panel. As shown in Figure 7.3 A, there was a greater filipin signal in the small intestine of  $\delta$ WD mice compared with small intestine of WT mice. To further investigate the role of the WD domain in tissue cholesterol accumulation, the small intestine of  $\delta$ WD<sup>IEC</sup> was also sectioned and stained with filipin. The representative images are shown in Figure 7.4 B, which indicates  $\delta$ WD<sup>IEC</sup> also have a higher level of cholesterol level in their intestine. To further study this, the sections were observed under 63X objective on a confocal microscope (ZESIS, US). The representative images were shown in Figure 7.4 C and D. All those data indicate that ATG16L1's WD domain maintains cholesterol distribution in the small intestine.



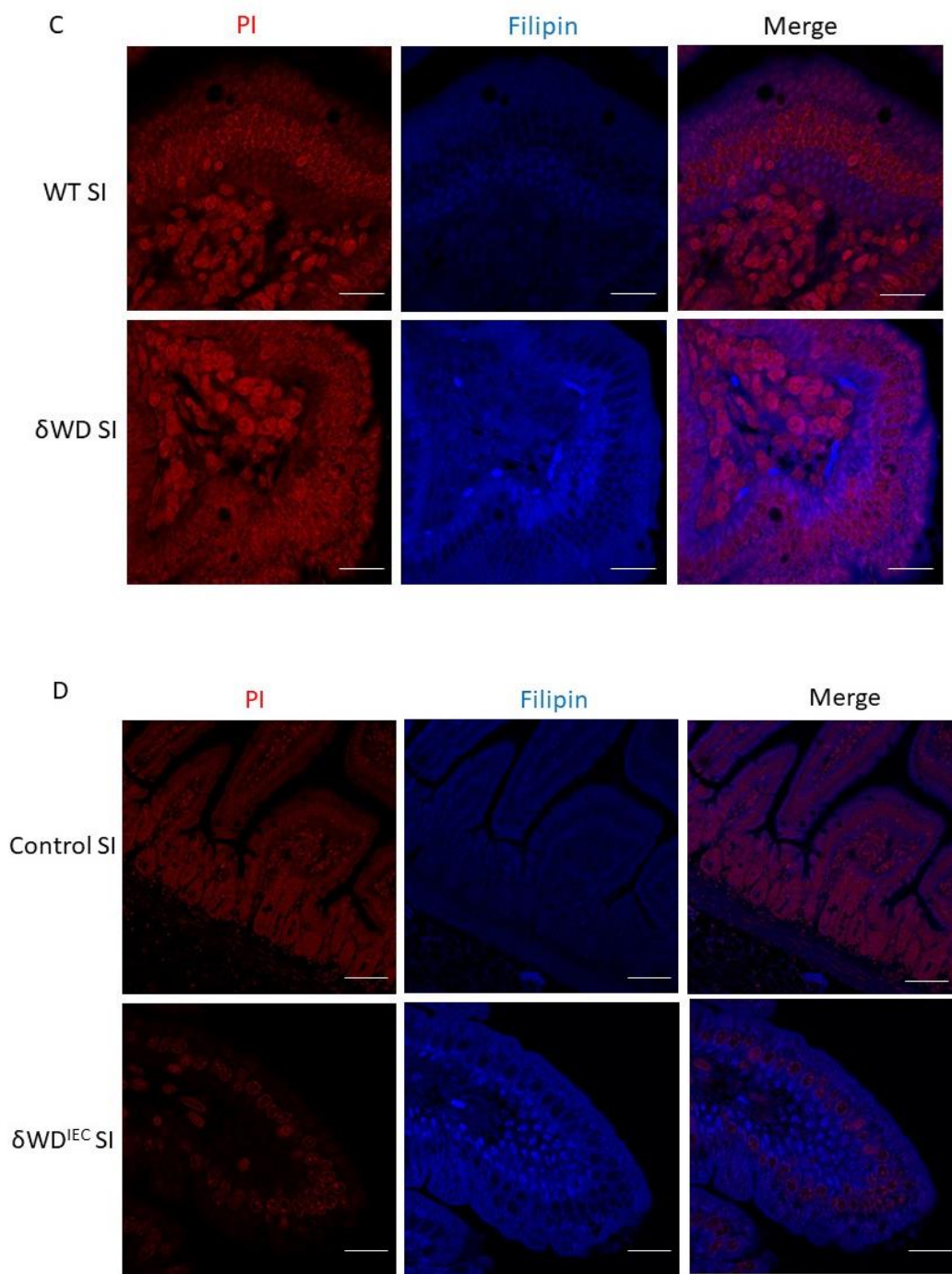


**Figure 7.4 Filipin staining of small intestine** Small intestines were harvested from  $\delta$ WD mice and WT mice and fixed with formalin. Then tissues were embedded in paraffin and cut with a microtome. The sections were dewaxed and stained with filipin for 2hours at room temperature. After filipin staining, the sections were counterstained with PI to identify nuclei and imaged with an Apotome microscope or confocal microscope. The left panel showed the PI staining (red) of the

SI, PI is a dye which often used to stain cells and nucleic acid. The quantum yield of PI is enhanced 20-30 fold after binding to DNA. Thus the nucleus is defined as the bright red dots in the left panel. Filipin binds to cholesterol and showed as blue in the middle panel. The merged image is in the right panel.

**A** Apotome image of small intestine from  $\delta\text{WD}^{\text{IEC}}$  and control mice. There was a greater filipin signal in the small intestine of  $\delta\text{WD}^{\text{IEC}}$  mice compared with the small intestine of control mice. Magnification 20X, scale bars: 50  $\mu\text{m}$ .

**B** Apotome image of small intestine from WT and  $\delta\text{WD}$ . There was a greater filipin signal in the small intestine of  $\delta\text{WD}$  mice compared with small intestine of WT mice. Magnification 20X, scale bars: 50  $\mu\text{m}$ .

**C** Confocal images of small intestine from WT and  $\delta\text{WD}$  mice. there was a greater filipin signal in the small intestine of  $\delta\text{WD}$  mice compared with small intestine of WT mice. Magnification 63X, scale bars: 11  $\mu\text{m}$ .

**D** Confocal images of small intestine from  $\delta\text{WD}^{\text{IEC}}$  and control mice. there was a greater filipin signal in the small intestine of  $\delta\text{WD}^{\text{IEC}}$  mice compared with the small intestine of control mice. Magnification 63X, scale bars: 11  $\mu\text{m}$ .

## 7.3 Discussion

### 7.3.i. Background.

The results presented in chapters 5 and 6 showed that the WD domain of ATG16L1 restricted *S. Typhimurium* replication in cell culture, and ‘*in vivo*’ following oral challenge in mice. Villin-cre mediated expression of the  $\delta$ WD mutation showed that protection against infection required expression of the WD domain in gut epithelial cells. During the course of this work, Xu et al showed that expression of SopF by *S. Typhimurium* inhibits interactions between the WD domain of ATG16L1 and the v-ATPase in the membrane of the SCV. This interaction is thought to promote replication of *S. Typhimurium* by preventing recruitment of LC3 to the SCV and degradation in lysosomes. This made it possible for the increased replication of *S. Typhimurium* seen in  $\delta$ WD cells and  $\delta$ WD mice, which could be explained because they lacked the ability to activate the v-ATPase-WD pathway. The results from chapter 7, however, suggested that the WD domain may influence the replication of *S. Typhimurium* by pathways separate from binding to the v-ATPase. During this period a study by Tan et al revealed that ATG16L1 plays an important role in maintaining plasma membrane integrity by promoting plasma membrane repair, and deficiency in ATG16L1 causes cellular cholesterol accumulation both *in vivo* and *in vitro*. This phenotype can be rescued by re-expressing full-length ATG16L1, but not the T300A variant or  $\delta$ WD deletion mutant (Tan, Mellouk et al. 2018). Furthermore, cholesterol plays a crucial role in the invasion (Huang 2011, Huang 2014, Alvarez, Glover et al. 2017) and intracellular replication of *S. Typhimurium* (Catron, Sylvester et al. 2002, Garner, Hayward et al. 2002). This prompted us to study cholesterol distribution in  $\delta$ WD cells and  $\delta$ WD mice.

### 7.3.ii. The lack of WD domain of ATG16L1 increases cellular cholesterol.

Cellular cholesterol was compared using fluorescent probes, such as filipin and mCherry-D4H, in  $\delta$ WD MEFs and WT MEFs. Loss of the WD domain resulted in cellular cholesterol accumulation. We also stained cholesterol in the paraffin-embedded small intestine sections of  $\delta$ WD and  $\delta$ WD<sup>IEC</sup> mice. The results indicated that *atg16L1 $\delta$ WD* caused cholesterol accumulation both in MEFs and in epithelial cells of the small intestine. MEFs lacking ATG16L1, or expressing ATG16L1 lacking the WD domain, also showed increased sensitivity to permeabilization with digitonin suggesting a defect in membrane repair. This was more pronounced in the ATG16L1 KO cells than  $\delta$ WD, suggesting that autophagy and non-canonical autophagy may both play a role in membrane repair. Staining of infected cells with the cholesterol sensor DH4 showed accumulation of cholesterol around vacuoles containing *S. Typhimurium*. The link between cholesterol and *S. Typhimurium* replication was tested by depleting cholesterol with T0901317. As in previous chapters, replication was greater in  $\delta$ WD MEFs compared to WT cells, and in each case, replication was reduced by approximately one-half when cholesterol was depleted by T0901317. The results showed that the loss of ATG16L1's WD domain increases intracellular cholesterol levels may restrict replication *S. Typhimurium* replication by modulating cholesterol distribution.

### **7.3.iii. Membrane repair, cholesterol and the WD domain of ATG16L1.**

The role played by the WD domain of ATG16L1 in membrane repair during bacterial infection was studied using *Listeria monocytogenes* as a model (Tan, Mellouk et al. 2018). Unlike *S. Typhimurium*, *Listeria* generates a pore-forming toxin called listeriolysin (LLO) that prevents vacuole acidification and helps the bacteria escape from the vacuole into the cytoplasm. The action of LLO is inhibited by cellular pathways such as lysosomal exocytosis that repair damaged membranes (Gedde, Higgins et al. 2000). Tan et al showed that MEFs lacking autophagy proteins ATG5, ATG12 or ATG16 showed reduced repair of the plasm membrane induced by the

cholesterol-dependent pore-forming Pneumolysin from *Streptococcus* or the sterol-based mild detergent digitonin. Defects in membrane repair were also seen for the T300A mutant of ATG16L1 and ATG16L1 lacking the WD domain (Tan, Mellouk et al. 2018). Further experiments by Tan et al showed that ATG16L1 facilitated lysosome exocytosis by allowing lysosomes to fuse with the plasma membrane to provide lipids required for membrane repair. Accumulation of cholesterol in lysosomes reduces lysosome exocytosis (Xu, Toops et al. 2012) and, similar to the result from this chapter, Tan et al showed that loss of ATG16L1 or the WD domain of ATG16L1 resulted in increased cholesterol. Tan et al were able to show that the cholesterol was located to LAMP positive lysosomes and that depletion of cholesterol by T0901317 restored membrane repair. Cell to cell spread of *Listeria* is promoted by the LLO-mediated membrane damage. Tan et al showed that loss of ATG16L1 resulted in reduced membrane repair during *Listeria* infection and an increased cell to cell spread that could be reversed if the accumulated cholesterol was depleted by T0901317 (Tan, Mellouk et al. 2018).

It would be interesting to follow up on these observations for *S. Typhimurium*. The LLO of *Listeria* is required for the bacteria to escape from the vacuole and for later escape from actin-induced pseudopodia that project into neighbouring cells. Both of these events are inhibited by ATG16L1 and its ability to lower intracellular cholesterol and facilitate lysosome exocytosis. *S. Typhimurium* do not make a pore-forming toxin but it appears from the results in this chapter that the regulation of cholesterol by the WD domain of ATG16L1 does restrict *S. Typhimurium* replication. We have shown defects in membrane repair in  $\delta$ WD MEFs, and therefore it will be interesting to determine if this results from reduced lysosome exocytosis and if lysosomes and/or SCVs accumulate cholesterol in  $\delta$ WD MEFs. It is possible that defects in membrane repair facilitate the escape of *S. Typhimurium* from the SCV into the cytoplasm, or allow the SCV to access nutrients needed for replication and formation of the SIF.

### **7.3.iv. Plasma membrane or cytosolic cholesterol inhabits *S.***

#### **Typhimurium infection.**

The role of plasma membrane cholesterol in *S. Typhimurium* infection has been studied previously and several mechanisms have been proposed. Huang identified the critical roles of plasma membrane cholesterol in *S. Typhimurium*-induced anti-inflammatory response and *S. Typhimurium*-induced autophagy in IECs cell lines (Huang 2011, Huang 2014). Huang treated Caco-2 cells with methyl-beta-cyclodextrin (M $\beta$ CD) to deplete membrane cholesterol. The depletion of cholesterol induces autophagy (Cheng, Ohsaki et al. 2006), and this may increase the recognition of *S. Typhimurium* in damaged SCVs and *S. Typhimurium* released to the cytosol (Birmingham and Brumell 2006) increasing the clearance of the pathogen (Birmingham, Smith et al. 2006). Alvarez et al. published a similar study more recently in 2017. In the study, Alvarez et al. identified a gene *VAC14* which plays an important role in cellular cholesterol trafficking and homeostasis and is an inhibitor for *S.Typhi* infection. The silencing of *VAC14* increased intracellular cholesterol levels, which results in the increasing invasion of *S.Typhi* and an increase of Typhoid fever susceptibility in humans. Then they treated zebrafish with ezetimibe, a drug demonstrated to reduce cholesterol levels in zebrafish larvae, before challenging zebrafish with *S.Typhi*. Improved survival and bacterial clearance were observed in ezetimibe-treated zebrafish compared with DMSO-treated controls. Similar to Huang's study, they depleted cholesterol from the plasma membranes with M $\beta$ CD treatment and determined that increasing the level of cholesterol in the plasma membrane facilitates *S.Typhi* invasion (Alvarez, Glover et al. 2017). M $\beta$ CD treatment was considered as a traditional way of extracting cholesterols from plasma membranes (Ilangumaran and Hoessli 1998, Mahammad S 2015), but some studies claimed that M $\beta$ CD extracts similar proportions of cholesterol from the Triton X-100 resistant (lipid raft enriched) as it does from other cellular fractions, furthermore cells rapidly reestablish the relative differences in cholesterol concentration between

different compartments (Mahammad and Parmryd 2008). Thus, further study is needed to determine whether plasma membrane cholesterol or cytosolic cholesterol plays a role in facilitating *S. Typhimurium* invasion.

### **7.3.v. Other roles for cholesterol during *S. Typhimurium* infection.**

Cholesterol sometimes plays a role in maintaining *S. Typhimurium* intracellular survival (Scott, Cuellar-Mata et al. 2002). Studies also show that intracellular cholesterol accumulation around SCVs promotes intracellular *S. Typhimurium* replication (Brumell, Tang et al. 2001, Catron, Sylvester et al. 2002, Garner, Hayward et al. 2002). A study found that more than 30% of total cellular cholesterol accumulated around SCVs at the late stage of infection and SPI-2 effectors were critical for the accumulation of cholesterol to the SCV in macrophages (Catron, Sylvester et al. 2002). Another study identified an SPI-2 effector, named SseJ, whose major role is to increase cholesterol esterification in host cells (Nawabi, Catron et al. 2008). Esterification of cholesterol increases the solubility of cholesterol allowing storage in lipid droplets, which may increase the availability of cholesterol to *S. Typhimurium*.  $\delta SseJ$  mutants reduce cholesterol esterification and lipid droplet formation in host cells.  $\delta SseJ$  mutants also have altered SCV dynamics (Ruiz-Albert, Yu et al. 2002) and showed a defect in virulence in mice infection models (Ruiz-Albert, Yu et al. 2002, Lawley, Chan et al. 2006). All these studies indicate that cholesterol and its esterification are important for bacterial survival and proliferation in the host. But how cholesterol contributes to *S. Typhimurium* intracellular survival and proliferation is still unclear and will be an important topic in future studies.

### **7.3.vi. Summary.**

In the present study, we determined that deficiency in Atg16L1's WD domain caused cellular cholesterol accumulation. We also determined that intracellular cholesterol

accumulates around *S. Typhimurium* by infecting mCherry-D4H transfected MEFs with GFP labeled JH3009 and determine the co-localization of D4H with GFP labeled *S. Typhimurium*. Then we treated both WT and  $\delta$ WD MEFs with T0901317, a drug that reduces cellular cholesterol level, prior to JH3009 infection. Results indicate a reduction in cellular cholesterol level significantly reduced intracellular *S. Typhimurium* replication in both WT and  $\delta$ WD MEFs. All these data suggest that the WD domain limits *S. Typhimurium* infection via maintaining cellular cholesterol homeostasis.

## Chapter 8 Discussion and further perspective

### 8.1 Discussion.

ATG16 in yeast contains the N-terminal CCD but lacks the C-terminal WD domain seen in higher eukaryotes, even so yeast ATG16 is still able to activate canonical autophagy. The WD40 domain makes up about 60% of the 66kDa ATG16L1 of higher eukaryotes, such as plants insects and mammals, and is not required for canonical autophagy. Studies in our lab in collaboration with Oliver Florey and colleagues show that the WD domain is required for non-canonical LC-3 lipidation on single membranes (Fletcher et al). This process was identified firstly in macrophages and referred to as LAP (Sanjuan et al 2007). LAP has been found to facilitate the removal of bacteria by phagocytosis from cells in culture (Martinez, Malireddi et al. 2015, reviewed in Schille, Crauwels et al. 2018) but studies ‘in vivo’ are rare because of a lack of suitable mouse models.

The work described in this thesis uses a new mouse model where a stop codon was inserted at aa 230 of the Atg16L1 gene. This preserved the ATG5 binding domain and WIPI2b binding site in CCD, which is essential for autophagy, but removed the 7 WD repeats which are required for LAP. These mice, named  $\delta$ WD mice, are defective in LAP but maintain normal autophagy. Further studies confirmed that these mice were fertile and maintained a normal immune system compared with WT mice, which makes them suitable for infection studies (Rai, Arasteh et al. 2019).

*S. Typhimurium* has been used extensively to study host-bacterial interactions. Many early studies focused on the role of autophagy in removing intracellular *S. Typhimurium*. Most of these studies were conducted on cell lines lacking genes essential for autophagy and tissue specific ATG knockout mice (Conway, Kuballa et al. 2013, Zhang, Zheng et al. 2017, Zhang, Zheng et al. 2017). However, at that time

the significance of LAP was underappreciated because the KO cells and mice used were defective in both ATG and LAP. Since then RUBICON KO mice have been developed and have been used to study LAP during fungal infection '*in vivo*', but thus far they have not been used to study *Salmonella*. These RUBICON knockout mice also showed a pro-inflammatory phenotype in their immune response and developed autoimmune diseases (Martinez, Malireddi et al. 2015, Martinez, Cunha et al. 2016) which may compromise infection studies.

In this thesis,  $\delta$ WD mice and cells derived from them were used to determine if the loss of WD domain increased sensitivity to *S. Typhimurium* infection. *S. Typhimurium* replicated faster in  $\delta$ WD MEFs compared with WT MEFs.  $\delta$ WD mice showed a higher mortality rate following oral gavage with *S. Typhimurium* strain JH3009 and a more severe weight loss compared with littermate controls. There was greater bacterial dissemination to tissues and severe damage was seen in the liver and spleen possibly caused by lymphocyte infiltration. These data indicate the WD domain of Atg16L1 plays an important role in restricting *S. Typhimurium* infection in mice. Then we used flox-cre recombination to determine the role of the WD domain in either IECs or myeloid cells during infection. The  $\delta$ WD<sup>IEC</sup> mice showed a high mortality rate and severe weight loss compared with littermate controls and also showed greater dissemination of bacteria to the liver and spleen. In contrast,  $\delta$ WD<sup>phage</sup> mice showed no difference in weight loss, mortality rate and bacterial dissemination to tissues compared to littermate controls. These experiments showed that the WD domain of ATG16L1 restricted *Salmonella* infection in intestinal epithelial cells.

A study conducted by Conway et al. used a specific knockout of ATG16L1 in gut epithelium mice model and found that lack of full-length ATG16L1 caused abnormality in Paneth cells and increased mice susceptibility to *S. Typhimurium* infection (Conway, Kuballa et al. 2013). In contrast, the abolition of ATG16L1 in mononuclear cells did not increase the virulence of *S. Typhimurium* in mice (Conway,

Kuballa et al. 2013). In the present study, we also found that loss of LAP in gut epithelial cells, but not myeloid cells, played crucial roles in controlling *S.Typhimurium* infection in mice. Myeloid cells, such as macrophages, act as transporters for *S.Typhimurium* dissemination from gut epithelium to other tissues and sites for *S.Typhimurium* replication in liver and spleen (Watson and Holden 2010). Macrophages are also involved in the adaptive immune response because they present antigens to T cells. It is very strange that LAP, an innate pathway that limits intracellular bacterial survival and promotes antigen presentation, in macrophages failed to play any significant roles in controlling *S.Typhimurium* infection in mice. It is likely that *S.Typhimurium* has developed some effector mechanism to avoid LAP and promote its survival in macrophages. In a recent study, Wei et al studied the immune response of C57/BL6 mice to *S.Typhimurium* strains. Only an attenuated *S.Typhimurium* strain, CVCC541, induced anti-*S. Typhimurium* adaptive immune response at 11 days post infection (Wei, Huang et al. 2019). In contrast, the *SL1344* strain used in our study failed to induce a significant adaptive immune response. Thus, it is possible that we were unable to see a role for LAP in myeloid cells because the mice were only followed for 6 days.

During the course of this study, an SPI-1 T3SS effector, STM1239 was identified and renamed *SopF* (Cheng, Wang et al. 2017). *SopF* was found to promote intracellular survival of *S.Typhimurium* by stabilising the nascent SCV and blocking xenophagy (Lau, Haeberle et al. 2019, Xu, Zhou et al. 2019). Interestingly, Xu et al revealed that v-ATPase binds with WD domain of ATG16L1 to recruit LC-3 to SCV membranes and this process can be blocked by *SopF* (Xu, Zhou et al. 2019). This finding provides valuable insight and raises the possibility that  $\delta$ WD mice lack the ability to use the ATG16L1WD-v-ATPase axis to recruit LC-3 to SCV membrane and this results in an increase in sensitivity to *S.Typhimurium* infections. To study this, a *SopF* deficient *S.Typhimurium* strain was first generated in SL1344, then transduced to JH3009 strain, and named JH3009 <sup>$\delta$ SopF</sup>. The loss of *SopF* caused a significant increase in the

percentage of LC-3 decorated Salmonella in WT MEFs while the percentage in  $\delta$ WD MEFs remained low, as would be expected for cells lacking the WD domain. Interestingly, the percentage of LC-3 decorated vacuoles in WT MEFs infected with JH3009 or JH3009 $\delta$ SopF was similar at early time points suggesting that SopF does not inhibit LC3 recruitment at early times of infection. Similar to the results of Xu et al, JH3009 $\delta$ SopF showed a reduced replication rate in MEFs and reduced virulence in WT mice. These data confirm that the ATG16L1WD-V-ATPase axis inhibits *S.Typhimurium* replication both *in vitro* and *in vivo*, and this inhibition can be blocked by SopF.

Interestingly,  $\delta$ Sopf Salmonella replicated faster in  $\delta$ WD MEFs and HEK cells and was more virulent in  $\delta$ WD mice compared to littermate control. The  $\delta$ WD cells and  $\delta$ WD mice lack the ATG16L1WD-V-ATPase axis that is the target of SopF. This raised the possibility that the WD domain is also involved in a pathway independent of the ATG16L1WD-v-ATPase axis. Another explanation is that the level of expression of SopF is not sufficient to block all interactions between the WD domain and v-ATPase. However, recruitment of LC-3 to WT *S.Typhimurium* SCVs showed no difference between WT and  $\delta$ WD MEFs, which suggests the expression level of SopF is sufficient to completely block the WD-v-ATPase axis.

During the course of this thesis work, a study from Tan et al revealed that ATG16L1 is involved in trafficking cholesterol between the cytosol, endosomes and plasma membrane (Tan, Mellouk et al. 2018) and a deficiency in ATG16L1 results in cellular cholesterol accumulation both *in vivo* and *in vitro*. This phenotype can only be rescued by expressing the full length ATG16L1 and not by the CCD domain alone indicating a role for the WD domain in this process. Furthermore, some early studies showed (Catron, Sylvester et al. 2002, Garner, Hayward et al. 2002) that cholesterol plays an important role during the invasion and replication of *S.Typhimurium* (Huang 2011, Huang 2014). These findings provided possibilities that cholesterol may play a

role in the ATG16L1-WD-v-ATPase independent pathway that restricts *S.Typhimurium* replication.

Similar to the results of Tan et al, we found that cholesterol accumulated in  $\delta$ WD MEFs compared with WT MEFs. A plasma membrane repair assay also confirmed that  $\delta$ WD MEFs showed deficiency in membrane repair. The link between *S.Typhimurium* and intracellular cholesterol accumulation was confirmed when replication in  $\delta$ WD MEFs was reduced by T0901317 a drug that removes cholesterol from cells. These data showed that the WD domain of ATG16L1 reduced cholesterol levels in cells and the SI, and this might restrict *S.Typhimurium* replication in MEFs and reduce the sensitivity of mice to *S.Typhimurium* infections.

## **8.2 Future perspective.**

The discovery that non-canonical autophagy pathways, such as LAP, conjugate LC3 to endosomes and phagosomes containing pathogens as they enter cells has given a new perspective on how autophagy proteins can control infection. It is known that LC3 recruitment during infection is triggered by TLR-signalling through Rubicon and ROS production and can be mediated by the vATPase: ATG16L1 axis. Studies in this thesis using  $\delta$ WD cells and  $\delta$ WD mice show that the WD domain may also control infection by influencing cholesterol distribution. This raises interesting questions concerning how the WD domain controls cholesterol transport, and if this is important during infection '*in vivo*'. Does the WD domain regulate sterol binding proteins able to transfer cholesterol directly from one membrane compartment to another, or does the WD domain influence cholesterol transport out of lysosomes through cholesterol transporters? Will depletion of cholesterol from  $\delta$ WD mice reduce their sensitivity to *S.Typhimurium* *in vivo*?

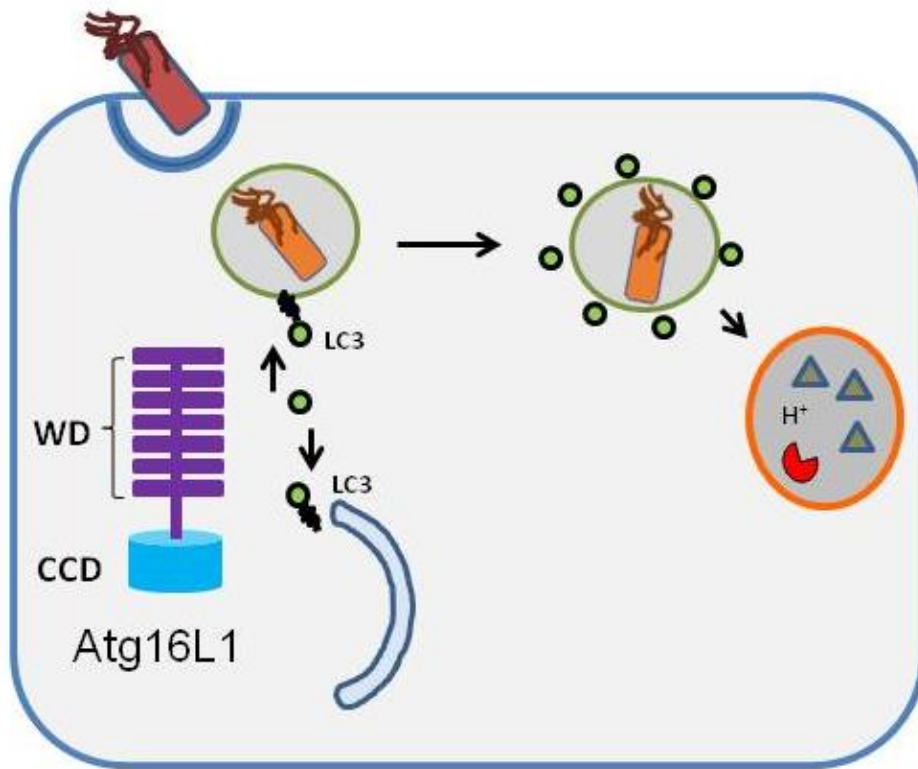
It is now appreciated that pathogens such as *Listeria monocytogenes* can further activate LC3 recruitment during membrane repair when pore forming toxins generate

pores in endosome and phagosome membranes. The availability of  $\delta$ SopF strains developed in this thesis will allow investigators to determine if membrane damage and pore formation are important during *S.Typhimurium* infection independently of the vATPase: ATG16L1 axis. It will be interesting to determine if the accumulation of cholesterol results from reduced lysosomal exocytosis during membrane repair. The accumulation of nutrient rich lysosomes in the cytoplasm allows *S.Typhimurium* to get easy access to nutrients by the formation of SIF to gain nutrients from endolysosome compartments. We have shown a deficiency of membrane repair in  $\delta$ WD and Atg16L1 knockout MEFs, this may alter the ability of SIFs to interact with endolysosome membranes. It will be interesting to see if these defects can also promote the escape of *S.Typhimurium* from SCV into the cytoplasm.

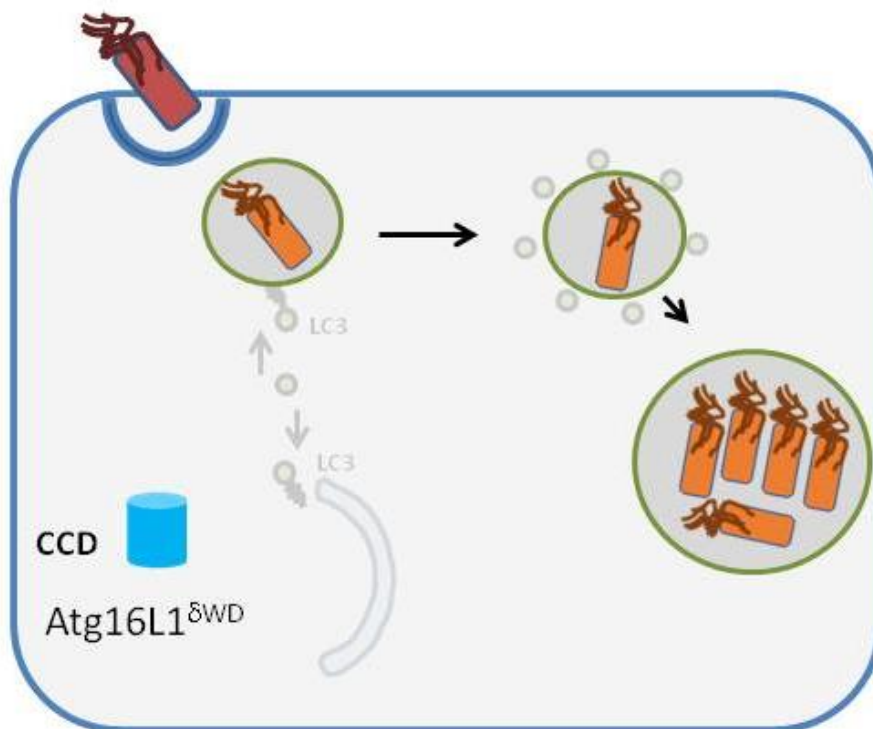
Taken together the above information could underpin the search for new *Salmonella*-associated signals leading to LC3 conjugation, membrane damage, and cholesterol redistribution. This may also stimulate a search for novel virulence factors able to slow LC3 recruitment and cholesterol redistribution.

Key questions still remain on the role played by LAP ‘*in vivo*’, particularly within phagocytic cells and how this may influence acquired immune responses. LAP plays important roles in antigen presenting, which play important roles in the adaptive immune response. Despite the loss of LAP in macrophages which might affect antigen presenting,  $\delta$ WD<sup>phage</sup> mice showed no difference after *S.Typhimurium* infection compared with littermates controls. This may be because the mice were studied before the development of the acquired immune response at about 11 days post infection. (Wei, Huang et al. 2019). The  $\delta$ WD<sup>phage</sup> mice developed in this thesis will be very valuable in dissecting the role played by the WD domain and LAP during acquired immune responses later during infection.

A



B



C

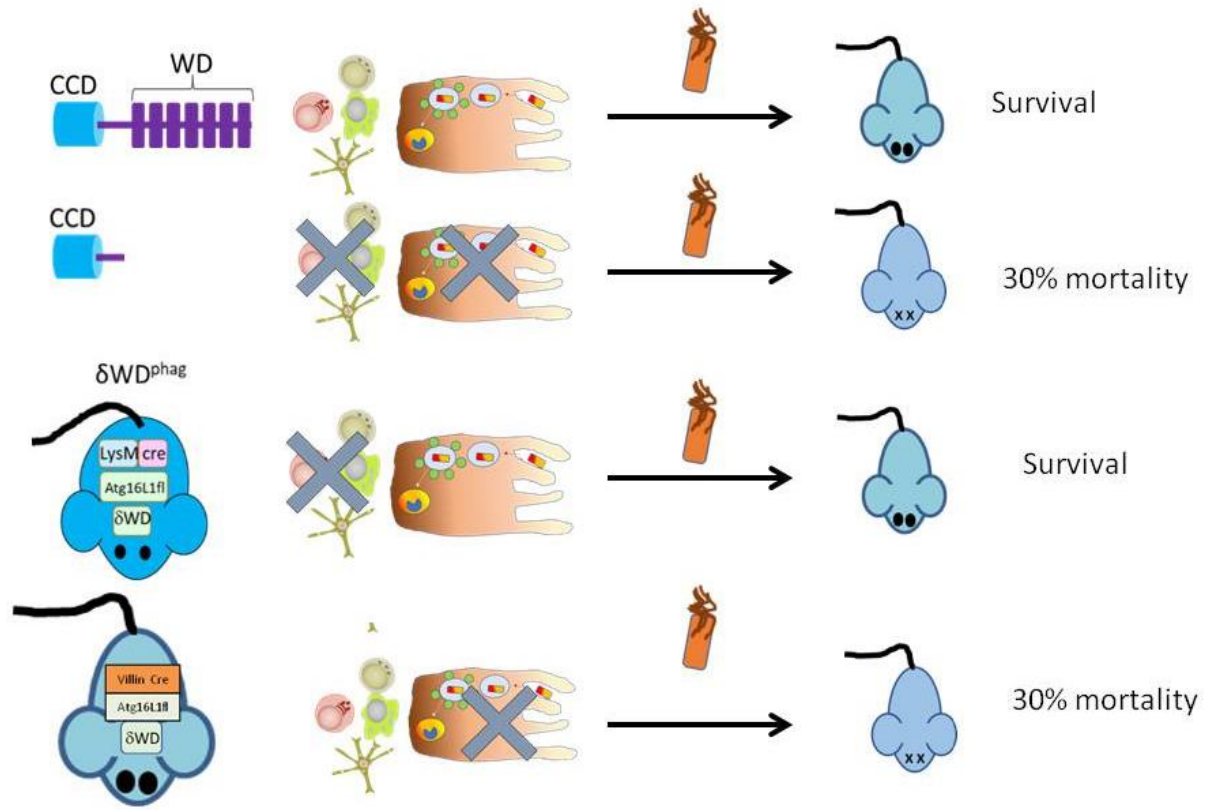
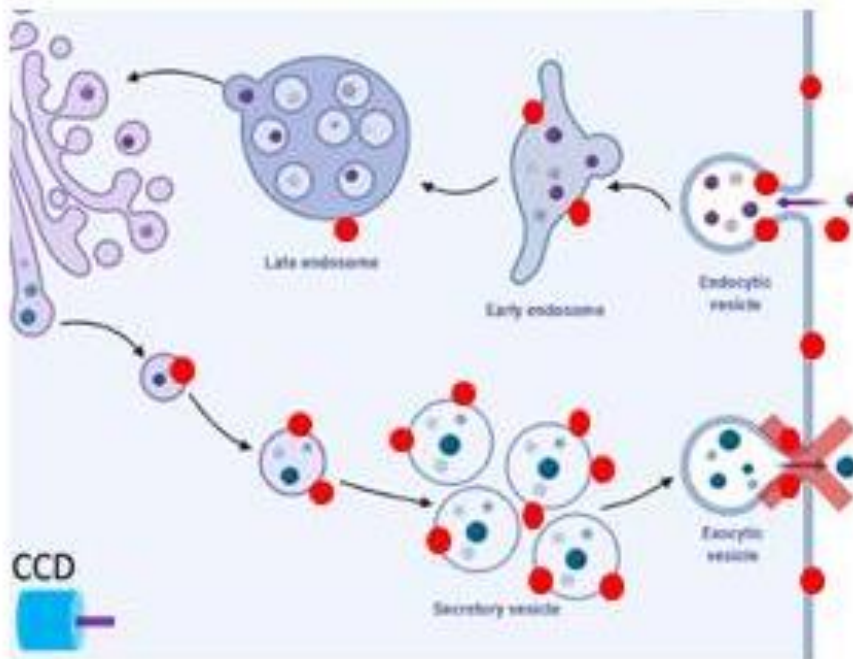
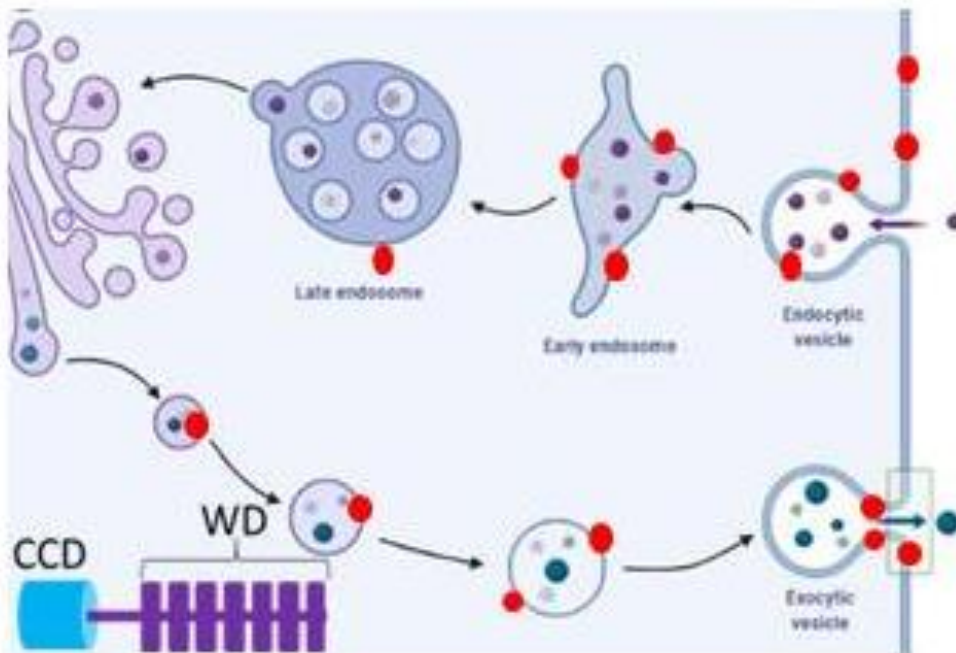


**Figure 8.1 Main findings of this thesis. A&B** WD domain of ATG16L1 recruits LC-3 to early endo-lysosomal compartments (SCVs) and increases lysosome fusion, which results in the removal of invading *S. Typhimurium*. Loss of WD domain increases *S. Typhimurium* replication. **C** *In vivo* studies showed that WD domain of Atg16L1 protects mice from *S. Typhimurium* infection. Infection studies of tissue-specific knock out mice revealed that WD domain in intestinal epithelial cells, not myeloid cells protect mice from *S. Typhimurium* infection.

A



**B**

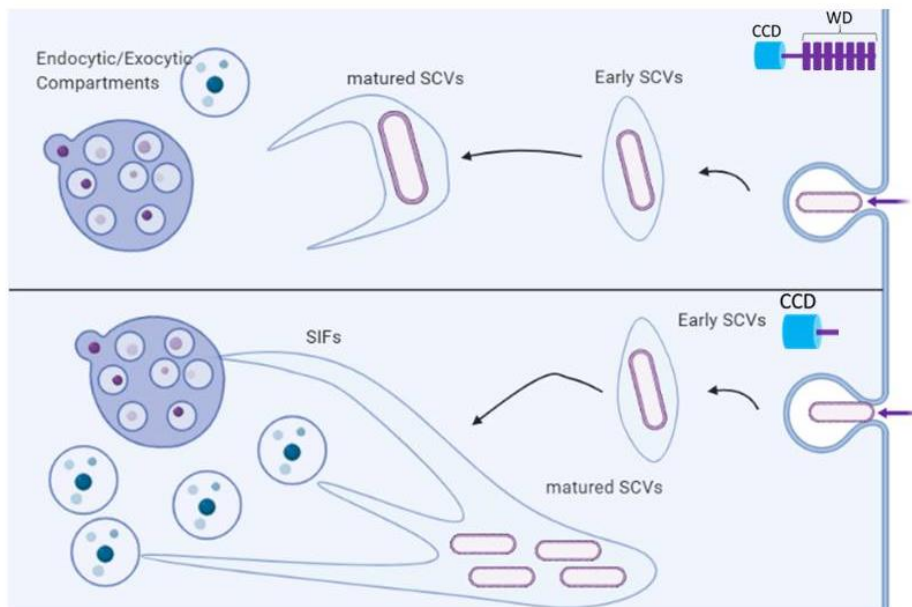


**Figure 8.2 How does cholesterol accumulation affects Salmonella replication? A hypothesis.**

**A** The WD domain of ATG16L1 facilitates exocytosis and movement of cholesterol to the plasma membrane. Reduced exocytosis increases intracellular endocytic and exocytic compartments. Red dots are referred as cholesterol. **B** Accumulated endocytic and exocytic compartments provide nutrients to intracellular *Salmonella* through SIF and promote intracellular replication.

## Reference

- Abrahams, G. L., P. Muller and M. Hensel (2006). "Functional dissection of SseF, a type III effector protein involved in positioning the salmonella-containing vacuole." Traffic **7**(8): 950-965.
- Agbaje, M., R. H. Begum, M. A. Oyekunle, O. E. Ojo and O. T. Adenubi (2011). "Evolution of Salmonella nomenclature: a critical note." Folia Microbiol (Praha) **56**(6): 497-503.
- Ahmer, B. M., M. Tran and F. Heffron (1999). "The virulence plasmid of Salmonella typhimurium is self-transmissible." J Bacteriol **181**(4): 1364-1368.
- Alvarez, M. I., L. C. Glover, P. Luo, L. Wang, E. Theusch, S. H. Oehlers, E. M. Walton, T. T. B. Tram, Y. L. Kuang, J. I. Rotter, C. M. McClean, N. T. Chinh, M. W. Medina, D. M. Tobin, S. J. Dunstan and D. C. Ko (2017). "Human genetic variation in VAC14 regulates Salmonella invasion and typhoid fever through modulation of cholesterol." Proc Natl Acad Sci U S A **114**(37): E7746-E7755.
- Anishkin, A. and C. Kung (2013). "Stiffened lipid platforms at molecular force foci." Proc Natl Acad Sci U S A **110**(13): 4886-4892.
- Aserkoff, B. and J. V. Bennett (1969). "Effect of antibiotic therapy in acute salmonellosis on the fecal excretion of salmonellae." N Engl J Med **281**(12): 636-640.
- Ault, A., S. M. Tennant, J. P. Gorres, M. Eckhaus, N. G. Sandler, A. Roque, S. Livio, S. Bao, K. E. Foulds, S. F. Kao, M. Roederer, P. Schmidlein, M. A. Boyd, M. F. Pasetti, D. C. Douek, J. D. Estes, G. J. Nabel, M. M. Levine and S. S. Rao (2013). "Safety and tolerability of a live oral Salmonella typhimurium vaccine candidate in SIV-infected nonhuman primates." Vaccine **31**(49): 5879-5888.
- Baison-Olmo, F., E. Cardenal-Munoz and F. Ramos-Morales (2012). "PipB2 is a substrate of the Salmonella pathogenicity island 1-encoded type III secretion system." Biochem Biophys Res Commun **423**(2): 240-246.
- Bao, Y. and X. Cao (2011). "Revisiting the protective and pathogenic roles of

- neutrophils: Ly-6G is key!" European Journal of Immunology **41**(9): 2535-2538.
- Baorto, D. M., Z. Gao, R. Malaviya, M. L. Dustin, A. van der Merwe, D. M. Lublin and S. N. Abraham (1997). "Survival of FimH-expressing enterobacteria in macrophages relies on glycolipid traffic." Nature **389**(6651): 636-639.
- Barton Behravesh, C., R. K. Mody, J. Jungk, L. Gaul, J. T. Redd, S. Chen, S. Cosgrove, E. Hedican, D. Sweat, L. Chavez-Hausser, S. L. Snow, H. Hanson, T. A. Nguyen, S. V. Sodha, A. L. Boore, E. Russo, M. Mikoleit, L. Theobald, P. Gerner-Smidt, R. M. Hoekstra, F. J. Angulo, D. L. Swerdlow, R. V. Tauxe, P. M. Griffin and I. T. Williams (2011). "2008 outbreak of Salmonella Saintpaul infections associated with raw produce." N Engl J Med **364**(10): 918-927.
- Baumler, A. and F. C. Fang (2013). "Host specificity of bacterial pathogens." Cold Spring Harb Perspect Med **3**(12): a010041.
- Bedard, K. and K. H. Krause (2007). "The NOX family of ROS-generating NADPH oxidases: physiology and pathophysiology." Physiol Rev **87**(1): 245-313.
- Behrends, C. and S. Fulda (2012). "Receptor proteins in selective autophagy." Int J Cell Biol **2012**: 673290.
- Bel, S., M. Pendse, Y. Wang, Y. Li, K. A. Ruhn, B. Hassell, T. Leal, S. E. Winter, R. J. Xavier and L. V. Hooper (2017). "Paneth cells secrete lysozyme via secretory autophagy during bacterial infection of the intestine." Science **357**(6355): 1047-1052.
- Berger, C. N., R. K. Shaw, D. J. Brown, H. Mather, S. Clare, G. Dougan, M. J. Pallen and G. Frankel (2009). "Interaction of Salmonella enterica with basil and other salad leaves." ISME J **3**(2): 261-265.
- Berger, C. N., S. V. Sodha, R. K. Shaw, P. M. Griffin, D. Pink, P. Hand and G. Frankel (2010). "Fresh fruit and vegetables as vehicles for the transmission of human pathogens." Environ Microbiol **12**(9): 2385-2397.
- Beuzon, C. R., S. P. Salcedo and D. W. Holden (2002). "Growth and killing of a Salmonella enterica serovar Typhimurium sifA mutant strain in the cytosol of different host cell lines." Microbiology (Reading) **148**(Pt 9): 2705-2715.

- Birmingham, C. L. and J. H. Brumell (2006). "Autophagy recognizes intracellular *Salmonella enterica* serovar Typhimurium in damaged vacuoles." Autophagy **2**(3): 156-158.
- Birmingham, C. L., A. C. Smith, M. A. Bakowski, T. Yoshimori and J. H. Brumell (2006). "Autophagy controls *Salmonella* infection in response to damage to the *Salmonella*-containing vacuole." J Biol Chem **281**(16): 11374-11383.
- Blondel, C. J., J. C. Jimenez, I. Contreras and C. A. Santiviago (2009). "Comparative genomic analysis uncovers 3 novel loci encoding type six secretion systems differentially distributed in *Salmonella* serotypes." BMC Genomics **10**: 354.
- Boada-Romero, E., M. Letek, A. Fleischer, K. Pallauf, C. Ramon-Barros and F. X. Pimentel-Muinos (2013). "TMEM59 defines a novel ATG16L1-binding motif that promotes local activation of LC3." EMBO J **32**(4): 566-582.
- Boada-Romero, E., I. Serramito-Gomez, M. P. Sacristan, D. L. Boone, R. J. Xavier and F. X. Pimentel-Muinos (2016). "The T300A Crohn's disease risk polymorphism impairs function of the WD40 domain of ATG16L1." Nat Commun **7**: 11821.
- Bonilla, F. A. and H. C. Oettgen (2010). "Adaptive immunity." J Allergy Clin Immunol **125**(2 Suppl 2): S33-40.
- Boumart, Z., P. Velge and A. Wiedemann (2014). "Multiple invasion mechanisms and different intracellular Behaviors: a new vision of *Salmonella*-host cell interaction." FEMS Microbiol Lett **361**(1): 1-7.
- Boyle, E. C., N. F. Brown and B. B. Finlay (2006). "*Salmonella enterica* serovar Typhimurium effectors SopB, SopE, SopE2 and SipA disrupt tight junction structure and function." Cellular Microbiology **8**(12): 1946-1957.
- Braden, C. R. (2006). "*Salmonella enterica* serotype Enteritidis and eggs: a national epidemic in the United States." Clin Infect Dis **43**(4): 512-517.
- Branchu, P., M. Bawn and R. A. Kingsley (2018). "Genome Variation and Molecular Epidemiology of *Salmonella enterica* Serovar Typhimurium Pathovariants." Infection and Immunity **86**(8).

- Brenner, F. W., R. G. Villar, F. J. Angulo, R. Tauxe and B. Swaminathan (2000). "Salmonella nomenclature." J Clin Microbiol **38**(7): 2465-2467.
- Brown, N. F., L. D. Rogers, K. L. Sanderson, J. W. Gouw, E. L. Hartland and L. J. Foster (2014). "A horizontally acquired transcription factor coordinates Salmonella adaptations to host microenvironments." mBio **5**(5): e01727-01714.
- Broz, P. and V. M. Dixit (2016). "Inflammasomes: mechanism of assembly, regulation and signalling." Nat Rev Immunol **16**(7): 407-420.
- Brumell, J. H., P. Tang, S. D. Mills and B. B. Finlay (2001). "Characterization of Salmonella-induced filaments (Sifs) reveals a delayed interaction between Salmonella-containing vacuoles and late endocytic compartments." Traffic **2**(9): 643-653.
- Buckle, G. C., C. L. Walker and R. E. Black (2012). "Typhoid fever and paratyphoid fever: Systematic review to estimate global morbidity and mortality for 2010." J Glob Health **2**(1): 010401.
- Butler, T., W. R. Bell, J. Levin, N. N. Linh and K. Arnold (1978). "Typhoid fever. Studies of blood coagulation, bacteremia, and endotoxemia." Arch Intern Med **138**(3): 407-410.
- Butler, T., M. Ho, G. Acharya, M. Tiwari and H. Gallati (1993). "Interleukin-6, gamma interferon, and tumor necrosis factor receptors in typhoid fever related to outcome of antimicrobial therapy." Antimicrob Agents Chemother **37**(11): 2418-2421.
- Cadwell, K., J. Y. Liu, S. L. Brown, H. Miyoshi, J. Loh, J. K. Lennerz, C. Kishi, W. Kc, J. A. Carrero, S. Hunt, C. D. Stone, E. M. Brunt, R. J. Xavier, B. P. Sleckman, E. Li, N. Mizushima, T. S. Stappenbeck and H. W. t. Virgin (2008). "A key role for autophagy and the autophagy gene Atg16l1 in mouse and human intestinal Paneth cells." Nature **456**(7219): 259-263.
- Cadwell, K., K. K. Patel, M. Komatsu, H. W. t. Virgin and T. S. Stappenbeck (2009). "A common role for Atg16L1, Atg5 and Atg7 in small intestinal Paneth cells and Crohn disease." Autophagy **5**(2): 250-252.

- Cano, D. A., M. Martinez-Moya, M. G. Pucciarelli, E. A. Groisman, J. Casadesus and F. Garcia-Del Portillo (2001). "Salmonella enterica serovar Typhimurium response involved in attenuation of pathogen intracellular proliferation." Infection and Immunity **69**(10): 6463-6474.
- Catron, D. M., M. D. Sylvester, Y. Lange, M. Kadekoppala, B. D. Jones, D. M. Monack, S. Falkow and K. Haldar (2002). "The Salmonella-containing vacuole is a major site of intracellular cholesterol accumulation and recruits the GPI-anchored protein CD55." Cellular Microbiology **4**(6): 315-328.
- Cavallaro, E., K. Date, C. Medus, S. Meyer, B. Miller, C. Kim, S. Nowicki, S. Cosgrove, D. Sweat, Q. Phan, J. Flint, E. R. Daly, J. Adams, E. Hyytia-Trees, P. Gerner-Smidt, R. M. Hoekstra, C. Schwensohn, A. Langer, S. V. Sodha, M. C. Rogers, F. J. Angulo, R. V. Tauxe, I. T. Williams and C. B. Behravesh (2011). "Salmonella typhimurium infections associated with peanut products." N Engl J Med **365**(7): 601-610.
- Centers for Disease, C. and Prevention (2008). "Outbreak of Salmonella serotype Saintpaul infections associated with multiple raw produce items--United States, 2008." MMWR Morb Mortal Wkly Rep **57**(34): 929-934.
- Chan, E. Y. (2009). "mTORC1 phosphorylates the ULK1-mAtg13-FIP200 autophagy regulatory complex." Science Signaling **2**(84): pe51.
- Chatterjee, S., E. R. Smith, K. Hanada, V. L. Stevens and S. Mayor (2001). "GPI anchoring leads to sphingolipid-dependent retention of endocytosed proteins in the recycling endosomal compartment." EMBO J **20**(7): 1583-1592.
- Cheng, J., Y. Ohsaki, K. Tauchi-Sato, A. Fujita and T. Fujimoto (2006). "Cholesterol depletion induces autophagy." Biochem Biophys Res Commun **351**(1): 246-252.
- Cheng, S., L. Wang, Q. Liu, L. Qi, K. Yu, Z. Wang, M. Wu, Y. Liu, J. Fu, M. Hu, M. Li, D. Zhou and X. Liu (2017). "Identification of a Novel Salmonella Type III Effector by Quantitative Secretome Profiling." Mol Cell Proteomics **16**(12): 2219-2228.
- Chu, H., A. Khosravi, I. P. Kusumawardhani, A. H. Kwon, A. C. Vasconcelos, L. D.

- Cunha, A. E. Mayer, Y. Shen, W. L. Wu, A. Kambal, S. R. Targan, R. J. Xavier, P. B. Ernst, D. R. Green, D. P. McGovern, H. W. Virgin and S. K. Mazmanian (2016). "Gene-microbiota interactions contribute to the pathogenesis of inflammatory bowel disease." Science **352**(6289): 1116-1120.
- Chu, Y., S. Gao, T. Wang, J. Yan, G. Xu, Y. Li, H. Niu, R. Huang and S. Wu (2016). "A novel contribution of spvB to pathogenesis of Salmonella Typhimurium by inhibiting autophagy in host cells." Oncotarget **7**(7): 8295-8309.
- Churchward, M. A. and J. R. Coorssen (2009). "Cholesterol, regulated exocytosis and the physiological fusion machine." Biochemical Journal **423**(1): 1-14.
- Clausen, B. E., C. Burkhardt, W. Reith, R. Renkawitz and I. Forster (1999). "Conditional gene targeting in macrophages and granulocytes using LysMcre mice." Transgenic Res **8**(4): 265-277.
- Clevers, H. C. and C. L. Bevins (2013). "Paneth cells: maestros of the small intestinal crypts." Annu Rev Physiol **75**: 289-311.
- Cliffe, L. J., N. E. Humphreys, T. E. Lane, C. S. Potten, C. Booth and R. K. Grencis (2005). "Accelerated intestinal epithelial cell turnover: a new mechanism of parasite expulsion." Science **308**(5727): 1463-1465.
- Conway, K. L., P. Kuballa, J. H. Song, K. K. Patel, A. B. Castoreno, O. H. Yilmaz, H. B. Jijon, M. Zhang, L. N. Aldrich, E. J. Villablanca, J. M. Peloquin, G. Goel, I. A. Lee, E. Mizoguchi, H. N. Shi, A. K. Bhan, S. Y. Shaw, S. L. Schreiber, H. W. Virgin, A. F. Shamji, T. S. Stappenbeck, H. C. Reinecker and R. J. Xavier (2013). "Atg16l1 is required for autophagy in intestinal epithelial cells and protection of mice from Salmonella infection." Gastroenterology **145**(6): 1347-1357.
- Cossart, P. and A. Helenius (2014). "Endocytosis of viruses and bacteria." Cold Spring Harb Perspect Biol **6**(8).
- Costa, L. F., T. A. Paixao, R. M. Tsolis, A. J. Baumler and R. L. Santos (2012). "Salmonellosis in cattle: advantages of being an experimental model." Res Vet Sci **93**(1): 1-6.
- Crouse, J., H. C. Xu, P. A. Lang and A. Oxenius (2015). "NK cells regulating T cell

- responses: mechanisms and outcome." Trends Immunol **36**(1): 49-58.
- Crump, J. A., S. P. Luby and E. D. Mintz (2004). "The global burden of typhoid fever." Bull World Health Organ **82**(5): 346-353.
- Cunha, L. D., M. Yang, R. Carter, C. Guy, L. Harris, J. C. Crawford, G. Quarato, E. Boada-Romero, H. Kalkavan, M. D. L. Johnson, S. Natarajan, M. E. Turnis, D. Finkelstein, J. T. Opferman, C. Gawad and D. R. Green (2018). "LC3-Associated Phagocytosis in Myeloid Cells Promotes Tumor Immune Tolerance." Cell **175**(2): 429-441 e416.
- D'Costa, V. M., V. Braun, M. Landekic, R. Shi, A. Proteau, L. McDonald, M. Cygler, S. Grinstein and J. H. Brummel (2015). "Salmonella Disrupts Host Endocytic Trafficking by SopD2-Mediated Inhibition of Rab7." Cell Reports **12**(9): 1508-1518.
- Dagan, T., R. Blehman and D. Graur (2006). "The "domino theory" of gene death: gradual and mass gene extinction events in three lineages of obligate symbiotic bacterial pathogens." Mol Biol Evol **23**(2): 310-316.
- Dall'Armi, C., K. A. Devereaux and G. Di Paolo (2013). "The role of lipids in the control of autophagy." Current Biology **23**(1): R33-45.
- de Jong, H. K., C. M. Parry, T. van der Poll and W. J. Wiersinga (2012). "Host-pathogen interaction in invasive Salmonellosis." PLoS Pathog **8**(10): e1002933.
- Deiwick, J., S. P. Salcedo, E. Boucrot, S. M. Gilliland, T. Henry, N. Petermann, S. R. Waterman, J. P. Gorvel, D. W. Holden and S. Meresse (2006). "The translocated Salmonella effector proteins SseF and SseG interact and are required to establish an intracellular replication niche." Infection and Immunity **74**(12): 6965-6972.
- Delves, P. J., Martin, S.J., Burton, D.R., and Roitt, I.M (2011). Roitt's essential immunology.
- Deng, W., S. R. Liou, G. Plunkett, 3rd, G. F. Mayhew, D. J. Rose, V. Burland, V. Kodoyianni, D. C. Schwartz and F. R. Blattner (2003). "Comparative genomics of Salmonella enterica serovar Typhi strains Ty2 and CT18." J Bacteriol **185**(7): 2330-2337.

- Deretic, V., T. Saitoh and S. Akira (2013). "Autophagy in infection, inflammation and immunity." Nat Rev Immunol **13**(10): 722-737.
- Domingues, L., D. W. Holden and L. J. Mota (2014). "The Salmonella effector SteA contributes to the control of membrane dynamics of Salmonella-containing vacuoles." Infection and Immunity **82**(7): 2923-2934.
- Dooley, H. C., M. Razi, H. E. Polson, S. E. Girardin, M. I. Wilson and S. A. Tooze (2014). "WIPI2 links LC3 conjugation with PI3P, autophagosome formation, and pathogen clearance by recruiting Atg12-5-16L1." Molecular Cell **55**(2): 238-252.
- Dufresne, K. a. D., F. (2017). "Salmonella fimbriae: What is the clue to their hairdo? In: Current Topics in Salmonella and Salmonellosis. ." InTechOpen, London.
- Edsall, G., S. Gaines, M. Landy, W. D. Tigertt, H. Sprinz, R. J. Trapani, A. D. Mandel and A. S. Benenson (1960). "Studies on infection and immunity in experimental typhoid fever. I. Typhoid fever in chimpanzees orally infected with Salmonella typhosa." Journal of Experimental Medicine **112**: 143-166.
- el Marjou, F., K. P. Janssen, B. H. Chang, M. Li, V. Hindie, L. Chan, D. Louvard, P. Chambon, D. Metzger and S. Robine (2004). "Tissue-specific and inducible Cre-mediated recombination in the gut epithelium." Genesis **39**(3): 186-193.
- Ericsson, A. C., M. J. Crim and C. L. Franklin (2013). "A brief history of animal modeling." Mo Med **110**(3): 201-205.
- Fabrega, A. and J. Vila (2013). "Salmonella enterica serovar Typhimurium skills to succeed in the host: virulence and regulation." Clin Microbiol Rev **26**(2): 308-341.
- Feasey, N. A., G. Dougan, R. A. Kingsley, R. S. Heyderman and M. A. Gordon (2012). "Invasive non-typhoidal salmonella disease: an emerging and neglected tropical disease in Africa." Lancet **379**(9835): 2489-2499.
- Feng, Z. Z., A. J. Jiang, A. W. Mao, Y. Feng, W. Wang, J. Li, X. Zhang, K. Xing and X. Peng (2018). "The Salmonella effectors SseF and SseG inhibit Rab1A-mediated autophagy to facilitate intracellular bacterial survival and replication." J Biol Chem **293**(25): 9662-9673.
- Ferrari, G., H. Langen, M. Naito and J. Pieters (1999). "A coat protein on phagosomes

- involved in the intracellular survival of mycobacteria." Cell **97**(4): 435-447.
- Figueira, R. and D. W. Holden (2012). "Functions of the Salmonella pathogenicity island 2 (SPI-2) type III secretion system effectors." Microbiology **158**(Pt 5): 1147-1161.
- Firoz Mian, M., E. A. Pek, M. J. Chenoweth and A. A. Ashkar (2011). "Humanized mice are susceptible to Salmonella typhi infection." Cell Mol Immunol **8**(1): 83-87.
- Fletcher, K., R. Ulferts, E. Jacquin, T. Veith, N. Gammoh, J. M. Arasteh, U. Mayer, S. R. Carding, T. Wileman, R. Beale and O. Florey (2018). "The WD40 domain of ATG16L1 is required for its non-canonical role in lipidation of LC3 at single membranes." EMBO J **37**(4).
- Florey, O., N. Gammoh, S. E. Kim, X. Jiang and M. Overholtzer (2015). "V-ATPase and osmotic imbalances activate endolysosomal LC3 lipidation." Autophagy **11**(1): 88-99.
- Foley, S. L., A. M. Lynne and R. Nayak (2008). "Salmonella challenges: prevalence in swine and poultry and potential pathogenicity of such isolates." J Anim Sci **86**(14 Suppl): E149-162.
- Forgac, M. (2007). "Vacuolar ATPases: rotary proton pumps in physiology and pathophysiology." Nat Rev Mol Cell Biol **8**(11): 917-929.
- Fournier, J. B., K. Knox, M. Harris and M. Newstein (2015). "Family Outbreaks of Nontyphoidal Salmonellosis following a Meal of Guinea Pigs." Case Rep Infect Dis **2015**: 864640.
- Freeman, J. A., C. Rappl, V. Kuhle, M. Hensel and S. I. Miller (2002). "SpiC is required for translocation of Salmonella pathogenicity island 2 effectors and secretion of translocon proteins SseB and SseC." J Bacteriol **184**(18): 4971-4980.
- Freidl, G., S. Schoss, M. Te Wierik, M. Heck, P. Tolsma, A. Urbanus, I. Slegers-Fitz-James and I. Friesema (2018). "Tracing Back the Source of an Outbreak of Salmonella Typhimurium; National Outbreak Linked to the Consumption of Raw and Undercooked Beef Products, the Netherlands, October to December 2015."

PLoS Curr **10**.

- Friesema, I., A. de Jong, A. Hofhuis, M. Heck, H. van den Kerkhof, R. de Jonge, D. Hameryck, K. Nagel, G. van Vilsteren, P. van Beek, D. Notermans and W. van Pelt (2014). "Large outbreak of Salmonella Thompson related to smoked salmon in the Netherlands, August to December 2012." Euro Surveill **19**(39).
- Friesema, I. H., B. Schimmer, J. A. Ros, H. J. Ober, M. E. Heck, C. M. Swaan, C. M. de Jager, R. M. Peran i Sala and W. van Pelt (2012). "A regional Salmonella enterica serovar Typhimurium outbreak associated with raw beef products, The Netherlands, 2010." Foodborne Pathog Dis **9**(2): 102-107.
- Fujioka, Y., N. N. Noda, H. Nakatogawa, Y. Ohsumi and F. Inagaki (2010). "Dimeric coiled-coil structure of Saccharomyces cerevisiae Atg16 and its functional significance in autophagy." J Biol Chem **285**(2): 1508-1515.
- Fujita, N., T. Itoh, H. Omori, M. Fukuda, T. Noda and T. Yoshimori (2008). "The Atg16L complex specifies the site of LC3 lipidation for membrane biogenesis in autophagy." Molecular Biology of the Cell **19**(5): 2092-2100.
- Fujita, N., E. Morita, T. Itoh, A. Tanaka, M. Nakaoka, Y. Osada, T. Umemoto, T. Saitoh, H. Nakatogawa, S. Kobayashi, T. Haraguchi, J. L. Guan, K. Iwai, F. Tokunaga, K. Saito, K. Ishibashi, S. Akira, M. Fukuda, T. Noda and T. Yoshimori (2013). "Recruitment of the autophagic machinery to endosomes during infection is mediated by ubiquitin." J Cell Biol **203**(1): 115-128.
- Gal-Mor, O., J. Suez, D. Elhadad, S. Porwollik, E. Leshem, L. Valinsky, M. McClelland, E. Schwartz and G. Rahav (2012). "Molecular and cellular characterization of a Salmonella enterica serovar Paratyphi a outbreak strain and the human immune response to infection." Clinical and Vaccine Immunology **19**(2): 146-156.
- Galan, J. E. and R. Curtiss, 3rd (1989). "Virulence and vaccine potential of phoP mutants of Salmonella typhimurium." Microb Pathog **6**(6): 433-443.
- Gallois, A., J. R. Klein, L. A. Allen, B. D. Jones and W. M. Nauseef (2001). "Salmonella pathogenicity island 2-encoded type III secretion system mediates

- exclusion of NADPH oxidase assembly from the phagosomal membrane." J Immunol **166**(9): 5741-5748.
- Gammoh, N., O. Florey, M. Overholtzer and X. Jiang (2013). "Interaction between FIP200 and ATG16L1 distinguishes ULK1 complex-dependent and -independent autophagy." Nat Struct Mol Biol **20**(2): 144-149.
- Garcia-Gil, A., C. S. Galan-Enriquez, A. Perez-Lopez, P. Nava, C. Alpuche-Aranda and V. Ortiz-Navarrete (2018). "SopB activates the Akt-YAP pathway to promote Salmonella survival within B cells." Virulence **9**(1): 1390-1402.
- Garcia Urena, M. A., M. Velasco Garcia, F. J. Carnero, E. Sancho Narvaez, P. A. Perez de la Lastra and A. Rodriguez Guzman (1999). "[Extraintestinal salmonellosis localized in the spleen]." Rev Esp Enferm Dig **91**(2): 153-154.
- Garner, M. J., R. D. Hayward and V. Koronakis (2002). "The Salmonella pathogenicity island 1 secretion system directs cellular cholesterol redistribution during mammalian cell entry and intracellular trafficking." Cellular Microbiology **4**(3): 153-165.
- Gatfield, J. and J. Pieters (2000). "Essential role for cholesterol in entry of mycobacteria into macrophages." Science **288**(5471): 1647-1650.
- Gedde, M. M., D. E. Higgins, L. G. Tilney and D. A. Portnoy (2000). "Role of listeriolysin O in cell-to-cell spread of *Listeria monocytogenes*." Infection and Immunity **68**(2): 999-1003.
- Geddes, K., F. Cruz and F. Heffron (2007). "Analysis of cells targeted by Salmonella type III secretion in vivo." PLoS Pathog **3**(12): e196.
- Geng, S., Y. Wang, Y. Xue, H. Wang, Y. Cai, J. Zhang, P. Barrow, Z. Pan and X. Jiao (2019). "The SseL protein inhibits the intracellular NF-kappaB pathway to enhance the virulence of *Salmonella Pullorum* in a chicken model." Microb Pathog **129**: 1-6.
- Glasgow, A. A., H. T. Wong and D. Tullman-Ercek (2017). "A Secretion-Amplification Role for *Salmonella enterica* Translocon Protein SipD." ACS Synth Biol **6**(6): 1006-1015.

- Glynn, J. R. and S. R. Palmer (1992). "Incubation period, severity of disease, and infecting dose: evidence from a Salmonella outbreak." Am J Epidemiol **136**(11): 1369-1377.
- Gomes, L. C. and I. Dikic (2014). "Autophagy in antimicrobial immunity." Molecular Cell **54**(2): 224-233.
- Gonzalez-Escobedo, G., K. M. La Perle and J. S. Gunn (2013). "Histopathological analysis of Salmonella chronic carriage in the mouse hepatopancreatobiliary system." PLoS One **8**(12): e84058.
- Gopinath, A., T. A. Allen, C. J. Bridgwater, C. M. Young and M. J. Worley (2019). "The Salmonella type III effector SpvC triggers the reverse transmigration of infected cells into the bloodstream." PLoS One **14**(12): e0226126.
- Gordon, M. A. (2008). "Salmonella infections in immunocompromised adults." J Infect **56**(6): 413-422.
- Graham, S. M. (2010). "Nontyphoidal salmonellosis in Africa." Curr Opin Infect Dis **23**(5): 409-414.
- Gulati, A., R. Shukla and A. Mukhopadhyaya (2019). "Salmonella Effector SteA Suppresses Proinflammatory Responses of the Host by Interfering With IkappaB Degradation." Front Immunol **10**: 2822.
- Gulig, P. A. and T. J. Doyle (1993). "The Salmonella typhimurium virulence plasmid increases the growth rate of salmonellae in mice." Infection and Immunity **61**(2): 504-511.
- Gunster, R. A., S. A. Matthews, D. W. Holden and T. L. M. Thurston (2017). "SseK1 and SseK3 Type III Secretion System Effectors Inhibit NF-kappaB Signaling and Necroptotic Cell Death in Salmonella-Infected Macrophages." Infection and Immunity **85**(3).
- Gutierrez, M. G., S. S. Master, S. B. Singh, G. A. Taylor, M. I. Colombo and V. Deretic (2004). "Autophagy is a defense mechanism inhibiting BCG and Mycobacterium tuberculosis survival in infected macrophages." Cell **119**(6): 753-766.

- Haeusler, G. M. and N. Curtis (2013). "Non-typhoidal Salmonella in children: microbiology, epidemiology and treatment." Adv Exp Med Biol **764**: 13-26.
- Hampe, J., A. Franke, P. Rosenstiel, A. Till, M. Teuber, K. Huse, M. Albrecht, G. Mayr, F. M. De La Vega, J. Briggs, S. Gunther, N. J. Prescott, C. M. Onnie, R. Hasler, B. Sipos, U. R. Folsch, T. Lengauer, M. Platzer, C. G. Mathew, M. Krawczak and S. Schreiber (2007). "A genome-wide association scan of nonsynonymous SNPs identifies a susceptibility variant for Crohn disease in ATG16L1." Nat Genet **39**(2): 207-211.
- Hanada, T., N. N. Noda, Y. Satomi, Y. Ichimura, Y. Fujioka, T. Takao, F. Inagaki and Y. Ohsumi (2007). "The Atg12-Atg5 conjugate has a novel E3-like activity for protein lipidation in autophagy." J Biol Chem **282**(52): 37298-37302.
- Haneda, T., Y. Ishii, H. Shimizu, K. Ohshima, N. Iida, H. Danbara and N. Okada (2012). "Salmonella type III effector SpvC, a phosphothreonine lyase, contributes to reduction in inflammatory response during intestinal phase of infection." Cellular Microbiology **14**(4): 485-499.
- Hapfelmeier, S. and W. D. Hardt (2005). "A mouse model for S. typhimurium-induced enterocolitis." Trends Microbiol **13**(10): 497-503.
- Hara, T., A. Takamura, C. Kishi, S. Iemura, T. Natsume, J. L. Guan and N. Mizushima (2008). "FIP200, a ULK-interacting protein, is required for autophagosome formation in mammalian cells." J Cell Biol **181**(3): 497-510.
- Hautefort, I., M. J. Proenca and J. C. Hinton (2003). "Single-copy green fluorescent protein gene fusions allow accurate measurement of Salmonella gene expression in vitro and during infection of mammalian cells." Appl Environ Microbiol **69**(12): 7480-7491.
- Heckmann, B. L., E. Boada-Romero, L. D. Cunha, J. Magne and D. R. Green (2017). "LC3-Associated Phagocytosis and Inflammation." J Mol Biol **429**(23): 3561-3576.
- Heckmann, B. L., E. Boada-Romero, L. D. Cunha, J. Magne and D. R. Green (2017). "LC3-Associated Phagocytosis and Inflammation." Journal of molecular biology.

- Heckmann, B. L. and D. R. Green (2019). "LC3-associated phagocytosis at a glance." Journal of Cell Science **132**(5).
- Heckmann, B. L., B. J. W. Teubner, E. Boada-Romero, B. Tummers, C. Guy, P. Fitzgerald, U. Mayer, S. Carding, S. S. Zakharenko, T. Wileman and D. R. Green (2020). "Noncanonical function of an autophagy protein prevents spontaneous Alzheimer's disease." Sci Adv **6**(33): eabb9036.
- Heckmann, B. L., B. J. W. Teubner, B. Tummers, E. Boada-Romero, L. Harris, M. Yang, C. S. Guy, S. S. Zakharenko and D. R. Green (2019). "LC3-Associated Endocytosis Facilitates beta-Amyloid Clearance and Mitigates Neurodegeneration in Murine Alzheimer's Disease." Cell **178**(3): 536-551 e514.
- Henao-Mejia, J., E. Elinav, T. Strowig and R. A. Flavell (2012). "Inflammasomes: far beyond inflammation." Nature Immunology **13**(4): 321-324.
- Henault, J., J. Martinez, J. M. Riggs, J. Tian, P. Mehta, L. Clarke, M. Sasai, E. Latz, M. M. Brinkmann, A. Iwasaki, A. J. Coyle, R. Kolbeck, D. R. Green and M. A. Sanjuan (2012). "Noncanonical autophagy is required for type I interferon secretion in response to DNA-immune complexes." Immunity **37**(6): 986-997.
- Henry, R. M., A. D. Hoppe, N. Joshi and J. A. Swanson (2004). "The uniformity of phagosome maturation in macrophages." J Cell Biol **164**(2): 185-194.
- Henry, T., C. Couillault, P. Rockenfeller, E. Boucrot, A. Dumont, N. Schroeder, A. Hermant, L. A. Knodler, P. Lecine, O. Steele-Mortimer, J. P. Borg, J. P. Gorvel and S. Meresse (2006). "The Salmonella effector protein PipB2 is a linker for kinesin-1." Proc Natl Acad Sci U S A **103**(36): 13497-13502.
- Hensel, M., J. E. Shea, B. Raupach, D. Monack, S. Falkow, C. Gleeson, T. Kubo and D. W. Holden (1997). "Functional analysis of ssaJ and the ssaK/U operon, 13 genes encoding components of the type III secretion apparatus of Salmonella Pathogenicity Island 2." Mol Microbiol **24**(1): 155-167.
- Herhaus, L. and I. Dikic (2018). "Regulation of Salmonella-host cell interactions via the ubiquitin system." Int J Med Microbiol **308**(1): 176-184.
- Hohmann, E. L. (2001). "Nontyphoidal salmonellosis." Clin Infect Dis **32**(2): 263-269.

- Holt, K. E., N. R. Thomson, J. Wain, G. C. Langridge, R. Hasan, Z. A. Bhutta, M. A. Quail, H. Norbertczak, D. Walker, M. Simmonds, B. White, N. Bason, K. Mungall, G. Dougan and J. Parkhill (2009). "Pseudogene accumulation in the evolutionary histories of *Salmonella enterica* serovars Paratyphi A and Typhi." BMC Genomics **10**: 36.
- House, D., J. Wain, V. A. Ho, T. S. Diep, N. T. Chinh, P. V. Bay, H. Vinh, M. Duc, C. M. Parry, G. Dougan, N. J. White, T. T. Hien and J. J. Farrar (2001). "Serology of typhoid fever in an area of endemicity and its relevance to diagnosis." J Clin Microbiol **39**(3): 1002-1007.
- Huang, F. C. (2011). "Plasma membrane cholesterol plays a critical role in the *Salmonella*-induced anti-inflammatory response in intestinal epithelial cells." Cell Immunol **271**(2): 480-487.
- Huang, F. C. (2014). "The critical role of membrane cholesterol in salmonella-induced autophagy in intestinal epithelial cells." Int J Mol Sci **15**(7): 12558-12572.
- Humphreys, D., A. Davidson, P. J. Hume and V. Koronakis (2012). "*Salmonella* virulence effector SopE and Host GEF ARNO cooperate to recruit and activate WAVE to trigger bacterial invasion." Cell Host Microbe **11**(2): 129-139.
- Ichimura, Y., T. Kirisako, T. Takao, Y. Satomi, Y. Shimonishi, N. Ishihara, N. Mizushima, I. Tanida, E. Kominami, M. Ohsumi, T. Noda and Y. Ohsumi (2000). "A ubiquitin-like system mediates protein lipidation." Nature **408**(6811): 488-492.
- Ilangumaran, S. and D. C. Hoessli (1998). "Effects of cholesterol depletion by cyclodextrin on the sphingolipid microdomains of the plasma membrane." Biochemical Journal **335** ( Pt 2): 433-440.
- Imanishi, M., D. S. Rotstein, R. Reimschuessel, C. A. Schwensohn, D. H. Woody, Jr., S. W. Davis, A. D. Hunt, K. D. Arends, M. Achen, J. Cui, Y. Zhang, L. F. Denny, Q. N. Phan, L. A. Joseph, C. C. Tuite, J. R. Tataryn and C. B. Behravesh (2014). "Outbreak of *Salmonella enterica* serotype Infantis infection in humans linked to dry dog food in the United States and Canada, 2012." J Am Vet Med Assoc **244**(5): 545-553.

- Jackson, B. R., P. M. Griffin, D. Cole, K. A. Walsh and S. J. Chai (2013). "Outbreak-associated *Salmonella enterica* serotypes and food Commodities, United States, 1998-2008." Emerg Infect Dis **19**(8): 1239-1244.
- Jantsch, J., D. Chikkaballi and M. Hensel (2011). "Cellular aspects of immunity to intracellular *Salmonella enterica*." Immunol Rev **240**(1): 185-195.
- Jarvik, T., C. Smillie, E. A. Groisman and H. Ochman (2010). "Short-term signatures of evolutionary change in the *Salmonella enterica* serovar typhimurium 14028 genome." J Bacteriol **192**(2): 560-567.
- Jennings, E., D. Esposito, K. Rittinger and T. L. M. Thurston (2018). "Structure-function analyses of the bacterial zinc metalloprotease effector protein GtgA uncover key residues required for deactivating NF-kappaB." J Biol Chem **293**(39): 15316-15329.
- Jennings, E., T. L. M. Thurston and D. W. Holden (2017). "Salmonella SPI-2 Type III Secretion System Effectors: Molecular Mechanisms And Physiological Consequences." Cell Host Microbe **22**(2): 217-231.
- Jiang, L., P. Wang, X. Song, H. Zhang, S. Ma, J. Wang, W. Li, R. Lv, X. Liu, J. Yan, H. Zhou, D. Huang, Z. Cheng, C. Yang, L. Feng and L. Wang (2021). "Salmonella Typhimurium reprograms macrophage metabolism via T3SS effector SopE2 to promote intracellular replication and virulence." Nat Commun **12**(1): 879.
- Johnson, R., A. Byrne, C. N. Berger, E. Klemm, V. F. Crepin, G. Dougan and G. Frankel (2017). "The Type III Secretion System Effector SptP of *Salmonella enterica* Serovar Typhi." J Bacteriol **199**(4).
- Johnson, R., E. Mylona and G. Frankel (2018). "Typhoidal *Salmonella*: Distinctive virulence factors and pathogenesis." Cellular Microbiology **20**(9): e12939.
- Jung, C. H., C. B. Jun, S. H. Ro, Y. M. Kim, N. M. Otto, J. Cao, M. Kundu and D. H. Kim (2009). "ULK-Atg13-FIP200 complexes mediate mTOR signaling to the autophagy machinery." Molecular Biology of the Cell **20**(7): 1992-2003.
- Kabeya, Y., N. Mizushima, A. Yamamoto, S. Oshitani-Okamoto, Y. Ohsumi and T. Yoshimori (2004). "LC3, GABARAP and GATE16 localize to autophagosomal

- membrane depending on form-II formation." Journal of Cell Science **117**(Pt 13): 2805-2812.
- Kamanova, J., H. Sun, M. Lara-Tejero and J. E. Galan (2016). "The Salmonella Effector Protein SopA Modulates Innate Immune Responses by Targeting TRIM E3 Ligase Family Members." PLoS Pathog **12**(4): e1005552.
- Kaur, J. and S. K. Jain (2012). "Role of antigens and virulence factors of Salmonella enterica serovar Typhi in its pathogenesis." Microbiol Res **167**(4): 199-210.
- Kent, T. H., S. B. Formal and E. H. Labrec (1966). "Salmonella gastroenteritis in rhesus monkeys." Arch Pathol **82**(3): 272-279.
- Kihara, A., T. Noda, N. Ishihara and Y. Ohsumi (2001). "Two distinct Vps34 phosphatidylinositol 3-kinase complexes function in autophagy and carboxypeptidase Y sorting in *Saccharomyces cerevisiae*." J Cell Biol **152**(3): 519-530.
- Kim, J. H., S. B. Hong, J. K. Lee, S. Han, K. H. Roh, K. E. Lee, Y. K. Kim, E. J. Choi and H. K. Song (2015). "Insights into autophagosome maturation revealed by the structures of ATG5 with its interacting partners." Autophagy **11**(1): 75-87.
- Kim, Y. G., J. H. Kim and K. J. Kim (2009). "Crystal structure of the Salmonella enterica serovar typhimurium virulence factor SrfJ, a glycoside hydrolase family enzyme." J Bacteriol **191**(21): 6550-6554.
- Kim, Y. K., J. S. Shin and M. H. Nahm (2016). "NOD-Like Receptors in Infection, Immunity, and Diseases." Yonsei Med J **57**(1): 5-14.
- Kimura, T., A. Jain, S. W. Choi, M. A. Mandell, K. Schroder, T. Johansen and V. Deretic (2015). "TRIM-mediated precision autophagy targets cytoplasmic regulators of innate immunity." J Cell Biol **210**(6): 973-989.
- Kirisako, T., Y. Ichimura, H. Okada, Y. Kabeya, N. Mizushima, T. Yoshimori, M. Ohsumi, T. Takao, T. Noda and Y. Ohsumi (2000). "The reversible modification regulates the membrane-binding state of Apg8/Aut7 essential for autophagy and the cytoplasm to vacuole targeting pathway." J Cell Biol **151**(2): 263-276.
- Klionsky, D. J., F. C. Abdalla, H. Abeliovich, R. T. Abraham, A. Acevedo-Arozena, K.

Adeli, L. Agholme, M. Agnello, P. Agostinis, J. A. Aguirre-Ghiso, H. J. Ahn, O. Ait-Mohamed, S. Ait-Si-Ali, T. Akematsu, S. Akira, H. M. Al-Younes, M. A. Al-Zeer, M. L. Albert, R. L. Albin, J. Alegre-Abarrategui, M. F. Aleo, M. Alirezaei, A. Almasan, M. Almonte-Becerril, A. Amano, R. Amaravadi, S. Amarnath, A. O. Amer, N. Andrieu-Abadie, V. Anantharam, D. K. Ann, S. Anoopkumar-Dukie, H. Aoki, N. Apostolova, G. Arancia, J. P. Aris, K. Asanuma, N. Y. Asare, H. Ashida, V. Askanas, D. S. Askew, P. Auberger, M. Baba, S. K. Backues, E. H. Baehrecke, B. A. Bahr, X. Y. Bai, Y. Bailly, R. Baiocchi, G. Baldini, W. Balduini, A. Ballabio, B. A. Bamber, E. T. Bampton, G. Banhegyi, C. R. Bartholomew, D. C. Bassham, R. C. Bast, Jr., H. Batoko, B. H. Bay, I. Beau, D. M. Bechet, T. J. Begley, C. Behl, C. Behrends, S. Bekri, B. Bellaire, L. J. Bendall, L. Benetti, L. Berliocchi, H. Bernardi, F. Bernassola, S. Besteiro, I. Bhatia-Kissova, X. Bi, M. Biard-Piechaczyk, J. S. Blum, L. H. Boise, P. Bonaldo, D. L. Boone, B. C. Bornhauser, K. R. Bortoluci, I. Bossis, F. Bost, J. P. Bourquin, P. Boya, M. Boyer-Guittaut, P. V. Bozhkov, N. R. Brady, C. Brancolini, A. Brech, J. E. Brenman, A. Brennand, E. H. Bresnick, P. Brest, D. Bridges, M. L. Bristol, P. S. Brookes, E. J. Brown, J. H. Brumell, N. Brunetti-Pierri, U. T. Brunk, D. E. Bulman, S. J. Bultman, G. Bultynck, L. F. Burbulla, W. Bursch, J. P. Butchar, W. Buzgariu, S. P. Bydlowski, K. Cadwell, M. Cahova, D. Cai, J. Cai, Q. Cai, B. Calabretta, J. Calvo-Garrido, N. Camougrand, M. Campanella, J. Campos-Salinas, E. Candi, L. Cao, A. B. Caplan, S. R. Carding, S. M. Cardoso, J. S. Carew, C. R. Carlin, V. Carmignac, L. A. Carneiro, S. Carra, R. A. Caruso, G. Casari, C. Casas, R. Castino, E. Cebollero, F. Cecconi, J. Celli, H. Chaachouay, H. J. Chae, C. Y. Chai, D. C. Chan, E. Y. Chan, R. C. Chang, C. M. Che, C. C. Chen, G. C. Chen, G. Q. Chen, M. Chen, Q. Chen, S. S. Chen, W. Chen, X. Chen, Y. G. Chen, Y. Chen, Y. J. Chen, Z. Chen, A. Cheng, C. H. Cheng, Y. Cheng, H. Cheong, J. H. Cheong, S. Cherry, R. Chess-Williams, Z. H. Cheung, E. Chevet, H. L. Chiang, R. Chiarelli, T. Chiba, L. S. Chin, S. H. Chiou, F. V. Chisari, C. H. Cho, D. H. Cho, A. M. Choi, D. Choi, K. S. Choi, M. E. Choi, S. Chouaib, D. Choubey, V. Choubey, C. T. Chu, T. H. Chuang,

S. H. Chueh, T. Chun, Y. J. Chwae, M. L. Chye, R. Ciarcia, M. R. Ciriolo, M. J. Clague, R. S. Clark, P. G. Clarke, R. Clarke, P. Codogno, H. A. Coller, M. I. Colombo, S. Comincini, M. Condello, F. Condorelli, M. R. Cookson, G. H. Coombs, I. Coppens, R. Corbalan, P. Cossart, P. Costelli, S. Costes, A. Coto-Montes, E. Couve, F. P. Coxon, J. M. Cregg, J. L. Crespo, M. J. Cronje, A. M. Cuervo, J. J. Cullen, M. J. Czaja, M. D'Amelio, A. Darfeuille-Michaud, L. M. Davids, F. E. Davies, M. De Felici, J. F. de Groot, C. A. de Haan, L. De Martino, A. De Milito, V. De Tata, J. Debnath, A. Degterev, B. Dehay, L. M. Delbridge, F. Demarchi, Y. Z. Deng, J. Dengjel, P. Dent, D. Denton, V. Deretic, S. D. Desai, R. J. Devenish, M. Di Gioacchino, G. Di Paolo, C. Di Pietro, G. Diaz-Araya, I. Diaz-Laviada, M. T. Diaz-Meco, J. Diaz-Nido, I. Dikic, S. P. Dinesh-Kumar, W. X. Ding, C. W. Distelhorst, A. Diwan, M. Djavaheri-Mergny, S. Dokudovskaya, Z. Dong, F. C. Dorsey, V. Dosenko, J. J. Dowling, S. Doxsey, M. Dreux, M. E. Drew, Q. Duan, M. A. Duchosal, K. Duff, I. Dugail, M. Durbeej, M. Duszenko, C. L. Edelstein, A. L. Edinger, G. Egea, L. Eichinger, N. T. Eissa, S. Ekmekcioglu, W. S. El-Deiry, Z. Elazar, M. Elgendy, L. M. Ellerby, K. E. Eng, A. M. Engelbrecht, S. Engelender, J. Erenpreisa, R. Escalante, A. Esclatine, E. L. Eskelinen, L. Espert, V. Espina, H. Fan, J. Fan, Q. W. Fan, Z. Fan, S. Fang, Y. Fang, M. Fanto, A. Fanzani, T. Farkas, J. C. Farre, M. Faure, M. Fechheimer, C. G. Feng, J. Feng, Q. Feng, Y. Feng, L. Fesus, R. Feuer, M. E. Figueiredo-Pereira, G. M. Fimia, D. C. Fingar, S. Finkbeiner, T. Finkel, K. D. Finley, F. Fiorito, E. A. Fisher, P. B. Fisher, M. Flajolet, M. L. Florez-McClure, S. Florio, E. A. Fon, F. Fornai, F. Fortunato, R. Fotedar, D. H. Fowler, H. S. Fox, R. Franco, L. B. Frankel, M. Fransen, J. M. Fuentes, J. Fueyo, J. Fujii, K. Fujisaki, E. Fujita, M. Fukuda, R. H. Furukawa, M. Gaestel, P. Gailly, M. Gajewska, B. Galliot, V. Galy, S. Ganesh, B. Ganetzky, I. G. Ganley, F. B. Gao, G. F. Gao, J. Gao, L. Garcia, G. Garcia-Manero, M. Garcia-Marcos, M. Garmyn, A. L. Gartel, E. Gatti, M. Gautel, T. R. Gawriluk, M. E. Gegg, J. Geng, M. Germain, J. E. Gestwicki, D. A. Gewirtz, S. Ghavami, P. Ghosh, A. M. Giammarioli, A. N. Giatromanolaki, S. B. Gibson,

R. W. Gilkerson, M. L. Ginger, H. N. Ginsberg, J. Golab, M. S. Goligorsky, P. Golstein, C. Gomez-Manzano, E. Goncu, C. Gongora, C. D. Gonzalez, R. Gonzalez, C. Gonzalez-Estevez, R. A. Gonzalez-Polo, E. Gonzalez-Rey, N. V. Gorbunov, S. Gorski, S. Goruppi, R. A. Gottlieb, D. Gozuacik, G. E. Granato, G. D. Grant, K. N. Green, A. Gregorc, F. Gros, C. Grose, T. W. Grunt, P. Gual, J. L. Guan, K. L. Guan, S. M. Guichard, A. S. Gukovskaya, I. Gukovsky, J. Gunst, A. B. Gustafsson, A. J. Halayko, A. N. Hale, S. K. Halonen, M. Hamasaki, F. Han, T. Han, M. K. Hancock, M. Hansen, H. Harada, M. Harada, S. E. Hardt, J. W. Harper, A. L. Harris, J. Harris, S. D. Harris, M. Hashimoto, J. A. Haspel, S. Hayashi, L. A. Hazelhurst, C. He, Y. W. He, M. J. Hebert, K. A. Heidenreich, M. H. Helfrich, G. V. Helgason, E. P. Henske, B. Herman, P. K. Herman, C. Hetz, S. Hilfiker, J. A. Hill, L. J. Hocking, P. Hofman, T. G. Hofmann, J. Hohfeld, T. L. Holyoake, M. H. Hong, D. A. Hood, G. S. Hotamisligil, E. J. Houwerzijl, M. Hoyer-Hansen, B. Hu, C. A. Hu, H. M. Hu, Y. Hua, C. Huang, J. Huang, S. Huang, W. P. Huang, T. B. Huber, W. K. Huh, T. H. Hung, T. R. Hupp, G. M. Hur, J. B. Hurley, S. N. Hussain, P. J. Hussey, J. J. Hwang, S. Hwang, A. Ichihara, S. Ilkhanizadeh, K. Inoki, T. Into, V. Iovane, J. L. Iovanna, N. Y. Ip, Y. Isaka, H. Ishida, C. Isidoro, K. Isobe, A. Iwasaki, M. Izquierdo, Y. Izumi, P. M. Jaakkola, M. Jaattela, G. R. Jackson, W. T. Jackson, B. Janji, M. Jendrach, J. H. Jeon, E. B. Jeung, H. Jiang, J. X. Jiang, M. Jiang, Q. Jiang, X. Jiang, A. Jimenez, M. Jin, S. Jin, C. O. Joe, T. Johansen, D. E. Johnson, G. V. Johnson, N. L. Jones, B. Joseph, S. K. Joseph, A. M. Joubert, G. Juhasz, L. Juillerat-Jeanneret, C. H. Jung, Y. K. Jung, K. Kaarniranta, A. Kaasik, T. Kabuta, M. Kadowaki, K. Kagedal, Y. Kamada, V. O. Kaminsky, H. H. Kampinga, H. Kanamori, C. Kang, K. B. Kang, K. I. Kang, R. Kang, Y. A. Kang, T. Kanki, T. D. Kanneganti, H. Kanno, A. G. Kanthasamy, A. Kanthasamy, V. Karantza, G. P. Kaushal, S. Kaushik, Y. Kawazoe, P. Y. Ke, J. H. Kehrl, A. Kelekar, C. Kerkhoff, D. H. Kessel, H. Khalil, J. A. Kiel, A. A. Kiger, A. Kihara, D. R. Kim, D. H. Kim, E. K. Kim, H. R. Kim, J. S. Kim, J. H. Kim, J. C. Kim, J. K. Kim, P. K. Kim, S. W. Kim, Y. S. Kim, Y. Kim, A.

Kimchi, A. C. Kimmelman, J. S. King, T. J. Kinsella, V. Kirkin, L. A. Kirshenbaum, K. Kitamoto, K. Kitazato, L. Klein, W. T. Klimecki, J. Klucken, E. Knecht, B. C. Ko, J. C. Koch, H. Koga, J. Y. Koh, Y. H. Koh, M. Koike, M. Komatsu, E. Kominami, H. J. Kong, W. J. Kong, V. I. Korolchuk, Y. Kotake, M. I. Koukourakis, J. B. Kouri Flores, A. L. Kovacs, C. Kraft, D. Krainc, H. Kramer, C. Kretz-Remy, A. M. Krichevsky, G. Kroemer, R. Kruger, O. Krut, N. T. Ktistakis, C. Y. Kuan, R. Kucharczyk, A. Kumar, R. Kumar, S. Kumar, M. Kundu, H. J. Kung, T. Kurz, H. J. Kwon, A. R. La Spada, F. Lafont, T. Lamark, J. Landry, J. D. Lane, P. Lapaquette, J. F. Laporte, L. Laszlo, S. Lavandero, J. N. Lavoie, R. Layfield, P. A. Lazo, W. Le, L. Le Cam, D. J. Ledbetter, A. J. Lee, B. W. Lee, G. M. Lee, J. Lee, J. H. Lee, M. Lee, M. S. Lee, S. H. Lee, C. Leeuwenburgh, P. Legembre, R. Legouis, M. Lehmann, H. Y. Lei, Q. Y. Lei, D. A. Leib, J. Leiro, J. J. Lemasters, A. Lemoine, M. S. Lesniak, D. Lev, V. V. Levenson, B. Levine, E. Levy, F. Li, J. L. Li, L. Li, S. Li, W. Li, X. J. Li, Y. B. Li, Y. P. Li, C. Liang, Q. Liang, Y. F. Liao, P. P. Liberski, A. Lieberman, H. J. Lim, K. L. Lim, K. Lim, C. F. Lin, F. C. Lin, J. Lin, J. D. Lin, K. Lin, W. W. Lin, W. C. Lin, Y. L. Lin, R. Linden, P. Lingor, J. Lippincott-Schwartz, M. P. Lisanti, P. B. Liton, B. Liu, C. F. Liu, K. Liu, L. Liu, Q. A. Liu, W. Liu, Y. C. Liu, Y. Liu, R. A. Lockshin, C. N. Lok, S. Lonial, B. Loos, G. Lopez-Berestein, C. Lopez-Otin, L. Lossi, M. T. Lotze, P. Low, B. Lu, Z. Lu, F. Luciano, N. W. Lukacs, A. H. Lund, M. A. Lynch-Day, Y. Ma, F. Macian, J. P. MacKeigan, K. F. Macleod, F. Madeo, L. Maiuri, M. C. Maiuri, D. Malagoli, M. C. Malicdan, W. Malorni, N. Man, E. M. Mandelkow, S. Manon, I. Manov, K. Mao, X. Mao, Z. Mao, P. Marambaud, D. Marazziti, Y. L. Marcel, K. Marchbank, P. Marchetti, S. J. Marciniak, M. Marcondes, M. Mardi, G. Marfe, G. Marino, M. Markaki, M. R. Marten, S. J. Martin, C. Martinand-Mari, W. Martinet, M. Martinez-Vicente, M. Masini, P. Matarrese, S. Matsuo, R. Matteoni, A. Mayer, N. M. Mazure, D. J. McConkey, M. J. McConnell, C. McDermott, C. McDonald, G. M. McInerney, S. L. McKenna, B. McLaughlin, P. J. McLean, C. R. McMaster, G. A. McQuibban, A. J. Meijer, M. H. Meisler, A.

Melendez, T. J. Melia, G. Melino, M. A. Mena, J. A. Menendez, R. F. Menna-Barreto, M. B. Menon, F. M. Menzies, C. A. Mercer, A. Merighi, D. E. Merry, S. Meschini, C. G. Meyer, T. F. Meyer, C. Y. Miao, J. Y. Miao, P. A. Michels, C. Michiels, D. Mijaljica, A. Milojkovic, S. Minucci, C. Miracco, C. K. Miranti, I. Mitroulis, K. Miyazawa, N. Mizushima, B. Mograbi, S. Mohseni, X. Molero, B. Mollereau, F. Mollinedo, T. Momoi, I. Monastyrska, M. M. Monick, M. J. Monteiro, M. N. Moore, R. Mora, K. Moreau, P. I. Moreira, Y. Moriyasu, J. Moscat, S. Mostowy, J. C. Mottram, T. Motyl, C. E. Moussa, S. Muller, K. Munger, C. Munz, L. O. Murphy, M. E. Murphy, A. Musaro, I. Mysorekar, E. Nagata, K. Nagata, A. Nahimana, U. Nair, T. Nakagawa, K. Nakahira, H. Nakano, H. Nakatogawa, M. Nanjundan, N. I. Naqvi, D. P. Narendra, M. Narita, M. Navarro, S. T. Nawrocki, T. Y. Nazarko, A. Nemchenko, M. G. Netea, T. P. Neufeld, P. A. Ney, I. P. Nezis, H. P. Nguyen, D. Nie, I. Nishino, C. Nislow, R. A. Nixon, T. Noda, A. A. Noegel, A. Nogalska, S. Noguchi, L. Notterpek, I. Novak, T. Nozaki, N. Nukina, T. Nurnberger, B. Nyfeler, K. Obara, T. D. Oberley, S. Oddo, M. Ogawa, T. Ohashi, K. Okamoto, N. L. Oleinick, F. J. Oliver, L. J. Olsen, S. Olsson, O. Opota, T. F. Osborne, G. K. Ostrander, K. Otsu, J. H. Ou, M. Ouimet, M. Overholtzer, B. Ozpolat, P. Paganetti, U. Pagnini, N. Pallet, G. E. Palmer, C. Palumbo, T. Pan, T. Panaretakis, U. B. Pandey, Z. Papackova, I. Papassideri, I. Paris, J. Park, O. K. Park, J. B. Parys, K. R. Parzych, S. Patschan, C. Patterson, S. Pattingre, J. M. Pawelek, J. Peng, D. H. Perlmutter, I. Perrotta, G. Perry, S. Pervaiz, M. Peter, G. J. Peters, M. Petersen, G. Petrovski, J. M. Phang, M. Piacentini, P. Pierre, V. Pierrefite-Carle, G. Pierron, R. Pinkas-Kramarski, A. Piras, N. Piri, L. C. Plataniias, S. Poggeler, M. Poirot, A. Poletti, C. Pous, M. Pozuelo-Rubio, M. Praetorius-Ibba, A. Prasad, M. Prescott, M. Priault, N. Produit-Zengaffinen, A. Progulske-Fox, T. Proikas-Cezanne, S. Przedborski, K. Przyklenk, R. Puertollano, J. Puyal, S. B. Qian, L. Qin, Z. H. Qin, S. E. Quaggin, N. Raben, H. Rabinowich, S. W. Rabkin, I. Rahman, A. Rami, G. Ramm, G. Randall, F. Randow, V. A. Rao, J. C. Rathmell, B. Ravikumar, S. K. Ray, B. H.

Reed, J. C. Reed, F. Reggiori, A. Regnier-Vigouroux, A. S. Reichert, J. J. Reiners, Jr., R. J. Reiter, J. Ren, J. L. Revuelta, C. J. Rhodes, K. Ritis, E. Rizzo, J. Robbins, M. Roberge, H. Roca, M. C. Roccheri, S. Rocchi, H. P. Rodemann, S. Rodriguez de Cordoba, B. Rohrer, I. B. Roninson, K. Rosen, M. M. Rost-Roszkowska, M. Rouis, K. M. Rouschop, F. Rovetta, B. P. Rubin, D. C. Rubinsztein, K. Ruckdeschel, E. B. Rucker, 3rd, A. Rudich, E. Rudolf, N. Ruiz-Opazo, R. Russo, T. E. Rusten, K. M. Ryan, S. W. Ryter, D. M. Sabatini, J. Sadoshima, T. Saha, T. Saitoh, H. Sakagami, Y. Sakai, G. H. Salekdeh, P. Salomoni, P. M. Salvaterra, G. Salvesen, R. Salvioli, A. M. Sanchez, J. A. Sanchez-Alcazar, R. Sanchez-Prieto, M. Sandri, U. Sankar, P. Sansanwal, L. Santambrogio, S. Saran, S. Sarkar, M. Sarwal, C. Sasakawa, A. Sasnauskiene, M. Sass, K. Sato, M. Sato, A. H. Schapira, M. Scharl, H. M. Schatzl, W. Scheper, S. Schiaffino, C. Schneider, M. E. Schneider, R. Schneider-Stock, P. V. Schoenlein, D. F. Schorderet, C. Schuller, G. K. Schwartz, L. Scorrano, L. Sealy, P. O. Seglen, J. Segura-Aguilar, I. Seiliez, O. Seleverstov, C. Sell, J. B. Seo, D. Separovic, V. Setaluri, T. Setoguchi, C. Settembre, J. J. Shacka, M. Shanmugam, I. M. Shapiro, E. Shaulian, R. J. Shaw, J. H. Shelhamer, H. M. Shen, W. C. Shen, Z. H. Sheng, Y. Shi, K. Shibuya, Y. Shidoji, J. J. Shieh, C. M. Shih, Y. Shimada, S. Shimizu, T. Shintani, O. S. Shirihai, G. C. Shore, A. A. Sibirny, S. B. Sidhu, B. Sikorska, E. C. Silva-Zacarin, A. Simmons, A. K. Simon, H. U. Simon, C. Simone, A. Simonsen, D. A. Sinclair, R. Singh, D. Sinha, F. A. Sinicrope, A. Sirko, P. M. Siu, E. Sivridis, V. Skop, V. P. Skulachev, R. S. Slack, S. S. Smaili, D. R. Smith, M. S. Soengas, T. Soldati, X. Song, A. K. Sood, T. W. Soong, F. Sotgia, S. A. Spector, C. D. Spies, W. Springer, S. M. Srinivasula, L. Stefanis, J. S. Steffan, R. Stendel, H. Stenmark, A. Stephanou, S. T. Stern, C. Sternberg, B. Stork, P. Stralfors, C. S. Subauste, X. Sui, D. Sulzer, J. Sun, S. Y. Sun, Z. J. Sun, J. J. Sung, K. Suzuki, T. Suzuki, M. S. Swanson, C. Swanton, S. T. Sweeney, L. K. Sy, G. Szabadkai, I. Tabas, H. Taegtmeier, M. Tafani, K. Takacs-Vellai, Y. Takano, K. Takegawa, G. Takemura, F. Takeshita, N. J. Talbot, K. S. Tan, K. Tanaka, D. Tang, I. Tanida, B. A. Tannous,

N. Tavernarakis, G. S. Taylor, G. A. Taylor, J. P. Taylor, L. S. Terada, A. Terman, G. Tettamanti, K. Thevissen, C. B. Thompson, A. Thorburn, M. Thumm, F. Tian, Y. Tian, G. Tocchini-Valentini, A. M. Tolkovsky, Y. Tomino, L. Tonges, S. A. Tooze, C. Tournier, J. Tower, R. Towns, V. Trajkovic, L. H. Travassos, T. F. Tsai, M. P. Tschan, T. Tsubata, A. Tsung, B. Turk, L. S. Turner, S. C. Tyagi, Y. Uchiyama, T. Ueno, M. Umekawa, R. Umemiya-Shirafuji, V. K. Unni, M. I. Vaccaro, E. M. Valente, G. Van den Berghe, I. J. van der Klei, W. van Doorn, L. F. van Dyk, M. van Egmond, L. A. van Grunsven, P. Vandenabeele, W. P. Vandenberghe, I. Vanhorebeek, E. C. Vaquero, G. Velasco, T. Vellai, J. M. Vicencio, R. D. Vierstra, M. Vila, C. Vindis, G. Viola, M. T. Viscomi, O. V. Voitsekhovskaja, C. von Haefen, M. Votruba, K. Wada, R. Wade-Martins, C. L. Walker, C. M. Walsh, J. Walter, X. B. Wan, A. Wang, C. Wang, D. Wang, F. Wang, G. Wang, H. Wang, H. G. Wang, H. D. Wang, J. Wang, K. Wang, M. Wang, R. C. Wang, X. Wang, Y. J. Wang, Y. Wang, Z. Wang, Z. C. Wang, D. G. Wansink, D. M. Ward, H. Watada, S. L. Waters, P. Webster, L. Wei, C. C. Weihl, W. A. Weiss, S. M. Welford, L. P. Wen, C. A. Whitehouse, J. L. Whitton, A. J. Whitworth, T. Wileman, J. W. Wiley, S. Wilkinson, D. Willbold, R. L. Williams, P. R. Williamson, B. G. Wouters, C. Wu, D. C. Wu, W. K. Wu, A. Wyttenbach, R. J. Xavier, Z. Xi, P. Xia, G. Xiao, Z. Xie, D. Z. Xu, J. Xu, L. Xu, X. Xu, A. Yamamoto, S. Yamashina, M. Yamashita, X. Yan, M. Yanagida, D. S. Yang, E. Yang, J. M. Yang, S. Y. Yang, W. Yang, W. Y. Yang, Z. Yang, M. C. Yao, T. P. Yao, B. Yeganeh, W. L. Yen, J. J. Yin, X. M. Yin, O. J. Yoo, G. Yoon, S. Y. Yoon, T. Yorimitsu, Y. Yoshikawa, T. Yoshimori, K. Yoshimoto, H. J. You, R. J. Youle, A. Younes, L. Yu, S. W. Yu, W. H. Yu, Z. M. Yuan, Z. Yue, C. H. Yun, M. Yuzaki, O. Zabirnyk, E. Silva-Zacarin, D. Zacks, E. Zacksenhaus, N. Zaffaroni, Z. Zakeri, H. J. Zeh, 3rd, S. O. Zeitlin, H. Zhang, H. L. Zhang, J. Zhang, J. P. Zhang, L. Zhang, M. Y. Zhang, X. D. Zhang, M. Zhao, Y. F. Zhao, Y. Zhao, Z. J. Zhao, X. Zheng, B. Zhivotovsky, Q. Zhong, C. Z. Zhou, C. Zhu, W. G. Zhu, X. F. Zhu, X. Zhu, Y. Zhu, T. Zoladek, W. X. Zong, A. Zorzano, J. Zschocke and B. Zuckerbraun

- (2012). "Guidelines for the use and interpretation of assays for monitoring autophagy." Autophagy **8**(4): 445-544.
- Knodler, L. A., V. Nair and O. Steele-Mortimer (2014). "Quantitative assessment of cytosolic Salmonella in epithelial cells." PLoS One **9**(1): e84681.
- Knodler, L. A. and O. Steele-Mortimer (2003). "Taking possession: biogenesis of the Salmonella-containing vacuole." Traffic **4**(9): 587-599.
- Knodler, L. A., B. A. Vallance, J. Celli, S. Winfree, B. Hansen, M. Montero and O. Steele-Mortimer (2010). "Dissemination of invasive Salmonella via bacterial-induced extrusion of mucosal epithelia." Proc Natl Acad Sci U S A **107**(41): 17733-17738.
- Knodler, L. A., B. A. Vallance, M. Hensel, D. Jackel, B. B. Finlay and O. Steele-Mortimer (2003). "Salmonella type III effectors PipB and PipB2 are targeted to detergent-resistant microdomains on internal host cell membranes." Mol Microbiol **49**(3): 685-704.
- Knuff, K. and B. B. Finlay (2017). "What the SIF Is Happening-The Role of Intracellular Salmonella-Induced Filaments." Front Cell Infect Microbiol **7**: 335.
- Kolodziejek, A. M. and S. I. Miller (2015). "Salmonella modulation of the phagosome membrane, role of SseJ." Cellular Microbiology **17**(3): 333-341.
- Kraus, M. D., B. Amatya and Y. Kimula (1999). "Histopathology of typhoid enteritis: morphologic and immunophenotypic findings." Mod Pathol **12**(10): 949-955.
- Kroger, C., S. C. Dillon, A. D. Cameron, K. Papenfort, S. K. Sivasankaran, K. Hokamp, Y. Chao, A. Sittka, M. Hebrard, K. Handler, A. Colgan, P. Leekitcharoenphon, G. C. Langridge, A. J. Lohan, B. Loftus, S. Lucchini, D. W. Ussery, C. J. Dorman, N. R. Thomson, J. Vogel and J. C. Hinton (2012). "The transcriptional landscape and small RNAs of Salmonella enterica serovar Typhimurium." Proc Natl Acad Sci U S A **109**(20): E1277-1286.
- Kuhle, V. and M. Hensel (2002). "SseF and SseG are translocated effectors of the type III secretion system of Salmonella pathogenicity island 2 that modulate aggregation of endosomal compartments." Cellular Microbiology **4**(12): 813-824.

- Kuma, A., M. Komatsu and N. Mizushima (2017). "Autophagy-monitoring and autophagy-deficient mice." Autophagy **13**(10): 1619-1628.
- Kurita, A., H. Gotoh, M. Eguchi, N. Okada, S. Matsuura, H. Matsui, H. Danbara and Y. Kikuchi (2003). "Intracellular expression of the Salmonella plasmid virulence protein, SpvB, causes apoptotic cell death in eukaryotic cells." Microb Pathog **35**(1): 43-48.
- Kuznetsov, S. A. and V. I. Gelfand (1987). "18 kDa microtubule-associated protein: identification as a new light chain (LC-3) of microtubule-associated protein 1 (MAP-1)." FEBS Lett **212**(1): 145-148.
- Lassen, K. G., P. Kuballa, K. L. Conway, K. K. Patel, C. E. Becker, J. M. Peloquin, E. J. Villablanca, J. M. Norman, T. C. Liu, R. J. Heath, M. L. Becker, L. Fagbami, H. Horn, J. Mercer, O. H. Yilmaz, J. D. Jaffe, A. F. Shamji, A. K. Bhan, S. A. Carr, M. J. Daly, H. W. Virgin, S. L. Schreiber, T. S. Stappenbeck and R. J. Xavier (2014). "Atg16L1 T300A variant decreases selective autophagy resulting in altered cytokine signaling and decreased antibacterial defense." Proc Natl Acad Sci U S A **111**(21): 7741-7746.
- Lassen, K. G. and R. J. Xavier (2018). "Mechanisms and function of autophagy in intestinal disease." Autophagy **14**(2): 216-220.
- Lau, N., A. L. Haeberle, B. J. O'Keeffe, E. A. Latomanski, J. Celli, H. J. Newton and L. A. Knodler (2019). "SopF, a phosphoinositide binding effector, promotes the stability of the nascent Salmonella-containing vacuole." PLoS Pathog **15**(7): e1007959.
- Lawley, T. D., K. Chan, L. J. Thompson, C. C. Kim, G. R. Govoni and D. M. Monack (2006). "Genome-wide screen for Salmonella genes required for long-term systemic infection of the mouse." PLoS Pathog **2**(2): e11.
- Le Minor, L., G. Chamoiseau, E. Barbe, C. Charie-Marsaines and L. Egron (1969). "[10 new Salmonella serotypes isolated in Chad]." Ann Inst Pasteur (Paris) **116**(6): 775-780.
- Legesse-Miller, A., Y. Sagiv, A. Porat and Z. Elazar (1998). "Isolation and

- characterization of a novel low molecular weight protein involved in intra-Golgi traffic." J Biol Chem **273**(5): 3105-3109.
- Levine, M. M., R. E. Black and C. Lanata (1982). "Precise estimation of the numbers of chronic carriers of *Salmonella typhi* in Santiago, Chile, an endemic area." Journal of Infectious Diseases **146**(6): 724-726.
- Li, Y. Y., T. Wang, S. Gao, G. M. Xu, H. Niu, R. Huang and S. Y. Wu (2016). "Salmonella plasmid virulence gene *spvB* enhances bacterial virulence by inhibiting autophagy in a zebrafish infection model." Fish Shellfish Immunol **49**: 252-259.
- Liao, A. P., E. O. Petrof, S. Kuppireddi, Y. Zhao, Y. Xia, E. C. Claud and J. Sun (2008). "Salmonella type III effector *AvrA* stabilizes cell tight junctions to inhibit inflammation in intestinal epithelial cells." PLoS One **3**(6): e2369.
- Liao, Z., L. M. Cimasky, R. Hampton, D. H. Nguyen and J. E. Hildreth (2001). "Lipid rafts and HIV pathogenesis: host membrane cholesterol is required for infection by HIV type 1." AIDS Res Hum Retroviruses **17**(11): 1009-1019.
- Lievin-Le Moal, V. and A. L. Servin (2006). "The front line of enteric host defense against unwelcome intrusion of harmful microorganisms: mucins, antimicrobial peptides, and microbiota." Clin Microbiol Rev **19**(2): 315-337.
- Ligeon, L. A., M. Loi and C. Munz (2018). "LC3-Associated Phagocytosis and Antigen Presentation." Curr Protoc Immunol **123**(1): e60.
- Ligeon, L. A., S. Romao and C. Munz (2017). "Analysis of LC3-Associated Phagocytosis and Antigen Presentation." Methods Mol Biol **1519**: 145-168.
- Linehan, S. A. and D. W. Holden (2003). "The interplay between *Salmonella typhimurium* and its macrophage host--what can it teach us about innate immunity?" Immunology Letters **85**(2): 183-192.
- Linetti, A., A. Fratangeli, E. Taverna, P. Valnegri, M. Francolini, V. Cappello, M. Matteoli, M. Passafaro and P. Rosa (2010). "Cholesterol reduction impairs exocytosis of synaptic vesicles." Journal of Cell Science **123**(Pt 4): 595-605.
- Liscum, L. and N. J. Munn (1999). "Intracellular cholesterol transport." Biochim

Biophys Acta **1438**(1): 19-37.

- Liu, K., E. Zhao, G. Ilyas, G. Lalazar, Y. Lin, M. Haseeb, K. E. Tanaka and M. J. Czaja (2015). "Impaired macrophage autophagy increases the immune response in obese mice by promoting proinflammatory macrophage polarization." Autophagy **11**(2): 271-284.
- Liu, S. L., T. Ezaki, H. Miura, K. Matsui and E. Yabuuchi (1988). "Intact motility as a *Salmonella typhi* invasion-related factor." Infection and Immunity **56**(8): 1967-1973.
- Lofstrom, C., A. S. Hintzmann, G. Sorensen and D. L. Baggesen (2015). "Outbreak of *Salmonella enterica* serovar Typhimurium phage type DT41 in Danish poultry production." Vet Microbiol **178**(1-2): 167-172.
- Lossi, N. S., N. Rolhion, A. I. Magee, C. Boyle and D. W. Holden (2008). "The *Salmonella* SPI-2 effector SseJ exhibits eukaryotic activator-dependent phospholipase A and glycerophospholipid : cholesterol acyltransferase activity." Microbiology (Reading) **154**(Pt 9): 2680-2688.
- Lossi, N. S., N. Rolhion, A. I. Magee, C. Boyle and D. W. Holden (2008). "The *Salmonella* SPI-2 effector SseJ exhibits eukaryotic activator-dependent phospholipase A and glycerophospholipid : cholesterol acyltransferase activity." Microbiology **154**(Pt 9): 2680-2688.
- Lu, Q., C. C. Yokoyama, J. W. Williams, M. T. Baldrige, X. Jin, B. DesRochers, T. Bricker, C. B. Wilen, J. Bagaitkar, E. Loginicheva, A. Sergushichev, D. Creamalmeyer, B. C. Keller, Y. Zhao, A. Kambal, D. R. Green, J. Martinez, M. C. Dinauer, M. J. Holtzman, E. C. Crouch, W. Beatty, A. C. Boon, H. Zhang, G. J. Randolph, M. N. Artyomov and H. W. Virgin (2016). "Homeostatic Control of Innate Lung Inflammation by Vici Syndrome Gene *Epg5* and Additional Autophagy Genes Promotes Influenza Pathogenesis." Cell Host Microbe **19**(1): 102-113.
- Luo, J., L. Y. Jiang, H. Yang and B. L. Song (2019). "Intracellular Cholesterol Transport by Sterol Transfer Proteins at Membrane Contact Sites." Trends

Biochem Sci **44**(3): 273-292.

Luo, J., H. Yang and B. L. Song (2020). "Mechanisms and regulation of cholesterol homeostasis." Nat Rev Mol Cell Biol **21**(4): 225-245.

Lystad, A. H., S. R. Carlsson, L. R. de la Ballina, K. J. Kauffman, S. Nag, T. Yoshimori, T. J. Melia and A. Simonsen (2019). "Distinct functions of ATG16L1 isoforms in membrane binding and LC3B lipidation in autophagy-related processes." Nat Cell Biol **21**(3): 372-383.

Ma, J., C. Becker, C. A. Lowell and D. M. Underhill (2012). "Dectin-1-triggered recruitment of light chain 3 protein to phagosomes facilitates major histocompatibility complex class II presentation of fungal-derived antigens." J Biol Chem **287**(41): 34149-34156.

MacLennan, C., C. Fieschi, D. A. Lammas, C. Picard, S. E. Dorman, O. Sanal, J. M. MacLennan, S. M. Holland, T. H. Ottenhoff, J. L. Casanova and D. S. Kumararatne (2004). "Interleukin (IL)-12 and IL-23 are key cytokines for immunity against Salmonella in humans." Journal of Infectious Diseases **190**(10): 1755-1757.

MacLennan, C. A. (2014). "Out of Africa: links between invasive nontyphoidal Salmonella disease, typhoid fever, and malaria." Clin Infect Dis **58**(5): 648-650.

Madan, R., G. Krishnamurthy and A. Mukhopadhyay (2008). "SopE-mediated recruitment of host Rab5 on phagosomes inhibits Salmonella transport to lysosomes." Methods Mol Biol **445**: 417-437.

Mahammad, S. and I. Parmryd (2008). "Cholesterol homeostasis in T cells. Methyl-beta-cyclodextrin treatment results in equal loss of cholesterol from Triton X-100 soluble and insoluble fractions." Biochim Biophys Acta **1778**(5): 1251-1258.

Mahammad S, P. I. (2015). "Cholesterol depletion using methyl- $\beta$ -cyclodextrin." Methods Mol Biol **1232**: 11.

Majowicz, S. E., J. Musto, E. Scallan, F. J. Angulo, M. Kirk, S. J. O'Brien, T. F. Jones, A. Fazil and R. M. Hoekstra (2010). "The global burden of nontyphoidal Salmonella gastroenteritis." Clin Infect Dis **50**(6): 882-889.

- Malhotra, R., J. P. Warne, E. Salas, A. W. Xu and J. Debnath (2015). "Loss of Atg12, but not Atg5, in pro-opiomelanocortin neurons exacerbates diet-induced obesity." Autophagy **11**(1): 145-154.
- Malik-Kale, P., S. Winfree and O. Steele-Mortimer (2012). "The bimodal lifestyle of intracellular Salmonella in epithelial cells: replication in the cytosol obscures defects in vacuolar replication." PLoS One **7**(6): e38732.
- Mandal, B. K. and J. Brennan (1988). "Bacteraemia in salmonellosis: a 15 year retrospective study from a regional infectious diseases unit." BMJ **297**(6658): 1242-1243.
- Mannon, P. and W. Reinisch (2012). "Interleukin 13 and its role in gut defence and inflammation." Gut **61**(12): 1765-1773.
- Marr, J. S. (1999). "Typhoid Mary." Lancet **353**(9165): 1714.
- Martin, C. J., K. N. Peters and S. M. Behar (2014). "Macrophages clean up: efferocytosis and microbial control." Curr Opin Microbiol **17**: 17-23.
- Martinez, J., J. Almendinger, A. Oberst, R. Ness, C. P. Dillon, P. Fitzgerald, M. O. Hengartner and D. R. Green (2011). "Microtubule-associated protein 1 light chain 3 alpha (LC3)-associated phagocytosis is required for the efficient clearance of dead cells." Proc Natl Acad Sci U S A **108**(42): 17396-17401.
- Martinez, J., L. D. Cunha, S. Park, M. Yang, Q. Lu, R. Orchard, Q.-Z. Li, M. Yan, L. Janke and C. Guy (2016). "Noncanonical autophagy inhibits the autoinflammatory, lupus-like response to dying cells." Nature **533**(7601): 115-119.
- Martinez, J., L. D. Cunha, S. Park, M. Yang, Q. Lu, R. Orchard, Q. Z. Li, M. Yan, L. Janke, C. Guy, A. Linkermann, H. W. Virgin and D. R. Green (2016). "Noncanonical autophagy inhibits the autoinflammatory, lupus-like response to dying cells." Nature **533**(7601): 115-119.
- Martinez, J., R. K. Malireddi, Q. Lu, L. D. Cunha, S. Pelletier, S. Gingras, R. Orchard, J. L. Guan, H. Tan, J. Peng, T. D. Kanneganti, H. W. Virgin and D. R. Green (2015). "Molecular characterization of LC3-associated phagocytosis reveals distinct roles for Rubicon, NOX2 and autophagy proteins." Nat Cell Biol **17**(7):

893-906.

Martinez, J., R. S. Malireddi, Q. Lu, L. D. Cunha, S. Pelletier, S. Gingras, R. Orchard, J.-L. Guan, H. Tan and J. Peng (2015). "Molecular characterization of LC3-associated phagocytosis reveals distinct roles for Rubicon, NOX2 and autophagy proteins." Nature cell biology **17**(7): 893-906.

Mason, W. P. (1909). "'Typhoid Mary'." Science **30**(760): 117-118.

Masud, S., T. K. Prajsnar, V. Torraca, G. E. M. Lamers, M. Benning, M. Van Der Vaart and A. H. Meijer (2019). "Macrophages target Salmonella by Lc3-associated phagocytosis in a systemic infection model." Autophagy **15**(5): 796-812.

Masud, S., L. van der Burg, L. Storm, T. K. Prajsnar and A. H. Meijer (2019). "Rubicon-Dependent Lc3 Recruitment to Salmonella-Containing Phagosomes Is a Host Defense Mechanism Triggered Independently From Major Bacterial Virulence Factors." Front Cell Infect Microbiol **9**: 279.

Mathur, R., H. Oh, D. Zhang, S. G. Park, J. Seo, A. Koblansky, M. S. Hayden and S. Ghosh (2012). "A mouse model of Salmonella typhi infection." Cell **151**(3): 590-602.

Matsunaga, K., T. Saitoh, K. Tabata, H. Omori, T. Satoh, N. Kurotori, I. Maejima, K. Shirahama-Noda, T. Ichimura, T. Isobe, S. Akira, T. Noda and T. Yoshimori (2009). "Two Beclin 1-binding proteins, Atg14L and Rubicon, reciprocally regulate autophagy at different stages." Nat Cell Biol **11**(4): 385-396.

Matsuzawa-Ishimoto, Y., Y. Shono, L. E. Gomez, V. M. Hubbard-Lucey, M. Cammer, J. Neil, M. Z. Dewan, S. R. Lieberman, A. Lazrak, J. M. Marinis, A. Beal, P. A. Harris, J. Bertin, C. Liu, Y. Ding, M. R. M. van den Brink and K. Cadwell (2017). "Autophagy protein ATG16L1 prevents necroptosis in the intestinal epithelium." Journal of Experimental Medicine **214**(12): 3687-3705.

McClelland, M., K. E. Sanderson, S. W. Clifton, P. Latreille, S. Porwollik, A. Sabo, R. Meyer, T. Bieri, P. Ozersky, M. McLellan, C. R. Harkins, C. Wang, C. Nguyen, A. Berghoff, G. Elliott, S. Kohlberg, C. Strong, F. Du, J. Carter, C. Kremizki, D.

- Layman, S. Leonard, H. Sun, L. Fulton, W. Nash, T. Miner, P. Minx, K. Delehaunty, C. Fronick, V. Magrini, M. Nhan, W. Warren, L. Florea, J. Spieth and R. K. Wilson (2004). "Comparison of genome degradation in Paratyphi A and Typhi, human-restricted serovars of *Salmonella enterica* that cause typhoid." Nat Genet **36**(12): 1268-1274.
- McClelland, M., K. E. Sanderson, J. Spieth, S. W. Clifton, P. Latreille, L. Courtney, S. Porwollik, J. Ali, M. Dante, F. Du, S. Hou, D. Layman, S. Leonard, C. Nguyen, K. Scott, A. Holmes, N. Grewal, E. Mulvaney, E. Ryan, H. Sun, L. Florea, W. Miller, T. Stoneking, M. Nhan, R. Waterston and R. K. Wilson (2001). "Complete genome sequence of *Salmonella enterica* serovar Typhimurium LT2." Nature **413**(6858): 852-856.
- McCormick, B. A., S. I. Miller, D. Carnes and J. L. Madara (1995). "Transepithelial signaling to neutrophils by salmonellae: a novel virulence mechanism for gastroenteritis." Infection and Immunity **63**(6): 2302-2309.
- McCusker, M. P., K. Hokamp, J. F. Buckley, P. G. Wall, M. Martins and S. Fanning (2014). "Complete Genome Sequence of *Salmonella enterica* Serovar Agona Pulsed-Field Type SAGOXB.0066, Cause of a 2008 Pan-European Outbreak." Genome Announc **2**(1).
- McGhie, E. J., L. C. Brawn, P. J. Hume, D. Humphreys and V. Koronakis (2009). "Salmonella takes control: effector-driven manipulation of the host." Curr Opin Microbiol **12**(1): 117-124.
- McGourty, K., T. L. Thurston, S. A. Matthews, L. Pinaud, L. J. Mota and D. W. Holden (2012). "Salmonella inhibits retrograde trafficking of mannose-6-phosphate receptors and lysosome function." Science **338**(6109): 963-967.
- McGovern, V. J. and L. J. Slavutin (1979). "Pathology of salmonella colitis." Am J Surg Pathol **3**(6): 483-490.
- Meltzer, E. and E. Schwartz (2010). "Enteric fever: a travel medicine oriented view." Curr Opin Infect Dis **23**(5): 432-437.
- Menendez, A., E. T. Arena, J. A. Guttman, L. Thorson, B. A. Vallance, W. Vogl and B.

- B. Finlay (2009). "Salmonella infection of gallbladder epithelial cells drives local inflammation and injury in a model of acute typhoid fever." Journal of Infectious Diseases **200**(11): 1703-1713.
- Mermin, J., L. Hutwagner, D. Vugia, S. Shallow, P. Daily, J. Bender, J. Koehler, R. Marcus and F. J. Angulo (2004). "Reptiles, amphibians, and human Salmonella infection: a population-based, case-control study." Clin Infect Dis **38 Suppl 3**: S253-261.
- Mesquita, F. S., M. Thomas, M. Sachse, A. J. Santos, R. Figueira and D. W. Holden (2012). "The Salmonella deubiquitinase SseL inhibits selective autophagy of cytosolic aggregates." PLoS Pathog **8**(6): e1002743.
- Messer, J. S., S. F. Murphy, M. F. Logsdon, J. P. Lodolce, W. A. Grimm, S. J. Bartulis, T. P. Vogel, M. Burn and D. L. Boone (2013). "The Crohn's disease: associated ATG16L1 variant and Salmonella invasion." BMJ Open **3**(6).
- Meyerholz, D. K., T. J. Stabel, M. R. Ackermann, S. A. Carlson, B. D. Jones and J. Pohlenz (2002). "Early epithelial invasion by Salmonella enterica serovar Typhimurium DT104 in the swine ileum." Vet Pathol **39**(6): 712-720.
- Mizuno, Y., H. Takada, A. Nomura, C. H. Jin, H. Hattori, K. Ihara, T. Aoki, K. Eguchi and T. Hara (2003). "Th1 and Th1-inducing cytokines in Salmonella infection." Clinical and Experimental Immunology **131**(1): 111-117.
- Mizushima, N. and M. Komatsu (2011). "Autophagy: renovation of cells and tissues." Cell **147**(4): 728-741.
- Mizushima, N., A. Kuma, Y. Kobayashi, A. Yamamoto, M. Matsubae, T. Takao, T. Natsume, Y. Ohsumi and T. Yoshimori (2003). "Mouse Apg16L, a novel WD-repeat protein, targets to the autophagic isolation membrane with the Apg12-Apg5 conjugate." J Cell Sci **116**(Pt 9): 1679-1688.
- Mizushima, N., A. Kuma, Y. Kobayashi, A. Yamamoto, M. Matsubae, T. Takao, T. Natsume, Y. Ohsumi and T. Yoshimori (2003). "Mouse Apg16L, a novel WD-repeat protein, targets to the autophagic isolation membrane with the Apg12-Apg5 conjugate." Journal of Cell Science **116**(Pt 9): 1679-1688.

- Mizushima, N., T. Noda and Y. Ohsumi (1999). "Apg16p is required for the function of the Apg12p-Apg5p conjugate in the yeast autophagy pathway." EMBO J **18**(14): 3888-3896.
- Morgan, E., J. D. Campbell, S. C. Rowe, J. Bispham, M. P. Stevens, A. J. Bowen, P. A. Barrow, D. J. Maskell and T. S. Wallis (2004). "Identification of host-specific colonization factors of *Salmonella enterica* serovar Typhimurium." Mol Microbiol **54**(4): 994-1010.
- Mortimer, P. P. (1999). "Mr N the milker, and Dr Koch's concept of the healthy carrier." Lancet **353**(9161): 1354-1356.
- Muller, A. J., C. Hoffmann, M. Galle, A. Van Den Broeke, M. Heikenwalder, L. Falter, B. Misselwitz, M. Kremer, R. Beyaert and W. D. Hardt (2009). "The *S. Typhimurium* effector SopE induces caspase-1 activation in stromal cells to initiate gut inflammation." Cell Host Microbe **6**(2): 125-136.
- Munoz, L. E., K. Lauber, M. Schiller, A. A. Manfredi and M. Herrmann (2010). "The role of defective clearance of apoptotic cells in systemic autoimmunity." Nat Rev Rheumatol **6**(5): 280-289.
- Murray, P. J. and T. A. Wynn (2011). "Protective and pathogenic functions of macrophage subsets." Nat Rev Immunol **11**(11): 723-737.
- Murray PR, R. K., Pfaller MA (2009). Medical Microbiology (6th ed.). Philadelphia, PA, Mosby Elsevier. p. 307.
- Murray, R. A. and C. A. Lee (2000). "Invasion genes are not required for *Salmonella enterica* serovar typhimurium to breach the intestinal epithelium: evidence that salmonella pathogenicity island 1 has alternative functions during infection." Infection and Immunity **68**(9): 5050-5055.
- Murthy, A., Y. Li, I. Peng, M. Reichelt, A. K. Katakam, R. Noubade, M. Roose-Girma, J. DeVoss, L. Diehl, R. R. Graham and M. van Lookeren Campagne (2014). "A Crohn's disease variant in Atg1611 enhances its degradation by caspase 3." Nature **506**(7489): 456-462.
- Myeni, S. K., L. Wang and D. Zhou (2013). "SipB-SipC complex is essential for

- translocon formation." PLoS One **8**(3): e60499.
- Nakagawa, I., A. Amano, N. Mizushima, A. Yamamoto, H. Yamaguchi, T. Kamimoto, A. Nara, J. Funao, M. Nakata, K. Tsuda, S. Hamada and T. Yoshimori (2004). "Autophagy defends cells against invading group A Streptococcus." Science **306**(5698): 1037-1040.
- Nawabi, P., D. M. Catron and K. Haldar (2008). "Esterification of cholesterol by a type III secretion effector during intracellular Salmonella infection." Mol Microbiol **68**(1): 173-185.
- Newson, J. P. M., N. E. Scott, I. Yeuk Wah Chung, T. Wong Fok Lung, C. Giogha, J. Gan, N. Wang, R. A. Strugnell, N. F. Brown, M. Cygler, J. S. Pearson and E. L. Hartland (2019). "Salmonella Effectors SseK1 and SseK3 Target Death Domain Proteins in the TNF and TRAIL Signaling Pathways." Mol Cell Proteomics **18**(6): 1138-1156.
- Nicolay, N., L. Thornton, S. Cotter, P. Garvey, O. Bannon, P. McKeown, M. Cormican, I. Fisher, C. Little, N. Boxall, E. De Pinna, T. M. Peters, J. Cowden, R. Salmon, B. Mason, N. Irvine, P. Rooney and D. O'Flanagan (2011). "Salmonella enterica serovar Agona European outbreak associated with a food company." Epidemiology and Infection **139**(8): 1272-1280.
- Nishi, T. and M. Forgac (2002). "The vacuolar (H<sup>+</sup>)-ATPases--nature's most versatile proton pumps." Nat Rev Mol Cell Biol **3**(2): 94-103.
- Norkin, L. C., S. A. Wolfrom and E. S. Stuart (2001). "Association of caveolin with Chlamydia trachomatis inclusions at early and late stages of infection." Exp Cell Res **266**(2): 229-238.
- Nutrition, F.-C. f. F. S. a. A. (2008). FDA/CFSAN - Food Safety A to Z Reference Guide - Salmonella.
- Ochiai, R. L., X. Wang, L. von Seidlein, J. Yang, Z. A. Bhutta, S. K. Bhattacharya, M. Agtini, J. L. Deen, J. Wain, D. R. Kim, M. Ali, C. J. Acosta, L. Jodar and J. D. Clemens (2005). "Salmonella paratyphi A rates, Asia." Emerg Infect Dis **11**(11): 1764-1766.

- Odendall, C., N. Rolhion, A. Forster, J. Poh, D. J. Lamont, M. Liu, P. S. Freemont, A. D. Catling and D. W. Holden (2012). "The Salmonella kinase SteC targets the MAP kinase MEK to regulate the host actin cytoskeleton." Cell Host Microbe **12**(5): 657-668.
- Okoro, C. K., R. A. Kingsley, T. R. Connor, S. R. Harris, C. M. Parry, M. N. Al-Mashhadani, S. Kariuki, C. L. Msefula, M. A. Gordon, E. de Pinna, J. Wain, R. S. Heyderman, S. Obaro, P. L. Alonso, I. Mandomando, C. A. MacLennan, M. D. Tapia, M. M. Levine, S. M. Tennant, J. Parkhill and G. Dougan (2012). "Intracontinental spread of human invasive Salmonella Typhimurium pathovariants in sub-Saharan Africa." Nat Genet **44**(11): 1215-1221.
- Olsen, S. J., S. C. Bleasdale, A. R. Magnano, C. Landrigan, B. H. Holland, R. V. Tauxe, E. D. Mintz and S. Luby (2003). "Outbreaks of typhoid fever in the United States, 1960-99." Epidemiology and Infection **130**(1): 13-21.
- Opipari, A. and L. Franchi (2015). "Role of inflammasomes in intestinal inflammation and Crohn's disease." Inflamm Bowel Dis **21**(1): 173-181.
- Ortiz, D., E. M. Siegal, C. Kramer, B. K. Khandheria and E. Brauer (2014). "Nontyphoidal cardiac salmonellosis: two case reports and a review of the literature." Tex Heart Inst J **41**(4): 401-406.
- Otomo, C., Z. Metlagel, G. Takaesu and T. Otomo (2013). "Structure of the human ATG12~ATG5 conjugate required for LC3 lipidation in autophagy." Nat Struct Mol Biol **20**(1): 59-66.
- Ouimet, M., V. Franklin, E. Mak, X. Liao, I. Tabas and Y. L. Marcel (2011). "Autophagy regulates cholesterol efflux from macrophage foam cells via lysosomal acid lipase." Cell Metab **13**(6): 655-667.
- Paine, S., C. Thornley, M. Wilson, M. Dufour, K. Sexton, J. Miller, G. King, S. Bell, D. Bandaranayake and G. Mackereth (2014). "An outbreak of multiple serotypes of salmonella in New Zealand linked to consumption of contaminated tahini imported from Turkey." Foodborne Pathog Dis **11**(11): 887-892.
- Pardo-Roa, C., G. A. Salazar, L. P. Noguera, F. J. Salazar-Echegarai, O. P. Vallejos, I.

- D. Suazo, B. M. Schultz, I. Coronado-Arrazola, A. M. Kalergis and S. M. Bueno (2019). "Pathogenicity island excision during an infection by *Salmonella enterica* serovar Enteritidis is required for crossing the intestinal epithelial barrier in mice to cause systemic infection." PLoS Pathog **15**(12): e1008152.
- Parkhill, J., G. Dougan, K. D. James, N. R. Thomson, D. Pickard, J. Wain, C. Churcher, K. L. Mungall, S. D. Bentley, M. T. Holden, M. Sebaihia, S. Baker, D. Basham, K. Brooks, T. Chillingworth, P. Connor, A. Cronin, P. Davis, R. M. Davies, L. Dowd, N. White, J. Farrar, T. Feltwell, N. Hamlin, A. Haque, T. T. Hien, S. Holroyd, K. Jagels, A. Krogh, T. S. Larsen, S. Leather, S. Moule, P. O'Gaora, C. Parry, M. Quail, K. Rutherford, M. Simmonds, J. Skelton, K. Stevens, S. Whitehead and B. G. Barrell (2001). "Complete genome sequence of a multiple drug resistant *Salmonella enterica* serovar Typhi CT18." Nature **413**(6858): 848-852.
- Parry, C. M., T. T. Hien, G. Dougan, N. J. White and J. J. Farrar (2002). "Typhoid fever." N Engl J Med **347**(22): 1770-1782.
- Pasetti, M. F., M. M. Levine and M. B. Sztein (2003). "Animal models paving the way for clinical trials of attenuated *Salmonella enterica* serovar Typhi live oral vaccines and live vectors." Vaccine **21**(5-6): 401-418.
- Patel, T. A., M. Armstrong, S. D. Morris-Jones, S. G. Wright and T. Doherty (2010). "Imported enteric fever: case series from the hospital for tropical diseases, London, United Kingdom." Am J Trop Med Hyg **82**(6): 1121-1126.
- Paz, Y., Z. Elazar and D. Fass (2000). "Structure of GATE-16, membrane transport modulator and mammalian ortholog of autophagocytosis factor Aut7p." J Biol Chem **275**(33): 25445-25450.
- Peeters, P. M., E. F. Wouters and N. L. Reynaert (2015). "Immune Homeostasis in Epithelial Cells: Evidence and Role of Inflammasome Signaling Reviewed." Journal of Immunology Research **2015**: 828264.
- Perrett, C. A. and D. Zhou (2013). "*Salmonella* type III effector SopB modulates host cell exocytosis." Emerg Microbes Infect **2**(5): e32.

- Pohan, H. T. (2004). "Clinical and laboratory manifestations of typhoid fever at Persahabatan Hospital, Jakarta." Acta Med Indones **36**(2): 78-83.
- Popik, W., T. M. Alce and W. C. Au (2002). "Human immunodeficiency virus type 1 uses lipid raft-colocalized CD4 and chemokine receptors for productive entry into CD4(+) T cells." J Virol **76**(10): 4709-4722.
- Proikas-Cezanne, T., Z. Takacs, P. Donnes and O. Kohlbacher (2015). "WIPI proteins: essential PtdIns3P effectors at the nascent autophagosome." Journal of Cell Science **128**(2): 207-217.
- Rabsch, W., H. L. Andrews, R. A. Kingsley, R. Prager, H. Tschape, L. G. Adams and A. J. Baumler (2002). "Salmonella enterica serotype Typhimurium and its host-adapted variants." Infection and Immunity **70**(5): 2249-2255.
- Raffatellu, M., R. L. Santos, D. E. Verhoeven, M. D. George, R. P. Wilson, S. E. Winter, I. Godinez, S. Sankaran, T. A. Paixao, M. A. Gordon, J. K. Kolls, S. Dandekar and A. J. Baumler (2008). "Simian immunodeficiency virus-induced mucosal interleukin-17 deficiency promotes Salmonella dissemination from the gut." Nature Medicine **14**(4): 421-428.
- Rai, S., M. Arasteh, M. Jefferson, T. Pearson, Y. Wang, W. Zhang, B. Bicsak, D. Divekar, P. P. Powell, R. Naumann, N. Beraza, S. R. Carding, O. Florey, U. Mayer and T. Wileman (2019). "The ATG5-binding and coiled coil domains of ATG16L1 maintain autophagy and tissue homeostasis in mice independently of the WD domain required for LC3-associated phagocytosis." Autophagy **15**(4): 599-612.
- Rao, S., T. Xu, Y. Xia and H. Zhang (2020). "Salmonella and S. aureus Escape From the Clearance of Macrophages via Controlling TFEB." Frontiers in Microbiology **11**: 573844.
- Ray, K., B. Marteyn, P. J. Sansonetti and C. M. Tang (2009). "Life on the inside: the intracellular lifestyle of cytosolic bacteria." Nat Rev Microbiol **7**(5): 333-340.
- Richardson, L. A. (2015). "How Salmonella survives the macrophage's acid attack." PLoS Biol **13**(4): e1002117.

- Richter-Dahlfors, A., A. M. Buchan and B. B. Finlay (1997). "Murine salmonellosis studied by confocal microscopy: *Salmonella typhimurium* resides intracellularly inside macrophages and exerts a cytotoxic effect on phagocytes in vivo." Journal of Experimental Medicine **186**(4): 569-580.
- Rodriguez, M., I. de Diego and M. C. Mendoza (1998). "Extraintestinal salmonellosis in a general hospital (1991 to 1996): relationships between *Salmonella* genomic groups and clinical presentations." J Clin Microbiol **36**(11): 3291-3296.
- Rolhion, N., R. C. Furniss, G. Grabe, A. Ryan, M. Liu, S. A. Matthews and D. W. Holden (2016). "Inhibition of Nuclear Transport of NF- $\kappa$ B p65 by the *Salmonella* Type III Secretion System Effector SpvD." PLoS Pathog **12**(5): e1005653.
- Romanov, J., M. Walczak, I. Ibiricu, S. Schuchner, E. Ogris, C. Kraft and S. Martens (2012). "Mechanism and functions of membrane binding by the Atg5-Atg12/Atg16 complex during autophagosome formation." EMBO J **31**(22): 4304-4317.
- Romao, S., N. Gasser, A. C. Becker, B. Guhl, M. Bajagic, D. Vanoaica, U. Ziegler, J. Roesler, J. Dengjel, J. Reichenbach and C. Munz (2013). "Autophagy proteins stabilize pathogen-containing phagosomes for prolonged MHC II antigen processing." J Cell Biol **203**(5): 757-766.
- Romao, S. and C. Munz (2014). "LC3-associated phagocytosis." Autophagy **10**(3): 526-528.
- Roppenser, B., S. Grinstein and J. H. Brumell (2012). "Modulation of host phosphoinositide metabolism during *Salmonella* invasion by the type III secreted effector SopB." Methods Cell Biol **108**: 173-186.
- Rosselin, M., N. Abed, I. Virlogeux-Payant, E. Bottreau, P. Y. Sizaret, P. Velge and A. Wiedemann (2011). "Heterogeneity of type III secretion system (T3SS)-1-independent entry mechanisms used by *Salmonella* Enteritidis to invade different cell types." Microbiology (Reading) **157**(Pt 3): 839-847.
- Rosselin, M., I. Virlogeux-Payant, C. Roy, E. Bottreau, P. Y. Sizaret, L. Mijouin, P. Germon, E. Caron, P. Velge and A. Wiedemann (2010). "Rck of *Salmonella*

- enterica, subspecies enterica serovar enteritidis, mediates zipper-like internalization." Cell Res **20**(6): 647-664.
- Rotger, R. and J. Casadesus (1999). "The virulence plasmids of Salmonella." Int Microbiol **2**(3): 177-184.
- Roumagnac, P., F. X. Weill, C. Dolecek, S. Baker, S. Brisse, N. T. Chinh, T. A. Le, C. J. Acosta, J. Farrar, G. Dougan and M. Achtman (2006). "Evolutionary history of Salmonella typhi." Science **314**(5803): 1301-1304.
- Rout, W. R., S. B. Formal, G. J. Dammin and R. A. Giannella (1974). "Pathophysiology of Salmonella diarrhea in the Rhesus monkey: Intestinal transport, morphological and bacteriological studies." Gastroenterology **67**(1): 59-70.
- Ruan, H., Z. Zhang, L. Tian, S. Wang, S. Hu and J. J. Qiao (2016). "The Salmonella effector SopB prevents ROS-induced apoptosis of epithelial cells by retarding TRAF6 recruitment to mitochondria." Biochem Biophys Res Commun **478**(2): 618-623.
- Ruiz-Albert, J., X. J. Yu, C. R. Beuzon, A. N. Blakey, E. E. Galyov and D. W. Holden (2002). "Complementary activities of SseJ and SifA regulate dynamics of the Salmonella typhimurium vacuolar membrane." Mol Microbiol **44**(3): 645-661.
- Ryan, M. P., J. O'Dwyer and C. C. Adley (2017). "Evaluation of the Complex Nomenclature of the Clinically and Veterinary Significant Pathogen Salmonella." Biomed Research International **2017**: 3782182.
- Rychlik, I., D. Gregorova and H. Hradecka (2006). "Distribution and function of plasmids in Salmonella enterica." Vet Microbiol **112**(1): 1-10.
- Rytönen, A., J. Poh, J. Garmendia, C. Boyle, A. Thompson, M. Liu, P. Freemont, J. C. Hinton and D. W. Holden (2007). "SseL, a Salmonella deubiquitinase required for macrophage killing and virulence." Proc Natl Acad Sci U S A **104**(9): 3502-3507.
- Saitoh, T., N. Fujita, M. H. Jang, S. Uematsu, B. G. Yang, T. Satoh, H. Omori, T. Noda, N. Yamamoto, M. Komatsu, K. Tanaka, T. Kawai, T. Tsujimura, O.

- Takeuchi, T. Yoshimori and S. Akira (2008). "Loss of the autophagy protein Atg16L1 enhances endotoxin-induced IL-1beta production." Nature **456**(7219): 264-268.
- Salcedo, S. P. and D. W. Holden (2003). "SseG, a virulence protein that targets Salmonella to the Golgi network." EMBO J **22**(19): 5003-5014.
- Salcedo, S. P., M. Noursadeghi, J. Cohen and D. W. Holden (2001). "Intracellular replication of Salmonella typhimurium strains in specific subsets of splenic macrophages in vivo." Cellular Microbiology **3**(9): 587-597.
- Salem, M., O. H. Nielsen, K. Nys, S. Yazdanyar and J. B. Seidelin (2015). "Impact of T300A Variant of ATG16L1 on Antibacterial Response, Risk of Culture Positive Infections, and Clinical Course of Crohn's Disease." Clin Transl Gastroenterol **6**: e122.
- Samie, M., J. Lim, E. Verschuere, J. M. Baughman, I. Peng, A. Wong, Y. Kwon, Y. Senbabaoglu, J. A. Hackney, M. Keir, B. McKenzie, D. S. Kirkpatrick, M. van Lookeren Campagne and A. Murthy (2018). "Selective autophagy of the adaptor TRIF regulates innate inflammatory signaling." Nat Immunol **19**(3): 246-254.
- Sanjuan, M. A., C. P. Dillon, S. W. Tait, S. Moshiah, F. Dorsey, S. Connell, M. Komatsu, K. Tanaka, J. L. Cleveland, S. Withoff and D. R. Green (2007). "Toll-like receptor signalling in macrophages links the autophagy pathway to phagocytosis." Nature **450**(7173): 1253-1257.
- Santos, R. L., S. Zhang, R. M. Tsois, R. A. Kingsley, L. G. Adams and A. J. Baumler (2001). "Animal models of Salmonella infections: enteritis versus typhoid fever." Microbes and Infection **3**(14-15): 1335-1344.
- Schille, S., P. Crauwels, R. Bohn, K. Bagola, P. Walther and G. van Zandbergen (2018). "LC3-associated phagocytosis in microbial pathogenesis." Int J Med Microbiol **308**(1): 228-236.
- Schmidt, H. and M. Hensel (2004). "Pathogenicity islands in bacterial pathogenesis." Clin Microbiol Rev **17**(1): 14-56.
- Schroeder, S., M. Harries, R. Prager, A. Hofig, B. Ahrens, L. Hoffmann, W. Rabsch, E.

- Mertens and D. Rimek (2016). "A prolonged outbreak of Salmonella Infantis associated with pork products in central Germany, April-October 2013." Epidemiology and Infection **144**(7): 1429-1439.
- Scott, C. C., P. Cuellar-Mata, T. Matsuo, H. W. Davidson and S. Grinstein (2002). "Role of 3-phosphoinositides in the maturation of Salmonella-containing vacuoles within host cells." J Biol Chem **277**(15): 12770-12776.
- Sekirov, I., N. M. Tam, M. Jogova, M. L. Robertson, Y. Li, C. Lupp and B. B. Finlay (2008). "Antibiotic-induced perturbations of the intestinal microbiota alter host susceptibility to enteric infection." Infection and Immunity **76**(10): 4726-4736.
- Sellin, M. E., K. M. Maslowski, K. J. Maloy and W. D. Hardt (2015). "Inflammasomes of the intestinal epithelium." Trends Immunol **36**(8): 442-450.
- Sellin, M. E., A. A. Muller and W. D. Hardt (2018). "Consequences of Epithelial Inflammasome Activation by Bacterial Pathogens." J Mol Biol **430**(2): 193-206.
- Serramito-Gomez, I., E. Boada-Romero, K. Slowicka, L. Vereecke, G. Van Loo and F. X. Pimentel-Muinos (2019). "The anti-inflammatory protein TNFAIP3/A20 binds the WD40 domain of ATG16L1 to control the autophagic response, NFKB/NF-kappaB activation and intestinal homeostasis." Autophagy **15**(9): 1657-1659.
- Sezgin, E., I. Levental, S. Mayor and C. Eggeling (2017). "The mystery of membrane organization: composition, regulation and roles of lipid rafts." Nat Rev Mol Cell Biol **18**(6): 361-374.
- Shappo, M. O. E., Q. Li, Z. Lin, M. Hu, J. Ren, Z. Xu, Z. Pan and X. Jiao (2020). "SspH2 as anti-inflammatory candidate effector and its contribution in Salmonella Enteritidis virulence." Microb Pathog **142**: 104041.
- Sharma, D. and T. D. Kanneganti (2016). "The cell biology of inflammasomes: Mechanisms of inflammasome activation and regulation." J Cell Biol **213**(6): 617-629.
- Sharma, V., S. Verma, E. Seranova, S. Sarkar and D. Kumar (2018). "Selective Autophagy and Xenophagy in Infection and Disease." Front Cell Dev Biol **6**: 147.
- Sheikh, A., F. Khanam, M. A. Sayeed, T. Rahman, M. Pacek, Y. Hu, A. Rollins, M. S.

- Bhuiyan, S. Rollins, A. Kalsy, M. Arifuzzaman, D. T. Leung, D. A. Sarracino, B. Krastins, R. C. Charles, R. C. Larocque, A. Cravioto, S. B. Calderwood, W. A. Brooks, J. B. Harris, J. Labaer, F. Qadri and E. T. Ryan (2011). "Interferon-gamma and proliferation responses to *Salmonella enterica* Serotype Typhi proteins in patients with *S. Typhi* Bacteremia in Dhaka, Bangladesh." *PLoS Negl Trop Dis* **5**(6): e1193.
- Shi, Z., Z. Cai, J. Yu, T. Zhang, S. Zhao, E. Smeds, Q. Zhang, F. Wang, C. Zhao, S. Fu, S. Ghosh and D. Zhang (2012). "Toll-like receptor 11 (TLR11) prevents *Salmonella* penetration into the murine Peyer patches." *J Biol Chem* **287**(52): 43417-43423.
- Shin, J. S., Z. Gao and S. N. Abraham (2000). "Involvement of cellular caveolae in bacterial entry into mast cells." *Science* **289**(5480): 785-788.
- Shultz, L. D., F. Ishikawa and D. L. Greiner (2007). "Humanized mice in translational biomedical research." *Nat Rev Immunol* **7**(2): 118-130.
- Silverman, M. and M. Simon (1980). "Phase variation: genetic analysis of switching mutants." *Cell* **19**(4): 845-854.
- Slowicka, K., I. Serramito-Gomez, E. Boada-Romero, A. Martens, M. Sze, I. Petta, H. K. Vikkula, R. De Rycke, E. Parthoens, S. Lippens, S. N. Savvides, A. Wullaert, L. Vereecke, F. X. Pimentel-Muinos and G. van Loo (2019). "Physical and functional interaction between A20 and ATG16L1-WD40 domain in the control of intestinal homeostasis." *Nat Commun* **10**(1): 1834.
- Smith, C., A. M. Stringer, C. Mao, M. J. Palumbo and J. T. Wade (2016). "Mapping the Regulatory Network for *Salmonella enterica* Serovar Typhimurium Invasion." *mBio* **7**(5).
- Song, J., T. Willinger, A. Rongvaux, E. E. Eynon, S. Stevens, M. G. Manz, R. A. Flavell and J. E. Galan (2010). "A mouse model for the human pathogen *Salmonella typhi*." *Cell Host Microbe* **8**(4): 369-376.
- Sou, Y. S., I. Tanida, M. Komatsu, T. Ueno and E. Kominami (2006). "Phosphatidylserine in addition to phosphatidylethanolamine is an in vitro target

- of the mammalian Atg8 modifiers, LC3, GABARAP, and GATE-16." J Biol Chem **281**(6): 3017-3024.
- Sprenkeler, E. G., M. S. Gresnigt and F. L. van de Veerdonk (2016). "LC3-associated phagocytosis: a crucial mechanism for antifungal host defence against *Aspergillus fumigatus*." Cellular Microbiology **18**(9): 1208-1216.
- Stecher, B., R. Robbiani, A. W. Walker, A. M. Westendorf, M. Barthel, M. Kremer, S. Chaffron, A. J. Macpherson, J. Buer, J. Parkhill, G. Dougan, C. von Mering and W. D. Hardt (2007). "Salmonella enterica serovar typhimurium exploits inflammation to compete with the intestinal microbiota." PLoS Biol **5**(10): 2177-2189.
- Stoycheva, M. and M. Murdjeva (2005). "Serum levels of interferon-gamma, interleukin-12, tumour necrosis factor-alpha, and interleukin-10, and bacterial clearance in patients with gastroenteric Salmonella infection." Scand J Infect Dis **37**(1): 11-14.
- Stuart, B. M. and R. L. Pullen (1946). "Typhoid; clinical analysis of 360 cases." Arch Intern Med (Chic) **78**(6): 629-661.
- Sun, H., J. Kamanova, M. Lara-Tejero and J. E. Galan (2016). "A Family of Salmonella Type III Secretion Effector Proteins Selectively Targets the NF-kappaB Signaling Pathway to Preserve Host Homeostasis." PLoS Pathog **12**(3): e1005484.
- Swanson, J. A., M. T. Johnson, K. Beningo, P. Post, M. Mooseker and N. Araki (1999). "A contractile activity that closes phagosomes in macrophages." Journal of Cell Science **112 ( Pt 3)**: 307-316.
- Sztein, M. B. (2007). "Cell-mediated immunity and antibody responses elicited by attenuated *Salmonella enterica* Serovar Typhi strains used as live oral vaccines in humans." Clin Infect Dis **45 Suppl 1**: S15-19.
- Takeuchi, O. and S. Akira (2010). "Pattern recognition receptors and inflammation." Cell **140**(6): 805-820.
- Tan, J. M. J., N. Mellouk, S. E. Osborne, D. A. Ammendolia, D. N. Dyer, R. Li, D.

- Brunen, J. M. van Rijn, J. Huang, M. A. Czuczman, M. A. Cemma, A. M. Won, C. M. Yip, R. J. Xavier, D. A. MacDuff, F. Reggiori, J. Debnath, T. Yoshimori, P. K. Kim, G. D. Fairn, E. Coyaud, B. Raught, A. M. Muise, D. E. Higgins and J. H. Brumell (2018). "An ATG16L1-dependent pathway promotes plasma membrane repair and limits *Listeria monocytogenes* cell-to-cell spread." Nature Microbiology **3**(12): 1472-1485.
- Tan, J. M. J., N. Mellouk, S. E. Osborne, D. A. Ammendolia, D. N. Dyer, R. Li, D. Brunen, J. M. van Rijn, J. Huang, M. A. Czuczman, M. A. Cemma, A. M. Won, C. M. Yip, R. J. Xavier, D. A. MacDuff, F. Reggiori, J. Debnath, T. Yoshimori, P. K. Kim, G. D. Fairn, E. Coyaud, B. Raught, A. M. Muise, D. E. Higgins and J. H. Brumell (2018). "An ATG16L1-dependent pathway promotes plasma membrane repair and limits *Listeria monocytogenes* cell-to-cell spread." Nat Microbiol **3**(12): 1472-1485.
- Tanida, I., T. Ueno and E. Kominami (2004). "LC3 conjugation system in mammalian autophagy." Int J Biochem Cell Biol **36**(12): 2503-2518.
- Thiennimitr, P., S. E. Winter, M. G. Winter, M. N. Xavier, V. Tolstikov, D. L. Huseby, T. Sterzenbach, R. M. Tsohis, J. R. Roth and A. J. Baumler (2011). "Intestinal inflammation allows *Salmonella* to use ethanolamine to compete with the microbiota." Proc Natl Acad Sci U S A **108**(42): 17480-17485.
- Thompson, J. A., M. Liu, S. Helaine and D. W. Holden (2011). "Contribution of the PhoP/Q regulon to survival and replication of *Salmonella enterica* serovar Typhimurium in macrophages." Microbiology (Reading) **157**(Pt 7): 2084-2093.
- Thompson, L. J., S. J. Dunstan, C. Dolecek, T. Perkins, D. House, G. Dougan, T. H. Nguyen, T. P. Tran, C. D. Doan, T. P. Le, T. D. Nguyen, T. H. Tran, J. J. Farrar, D. Monack, D. J. Lynn, S. J. Popper and S. Falkow (2009). "Transcriptional response in the peripheral blood of patients infected with *Salmonella enterica* serovar Typhi." Proc Natl Acad Sci U S A **106**(52): 22433-22438.
- Threlfall, E. J., L. R. Ward, M. D. Hampton, A. M. Ridley, B. Rowe, D. Roberts, R. J. Gilbert, P. Van Someren, P. G. Wall and P. Grimont (1998). "Molecular

- fingerprinting defines a strain of *Salmonella enterica* serotype Anatum responsible for an international outbreak associated with formula-dried milk." *Epidemiology and Infection* **121**(2): 289-293.
- Thurston, T. L., M. P. Wandel, N. von Muhlinen, A. Foeglein and F. Randow (2012). "Galectin 8 targets damaged vesicles for autophagy to defend cells against bacterial invasion." *Nature* **482**(7385): 414-418.
- Tindall, B. J., P. A. Grimont, G. M. Garrity and J. P. Euzeby (2005). "Nomenclature and taxonomy of the genus *Salmonella*." *Int J Syst Evol Microbiol* **55**(Pt 1): 521-524.
- Tokunaga, F. and K. Iwai (2012). "LUBAC, a novel ubiquitin ligase for linear ubiquitination, is crucial for inflammation and immune responses." *Microbes and Infection* **14**(7-8): 563-572.
- Travassos, L. H., L. A. Carneiro, M. Ramjeet, S. Hussey, Y. G. Kim, J. G. Magalhaes, L. Yuan, F. Soares, E. Chea, L. Le Bourhis, I. G. Boneca, A. Allaoui, N. L. Jones, G. Nunez, S. E. Girardin and D. J. Philpott (2010). "Nod1 and Nod2 direct autophagy by recruiting ATG16L1 to the plasma membrane at the site of bacterial entry." *Nature Immunology* **11**(1): 55-62.
- Truong, D., K. C. Boddy, V. Canadien, D. Brabant, G. D. Fairn, V. M. D'Costa, E. Coyaud, B. Raught, D. Perez-Sala, W. S. Park, W. D. Heo, S. Grinstein and J. H. Brumell (2018). "Salmonella exploits host Rho GTPase signalling pathways through the phosphatase activity of SopB." *Cellular Microbiology* **20**(10): e12938.
- Tsolis, R. M., G. M. Young, J. V. Solnick and A. J. Baumler (2008). "From bench to bedside: stealth of enteroinvasive pathogens." *Nat Rev Microbiol* **6**(12): 883-892.
- Tsukada, M. and Y. Ohsumi (1993). "Isolation and characterization of autophagy-defective mutants of *Saccharomyces cerevisiae*." *FEBS Lett* **333**(1-2): 169-174.
- Upadhyay, S. and J. A. Philips (2019). "LC3-associated phagocytosis: host defense and microbial response." *Curr Opin Immunol* **60**: 81-90.
- van Asten, A. J. and J. E. van Dijk (2005). "Distribution of "classic" virulence factors among *Salmonella* spp." *FEMS Immunol Med Microbiol* **44**(3): 251-259.

- Van Cauteren, D., H. De Valk, C. Sommen, L. A. King, N. Jourdan-Da Silva, F. X. Weill, S. Le Hello, F. Megraud, V. Vaillant and J. C. Desenclos (2015). "Community Incidence of Campylobacteriosis and Nontyphoidal Salmonellosis, France, 2008-2013." Foodborne Pathog Dis **12**(8): 664-669.
- van de Vosse, E. and T. H. Ottenhoff (2006). "Human host genetic factors in mycobacterial and Salmonella infection: lessons from single gene disorders in IL-12/IL-23-dependent signaling that affect innate and adaptive immunity." Microbes and Infection **8**(4): 1167-1173.
- Van Detta, J. A. (1999). "'Typhoid Mary' meets the ADA: a case study of the 'direct threat' standard under the Americans with Disabilities Act." Harv J Law Public Policy **22**(3): 849-958.
- Vasanthakumar, T. and J. L. Rubinstein (2020). "Structure and Roles of V-type ATPases." Trends Biochem Sci **45**(4): 295-307.
- Viard, M., I. Parolini, M. Sargiacomo, K. Fecchi, C. Ramoni, S. Ablan, F. W. Ruscetti, J. M. Wang and R. Blumenthal (2002). "Role of cholesterol in human immunodeficiency virus type 1 envelope protein-mediated fusion with host cells." J Virol **76**(22): 11584-11595.
- Vogt, S. L., J. Pena-Diaz and B. B. Finlay (2015). "Chemical communication in the gut: Effects of microbiota-generated metabolites on gastrointestinal bacterial pathogens." Anaerobe **34**: 106-115.
- Vonaesch, P., M. E. Sellin, S. Cardini, V. Singh, M. Barthel and W. D. Hardt (2014). "The Salmonella Typhimurium effector protein SopE transiently localizes to the early SCV and contributes to intracellular replication." Cellular Microbiology **16**(12): 1723-1735.
- Wahid, R., R. Salerno-Goncalves, C. O. Tacket, M. M. Levine and M. B. Sztein (2007). "Cell-mediated immune responses in humans after immunization with one or two doses of oral live attenuated typhoid vaccine CVD 909." Vaccine **25**(8): 1416-1425.
- Wang, H., F. K. Bedford, N. J. Brandon, S. J. Moss and R. W. Olsen (1999).

- "GABA(A)-receptor-associated protein links GABA(A) receptors and the cytoskeleton." Nature **397**(6714): 69-72.
- Wang, X., S. Zhu, J. H. Zhao, H. X. Bao, H. Liu, T. M. Ding, G. R. Liu, Y. G. Li, R. N. Johnston, F. L. Cao, L. Tang and S. L. Liu (2019). "Genetic boundaries delineate the potential human pathogen *Salmonella bongori* into discrete lineages: divergence and speciation." BMC Genomics **20**(1): 930.
- Wang, Y., P. Sharma, M. Jefferson, W. Zhang, B. Bone, A. Kipar, D. Bitto, J. L. Coombes, T. Pearson, A. Man, A. Zhekova, Y. Bao, R. A. Tripp, S. R. Carding, Y. Yamauchi, U. Mayer, P. P. Powell, J. P. Stewart and T. Wileman (2021). "Non-canonical autophagy functions of ATG16L1 in epithelial cells limit lethal infection by influenza A virus." EMBO J: e105543.
- Wangdi, T., S. E. Winter and A. J. Baumler (2012). "Typhoid fever: "you can't hit what you can't see"." Gut Microbes **3**(2): 88-92.
- Watson, K. G. and D. W. Holden (2010). "Dynamics of growth and dissemination of *Salmonella* in vivo." Cellular Microbiology **12**(10): 1389-1397.
- Watson, R. O., S. L. Bell, D. A. MacDuff, J. M. Kimmey, E. J. Diner, J. Olivas, R. E. Vance, C. L. Stallings, H. W. Virgin and J. S. Cox (2015). "The Cytosolic Sensor cGAS Detects *Mycobacterium tuberculosis* DNA to Induce Type I Interferons and Activate Autophagy." Cell Host Microbe **17**(6): 811-819.
- Wei, S., J. Huang, Z. Liu, M. Wang, B. Zhang, Z. Lian, Y. Guo and H. Han (2019). "Differential immune responses of C57BL/6 mice to infection by *Salmonella enterica* serovar Typhimurium strain SL1344, CVCC541 and CMCC50115." Virulence **10**(1): 248-259.
- Wilhelm, L. P., L. Voilquin, T. Kobayashi, C. Tomasetto and F. Alpy (2019). "Intracellular and Plasma Membrane Cholesterol Labeling and Quantification Using Filipin and GFP-D4." Methods Mol Biol **1949**: 137-152.
- Wilkins, E. G. and C. Roberts (1988). "Extraintestinal salmonellosis." Epidemiology and Infection **100**(3): 361-368.
- Winsor, N., C. Krustev, J. Bruce, D. J. Philpott and S. E. Girardin (2019). "Canonical

- and noncanonical inflammasomes in intestinal epithelial cells." Cellular Microbiology **21**(11): e13079.
- Wisner, A. L. S., T. S. Desin, B. Koch, P. S. Lam, E. M. Berberov, C. S. Mickael, A. A. Potter and W. Koster (2010). "Salmonella enterica subspecies enterica serovar Enteritidis Salmonella pathogenicity island 2 type III secretion system: role in intestinal colonization of chickens and systemic spread." Microbiology (Reading) **156**(Pt 9): 2770-2781.
- Wong, L. H., A. T. Gatta and T. P. Levine (2019). "Lipid transfer proteins: the lipid commute via shuttles, bridges and tubes." Nat Rev Mol Cell Biol **20**(2): 85-101.
- Wooldridge, K. G., P. H. Williams and J. M. Ketley (1996). "Host signal transduction and endocytosis of *Campylobacter jejuni*." Microb Pathog **21**(4): 299-305.
- Woting, A. and M. Blaut (2018). "Small Intestinal Permeability and Gut-Transit Time Determined with Low and High Molecular Weight Fluorescein Isothiocyanate-Dextrans in C3H Mice." Nutrients **10**(6).
- Wu, M. Y. and J. H. Lu (2019). "Autophagy and Macrophage Functions: Inflammatory Response and Phagocytosis." Cells **9**(1).
- Xiao, Y. Q., C. G. Freire-de-Lima, W. P. Schiemann, D. L. Bratton, R. W. Vandivier and P. M. Henson (2008). "Transcriptional and translational regulation of TGF-beta production in response to apoptotic cells." J Immunol **181**(5): 3575-3585.
- Xu, J., K. A. Toops, F. Diaz, J. M. Carvajal-Gonzalez, D. Gravotta, F. Mazzoni, R. Schreiner, E. Rodriguez-Boulan and A. Lakkaraju (2012). "Mechanism of polarized lysosome exocytosis in epithelial cells." Journal of Cell Science **125**(Pt 24): 5937-5943.
- Xu, Y., P. Zhou, S. Cheng, Q. Lu, K. Nowak, A. K. Hopp, L. Li, X. Shi, Z. Zhou, W. Gao, D. Li, H. He, X. Liu, J. Ding, M. O. Hottiger and F. Shao (2019). "A Bacterial Effector Reveals the V-ATPase-ATG16L1 Axis that Initiates Xenophagy." Cell **178**(3): 552-566 e520.
- Xu, Z., L. Yang, S. Xu, Z. Zhang and Y. Cao (2015). "The receptor proteins: pivotal roles in selective autophagy." Acta Biochim Biophys Sin (Shanghai) **47**(8): 571-

580.

- Yang, S., Q. Deng, L. Sun, K. Dong, Y. Li, S. Wu and R. Huang (2019). "Salmonella effector SpvB interferes with intracellular iron homeostasis via regulation of transcription factor NRF2." Faseb Journal **33**(12): 13450-13464.
- Ye, Z., E. O. Petrof, D. Boone, E. C. Claud and J. Sun (2007). "Salmonella effector AvrA regulation of colonic epithelial cell inflammation by deubiquitination." American Journal of Pathology **171**(3): 882-892.
- Yeom, J., Y. Shao and E. A. Groisman (2020). "Small proteins regulate Salmonella survival inside macrophages by controlling degradation of a magnesium transporter." Proc Natl Acad Sci U S A **117**(33): 20235-20243.
- Yu, X. J., G. J. Grabe, M. Liu, L. J. Mota and D. W. Holden (2018). "SsaV Interacts with SsaL to Control the Translocon-to-Effector Switch in the Salmonella SPI-2 Type Three Secretion System." mBio **9**(5).
- Yu, X. J., M. Liu and D. W. Holden (2016). "Salmonella Effectors SseF and SseG Interact with Mammalian Protein ACBD3 (GCP60) To Anchor Salmonella-Containing Vacuoles at the Golgi Network." mBio **7**(4).
- Yu, X. J., J. Ruiz-Albert, K. E. Unsworth, S. Garvis, M. Liu and D. W. Holden (2002). "SpiC is required for secretion of Salmonella Pathogenicity Island 2 type III secretion system proteins." Cellular Microbiology **4**(8): 531-540.
- Zak, D. E., F. Schmitz, E. S. Gold, A. H. Diercks, J. J. Peschon, J. S. Valvo, A. Niemisto, I. Podolsky, S. G. Fallen, R. Suen, T. Stolyar, C. D. Johnson, K. A. Kennedy, M. K. Hamilton, O. M. Siggs, B. Beutler and A. Aderem (2011). "Systems analysis identifies an essential role for SHANK-associated RH domain-interacting protein (SHARPIN) in macrophage Toll-like receptor 2 (TLR2) responses." Proc Natl Acad Sci U S A **108**(28): 11536-11541.
- Zhang, H., L. Zheng, D. P. McGovern, A. M. Hamill, R. Ichikawa, Y. Kanazawa, J. Luu, K. Kumagai, M. Cilluffo, M. Fukata, S. R. Targan, D. M. Underhill, X. Zhang and D. Q. Shih (2017). "Myeloid ATG16L1 Facilitates Host-Bacteria Interactions in Maintaining Intestinal Homeostasis." J Immunol **198**(5): 2133-

2146.

- Zhang, K., A. Riba, M. Nietschke, N. Torow, U. Repnik, A. Putz, M. Fulde, A. Dupont, M. Hensel and M. Hornef (2018). "Minimal SPI1-T3SS effector requirement for *Salmonella enterocyte* invasion and intracellular proliferation in vivo." PLoS Pathog **14**(3): e1006925.
- Zhang, X., L. He, C. Zhang, C. Yu, Y. Yang, Y. Jia, X. Cheng, Y. Li, C. Liao, J. Li, Z. Yu and F. Du (2019). "The impact of sseK2 deletion on *Salmonella enterica* serovar typhimurium virulence in vivo and in vitro." BMC Microbiol **19**(1): 182.
- Zhang, Y., A. D. Hoppe and J. A. Swanson (2010). "Coordination of Fc receptor signaling regulates cellular commitment to phagocytosis." Proc Natl Acad Sci U S A **107**(45): 19332-19337.
- Zurawski, D. V. and M. A. Stein (2004). "The SPI2-encoded SseA chaperone has discrete domains required for SseB stabilization and export, and binds within the C-terminus of SseB and SseD." Microbiology **150**(Pt 7): 2055-2068.